FACULDADE DE ENGENHARIA DA UNIVERSIDADE DO PORTO

Evaluation and Optimization of an Industrial Utility System

João Alegre Queiroz

Doctoral Program in Refining, Petrochemical and Chemical Engineering

Academic supervisors: **Fernando Martins (UP – FEUP - LEPABE)**

Henrique Matos (UL - IST - CERENA)

Industrial coordinator: **Vítor Rodrigues (Dow Portugal)**

February 2016

Evaluation and Optimization of an Industrial Utility System

João Alegre Queiroz

Doctoral Program in Refining, Petrochemical and Chemical Engineering

Work financially supported by

under the program Bolsas de Doutoramento em Empresas
(SFRH/BDE/51013/2010).

February 2016

Resumo

Num contexto global, é fundamental reduzir a energia consumida com origem em combustíveis fósseis de forma a minimizar o impacto ambiental da atividade humana. A contribuição da indústria para a energia total consumida é bastante elevada (em 2013 correspondeu a 30% da energia total consumida mundialmente de acordo com Agência Internacional de Energia), pelo que a redução do consumo energético neste setor é bastante incentivada. Do ponto de vista da indústria, a redução de custos induzida pela minimização do consumo energético representa outro fator de extrema relevância.

A diminuição das reservas de combustíveis fósseis e o aumento da concentração dos gases com efeito de estufa motivam o desenvolvimento de um sistema sustentável que utilize menos combustíveis fósseis. De forma a minimizar a sua utilização duas vias deverão ser exploradas:

- Desenvolvimento e introdução de novas tecnologias de produção, armazenamento e utilização de energia, que não se baseiem em combustíveis fósseis;
- Medidas de conservação energética (intensificação) para utilização mais eficiente dos recursos energéticos.

O estudo que foi desenvolvido e é aqui apresentado foca-se nesta última estratégia e visa a aplicação de ferramentas e metodologias de otimização energética aplicáveis em ambiente industrial.

Numa instalação industrial de produção de produtos químicos é comum a utilização de vapor e água de arrefecimento como meios de distribuição energética de e para o processo. O foco deste estudo é o desenvolvimento de metodologias nos dois seguintes tópicos:

1. Avaliar o desempenho térmico e hidráulico dos sistemas de vapor e água de arrefecimento através de modelos suportados em ferramentas informáticas;
2. Identificar fontes de desperdício e oportunidades de melhoria que visem a melhoria do desempenho energético da unidade.

As ferramentas e metodologias desenvolvidas foram utilizadas para identificar oportunidades de melhoria na fábrica da Dow Portugal, em Estarreja. Foi possível identificar oportunidades de melhoria que reduziriam em cerca de 11% os custos energéticos operacionais, representado cerca de 1 M€ de poupança anual. Estas modificações também permitiram reduzir o tempo em que a torre de arrefecimento é o ponto de estrangulamento da fábrica, permitindo reduzir este período de 4.5% para 3% do tempo total de operação da fábrica.

Palavras-chave: energia; sistema de água de arrefecimento; sistema de vapor; integração de processo; tecnologia do estrangulamento térmico, método matricial

Abstract

In a global context, it is fundamental to reduce the fossil-based energy consumption to minimize the environmental impact of human activities. Industry's contribution to the total energy consumption is very high (in 2013 corresponded to 30% of the total energy consumption worldwide according to the International Energy Agency [1]), and thus reduction of energy use is highly motivated in this sector. From the industry viewpoint, cost savings represent another key driver for energy optimization.

The diminishing supplies of fossil fuels and increased greenhouse gas levels motivate research and development towards a sustainable energy system with less use of fossil fuels. To decrease this use, two main paths must be pursued:

- Development and introduction of new energy production techniques, not relying on fossil fuels;
- Energy conservation (intensification) measures to use energy more efficiently.

The study presented herein is focuses on the latter approach and aims for the application of energy optimization tools and methodologies, applicable in an industrial context.

Within a chemical manufacturing plant, steam and cooling water are two major utilities in regard to energy in- and output to/from the processes. The aim of this work is to contribute through the development of methods in two subjects:

1. Evaluating thermal and hydraulic performance of steam and cooling water systems through computer-based mathematical models;
2. Identifying waste sources and cost-effective retrofit improvements to the steam and cooling water systems.

The developed tools and methodologies were applied in a practical example of Dow Portugal, in Estarreja, to identify improvement opportunities. It was possible to identify possible modifications that could result in a 11% operational cost reduction, representing around 1 M€/yr savings. These modifications would also allow to reduce the time during which the cooling tower is the production bottleneck, allowing a reduction of this period from 4.5% to 3% of the total operating time.

Keywords: Energy; cooling tower; cooling water system; steam system; process integration; stream matching; pinch analysis; matrix method

Acknowledgements

I am truly grateful to my academic supervisors: Prof. Fernando Martins (UP-FEUP) and Prof. Henrique Matos (UL-IST) for all the support, guidance and advice that were fundamental to complete this endeavour. Without their commitment and encouragement most of the achievements of this project would have been compromised.

To my supervisor at Dow Portugal, Vitor Rodrigues, a word of deep gratitude for being key to the development of the project and for teaching me so many things at the professional level as well as the personal level. I will most certainly use much of his insights throughout my life.

I also acknowledge the Doctoral Program in Refining, Petrochemical and Chemical Engineering, Faculdade de Engenharia da Universidade do Porto, Instituto Superior Técnico, Fundação para a Ciência e a Tecnologia and Dow Portugal for making this project possible.

A big “Thank you!” is also owed to my parents, family and friends who supported me at all times and gave me words of advice and wisdom throughout this journey.

Finally, I have no words to express my gratitude towards Raquel and Afonso, whose love and patience was fundamental for the sanity of the author and without whom everything would be infinitely harder.

Table of contents

List of Figures

List of Tables

List of Abbreviations

CS	Case study
CP	Heat capacity flow rate [$kW \cdot C^{-1}$]
e.g.	*exempli gratia*
et al.	*et alii*
HX	Heat exchanger
i.e.	*id est*
MDA	4,4'-Diphenyl methyl diamine
MDI	Methylene diphenyl diisocyanate

Notation

$F(\lambda)$	=	Sum of squared error between experimental and model prediction values
G	=	Humid air mass flow (kg/h)
$H[F(\lambda)]$	=	Hessian matrix of $F(\lambda)$
I	=	Identity matrix
i	=	Rate of return (%)
L	=	Water mass flow (kg/h)
m	=	Number of data points in each sub-set
N	=	Number of equilibrium stages
n	=	Plant life (yrs)
P	=	Pressure (kPa)
Q	=	Enthalpy in stream (kJ)
RH	=	Relative humidity (%)
s	=	Search direction
T	=	Temperature (C)
x	=	Independent variables
y	=	Vapor composition on equilibrium stage
Y	=	Model output
$\bar{Y}$	=	Average value of the model output
$\hat{Y}$	=	Experimental value
β	=	Control coefficient in Levenberg-Marquardt method
$\Delta\lambda$	=	Increment of λ

ε = Allowable difference between two consecutive iterations

η = Efficiency (%)

λ = Model parameters

$\nabla F(\lambda)$ = Gradient of $F(\lambda)$

Subscripts

dm = Calculated using the direct method

fuel = Relative to fuel

i = Relative to component *i*

im = Calculated using the indirect method

j = Relative to stage *j*

k = k^{th} iteration

l = l^{th} experimental point

stm = Relative to steam

test = Relative to test data sub-set

trn = Relative to train data sub-set

val = Relative to validation data sub-set

Superscripts

atm = Relative to ambient conditions

a = Relative to air stream

exp = Experimental data

mod = Model predicted values

w = Relative to water stream

1 Introduction

This chapter describes the motivation, scope and context that led to the development of this thesis as well as the structure of the document.

1.1 Motivation

Increasing energy prices and environmental concerns motivate research and development towards systems with higher energy efficiency. Ultimately, companies that are able to produce products at lower manufacturing costs and lower environmental impacts have a competitive advantage.

The motivation that led to this study essentially was a set of problems arising from an industrial case-study. The development of a structured methodology and application to a real case was the basis for this thesis.

The industrial case-study problem behind this work can be described as follows:

I. Plant capacity increased throughout the years with several equipment being modified, added and removed;
II. Cooling tower and steam generation systems have never been replaced or upgraded in terms of capacity;
III. Energy costs represent a significant proportion of the manufacturing costs;
IV. Several process constraints hinder higher process integration.

Simply put, the aim of this work is to develop retrofit modifications that reduce utility consumption taking into consideration process constraints.

1.2 Scope

The scope of the research work is to describe a methodology that allows the evaluation and optimization of an existent industrial steam and cooling water system. This methodology should then be applied to the industrial case-study.

This thesis contributes through the development of strategies for decreasing the utility consumption that are related with the following specific topics:

1. Evaluation and optimization of steam and cooling water networks;
2. Identification of cost-effective options for designing and retrofitting heat exchanger networks;

The knowledge generated by this work is expected to contribute with tools that take into consideration not only the state of the art but also the real industrial limitations, generating both environmental benefits and capital savings.

1.3 Industrial context

The plant in which this study is focused, Dow Portugal S.U.L., manufactures polymeric methylene diphenyl diisocyanate (MDI). In 2009, a revamping project was implemented so that plant capacity almost doubled. However, the utility system was not modified and the plant was facing problems meeting the necessary cooling requirements, especially in summer months. Instead of applying a solution that would result in acquiring a cooling tower with higher capacity, with this project, it is intended to evaluate the entire process and utility system so that they are optimized. By minimizing energy consumption, the existent equipment, namely boilers and cooling towers, can be used even for higher plant capacity.

Polymeric MDI is then used in rigid foam insulation for the construction and refrigeration industries. It is also used for producing high resilience flexible, semi-rigid, and packaging polyurethane foams and in a number of non-foam applications such as adhesives, composite wood binder, plywood patching compounds, etc. [2].

In 1848, Wurtz was the first to synthesize isocyanates from the reaction of diethylsulfete and potassium-cyanate. Later, in 1984, Hentschel synthesized isocyanates by phosgenation of amine, creating what became the most common process in commercial applications [3]. PMDI is a brown liquid, stable over a wide range of temperatures. It is produced by the condensation of aniline and formaldehyde and subsequent phosgenation. The process leads to a mixture containing 2,4' and 2,2' monomeric isomers (MMDI) as well as 3-ring and higher molecular weight species (Figure 1.1) [2].

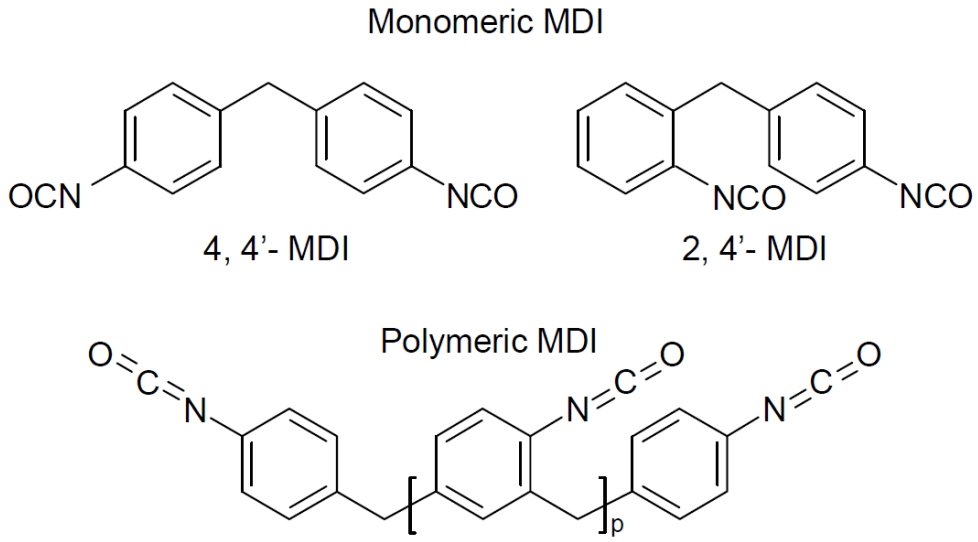

Figure 1.1 – Molecular structure of monomeric and polymeric MDI.

Besides reacting with water, methylene diphenyl diisocyanate (MDI) reacts with acids, alcohols, basic materials (*e.g.*, sodium hydroxide, ammonia, and amines), magnesium and aluminum (and their alloys), metal salts (*e.g.*, tin, iron, aluminum, and zinc chlorides), strong oxidizing agents (e.g., bleach and chlorine) and polyols. These reactions may be violent, generating heat, which can result in an increased evolution of isocyanate vapor and/or a buildup of pressure within closed containers as well as generating a solid residue that causes severe fouling [2].

The MDI plant operated by Dow Portugal is part of a chemical cluster located in Estarreja (Figure 1.2). The integration with other production facilities contributes to the overall success of the cluster since transportation costs are minimized and some common infrastructures are shared (*e.g.*, utilities, effluent treatment) [4].

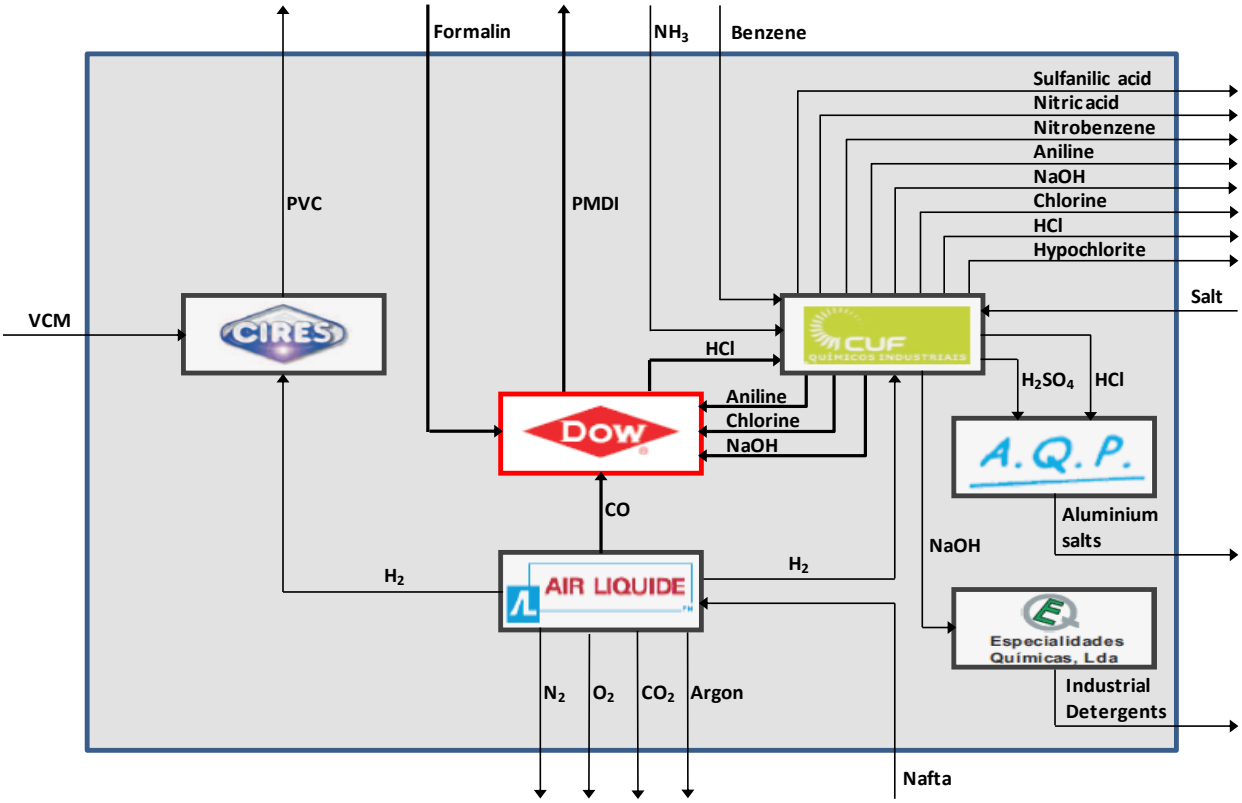

Figure 1.2 – Overview of the Estarreja chemical cluster [4].

The greatest issues affecting the Estarreja MDI process are: the dangerousness of phosgene, which turns any cross-exchange with a stream containing this material into a very difficult operation; the reactivity of the isocyanate group with a variety of nucleophiles including alcohols, amines and water, affecting the reliability of heat exchangers where water is used to cool down streams containing isocyanates; fouling of heat exchanger due to the fact that MDI is prone to crystallization, which requires special designed heat exchangers to handle these streams; and the fact that the heat exchangers are spread throughout the plant, requiring the streams to be moved great distances in some cases.

The main constraints affecting the process integration of the Estarreja MDI plant can be summarized as follows:

- Process safety issues
- Incompatible materials
- Operability issues
- Geographical distance

So, while there are several published works regarding the application of the pinch analysis methodology to practical case-studies [5-7]. To the author's best knowledge there is not any published work describing a methodology describing the application of pinch analysis to a process with several constraints to process integration.

1.3.1 Process description

Taking into account the nature of each reaction step, the process can be divided into four main sections: 4,4'-diphenylmethyldiamine (MDA) plant, Phosgene generation; MDA phosgenation and MDI finishing.

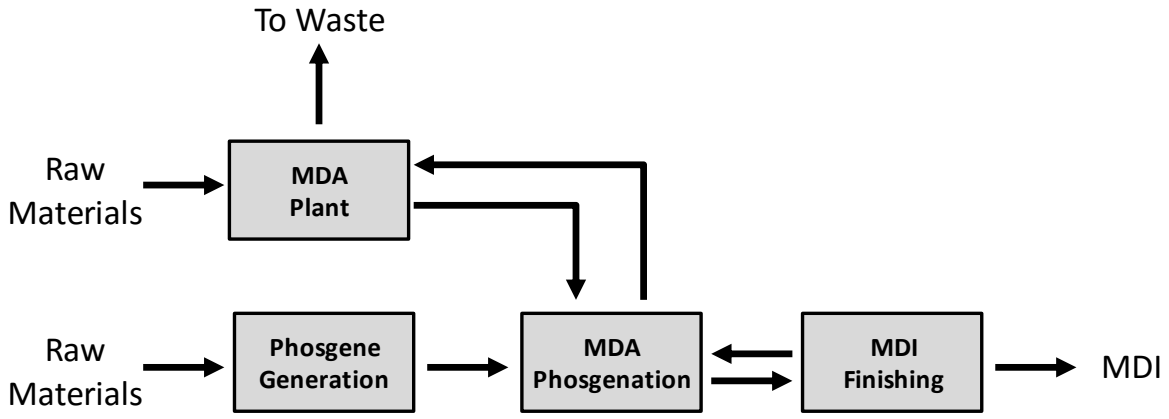

Figure 1.3 – Process block diagram.

Figure 1.4 shows the main reaction steps involved in the process. The condensation of aniline and formaldehyde in a hydrochloric acid medium, resulting in MDA and some other isomers with two or more aromatic rings, takes place in the "MDA Plant". Simultaneously, phosgene is continuously produced by reacting chlorine with carbon monoxide in the "Phosgenation Generation" section. Next, MDA is reacted with phosgene in a monochlorobenzene (MCB) solvent in the "MDA Phosgenation" section, resulting in an isocyanate mixture termed as crude MDI. Finally, the MCB solvent in which the phosgenation reaction took place is recovered and purified in the "MDI Finishing" section.

.

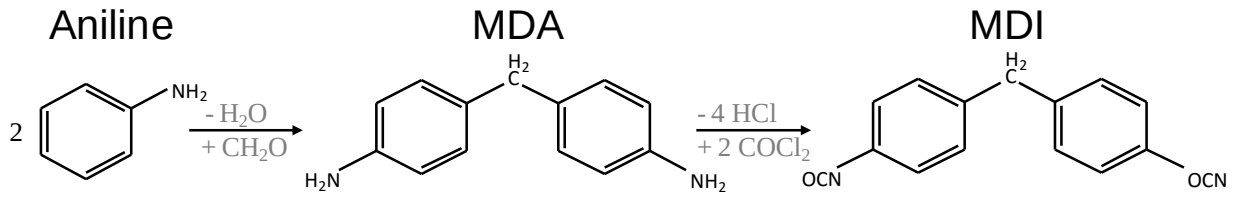

Figure 1.4 – Main products and reaction steps involved in the MDI manufacturing process.

1.4 Thesis outline

This document is organized in 6 chapters and 3 appendixes. Apart from the thesis outline, Chapter 1 presents the motivation, scope and context for this study. In Chapter 2, an overview of the state of the art methodologies used to evaluate and optimize the process energy efficiency is presented. An analysis of the utility system, namely steam and cooling water systems, is performed in Chapter 3. Energy targets for the hot and cold utilities are then presented in Chapter 4, where solutions to minimize energy consumption are also shown. Finally, the main conclusions taken from this study and recommendations for future work are given in Chapter 5. In Chapter 6 the references cited in this work are listed.

Appendix A1 has the equations and algorithms used for determining the psychometric data of air necessary for the cooling tower simulations. Appendix A2 shows the equations used in the stream matching methodology. In Appendix A3, the stream matching tools developed during this work are detailed.

In Figure 1.5, a word cloud with the terms used in this document is shown. The words that are most frequently used are within the “thermal energy” context, which is in fact the main subject addressed in this work.

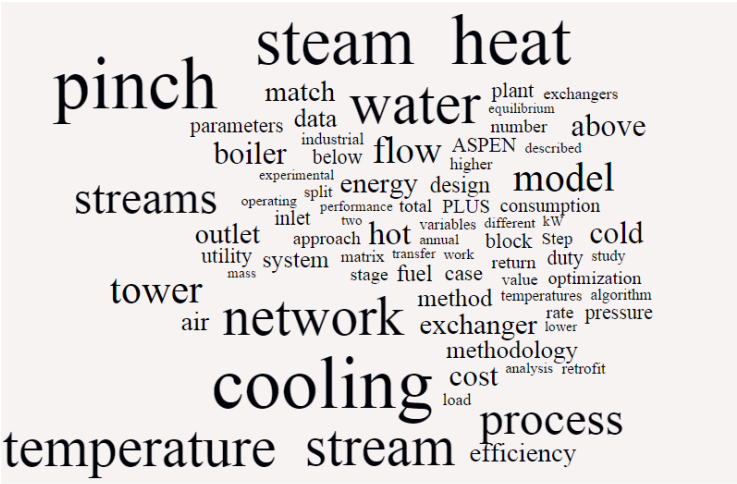

Figure 1.5 – Word cloud with the terms using in this thesis.

Figure 1.6 is a schematic representation of the thesis structure with a summary of the subjects addressed in each chapter.

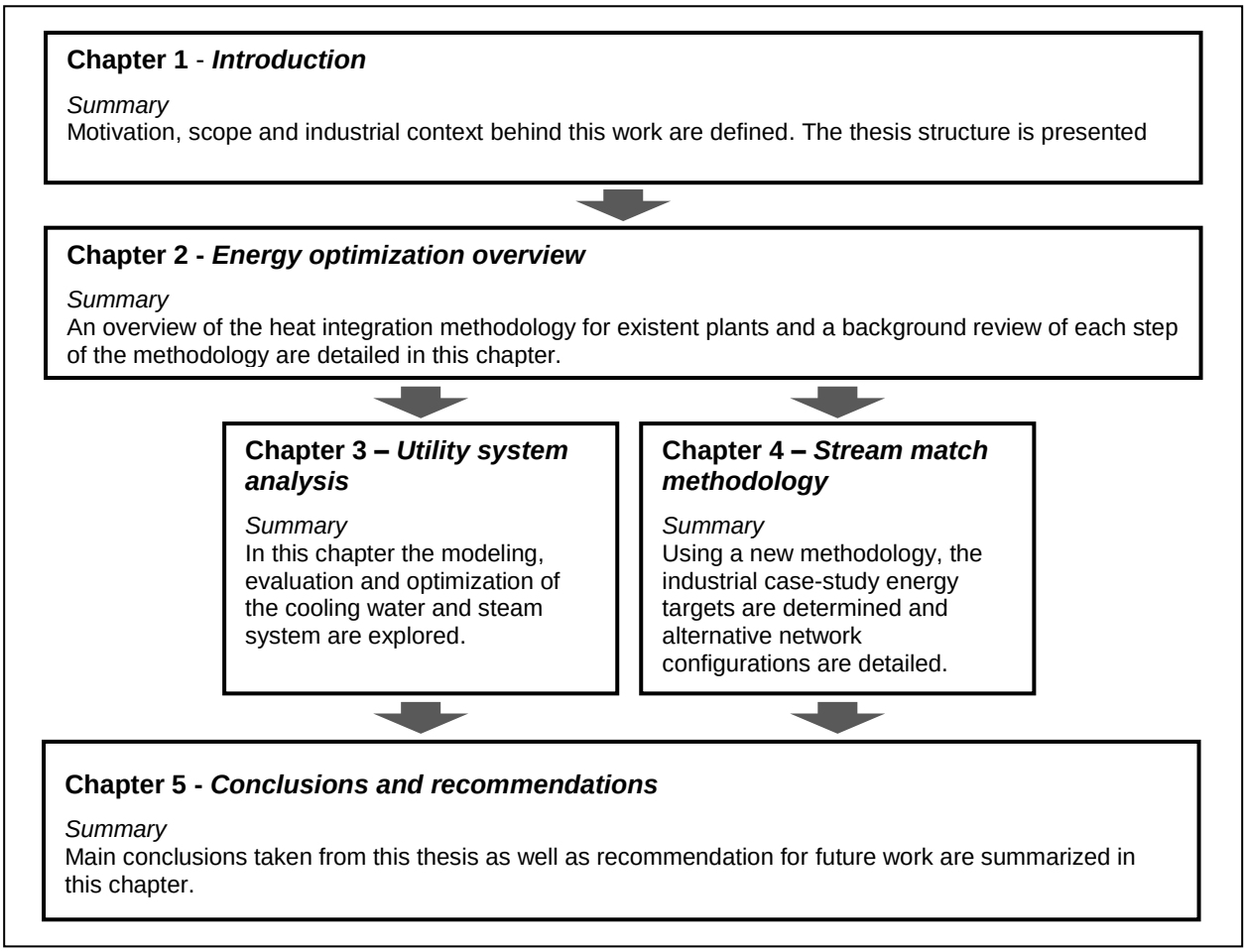

Figure 1.6 – Thesis structure and summary of each chapter.

2 Energy efficiency optimization overview

This chapter details the energy efficiency optimization methodology and techniques. It starts by introducing the energy optimization methodology for existent plants, listing the various steps. This is followed by the presentation of key concepts related to each step of the methodology.

Nowadays, practically all manufacturing industries are challenged with increasingly high energy prices and environmental regulations. An example of such regulations is the Kyoto Protocol, limiting the discharge of greenhouse gases. The fact that carbon dioxide is considered one of the main greenhouse gases and the energy sector is the primary source of carbon dioxide discharge implies that energy use is restricted as well [6]. The petrochemical industry is especially sensitive to this issue as it is a very energy intensive sector. Therefore, efforts to reduce energy consumption are being carried out not only in new plants but also in existent ones.

Retrofitting/revamping a plant consists on analyzing an existing plant and evaluating whether it can be improved, reducing energy consumption and emissions while increasing profitability. This process allows the existent plants to remain competitive within the industry despite being originally designed with outdated assumptions.

The purpose of this study is to present a methodology that can be used to evaluate and optimize the energy performance of existent chemical manufacturing plants. The Estarreja PMDI plant is used as a case study where the proposed methodologies are applied. Despite being a somewhat humorous image, Figure 2.1 represents the purpose of this work, *i.e.*, an effort is taken to minimize the quality and quantity of the resources that are used in the process, and therefore decreases waste as well, so that the operating costs are reduced.

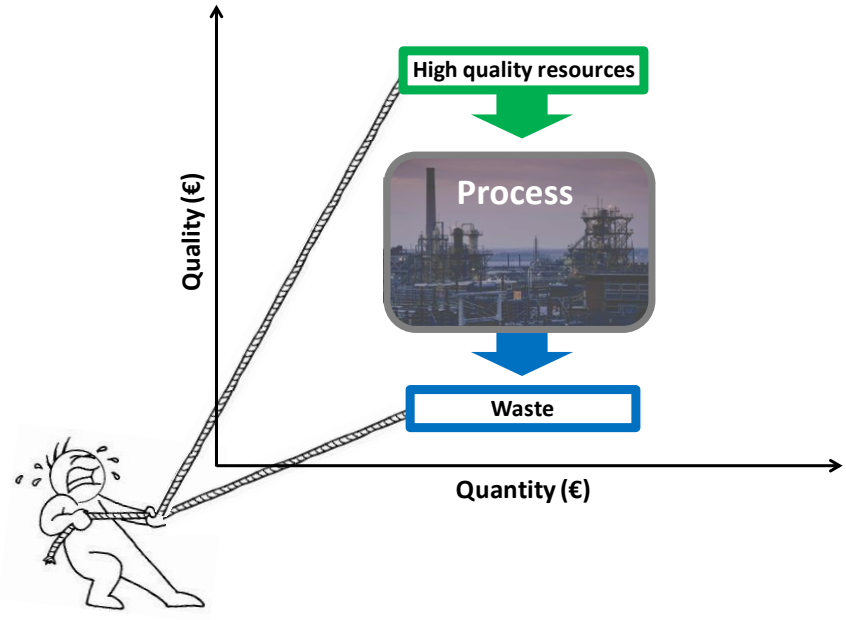

Figure 2.1 – An effort to reduce external utilities' quality and quantity is constantly pursued.

Although the main aim of this work is the energy optimization of an existent plant using Heat Integration techniques, a general note on Process Integration as boarder field study is recommended.

Process integration is a broad and active field that essentially aims for efficient use of raw materials and energy, therefore reducing the environmental footprint.

The definition of Process integration, as stated by the International Energy Agency (IEA) [8] is as follows:

"Systematic and general methods for designing integrated production systems, ranging from individual processes to total sites, with special emphasis on the efficient use of energy and reducing environmental effects."

The term Process Integration was widely diffused in the 1980's mainly due to the introduction of the Pinch concept by Linnhoff and his co-workers [9-11]. After the major advancements in Heat Integration that led to significant improvements in the oil, chemical and power industries, further developments into other fields followed. Due to the fact that the Pinch concept was initially applied to Heat Integration, the terms are sometimes taken as identical. However, although Heat Integration is still today a major subject of the Process Integration field (as shown in Figure 2.2), it is not exclusive. Nowadays, Process integration methodologies also cover areas such as Mass Integration and Water Integration [12].

Figure 2.2 – Word cloud showing the prominence of the Keywords that appear more frequently in the works returned by www.ScienceDirect.com with the search words "Process Integration" (August 2014).

The methodology followed in this work is presented in Figure 2.3 and is based on four main steps:

1. **Data extraction** – During this step, data was gathered either by direct measurements, design data or simulation models. The ideal source of information is a process model properly validated with plant data. Besides providing several operational parameters that in some cases are difficult to obtain directly, it allows the evaluation of the impacts that the implementation of projects have on the process. The outcome of this stage is therefore a set of process simulation models, validated with plant data;
2. **Utility system analysis** – Models of the steam and cooling water network systems were developed. The systems models allow the evaluation of the impacts that any process modification has on the utility system. Additionally, they allow the identification of possible improvements on the utility system itself.
3. **Retrofit heat exchanger network** – Based on stream material and energy balances, a retrofit study was performed. The outcome of this stage is the cold and hot utility targets, current network performance in relation to the targets and cross exchange possibilities;
4. **Site improvements** – Some of the alternatives generated during steps 2 and 3 are independent from each other and some are not. Taking into account the various alternatives, several combinations can be generated. The outcome of this stage is then a set of proposals with the respective costs and savings estimates.

Project ideas generated by this methodology are then evaluated and, if implemented, will contribute to a better energy efficiency of the site.

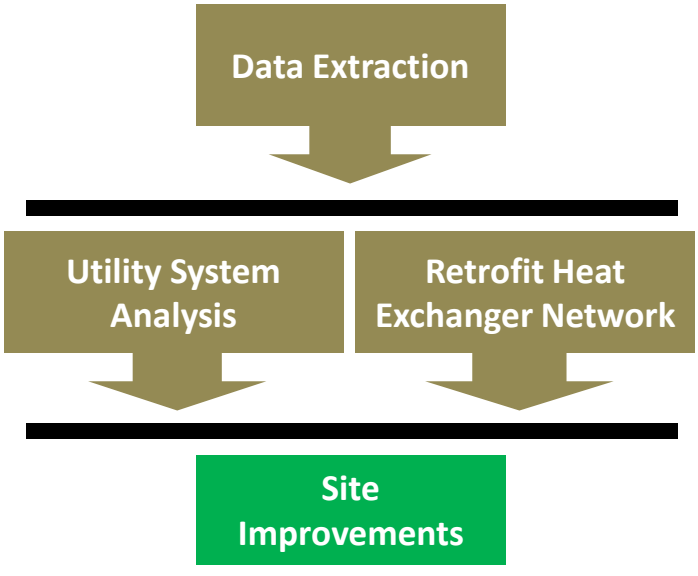

Figure 2.3 – Methodology for the overall process energy evaluation and optimization.

2.1 Data extraction

Data extraction is the key link between the process and the evaluation/optimization steps that lead to site improvements, the quality of the data collected during this phase is crucial for the validity of the subsequent steps of the methodology.

The simulation tool used in this work was ASPEN PLUS [13], which is a software extensively used in the petrochemical industry for steady state simulation and has been applied in feasibility studies of new designs, analysis of complex plants with recycles and optimization [13]. This process simulator delivers a comprehensive library of models that are user-editable as well as models that are organized by function, such as Mixers/Splitters, Separators, Heat Exchangers, Columns, or Reactors, etc. Additionally, ASPEN PLUS has a vast database of component properties along with an array of thermodynamic models that can also be edited according to the user needs.

In regard to the property methods used in the models it is fundamental to choose the appropriate package. Without quality input data and a good overall understanding of the modeled system from a chemical engineering perspective, the simulation results can easily be misinterpreted. Kinetic data and thermodynamic property methods can be the most likely source of error [14].

Regarding the Estarreja PMDI manufacturing plant, and before this study took place, process flowsheets diagrams (PFD's) as well as some ASPEN PLUS simulations were already available. These simulations are a fair representation of the process as they have been validated with plant data; therefore, they were used to perform the energy evaluation and optimization study.

Although it is possible to use only direct measurements, the ideal case is when this information is used to validate process models. Consolidated process models can then provide a reliable source of information for several operational variables and be used to evaluate the impact of the projects recommended by the application of this methodology.

For performing an evaluation and optimization study of a process unit, it is necessary to simulate and validate plant data. Simulation should provide a mass and energy balance consistent with plant measurements. Nowadays, most of the processes are already simulated and validated with plant data. However, it is important to cross-check all the available data to identify any inconsistency and correct it. The importance of the simulation is not only to provide analysis data to the following stages of the study but also to foresee the impact that any suggested modifications can promote on the process.

Although direct measurements portrait the process currently in operation, they may be inconsistent or simply unavailable. In such cases the best option is to use design data to populate the simulations.

In modern manufacturing industries, computer aided engineering is present in practically all activities related to process engineering. Flowsheeting is a key activity in process engineering and can be described as the calculation of all output information and some internal variables using all information from the inputs

[15]. The architecture of a flowsheeting software is determined by the strategy of computation. Three basic approaches have been developed over the years [16]:

- Sequential-Modular.
- Equation-Oriented.
- Simultaneous-Modular

In **Sequential-Modular (SM)** approach, the flowsheet model problem is partitioned into smaller (simpler) sub-problems (Figure 2.4) [17]. Problem decomposition is based on the structure (topology) of the flowsheet and is ideal for acyclic flowsheets (Figure 2.5.a).

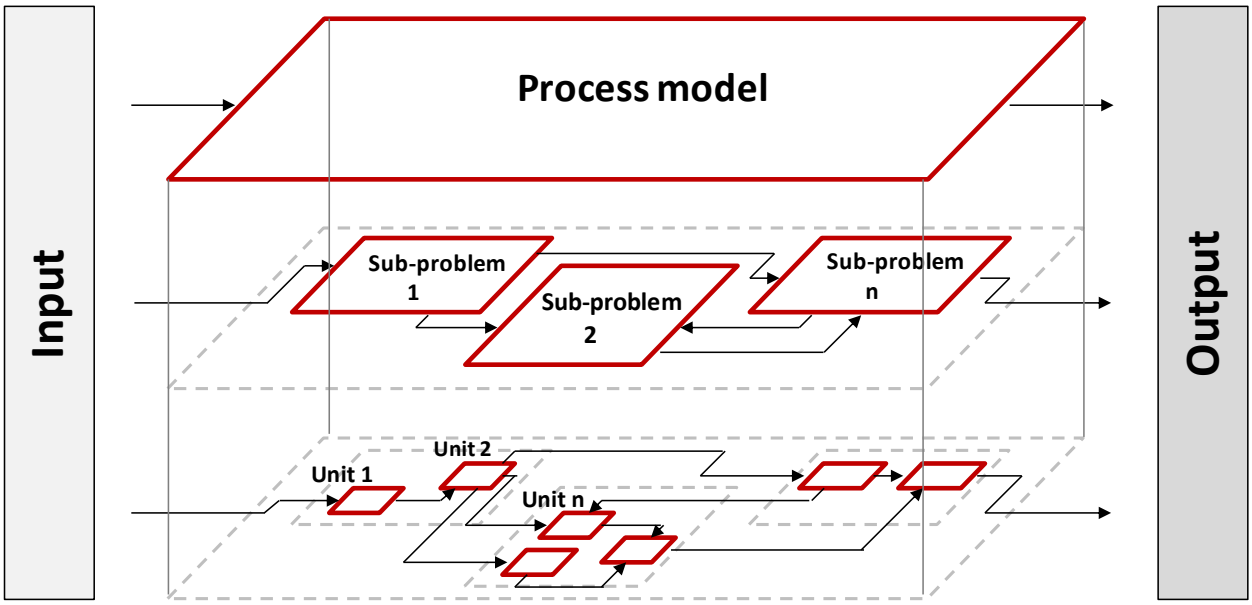

Figure 2.4 – Sequential-Modular architecture diagram (Adapted from [17]).

In acyclic systems, *i.e.*, without recycle streams (Figure 2.5.a), when the process feed streams and all the unit and operating parameters are known, the SM approach is relatively straightforward as the units are computed in a sequence where the output from one unit are the inputs for the next. In the example shown in Figure 2.5.a, given Stream 1, Unit A would be the first to be solved; Stream 2 would then be used to solve Unit B, and so on.

However, most processes involve recycles. Taking Figure 2.5.b as an example: Unit A could be directly solved with only the input information (Stream 1); Unit B cannot be solved unless both Streams 2 and 6 are known; conversely Unit C cannot be solved until Stream 3 is determined.

A possible approach to solve this problem is to apply a tearing algorithm: 1. Tear (guess) the stream in the recycle (Stream 6); 2. Perform a calculation pass through the flowsheet; 3. Evaluate the results by comparing the calculated with the estimated value; 4. If it did not converge, replace the tear value by the calculated value or by the average; 4. Iterate until convergence criteria are met.

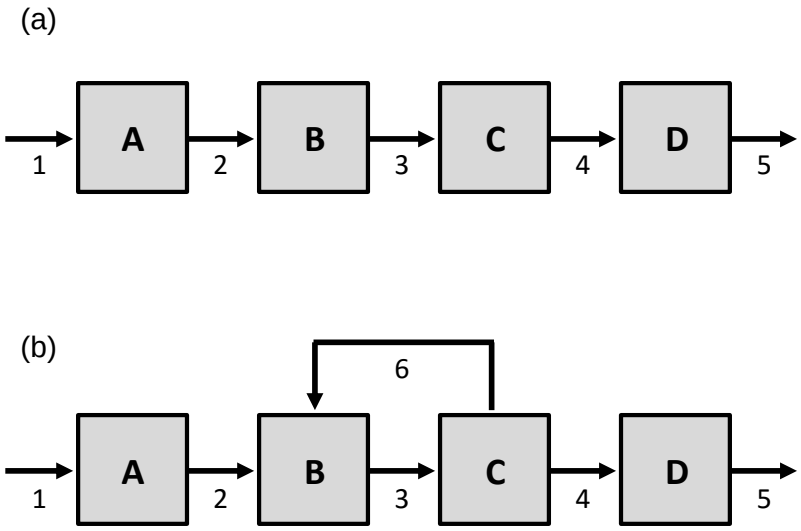

Figure 2.5 – Sequential modular approach (a) without recycle stream and (b) with recycle stream.

In **Equation-Oriented (EO)** approach, instead of tearing recycle streams and solving unit models in a modular fashion the simulator assembles all the equations describing a process model and attempts to solve them simultaneously.

Table 2.1 – Summary of characteristics of sequential-modular and equation-oriented architectures [15].

Sequential-modular	Equation-oriented
• Each unit operation is simulated sequentially	• All unit operations are simulated at once
• The flowsheet is decomposed	• The equations are sorted
• Iterative procedures using tear-streams	• All variables are updated at once
• Less flexible but more robust	• More flexible but less robust
• Initialization is important	• Initialization is very important
• Memory requirements are not very high	• Memory requirements may be very high

In **Simultaneous-Modular (SiM)** approach, the solution strategy is a combination of Sequential-Modular and Equation-Oriented approaches. Rigorous models are used at units' level, which are solved sequentially, while linear models are used at flowsheet level, solved globally. The linear models are updated based on results obtained with rigorous models. This architecture has been experimented in some academic products. It may be concluded that **SE** approach keeps a dominant position in steady state simulation. The **EO** approach has proved its potential in dynamic simulation, and real time optimisation. The solution for the future generations of flowsheeting software seems to be a fusion of these strategies [16].

2.2 Utility system analysis

Although sometimes regarded as a minor component of the manufacturing process, utilities are often as important as any other part of the technology as the savings achieved by an adequate design and operation of the utility system can frequently surpass the ones achieved when modifying the process.

In the petrochemical and refining industries, cooling water and steam are arguably the most used utilities for thermal energy distribution in the manufacturing processes [18] [19]. Water is often the preferred medium for energy transport not only due to its relatively low cost and abundance but also because it is a non-flammable and non-toxic resource .

The connection between the source/sink and the equipments that consume steam and cooling water is established by means of a more or less complex distribution network [20]. These systems are often not monitored and/or controlled, resulting in great material and energy waste. Modeling these systems can be achieved by using computer-based mathematical models, allowing engineers to monitor the performance of existent systems and create alternative operation scenarios.

While it is relatively common for process streams in chemical plants to have sufficient instrumentation, the utility systems that support production are often not well monitored. This can make it impossible to determine where unnecessary consumption or leaks are occurring. This work will provide essential information for identifying utility consumption and enable strategies to save energy and to improve efficiency.

To overcome the current high energy costs, refiners and petrochemical producers are looking for ways to improve their energy efficiency and reduce these unnecessary energy costs. Utility systems are characterized by a branched piping network, sending steam, air, water, electricity, etc. to and from the process units [21]. Often only the network's main headers and branches are instrumented, which leaves many areas unmonitored. This limited coverage may help calculate the overall consumption and identify the main suppliers' and consumers' performance, but it does not help close the material balance or identify possible leaks or wasted use. Engineers also do not have enough information to optimize the usage of these utilities across the site.

In regard to the systems optimization, although several different methods for energy systems analysis are available, often they can only be applied when designing a heat recovery network without any plant layout considerations. It is, however, not very often that new plants are built; instead, retrofitting of existing processes is carried out. The extreme case would be to remove all existing equipment and build a new optimized process from scratch, but this would result into significant capital waste. When retrofitting a system, already installed equipment must be taken into account as it represents sunken capital. On the other hand, the thermal and hydraulic impact that any modification has on the rest of the network must be carefully analyzed.

2.2.1 Cooling water system

The cooling water system in an industrial facility that usually comprises the cooling tower and the cooling water network. The cooling tower is responsible for rejecting waste energy to the environment by means of evaporative cooling. The cooling water network is essentially a heat exchanger network that is used for removing waste heat from the process.

2.2.1.1 *Cooling towers*

Cooling towers are widely employed in many industrial applications for rejecting waste heat from the process to the environment. The principle behind a cooling tower operation is evaporative cooling which, in theory, would allow circulating water to equal ambient air wet-bulb temperature. Evaporative cooling is a process with simultaneous mass and heat transfer between air and circulating water.

There are several methods and strategies related to the modeling of cooling towers with different levels of complexity. According to Jin *et al.* [22], the first theoretical analysis of cooling towers was performed by Dr. Fredrick Merkel in 1925. He proposed a theory relating evaporation and sensible heat transfer where there is counter flow contact of water and air. As described by Benton *et al.* [23], Merkel expressed the number of transfer units (NTU) as a function of the integral of the water temperature difference divided by the enthalpy gradient where, to reduce the governing relationships to a single separable ordinary differential equation, several simplifying assumptions were made: Merkel assumed that the Lewis factor, relating heat and mass transfer was equal to 1; the air exiting the tower was saturated with water vapor; and the reduction of water flow rate by evaporation was neglected in the energy balance.

Kloppers and Kröger [24] evaluated three methods used in cooling tower design, namely, Merkel, Poppe and effectiveness-NTU and gave a detailed derivation of the heat and mass-transfer equations of evaporative cooling in cooling towers. Based on Merkel equation, Picardo and Variyar [25] presented a power law that related packed height with excess air and determined equation parameters for air wet-bulb temperature between 10–34 ºC and cooling range between 40–20 ºC. They also showed that beyond a certain air flow the reduction in packed height does not justify the increase in energy utilization for air compression.

Castro *et al.* [26] developed an optimization model for a cooling water system composed of a counter flow tower and five heat exchangers where the thermal and hydraulic interactions in the overall process were considered. They observed that forced withdrawal of water upstream of the tower is an important resource for fulfilling cooling duty requirements. Khan *et al*. [27] presented a fouling growth model where it was demonstrated that the effectiveness of a cooling tower degrades significantly with time, indicating that for a low fouling risk level (p = 0.01), which is the probability of fill surface being fouled up to a critical level after which a cleaning is needed, there is about 6.0% decrease in effectiveness. Al-Waked and Behnia [28] applied computational fluid dynamics (CFD) for natural draft wet cooling tower. The difference between outlet air temperature predicted by the CFD model and design results was less than 3%. Jin *et al.* [22] proposed a model based on heat resistance and energy balance principles where empirical parameters were introduced, avoiding the need to specify geometrical parameters. Rubio-Castro *et al.* [29] determined

optimal cooling tower design parameters and temperature profiles across a counter flow cooling tower by applying a rigorous heat and mass transfer model. Nonlinear algebraic equations were solved using a discretization approach with a fourth-order Runge-Kutta algorithm. Given a set of experimental data to train the model, Hosoz *et al.* [30] suggested that applying artificial neural networks (ANN) for modeling the cooling tower performance avoided the solution of complex differential equations. Predicted and experimental values had correlation coefficients in the range of 0.975–0.994 and mean relative errors in the range of 0.89–4.64%. Pan *et al* [31] presented a data-driven model-based assessment strategy to investigate the performance of an industrial cooling tower. Considering one month test interval and based on water mass flow rate, water inlet temperature, air dry-bulb temperature, relative humidity and fan motor power consumption the predicted water outlet temperature was within a ±5% error band and presented a mean square error of 0.29 ºC. Serna-González *et al.* [32] used mixed-integer nonlinear programming (MINLP) techniques to evaluate the optimal conditions of a mechanical draft cooling tower that minimize the total annual cost for a given heat load, dry- and wet-bulb inlet air temperatures and temperature constraints on the cooling water network. Rao and Patel [33] compared the results obtained by Serna-González *et al.* [32] with the ones achieved when applying an artificial bee colony algorithm. Using the artificial bee colony algorithm resulted in an objective function value lower than the one achieved by Serna-González *et al.* [32] for all six case studies (improvement between 1.27% and 11.17%).

Xiaoni *et al.* [34] studied and developed a mathematical model of a seawater shower cooling tower and although the cooling performance decreases with increased salinity and is not as high as when compared to “freshwater” cooling towers, seawater is more readily available than freshwater in important chemical clusters around the world. On another study that uses seawater as a cooling medium, Sadafi *et al.* [35] investigated the spray nozzle configuration and established a dimensionless correlation to predict the distance from the nozzle after which the dry stream starts (wet length) and cooling efficiency.

As an alternative to the abovementioned methodologies, a different approach that does not involve the solution of differential equations can be used to model a cooling tower operation by applying an equilibrium stage. While the equilibrium stage method can hardly be used for design purposes without proper correlations that allow the determination of the height equivalent to a theoretical plate (HETP), it is demonstrated in this work that both the outlet water and air temperature predicted by the model are quite accurate when compared to the experimental values.

2.2.1.2 ***Cooling Water networks***

Cooling water networks have been studied in the past due to their importance in most industrial processes. The structure of a cooling water network influences the operation of the cooling tower as cooling water flow and cooling tower inlet temperature are variables that directly impact on the cooling tower performance. Thus, optimizing the cooling water network allows designing a cooling water network that eventually leads to requiring a lower capacity cooling tower, involving a lower capital investment. This can be of paramount importance in grassroot design or when retrofitting an existent plant with limited cooling tower capacity.

Kim and Smith [19] developed a methodology based on pinch technology that provided design guidelines for cooling water system design. In retrofitting situations, they concluded that better design of the cooling network, increasing cooling tower blowdown, taking hot blowdown and strategic use of air coolers, could be used to avoid investment in new cooling tower capacity.

Ponce-Ortega *et al.* [36] presented a mixed-integer nonlinear programming (MINLP) algorithm for the synthesis of cooling networks. The strategy was based on a superstructure that allowed a combination of arrangements in series and in parallel, considering simultaneously the capital cost for the coolers and the utility costs.

Gololo and Majozi [37] study focused mainly on cooling systems consisting of multiple cooling towers that supplied a common set of heat exchangers. The heat exchanger network was synthesized based on a mathematical optimization technique that defined a superstructure in which all opportunities for cooling water reuse were explored. They applied the proposed methodology to two case studies, rendering MINLP and NLP problems, depending on whether a cooling tower could supply only a dedicated set of coolers, MILNP problem, or could supply any coolers of the network, NLP problem.

A two-step methodology for the optimization of a cooling water network was developed by Sun *et al.* [38]. The first step of the methodology was to use a thermodynamic model to obtain an optimal cooler network and a second step, where the hydraulic model was established to obtain the optimal pump network with auxiliary pumps installed in parallel branch pipes. The authors identified savings of up to 23.3% of the cooler network cost and 11% of the pump network cost.

A numerical hydraulic model of a cooling water system in EPANET was built by Georgescu *et al.* [39]. Since EPANET does not have the possibility to insert some equipment into the network such as heat exchangers they used throttle valves with adjusted loss coefficients to simulate these equipments and account for their pressure drop. They adjusted the model with pressure loss measurements and concluded that the resulting model fitted field data.

The approach suggested in this work resulted from a combination of the cooling water hydraulic model, to determine the cooling water flow on each point of the network, and the thermodynamic model, to calculate the cooling water temperature on each point. The models allow a precise simulation of the cooling water network and serve as a basis for performing modification studies on the cooling water heat exchanger network.

2.2.2 Steam system

Steam is widely used within the chemical industry as medium to distribute thermal energy across the various process units. A steam system comprises steam generators where energy from any given source is transferred to water and steam is generated. Although the energy required to generate steam can be supplied by a variety of sources, such as an electric current passing through a resistance, solar and

geothermic energy, etc., within the chemical industry the energy is commonly provided either by burning fuel or cooling down a process stream.

The steam generated in the steam generator is then fed to a network where it is distributed to the various consumers. It is not uncommon to have a network where steam is distributed at different pressure and temperature levels. Steam is then either injected directly into the process or condensed in heat exchangers. Condensates can then be flashed to generate steam at a lower pressure or return to the steam generator.

2.2.2.1 *Steam generator*

As mentioned above, steam can be generated from various sources, being that the most common in process industries is that the energy is provided by either burning fuel or cooling down a process stream.

Fired steam boilers are used to produce steam by using the energy released by fuel combustion. Several parameters influence boiler efficiency and can therefore be optimized. These parameters are discussed elsewhere in Section 3.2, where a detailed analysis of boilers performance is presented.

Artificial neural networks (ANN) were applied by Kljajic *et al.* [40] to forecast the performance of fired boilers. They stated that the most influential parameters on boiler efficiency were oxygen content in flue gas, boiler maximum capacity and boiler load. Behera *et al.* [41] also used ANN to predict the performance of a refuse plastic fuel (RPF) boiler. Based on feed water pressure, feed water temperature, fuel conveyor speed, and incinerator exit temperature they were able to estimate the steam temperature, pressure, and mass flow rate. A different work developed by Strušnik *et al.* [42] where ANN were applied to develop a model that predicts the power production of a power plant and distributes the production between the boilers so that the latter operate at their highest efficiency.

Andreassen and Olsen [43] used mathematical optimization tools to solve a load allocation problem with minimum cost as the objective function. Given a certain steam demand in a plant with more than one boiler supplying the steam network, the method allowed the optimum load allocation to each boiler so that the operating cost was minimal. They applied the methodology to a paper mill case study where it was demonstrated that the optimum load optimization strategy gave tangible savings when compared to the equal load distribution strategy.

A study where an algorithm based on a second-order gradient search method that optimize the allocation of multiple industrial boilers consuming single or multiple fuel types was presented by Dunn and Du [44]. They showed through a variety of practical examples that the proposed methodology was capable of producing more favorable results in terms of operating costs than the base case scenario.

To support fuel management decisions in the steam production system of industrial boilers Rocco and Morabito [45] proposed a MILP model. The model covers variables such as fuel replenishment and its inventory control), boiler operational decisions (start-up, warm-up, and shutdown operations) and which boiler should produce steam.

Differently from the abovementioned approaches this work describes a methodology for optimizing the boiler load in a multi-boiler steam system. The load allocation of each boiler depends on the thermal efficiency of the boiler and plant demand.

2.2.2.2 ***Steam network***

The steam network consists on the distribution network of steam supply to the various users and the subsequent return of condensates to the steam generator. In large industrial plants steam is usually distributed at different pressure and temperature levels.

A mathematical approach for retrofit and optimization of total site steam distribution networks was developed by Chen *et al.* [46]. The MILNP formulation rendered a model where retrofit solutions of an inter-plant steam network were effectively achieved. They investigated the operational optimization of existing units, installation of new turbines, replacement of low-efficiency boilers and turbines and use of steam ejectors to upgrade a low pressure steam current to a level where it could be used in the plant.

Majane [47] presented a Model Predictive Control method (MPC) for pressure control of steam systems. A power plant simulator controlled by MPC helps to decide the location and the capacity of steam levelling components needed to stabilize the operation of the process.

Process integration techniques were used by Coetzee and Majozi [48] to study the steam system network synthesis. Their approach consisted on a hybrid method that combined pinch technology and mathematical optimization that minimized the steam flow. This was achieved by placing heat exchangers in series instead of the typical parallel configuration. By placing the heat exchangers in series it allows hot condensates to heat cold streams instead of using always steam.

Zhong *et al.* [49] proposed a hydraulic model of a steam network that took into consideration heat dissipation in pipes. The authors used the software HEATNET to build the simulation and introduced a control strategy to avoid steam stagnation by optimizing the heat load distribution.

In this work, a methodology for building a thermodynamic model of the steam network in ASPEN PLUS is described. This methodology describes the implementation of a model of the steam network that can then be used as a basis for optimization studies and for the evaluation of the impacts that any modification has on the overall balance of the steam network.

2.3 Retrofit heat exchanger networks

With the formalization of the pinch point concept by Umeda *et al.* [50] and Linnhoff and Flower [10, 11] in the late 1970's, it was possible to quantify the maximum recoverable heat and the minimum utilities requirement. The "best" heat exchanger network design that allows these targets to be met is yet another

problematic point as there is a trade-off between energy, heat transfer area and number of heat transfer units, as pictorially shown in Figure 2.1.

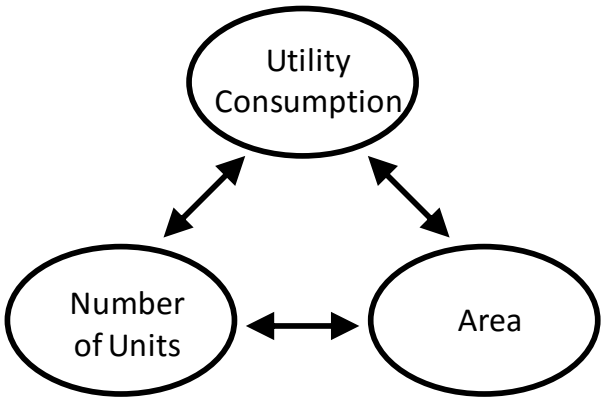

Figure 2.6 – Trade-offs in heat exchanger network design (Adapted from Yee and Grossman [51]).

Ever since the first developments in the heat exchanger network synthesis introduced by Linnhoff *et al.* in 1978 [9-11], several new extensions were introduced, incorporating existent and new methodologies into other process synthesis problems such as heat exchanger network retrofit.

According to Nordman [52], early approaches were mainly based on synthesis methods that were originally aimed for grass-root design. The retrofit methodologies usually consisted on generating grass-root designs and then selecting the design closest to the existing one for further development.

Retrofit methodologies can be clustered into pinch analysis methods, mathematical programming or a combination of both:

Pinch analysis methods use pinch analysis to solve retrofit problems. They employ the typical pinch tools such as composite curves, grand composite curves, etc., to retrofit heat exchanger networks. The retrofit process based on pinch methodologies rely on a strong user interaction. Although this can be an advantage in some cases, it can be very time consuming. Additionally, because heuristics play a major role during the process, the end result is strongly dependent on the user's experience and good judgment.

Mathematical programming methods comprise the solution of a mathematical model formulation using optimization methods. Considering network topology modifications such as stream splits, heat exchanger relocation or new exchanger as being subject to optimization renders a Mixed Integer problem. Moreover, the area equations that use the Log Mean Temperature difference (LMTD) are intrinsically non-linear. Thus, due to the aforementioned reasons, HEN retrofit is by nature formulated as Mixed Integer Non-Linear Programming (MINLP) problem. To overcome the inherent complexity of the MINLP problem, the formulation is usually simplified as Mixed Integer Linear Programming (MILP), Non-Linear Programming (NLP) or Linear Programming (LP) by making some assumptions and step-wise manipulation. As an alternative to deterministic methods that are often trapped at a local optimum, stochastic methods such as simulated annealing algorithms and genetic algorithms, are also employed [53]. As stated on the review of heat exchanger retrofit methodologies presented by Sreepathi and Rangaiah [54], mathematical

programming based methods are popular in academia but much less so in industrial practice due to the difficulty of setting up the problem models, particularly for practitioners.

Hybrid methods are the methods that make use of both pinch analysis and mathematical programming in an effort to combine the strengths of both. They allow user interaction and can also be applied to large problems.

2.3.1 Pinch analysis

As previously mentioned, pinch analysis was conceived greatly due to the contributions of Linnhoff and his co-workers at the Leeds University [9-11] in the late 1970's, with Imperial Chemical Industries (ICI) pioneering in the use of this technology [55]. Although pinch analysis was initially targeted for energy optimization applications, the concept was successfully translated to other fields such as wastewater minimization and other mass exchange networks and hydrogen pinch [56-58].

The objective of applying pinch analysis is to reduce the consumption of a given resource through process integration, usually thermal energy. It can be used during the design phase, where the heat exchanger network is configured so that the hot and cold utility consumption is minimized, or to retrofit existent units, which is achieved by evaluating how efficiently a resource is being used and what actions should be taken to close the gap between current consumption and the minimum consumption targets. The targets given by pinch analysis are conceptual and can hardly be achieved in a complex industrial process. Nonetheless, they set the goal for external resource consumption, giving an important incentive to find a network that is as close to this values as possible.

Kemp [55] summarized three different approaches for heat exchanger network retrofit using pinch analysis:

1. Develop a Minimum Energy Requirement (MER) heat exchanger network design as for a new plant but, where an option exists, select matches which already exist in the current network. This was the approach used in the earliest pinch studies;

2. Start with the existing network and work towards a MER design. Take the current ΔT_{min} and calculate the targets and the pinch temperature. The existing exchangers, heaters and coolers are plotted on the grid diagram and the pinch violators are identified. Finally, alternative configurations that add new matches which correct these problems are identified. This approach was described by Tjoe and Linnhoff [59];

3. Start with the existing network and identify the most critical changes required in the network structure to give a substantial energy reduction. This method will be appropriate if the MER design is so different in configuration from the existing layout that they are virtually incompatible.

Tjoe and Linnhoff [59] presented the first application of pinch tools to heat exchanger network retrofit, developing the concept of area efficiency in heat exchanger networks, α. Area efficiency is the ratio between the area of an existent network and, assuming the same energy consumption as the existing network, the area that would be required if the network was designed so that there was no crisscross heat transfer, *i.e.*, only vertical heat transfer was allowed . The method assumes that the area efficiency of the retrofit HEN is equal to that of the existing network, and this assumption is used to set targets for design [60].

The Cost Matrix approach presented by Carlsson *et al.* [61] takes into account the cost of structural changes implemented in the retrofit design, but it depends on accurate piping and other cost data for each potential match. According to Asante *et al.* [62], this methodology can be impractical in some cases, stating that considerable effort would is required to generate the necessary data for a moderately sized industrial process.

2.3.1.1 *Pinch concepts*

Within a process, there are some streams that need to be cooled down and others heated up. A stream that is at a given temperature and is heated up is defined as being a **cold stream,** whereas a stream that is cooled down is defined as a **hot stream**.

Heat can be supplied or removed from the process through the use of external utilities. They can be **hot utilities** (*e.g.* steam, hot oil, combustion gases) or **cold utilities** (*e.g.* cooling water, air, refrigeration fluid).

It was previously mentioned that pinch analysis produced a set of **energy targets**. This is in fact an important concept in pinch analysis. These targets refer to the thermodynamic targets that the process would meet if it was perfectly integrated. There are three important targets given by the heat pinch analysis: cold utility; hot utility and cross-exchange targets. The aim of the pinch engineer is then to identify the best network configuration that enables the process to move closer to these targets.

Another key concept of pinch analysis is the one of **pinch point**, often referred simply as “pinch”. This concept relates to the most constrained region of a heat exchanging network, *i.e.*, nowhere else than at this point does the minimum approach, ΔT_{min}, occurs [9]. Once the pinch point has been identified, it is possible to consider the process as two separate systems: one above and one below the pinch.

Based on the concepts described above, for a process to achieve minimum energy targets, pinch methodology states that three fundamental rules must be obeyed:

1. Heat must not be transferred across the pinch;
2. There must be no external cooling above the pinch;
3. There must be no external heating below the pinch.

2.3.1.2 *Temperature – Enthalpy representation*

The T-Q diagram is very useful in the pinch analysis methodology as it provides a visual representation of the streams' energy and temperature variation.

A variable described as the heat capacity flow rate, *CP* ($kW \cdot ºC^{-1}$), is introduced. This variable is considered as constant for each stream and is given by Equation (2.1), which is the product between the mass flow rate, *M* ($kg \cdot s^{-1}$), and the specific heat capacity at constant pressure C_p ($kJ \cdot kg^{-1} \cdot ºC^{-1}$).

$$CP = M \times C_p \quad \textbf{(2.1)}$$

The term "enthalpy", *Q* (kW), refers to the differential heat flow between the stream inlet and outlet stream conditions. It is given by Equation (2.2), which is the product between MC_p and the difference between the inlet, T_{in} (ºC), and outlet, T_{out} (ºC), temperatures.

$$Q = CP(T_{out} - T_{in}) \quad \textbf{(2.2)}$$

In a T-Q plot where temperature, *T*, is in the vertical axis and enthalpy, *Q*, the horizontal axis. Since enthalpy is a property that results from the difference between two thermodynamic states, the line segment can be drawn anywhere in the enthalpy axis as long as each stream is represented by a line segment with slope MC_p, that starts on T_{in} and finishes on T_{out}.

For two streams to cross-exchange there must be a temperature drive between the two and the hot stream must be hotter than the cold stream. So, in the T-Q plot, the hot stream must at all times be above the cold stream at a distance of at least ΔT_{min}.

In Figure 2.7, an example of a countercurrent heat exchanger is shown. A hot stream enters the heat exchanger at T_{Hin} with a target temperature of T_{Hout} and the cold stream enters the heat exchanger at T_{Cin} with a target temperature of T_{Cout}. Heat recovery reaches its maximum when the approach between the hot outlet and the cold inlet temperature is equal to ΔT_{min}. If this temperature approach was to be increased to $\Delta T > \Delta T_{min}$, the curves would be shifted (dashed line in Figure 2.7) and external utilities would be required.

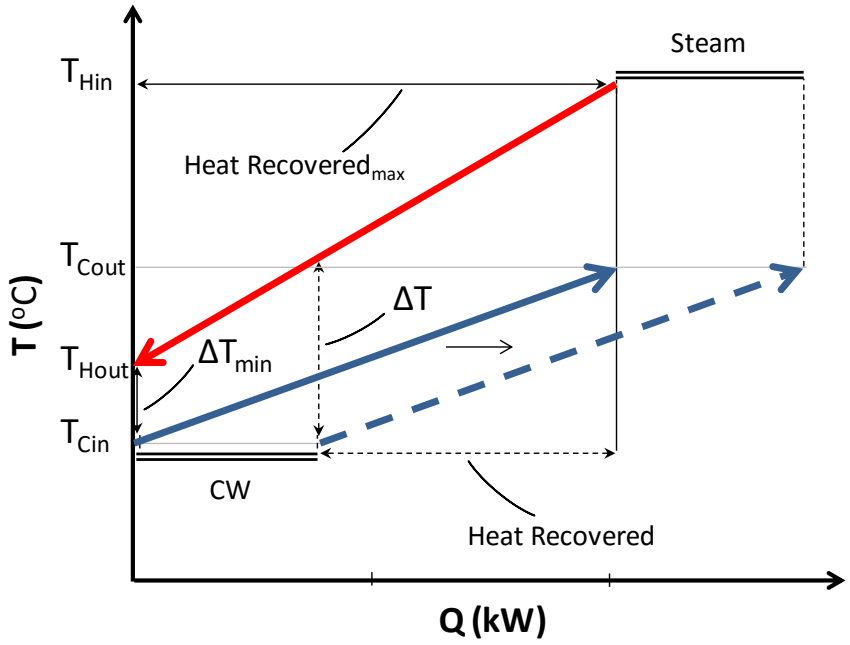

Figure 2.7 – Temperature-Enthalpy profile of a countercurrent heat exchanger.

2.3.1.3 *Composite curves*

In Figure 2.7, only two streams are represented but at an industrial level multiple streams are involved. To plot a T-Q that takes into account several streams, the concept of **composite curves** is introduced. The curve representing the available heat, or the hot streams, is referred to as the "hot composite curve" whereas the heat demand, or the cold streams, is the "cold composite curve".

To exemplify the construction of a composite curve, two hot streams are considered. In Figure 2.8, these streams are represented in a T-Q plot. Stream 1 has a MC_p of 50 kW·ºC^{-1}, and is cooled from 120 °C to 40 °C, releasing 4000 kW. Stream 2 is cooled from 160 °C to 80 °C with a MC_p of 25 kW·ºC^{-1} and releases 2000 kW.

Taking the example streams described above and the T-Q plot in Figure 2.7, it is possible to identify three distinct horizontal regions: One where only stream 1 exists, other where stream 1 and 2 coexist and another one where only stream 2 exists.

For plotting the hot composite curve, shown in Figure 2.9, the following procedure was applied:

- Between T^1_{out} and T^2_{out} only stream 1 exists, so the available heat is given by $MC_p{}^1(T^2_{out} - T^1_{out})$;
- Between T^2_{out} and T^1_{in} both streams 1 and coexist, so the available heat is given by $(MC_p{}^1+MC_p{}^2)\cdot(T^1_{in} - T^2_{out})$;
- Between T^2_{in} and T^1_{in}, only stream 2 exists, so the available heat is given by $MC_p{}^2(T^2_{in} - T^1_{in})$;

A similar procedure is followed to generate the cold composite curve.

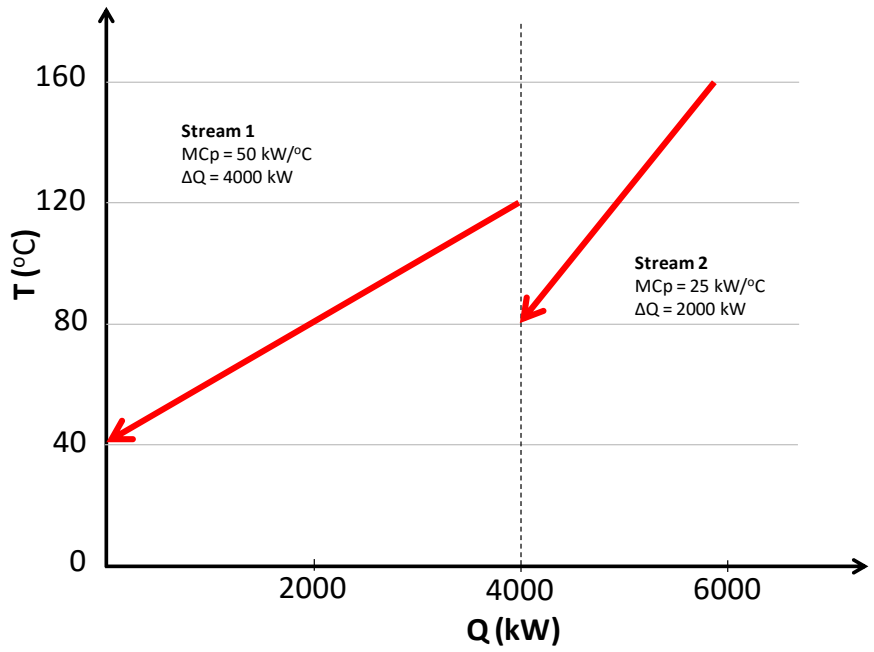

Figure 2.8 – Two hot streams represented in the T-Q plot.

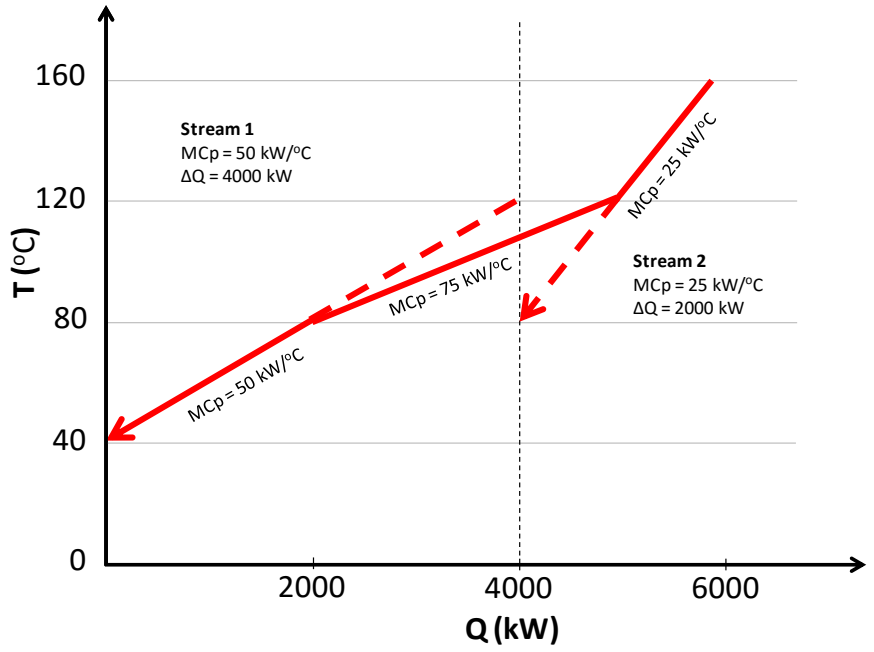

Figure 2.9 – Stream 1 and 2 combined in one single composite curve.

In Figure 2.10, hot and cold composite curves are combined in the same T-Q plot. This is achieved by positioning the left edge of the hot composite curve at $Q = 0$ and shifting the cold composite curve until the gap between the two curves equals ΔT_{min}.

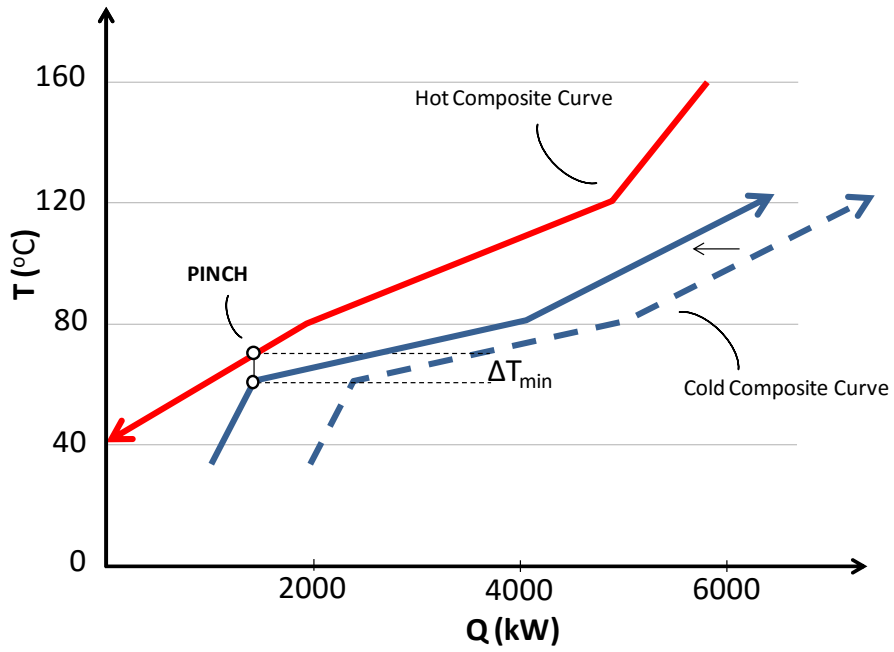

Figure 2.10 – Hot and cold composite curves in the same T-Q plot.

By combining the hot and cold composite curves in a single T-Q plot it is possible to determine the amount of heat recovered as well as the external utilities requirements. In Figure 2.11, the shaded area where the hot and cold composite curves coexist correspond to the total recoverable heat whereas the region where only the hot and cold curves exist correspond to the external cold and hot utility requirements, respectively.

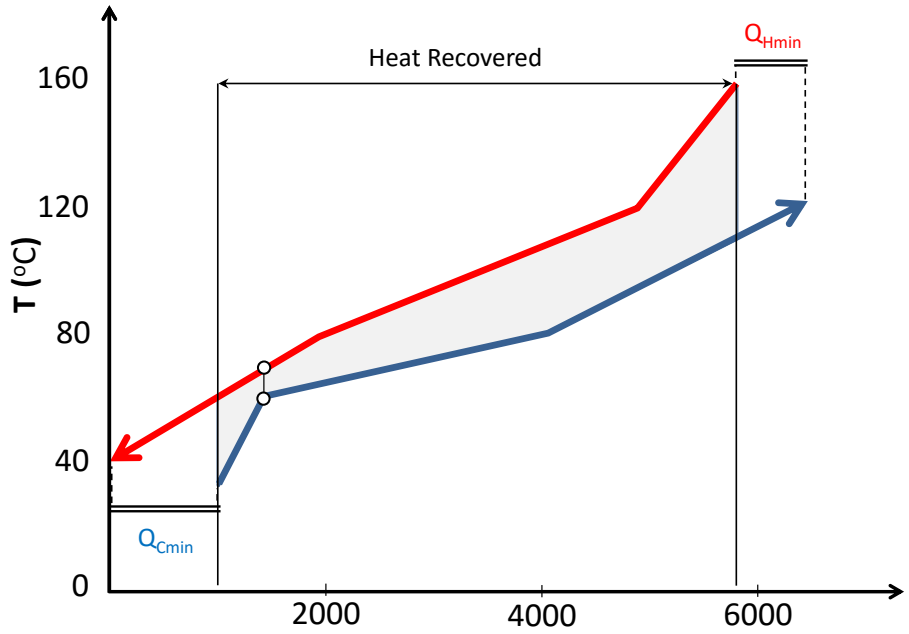

Figure 2.11 – Energy targets given by the combined composite curves.

2.3.1.4 *Grand Composite Curve (GCC)*

In most processes, heating and cooling are performed by using different utility levels (*e.g.* different steam levels, hot oil, cooling water, air, refrigeration). Since lower level utilities (closer to ambient conditions) are cheaper than higher level utilities (*e.g.* cooling water is cheaper than refrigeration), consumption of higher level utilities should be minimized by using lower level utilities, wherever it is viable.

Although composite curves are useful to determine the overall energy targets, they are hardly the best tool for identifying multiple utility targets. Conversely, The Grand Composite Curve (GCC) is a very convenient tool for setting the targets for the multiple utility levels.

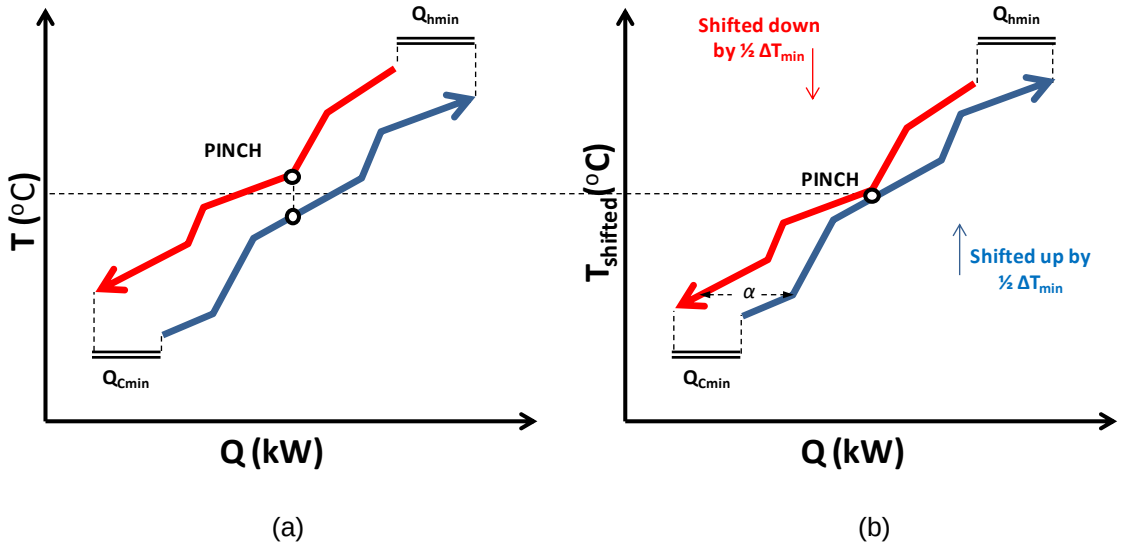

Figure 2.12 – Composite curve shifting.

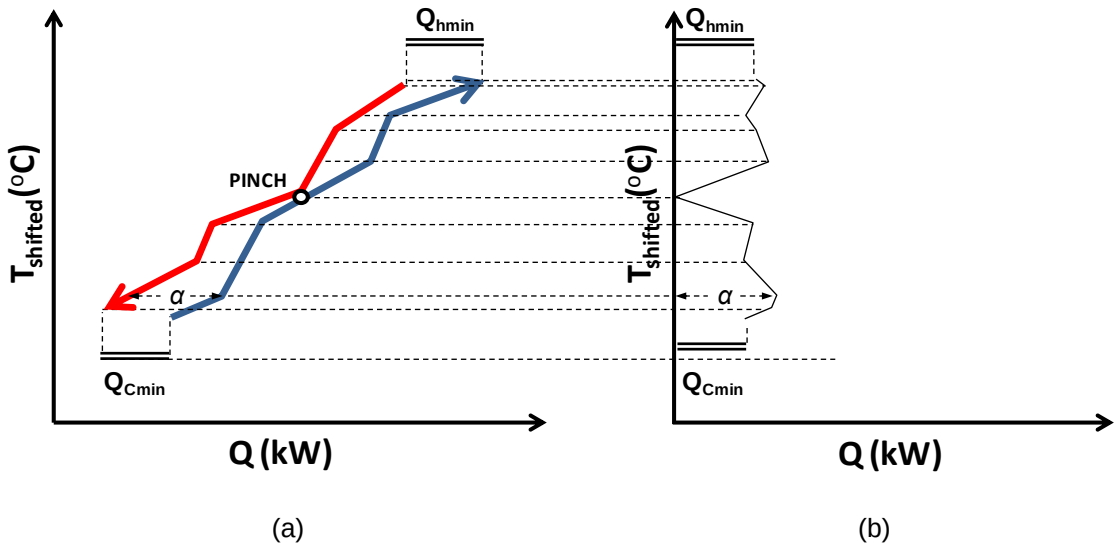

Figure 2.13 – Construction of the grand composite curve.

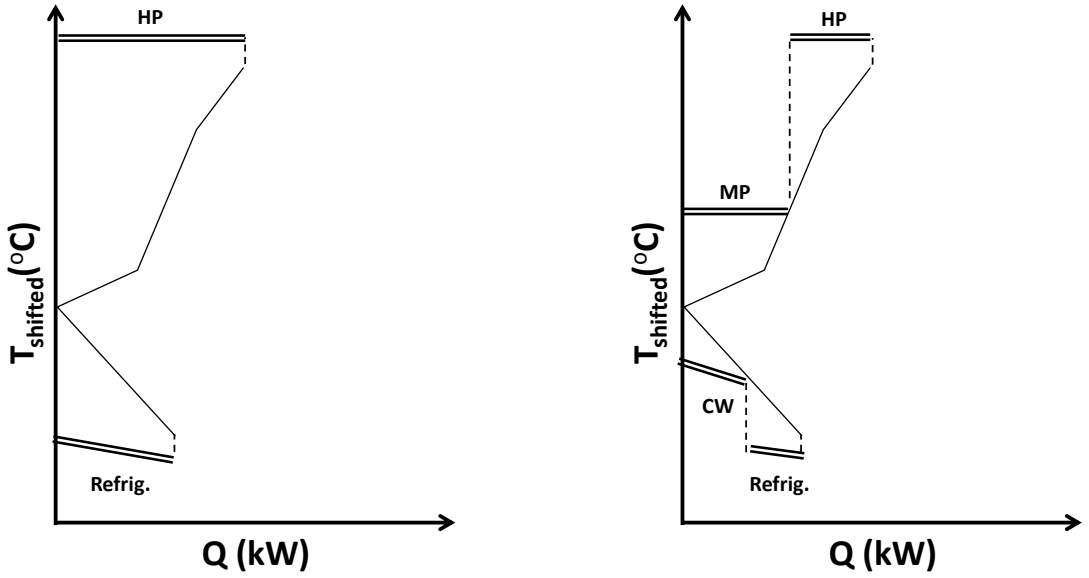

(a) (b)

Figure 2.14 – Grand Composite Curve used to determine utility targets in (a) a process with only two utility levels and (b) a process with multiple utilities levels.

Figure 2.15.a shows an example of perfectly integrated process *i.e.*, no heat transferred across the pinch and no cooling or heating above and below the pinch, respectively, as stated by the pinch rules.

In Figure 2.15.b, α amount of heat is transferred from above the pinch to below the pinch. The system above the pinch, which was before in heat balance with Q_{Hmin}, now loses α units of heat to the system below the pinch. To restore the heat balance, the hot utility must be increased by the same amount, that is, α units. Below the pinch, α units of heat are added to the system that had an excess of heat, therefore the cold utility requirement also increases by α units. In conclusion, the consequence of a cross-pinch heat transfer (α) is that both the hot and cold utility will increase by the cross-pinch duty (α).

Figure 2.15.c also shows γ amount of external cooling above the pinch and β amount of external heating below the pinch. The external cooling above the pinch of γ amount increases the hot utility demand by the same amount. Therefore, on an overall basis both the hot and cold utilities are increased by γ amount. Similarly, external heating below the pinch of β amount increases the overall hot and cold utility requirement by the same amount (*i.e.* β).

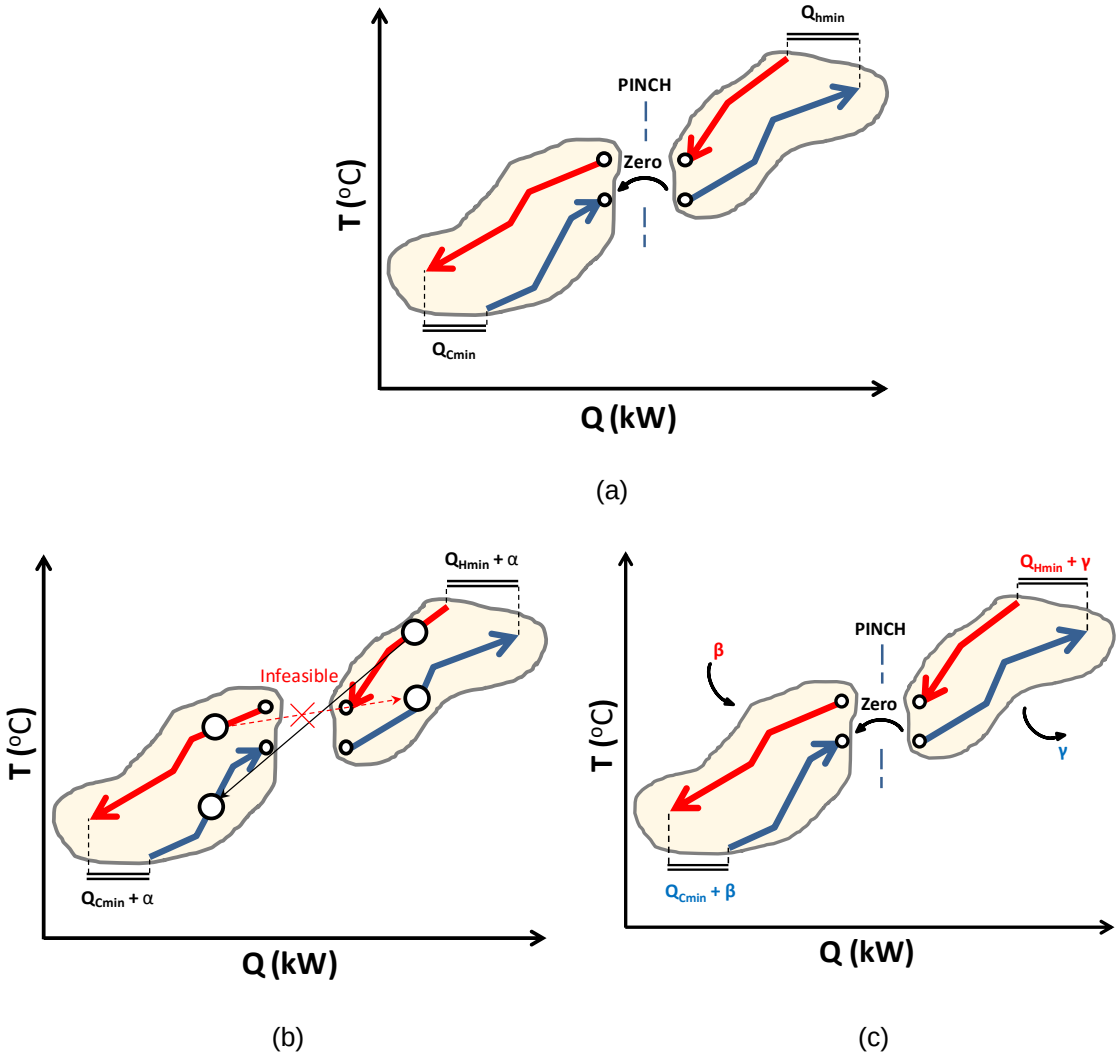

Figure 2.15 – Hot and cold composite curves for: (a) a process with minimum energy requirements, (b) a process where α amount of heat is transferred across the pinch and (c) a process with γ amount of external cooling and β amount of external heating above and below the pinch, respectively.

2.3.2 Mathematical programming

Cerda *et al.* [63] formulated an algorithm as a "transportation" problem, a well-known problem for which efficient algorithms exist, that allowed the minimum utility calculation for a heat exchanger network synthesis. In order to find the smallest number of matches in the process, a MILP model was relaxed into a linear programming "transportation" problem and solved. Later, Cerda and Westerberg [64] extended their work by formulating an algorithm that allowed the user to impose constraints disallowing the matching of stream pairs.

Papoulias and Grossman [65] proposed a similar approach by formulating a MILP problem based on "transshipment" models, being a considerably smaller variation of the "transportation" model, which was used for deriving network configurations. The minimum number of matches that should take place in the network is determined by means of the "transshipment" model involving the solution of a MILP, by means of a branch-and-bound method. The heat exchanger network configuration is not obtained directly from the

solution of the MILP “transshipment” model, but it contains all necessary information to derive the network by hand.

Barbaro and Bagajewicz [66] developed a Heat Integration Transportation (HIT) model for grassroots design, which was then extended to perform retrofit studies by Nguyen [67]. The retrofit methodology used a one-step MILP formulation that accounted for costs associated with addition and reduction of area, addition and relocation of heat exchangers and repiping. This study also showed modifications to the one-step formulation that gave some room for user interface, allowing users to allow/disallow stream splitting and heat exchanger relocation, limiting the number of new exchangers and relocations, etc. Later, Bagajewicz *et al.* [60] compared the utilization of pinch technology using the three-step procedure (targeting, design and evolution) and the reported HIT model in a crude unit pre-heating. They concluded that the solutions retrieved by HIT model had a higher Net Present Value (NPV) when compared with the solutions given by the pinch methodology.

Wang *et al.* [68] used a mathematical optimization method based on simulated annealing that incorporated the option of retrofitting the heat exchangers through Heat Transfer Enhancement (HTE) such as applying internal fins, twisted-tape inserts, coiled wire inserts or hiTran [69] for the tube side and/or applying helical baffles and external fins for the shell side. These technologies effectively change fluid flow characteristics, allowing a more efficient heat transfer between hot and cold streams. Enhanced heat exchangers require less heat transfer area for a given heat duty because of higher heat-transfer coefficients [70]. Pan *et al.* [71] detail in their study different intensified heat transfer techniques.

Becker and Maréchal [72] recently introduced a method to integrate industrial heat exchanger networks with restrictions between process sub-systems but where heat could be transferred indirectly through an intermediate heat transfer system. They formulated the problem as MILP problem so that the energy penalties introduced by the forbidden matches could be reduced by ensuring feasible solutions through the inclusion of intermediate heat transfer systems. However, this methodology cannot be applied when it is not possible to decompose the process into separate sub-systems.

2.3.3 Hybrid methods

Asante *et al.* [62] developed a methodology that combined pinch and mathematical optimization approaches, introducing the concept of network pinch and generating an automated and interactive methodology for heat exchanger retrofit. It consisted of two steps, the diagnosis stage and the optimization stage.

The diagnosis stage is used to identify and select optimal topology modifications to be made, combining the concepts of pinching matches and network pinch with mathematical programming techniques, resulting in a set of MILP problems.

For the optimization stage, the topology defined during the diagnosis stage is optimized with mathematical programming techniques, manipulating heat recovery and exchanger area using cost minimization as the optimization objective.

3 Utility system analysis

This chapter presents the modeling and evaluation of the cooling water and steam systems of the case study plant. By using the methodology described in this chapter it is possible to evaluate the performance of the current network as well as providing a tool for evaluating any plant modification that impacts on the utility systems.

The cooling water system described in this chapter is composed by the cooling water network, where waste heat of the process is throw out to the cooling water, and the cooling tower, where the heat is dissipated to the environment. For determining the flow on each heat exchanger a hydraulic model was implemented and for determining the temperatures on each point of the network as well as the behavior of the cooling tower a thermodynamic model was implemented.

3.1 Cooling water system

To determine the flow on each point of the cooling water network a hydraulic model was implemented. Then, to simulate the cooling water system thermodynamic behavior, a methodology for modeling with ASPEN PLUS an existent cooling tower and the cooling water network is presented. Finally, the performance of the cooling water system is evaluated.

3.1.1 Hydraulic model of cooling water network

The cooling water network consists on all the heat exchangers where cooling water is used to remove heat from the process. Cooling water then goes through the cooling tower, where waste heat is rejected to the environment.

Cooling tower performance depends on several parameters, where both inlet water temperature and flow are two important variables. On the other hand, they depend on the cooling water network configuration and duty. As a result, two approaches were considered for modeling the cooling water network and are presented as follows: Hydraulic simulation and thermodynamic simulation.

While hydraulic simulation provided with an estimate for the flow of cooling water going through each heat exchanger, thermodynamic simulation was used to determine the temperature on each point of the network. The inputs for the models were the network configuration together with each heat exchanger heat duty and cooling tower performance.

The Estarreja MDI plant cooling water network has a parallel arrangement, *i.e.*, fresh cooling water passes through each heat exchanger only once before returning to the cooling tower. After being cooled down in

the cooling tower, cooling water goes through three parallel pumps that feed a main supply duct. Heat exchangers are located between the supply and return ducts so that cooling water flows between them.

For the hydraulic simulation of the Estarreja MDI plant the SiNET software [73] was used. SiNET is a software tool developed by Epcon that allows the user to model complex liquid and gas networks in regard to the fluid hydraulic behavior. It computes the head loss imposed by pipe friction and fittings as well as pressure drop caused by pieces of equipment such as heat exchangers. For a given network configuration and pump curves, SiNET computes pressure and flow at each node of the network for a stated set of pressure and flow inputs.

A detailed survey of the cooling water network was carried out, resulting in the mapping of the network in terms of pipe length, size, elevation and fittings. The information related with piping configuration was retrieved from isometric drawings while heat exchanger design flow and pressure drop from the respective specification datasheet.

Together with pump curves, this data was then inserted into the SiNET model. The output of the model is the cooling water flow on each pipe segment and the pressure on each node.

In Figure 3.1 a detail of the cooling water pumps and the heat exchanger network is shown. A node is used whenever there is a split or a change in pipe dimension. Nodes are connected to each other by pipes where the number and type of fittings is specified. It is also possible to add pumps and heat exchangers to the network.

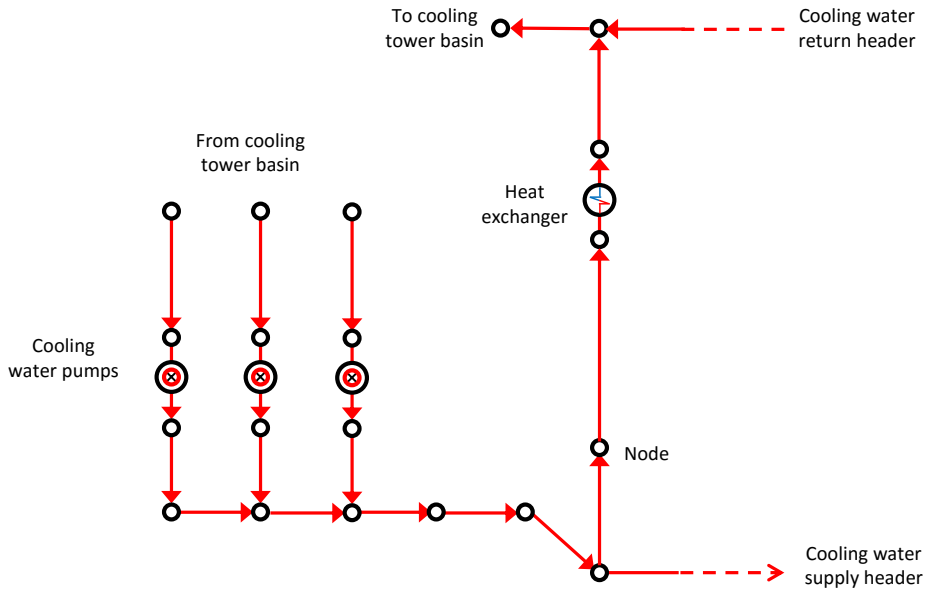

Figure 3.1 - Detail of the cooling water pumps and heat exchanger network in SiNET.

Figure 3.2 shows the cooling water network of Dow Portugal modeled on SiNET and Table 3.1 summarizes the network dimension.

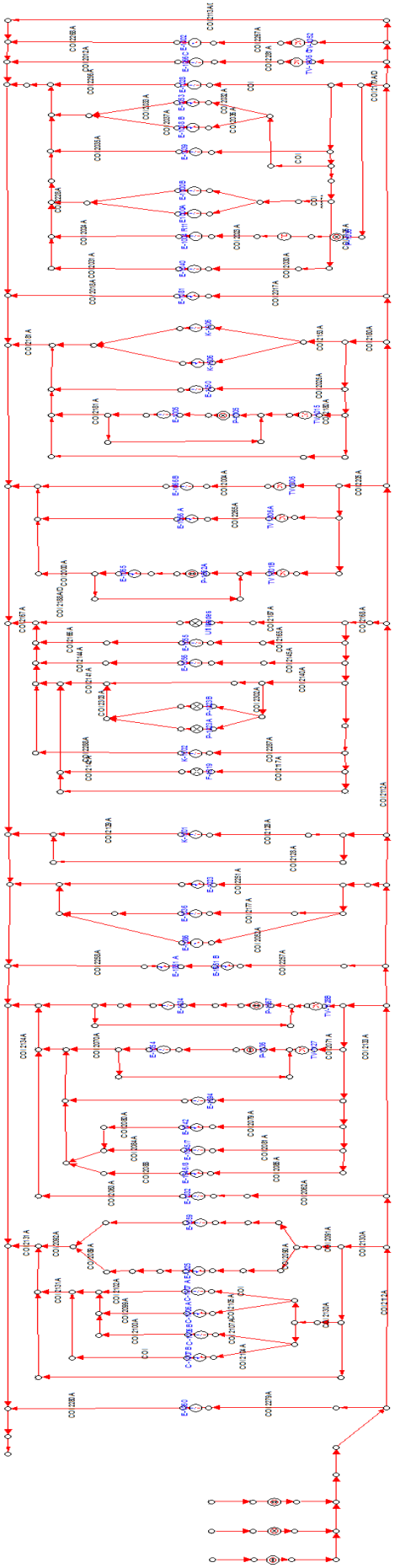

Figure 3.2 – The cooling water network in SiNET.

Table 3.1 – Cooling water hydraulic model dimension.

Nodes	310
Heat exchangers	41
Fittings	610

Results from the SiNET model indicate that the total cooling water flow is approximately 5678 $m^{3} \cdot h^{-1}$. Regarding the supply duct, pressure changes from 2.54 barg in the first node (closest to the cooling tower) to 2.24 barg in the last node (farthest from the cooling tower). In the return duct, pressure changes from 1.85 barg in last node (farthest from the cooling tower) to 1.56 barg in the first node (closest to the cooling tower).

Some differences between design and simulated flow values were verified. In some cases, there was a positive deviation while, in others, a negative variation was observed, meaning that the simulated value was either higher or lower than design, respectively.

Taking these deviations into consideration alternative configurations that minimize the deviations can be purposed. In the case of the modeled network adjusting pipe diameter reduces deviations and allow the modeled flow to be closer to the design value.

Figure 3.3 shows the relative deviations between simulated and design flow for the current network as well as for the case where pipe adjustments are implemented. It is possible to observe that the deviations between design and simulation are lower when the modifications are implemented.

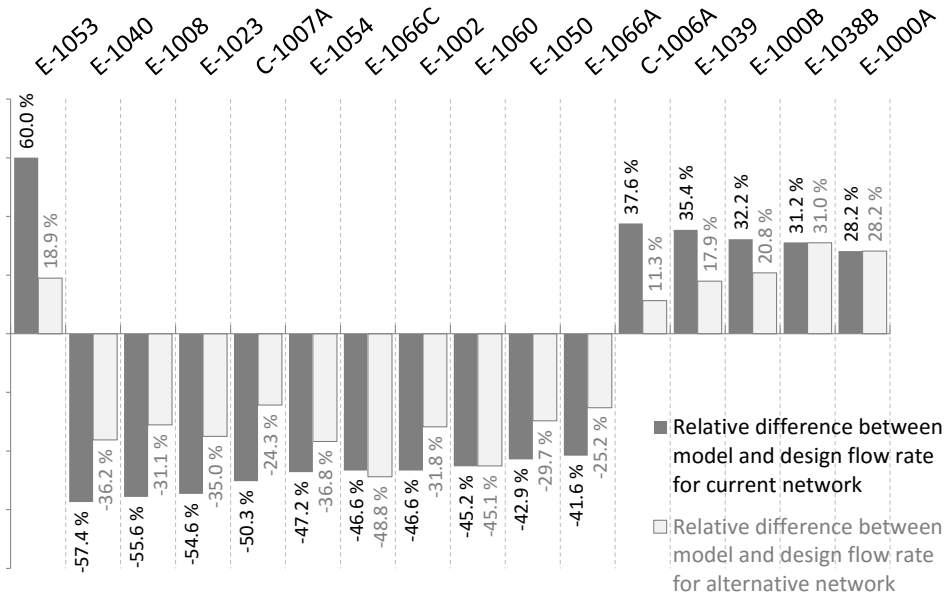

Figure 3.3 – Comparison between design and simulated flow of current network configuration. Relative difference between design and improved network configuration is also presented.

In this section, the main goal was to determine the hydraulic behavior of the cooling water network through the development of an accurate model. However, although this subject is not developed any further, it is possible to identify the places where deviations from design are higher and hence take corrective measures to balance the network. It is also possible to use the model to evaluate the impact that any change in the network has on the overall hydraulic performance of the network.

The cooling water flow on each heat exchanger determined by the hydraulic model are used ahead in the cooling water system thermodynamic model. The integration of the hydraulic model with the thermodynamic model provide a solid base for an accurate overall model of the cooling water system.

3.1.2 The cooling tower model

The aim of this section is to describe a methodology that enables the simulation of a counter flow, induced draft, cooling tower in ASPEN PLUS. The outcome of the proposed approach is a model able to simulate the behavior of a real cooling tower and is capable of working as a stand-alone model or be integrated into a larger simulation model. It should provide grounds for optimization studies, where off-design conditions such as water and air flow variations can be simulated; debottlenecking studies (where equipment limitations may be of interest as production rates are increased); and operability studies (where evolution of equipment performance can be assessed to help plant personnel troubleshoot operations).

Given a set of data consisting of water and air inlet temperature, water and air inlet flow, air inlet humidity and ambient pressure, the problem then consists in determining model parameters that mimic actual cooling tower performance. It is possible to use the model to calculate evaporation ratio and cooling tower heat duty. However, only the output variables which could be compared with the published data by Simpson and Sherwood [74] *i.e.*, water and air outlet temperatures, were presented in this work. Moreover, the model was developed considering the following assumptions:

1. Pressure drop across the cooling tower was not considered because the model was not used for design purposes and it has a minor effect when compared to ambient pressure;
2. The operation of cooling tower was assumed as an adiabatic process;
3. The water stream was considered to be pure as impurities in this stream do not significantly change equilibrium properties;
4. The cooling tower was in steady-state operation.

The proposed cooling tower model is implemented in ASPEN PLUS [75]. This process simulator provides several built-in model blocks that can be directly applied in process simulation. Additionally, this process simulator has an extensive physical property database where the stream properties required to model the material streams in a plant are available.

For simulating the cooling tower in ASPEN PLUS, an approach based on equilibrium stages is applied. For this purpose, ASPEN PLUS provides the RADFRAC built-in block considering neither reboiler nor condenser, which allows the calculation of the liquid and vapor/gas equilibrium on each equilibrium stage.

The methodology for modeling an existent cooling tower described herein was published in a scientific paper under the title: “Modeling of existing cooling towers in ASPEN PLUS using an equilibrium stage method” [76].

3.1.2.1 *Step 1 – Set up the model in ASPEN PLUS*

Cooling towers operate at relatively mild temperature and pressure so it can be assumed that the behavior of the thermodynamic equilibrium between water and air is close to ideality. This fact is confirmed comparing the results achieved using the Cooling Tower general model when applying the ideal property method and other method that takes into account non-idealities (NRTL). Moreover, considering a base case data and two scenarios with ±10% variations on RH^{in}, $T^{a\ in}$, $T^{w\ in}$, L^{in} and G^{in} the results are identical independently of the chosen property package (Table 3.2). Thus, it can be concluded that assuming an ideal behavior of the system substances (water and air) is a good approximation for this process.

Table 3.2 – Comparison between the outputs of the model considering NRTL and IDEAL property packages. The number of equilibrium stages was set to 2 and Murphree stage efficiencies to 1.

	Inputs					**Outputs**			
	RH^{in}	$T^{a\ in}$	$T^{w\ in}$	L^{in}	G^{in}	$T^{w\ out}$ (ºC)		$T^{a\ out}$ (ºC)	
	(%)	(ºC)	(ºC)	(kg/h)	(kg/h)	NRTL	IDEAL	NRTL	IDEAL
Base Case	***80***	***30***	***37***	***7.5***	***10***	***29.5***	***29.5***	***32.4***	***32.4***
+ 10%	88	33	41	8.3	11	33.3		35.9	
- 10%	71	27	33	6.7	9	25.6		28.6	

For defining the RADFRAC block in ASPEN PLUS, the following parameters were specified in the process simulator:

- Calculation type set as ‘Equilibrium’
- Inlet water entered the block ‘Above-Stage’ on the first stage
- Outlet water left the block on the last stage
- Inlet air entered the block ‘On-stage’ on the last stage
- Outlet air left the block on the first stage
- Reboiler and condenser set as ‘None’
- Efficiency type set as ‘Murphree efficiencies’ on each stage

Murphree efficiency is applied when accounting for deviations from ideality, *i.e.*, considering that in an equilibrium stage, liquid and vapor phases do not reach thermodynamic equilibrium. Eq. (3.1) defines Murphree vapor efficiency, $Eff_{i,j}^{M}$, for component i on stage j, where $y_{i,j}$ and $x_{i,j}$ are the vapor and liquid composition, respectively, and $y^{*}_{i,j}$ is the composition of the vapor that would be in equilibrium with the liquid leaving the equilibrium stage.

$$Eff_{i,j}^{M} = \frac{y_{i,j} - y_{i,j+1}}{y_{i,j}^{*} - y_{i,j+1}} \qquad \textbf{(3.1)}$$

Figure 3.4 shows a schematic representation of an equilibrium stage in a cooling tower.

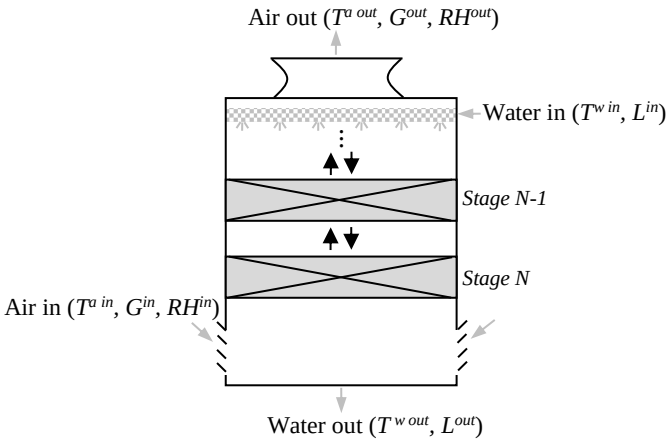

Figure 3.4 – Representation of a cooling tower with *N* equilibrium stages. The air stream enters the cooling tower at the bottom stage and leaves at the top stage; it is characterized by its dry bulb temperature (T^{a}), flow (G) and relative humidity (RH). Water stream enters the cooling tower at the top stage and leaves at the bottom stage; it is characterized by its temperature (T^{w}) and flow (L).

3.1.2.2 *Step 2 – Evaluation of the model parameters*

Once the general model representing the cooling tower has been implemented in ASPEN PLUS, it is necessary to evaluate the model parameters for a given cooling tower, by calculating the number of equilibrium stages and Murphree efficiency of each stage. Heat exchanger performance strongly depends on the cooling medium supply temperature, therefore the most relevant parameter when considering a cooling tower operation is the water temperature ($T^{w\,out}$) that this equipment is able to provide given certain operational conditions. Model parameters values are adjusted by using a set of experimental data

(l=1,…,m) and by minimizing objective function (F), which is the sum of the squared difference between experimental, $T_l^{w\,out,exp}$, and model outputs, $T_l^{w\,out,mod}$ [Eq. (3.2)].

$$F = \sum_{l=1}^{m} \left[T_l^{w\,out,exp} - T_l^{w\,out,mod}\right]^2 \quad \textbf{(3.2)}$$

Eq. (3.2) can be rewritten as Eq.(3.3) to give a more general formulation of the function to be minimized [77]. Each experimental measurement is described by x_l, which is the independent variables vector and corresponds to the measured inlet streams' values (Table 3.3). Model output, $T_l^{w\,out,mod}$ (x_l, λ_k), specified in Table 3.3 depends on both the independent variables, x_l, and the model parameters, λ_k. The minimization of the objective function is accomplished by applying the method described in this work, which consists on an iterative approach thus; model parameters are adjusted for each k^{th} iteration.

Table 3.3 – List of independent, dependent and model variables.

Independent variables [x]	**Model variables** [λ]	**Dependent variables** [$f(x, \lambda)$]
- Inlet air temperature	- Stage 1 efficiency	- Outlet water temperature
- Inlet water temperature	- Stage 2 efficiency	
- Inlet air flow	⋮ [(1)]	
- Inlet water flow	- Stage N efficiency	
- Inlet air humidity		

[(1)] The number of model variables depends on the number of equilibrium stages.

Ideally, the model would return an output, $T_l^{w\,out,mod}$ (x_l, λ_k), equal to the measured value, $T_l^{w\,out,exp}$, given a certain set of inlet parameters, x_l. Therefore, for m experimental data points, the goal is to find the model parameters that correspond to the minimum value of the objective function described by Eq. (3.3), $F(\lambda_k)$.

$$F(\lambda_k) = \sum_{l=1}^{m} \left[T_l^{w\,out,exp} - T^{w\,out,mod}(x_l, \lambda_k)\right]^2 \quad \textbf{(3.3)}$$

Regarding the particular case of a cooling tower, the parameter vector (λ_k) to be adjusted is the number of equilibrium stages, N, and Murphree stage efficiencies, $Eff_{i,j}^{M}$. Hence, the minimization problem is subject to the following constraints:

s.t. $0 < Eff_{i,j}^{M} \leq 1$

$N > 1$

N *is integer*

To evaluate the model parameters an algorithm was established, as shown in Figure 3.5. This algorithm was implemented in Microsoft Excel, using Visual Basic for Applications, and simulations were performed in ASPEN PLUS. Information flow between ASPEN PLUS [75] and Microsoft Office Excel [78] was established by Aspen Simulation Workbook [79].

Considering the set of experimental data regarding the operation of a given cooling tower, the first step is to divide it into three sub-sets: training (*trn*), validation (*val*) and test (*test*). Training and validation sub-sets are used to determine model parameters and are inputs of the algorithm; the test sub-set is used to confirm whether the model parameters returned by the algorithm are adequate when applied to an independent set of data.

When considering only a training sub-set to adjust model parameters, each iteration would bring the difference between model and experimental values closer to zero. However, the inconvenient of this approach is that there would be a point where the model is too adjusted to that specific set of data, resulting in a model very dependent of the data set used to train the model. To avoid this situation, a second set of data, the validation sub-set (*val*), is used to avoid the model overfitting. During the starting iterations, it is expected that the error between model and experimental values decreases for both training and validation sub-sets as model parameters start to be adjusted. Despite the fact that the objective function value for the training sub-set decreases as the algorithm progresses ($F_{trn}(\lambda_{k+1}) < F_{trn}(\lambda_k)$), there can be point where the value of the objective function regarding the validation sub-set reaches a local minimum and then starts to increase. Beyond this point, it is considered that the model becomes dependent of the training sub-set data and the inner algorithm stops (Figure 3.5), thus assuming that the model parameters corresponding to this minimum is the most adequate.

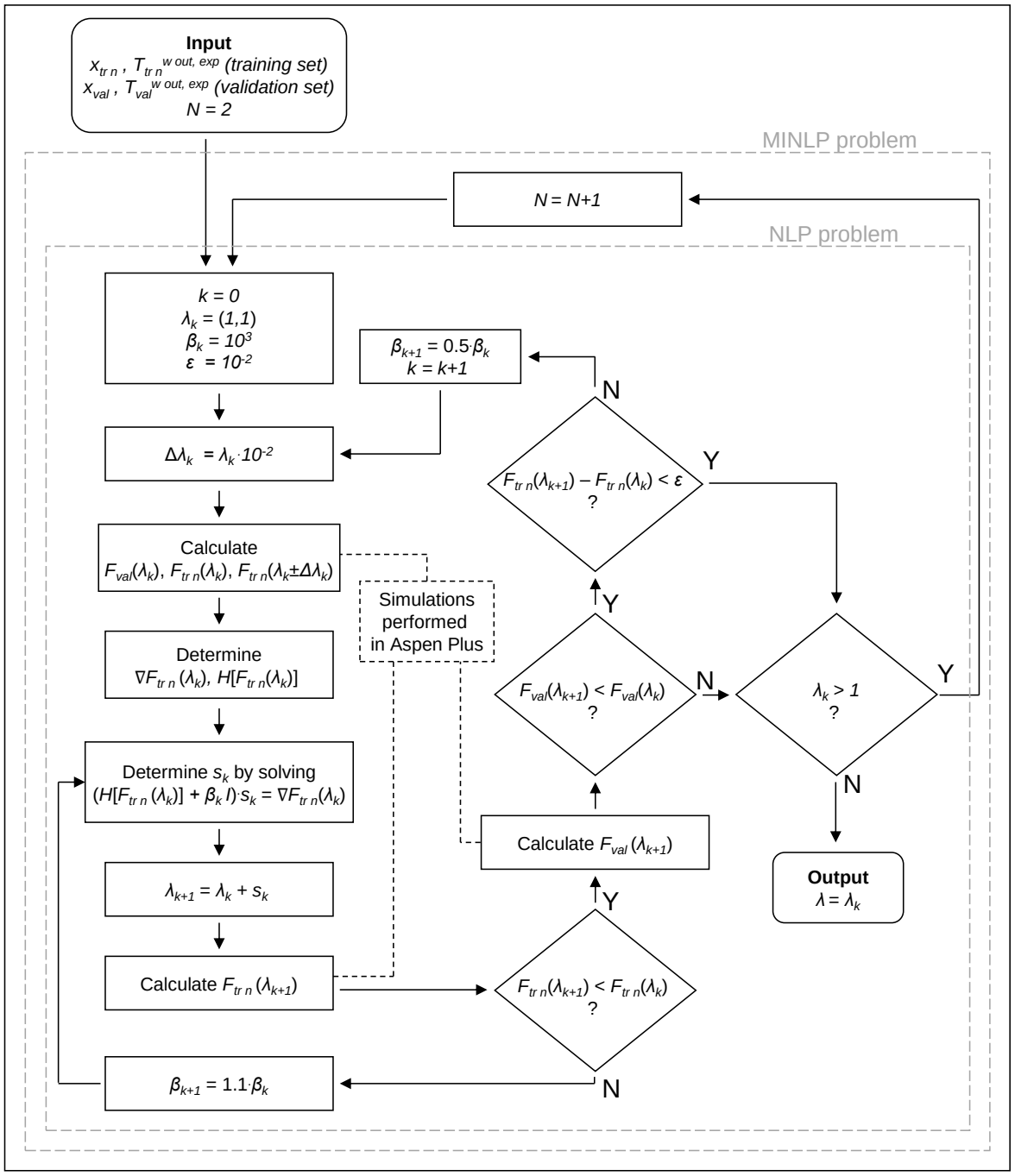

Figure 3.5 – Algorithm for the evaluation of the model parameters. The inner circle of the algorithm is a NLP problem whereas if the number of equilibrium stages is considered it is a MINLP problem.

Number of equilibrium stages (N)

The problem, as described, represents a mixed integer non-linear programming (MINLP) problem. The algorithm introduced in this work transform the MINLP into a non-linear problem (NLP) model by setting a fixed value to the number of stages, eliminating the integer variable. Figure 3.5 shows how the algorithm is structured and how the number of equilibrium stages initial estimate is confirmed at the end of inner algorithm

With this approach, the NLP minimization problem can be solved by using the Levenberg-Marquardt search method. The initial guess for the number of equilibrium stages is set to be the minimum allowed by ASPEN PLUS RADFRAC block, N = 2. Murphree efficiency for each stage is then determined using the Levenberg-Marquardt method and, if the algorithm generates a result corresponding to Murphree stage efficiencies higher than 1, the number of stages should be incremented to avoid an inconsistent stage efficiency value. The algorithm must then be reinitialized, taking into account the new number of equilibrium stages (N+1).

Murphree stage efficiencies ($Eff_{w,j}^{M}$)

Levenberg-Marquardt is in nature an improved Gauss-Newton method by incorporating steepest-descent method into the iterative update scheme, using a search direction between these two methods. In the Levenberg-Marquardt method the search direction, s_k, is determined by solving Eq. (3.4), where $H[F(\lambda_k)]$ is the Hessian matrix of $F(\lambda_k)$, β_k is the control coefficient of the Levenberg-Marquardt method, I is the identity matrix and $\nabla F(\lambda_k)$ is the gradient of $F(\lambda_k)$.

When β_k tends to zero Levenberg-Marquardt method approaches the Gauss-Newton method whereas when β_k tends to infinity the Levenberg-Marquardt method approaches the steepest-descent method. The values of β_k, during the iterative process, are chosen in the following way: when initializing the algorithm, β_k is set to a large value so that the Levenberg-Marquardt method manifests the robustness of the steepest-descent method, meaning that the initial guess can be chosen with less caution. For each iteration, if $F(\lambda_k + s_k) < F(\lambda_k)$, convergence is accelerated by decreasing β_k by a certain amount set by the user; otherwise, β_k is increased in order to enlarge the searching area [80].

$$(H[F(\lambda_k)] + \beta_k I)s_k = -\nabla F(\lambda_k) \quad \textbf{(3.4)}$$

The objective function is not described by an analytical expression; therefore, the gradient is calculated using the numeric method given by Eq. (3.5). The step size, $\Delta\lambda$, is an infinitesimal positive number that enables the numerical calculation of the gradient.

$$\nabla F(\lambda_k) = \frac{\left(F(\lambda_k + \Delta\lambda_k) - F(\lambda_k - \Delta\lambda_k)\right)}{2 \cdot \Delta\lambda_k} \quad \textbf{(3.5)}$$

Regarding the Hessian matrix, the calculation is performed by applying the expanded Taylor series truncated to the second trm, as shown in Eq. (3.6).

$$F(\lambda_k + \Delta\lambda_k) = F(\lambda_k) + \nabla F(\lambda_k) \cdot \Delta\lambda_k + \frac{1}{2} \cdot \Delta\lambda_k{}^T \cdot H[F(\lambda_k)] \cdot \Delta\lambda_k \quad \textbf{(3.6)}$$

3.1.2.3 *Step 3 –ASPEN PLUS and Microsoft Excel interaction*

As stated in Steps 1 and 2, the model outputs – which correspond to the outlet water temperature – are generated running an ASPEN PLUS simulation model. These results generated by the process simulator are fed into the minimization algorithm implemented in Microsoft Office Excel, which in turn will feed the simulator with new model parameters (Figure 3.6).

This two-way connection between the process simulator (ASPEN PLUS) and the minimization algorithm (Visual Basic for Application in Microsoft Office Excel) is provided by an interface between both software tools. The interface is guaranteed by Aspen Simulation Workbook, which allows a seamless data transfer between ASPEN PLUS and Microsoft Excel.

Aspen Simulation Workbook is a tool for interfacing AspenTech's process simulation models with Microsoft Office Excel worksheets. Aspen Simulation Workbook also has tools to link model variables to plant data tags, imported using third-party applications. These capabilities allow modeling experts to link models and plant data and publish the resulting models as Microsoft Office Excel worksheets [81].

Step 4 - Implementation of the proposed methodology

A step by step flowchart representing the actions that must be taken to implement the proposed methodology is shown in Figure 3.6.

Due to the comprehensive experimental data as well as detailed information about the experimental setup, the work of Simpson and Sherwood [74] is often used to evaluate the appropriateness of cooling tower models [27, 82, 83]. These authors published experimental data regarding the operation of two mechanical induced draft cooling towers, designated by tower R-1 and tower R-2. Although the ambient pressure is not mentioned in the work of Simpson and Sherwood [74], taking into account the nature of the work it is assumed that it remained approximately constant during the length of the experimental work. These two sets of published experimental data are used for validating the approach proposed in this work.

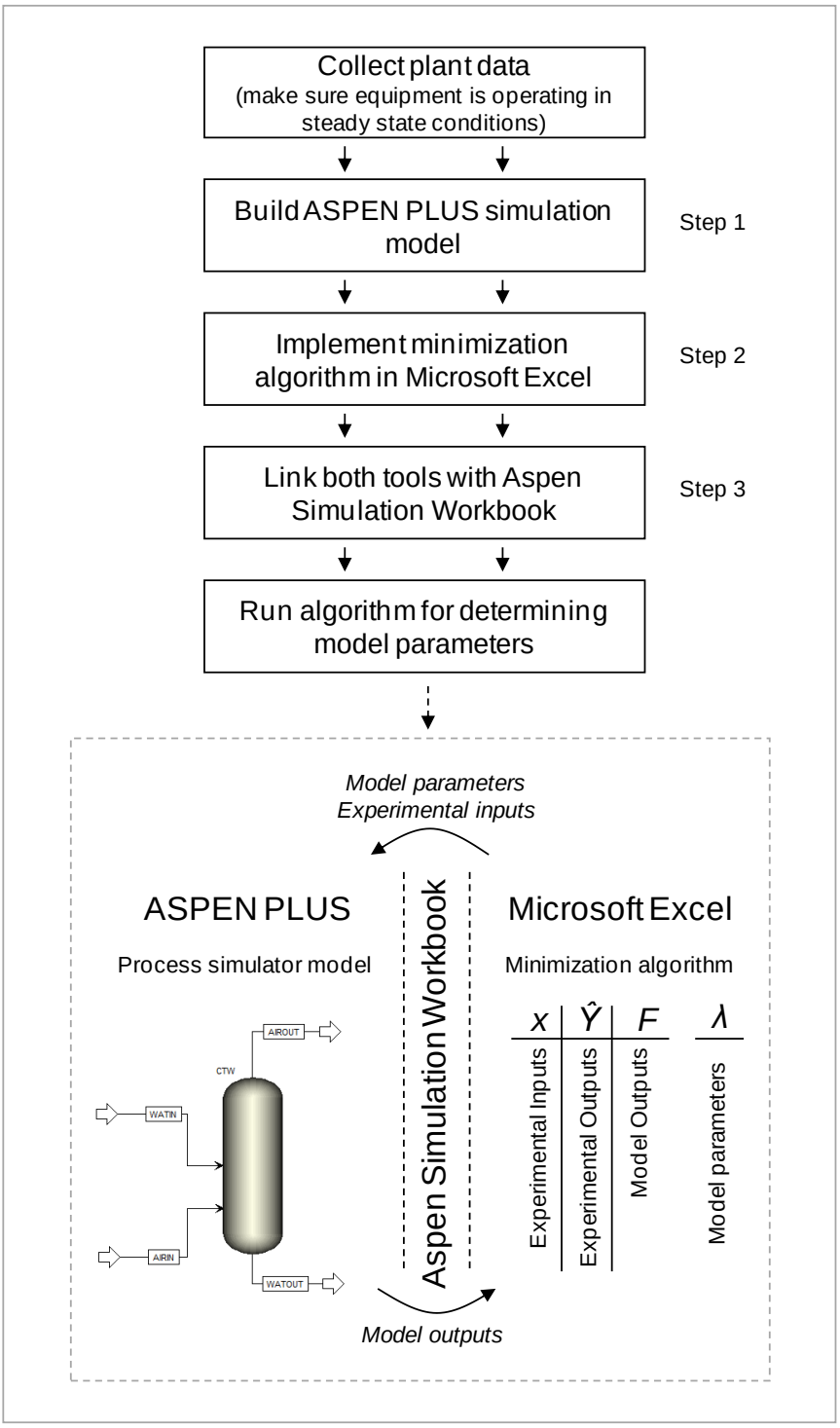

Figure 3.6 – Overall procedure flowchart showing the interaction between the process simulator (ASPEN PLUS) and the minimization algorithm (implemented in Microsoft Excel), being this interaction mediated by Aspen Simulation Workbook. The steps referred in this figure are described in detail in Section 2 of this work.

A third set of data (Table 3.4) was used to confirm the applicability of the proposed approach to a real industrial application, which corresponded to a set of experimental data collected from an industrial mechanical induced draft cooling tower.

The industrial cooling tower with the characteristics presented in Table 3.5 belongs to one of the manufacturing plants of Dow Chemical Company in Portugal. Water pumps and fan motors are equipped with fixed speed drives so that the water and air flow rate are kept static. The dry-bulb temperature and relative humidity were measured near the air entrance of the cooling tower with a data logger (Tinytag View 2 –TV4500). In- and outlet water temperature are both registered by an online process monitoring system. Since the atmospheric pressure is not monitored on site, this variable was retrieved from two weather stations 20 km away on opposite directions and the mean value was computed. The atmospheric pressure was obtained from Weather Underground website [84]. Due to the fact that the air outlet temperature was not monitored, the objective function that was minimized only took into account the outlet water temperature.

To train, validate and test the model, experimental data was divided in three sets. Data points were randomly split for training (*trn*), validating (*val*) and testing (*test*) with 60/20/20%, respectively. Data sets regarding tower R-1, R-2 and Dow's were defined by 49, 45 and 50 experimental measurements, respectively.

As stated in the algorithm illustrated in Figure 3.5, the procedure stops when the error associated to the validation sub-set increases or, for the case when the this value is continuously decreasing, the difference between the error associated to the training sub-set of two consecutive iterations is less than a pre-set value (ε). The stopping criteria that were verified for both tower R-1 and Dow's tower were $F_{val}(\lambda_{k+1}) > F_{val}(\lambda_k)$ and for tower R-2 $F_{trn}(\lambda_{k+1}) - F_{trn}(\lambda_k) < \varepsilon$. Figure 3.7 to Figure 3.9 show the evolution of the objective function in regard to the number of iterations.

Considering the algorithm for model identification described before, it was stated that additional equilibrium stages are added only when the algorithm returns stage efficiency values higher than 1. For the three case studies presented in this work, two equilibrium stages were sufficient to provide a good fit to experimental data, with both stage efficiencies lower than one.

The algorithm finished when k = 5, k = 4 and k = 8 for tower R-1, R-2 and Dow's, respectively. For tower R-1 and R-2 the procedure terminates when the objective function of the validation sub-set reached a local minimum while for Dow's cooling tower the algorithm stopped when the difference between two consecutive iterations of the training sub-set was lower than the established margin.

Murphree stage efficiencies for the three cooling towers were: $Eff_{w,1}^{M}$ = 0.93, $Eff_{w,2}^{M}$ = 0.85 for tower R-1; $Eff_{w,1}^{M}$ = 0.89, $Eff_{w,2}^{M}$ = 0.74 for tower R-2 and $Eff_{w,1}^{M}$ = 0.96, $Eff_{w,2}^{M}$ = 0.70 for Dow's tower.

Table 3.4 – Experimental and modeled values for Dow's cooling tower collected during one month period (20.May.2011 to 20.Jun.2011). Air and water flow correspond to design. Air outlet temperature was not monitored.

	P^{atm} (kPa)	$T^{a\ in,exp}$ (ºC)	RH^{in} (%)	$T^{w\ in,exp}$ (ºC)	$T^{w\ out,exp}$ (ºC)	$T^{w\ out,mod}$ (ºC)
Train	101.44	17.45	97.00	28.46	22.87	*22.93*
	101.95	15.97	91.65	27.38	21.74	*21.63*
	101.92	21.29	72.80	29.91	23.82	*23.95*
	101.85	20.26	67.62	28.79	22.70	*22.85*
	102.12	17.03	87.15	28.73	22.50	*22.47*
	101.11	21.22	85.47	31.01	25.14	*25.02*
	100.63	18.09	89.67	28.61	22.75	*22.93*
	102.19	19.71	79.10	29.77	23.55	*21.83*
	102.12	21.98	73.90	30.86	24.51	*24.69*
	102.09	17.41	80.22	28.73	22.36	*22.37*
	101.51	19.48	88.00	28.07	23.03	*23.16*
	101.14	19.71	79.10	29.77	23.55	*23.58*
	101.82	18.65	85.77	27.76	22.61	*22.61*
	101.78	17.79	92.47	29.31	23.30	*23.23*
	101.92	22.02	68.17	30.49	24.20	*24.26*
	102.02	19.36	81.87	30.02	23.68	*23.73*
	100.90	17.60	97.85	29.83	23.72	*23.59*
	101.14	17.62	81.60	27.65	21.83	*21.97*
	101.78	21.15	65.45	29.87	23.17	*23.51*
	101.58	27.27	37.98	30.88	24.49	*24.37*
	101.82	18.65	85.77	27.76	22.61	*22.62*
	101.78	26.93	35.40	30.31	24.06	*23.82*
	101.41	19.72	78.55	27.29	22.40	*22.47*
	101.65	19.50	68.97	28.81	22.74	*22.61*
	101.31	25.47	41.88	30.63	24.29	*23.94*
	101.44	22.65	74.97	31.15	24.86	*25.14*
	100.90	16.46	79.10	28.15	21.92	*21.65*
	101.51	24.76	51.58	30.91	24.65	*24.44*
	101.75	25.43	65.72	31.40	25.64	*25.82*
	101.78	21.75	75.52	28.93	23.65	*23.89*
Validation	102.02	21.85	62.77	30.11	23.78	*23.75*
	101.82	17.40	86.60	29.14	22.80	*22.79*
	101.88	19.79	62.22	28.95	22.64	*22.49*
	102.02	21.85	67.35	30.32	23.97	*24.50*
	101.31	22.30	75.25	31.39	25.26	*25.12*
	102.12	17.61	83.25	29.17	22.80	*22.77*
	102.02	21.89	73.35	30.82	24.44	*24.62*
	100.87	17.55	96.72	29.50	23.51	*23.40*
	101.88	19.79	62.22	28.95	22.64	*22.49*
	101.99	22.16	72.25	30.57	24.51	*24.56*
Test	101.88	19.79	62.22	28.95	22.64	*22.51*
	101.78	22.17	73.90	30.32	24.51	*24.53*
	101.85	18.07	85.20	29.44	23.16	*23.12*
	101.82	21.31	76.90	28.14	23.23	*23.40*
	101.78	20.71	75.25	30.17	24.05	*23.97*
	101.75	22.60	52.35	27.85	22.53	*22.43*
	101.78	20.71	52.35	28.11	22.03	*21.91*
	101.99	22.57	65.72	30.90	24.42	*24.49*
	102.02	16.31	83.55	28.10	21.79	*21.81*
	101.07	22.44	78.55	31.04	25.04	*25.16*

Table 3.5 – Dow's cooling tower design specifications.

Type	Induced draft Counter flow
Tower dimensions	H 12.85 m W 13.32 m L 37.58 m
Packing height	5.1 m
Water flow	5878 t/h
Water inlet temperature	36.7 ºC
Water outlet temperature	30.0 ºC
Air inlet wet-bulb temperature	26.7 ºC
Air flow	4505 t/h
Number of fans	3
Nominal fan power (each)	75 kW

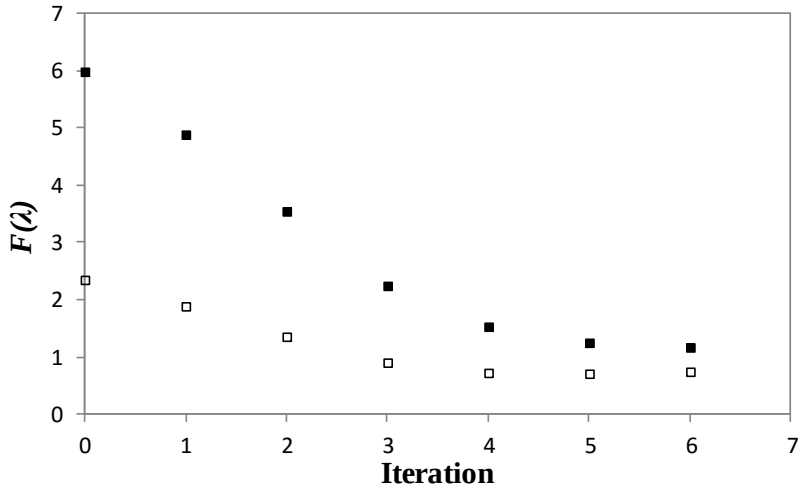

Figure 3.7 – Objective function evolution for tower R-1 for training [■] and validation [□] sub-sets.

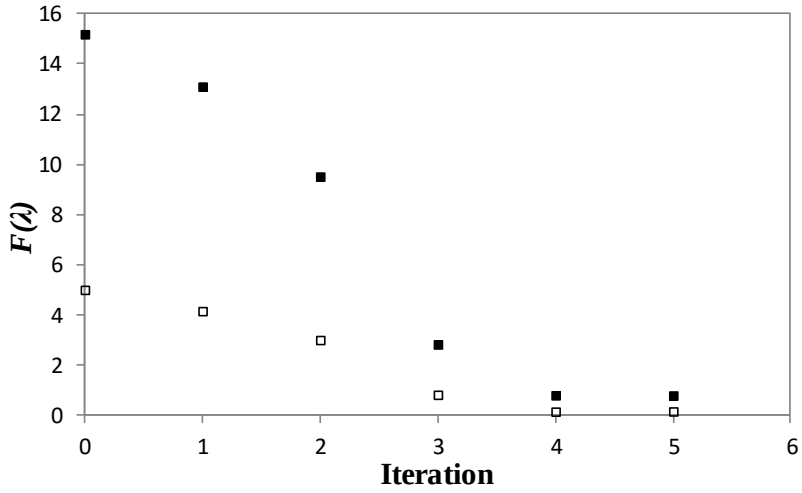

Figure 3.8 – Objective function evolution for tower R-2 for training [■] and validation [□] sub-sets.

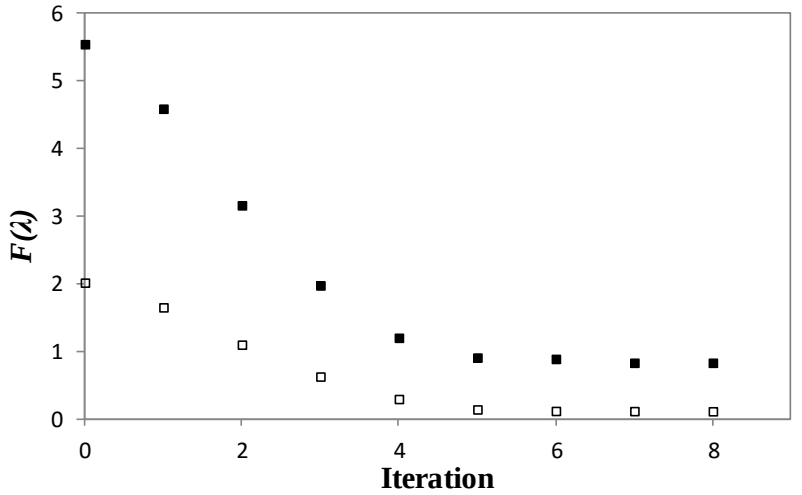

Figure 3.9 – Objective function evolution for Dow's tower for training [■] and validation [□] sub-sets.

The good agreement between predicted and experimental can be seen in Figure 3.10 to Figure 3.12 for water outlet temperatures.

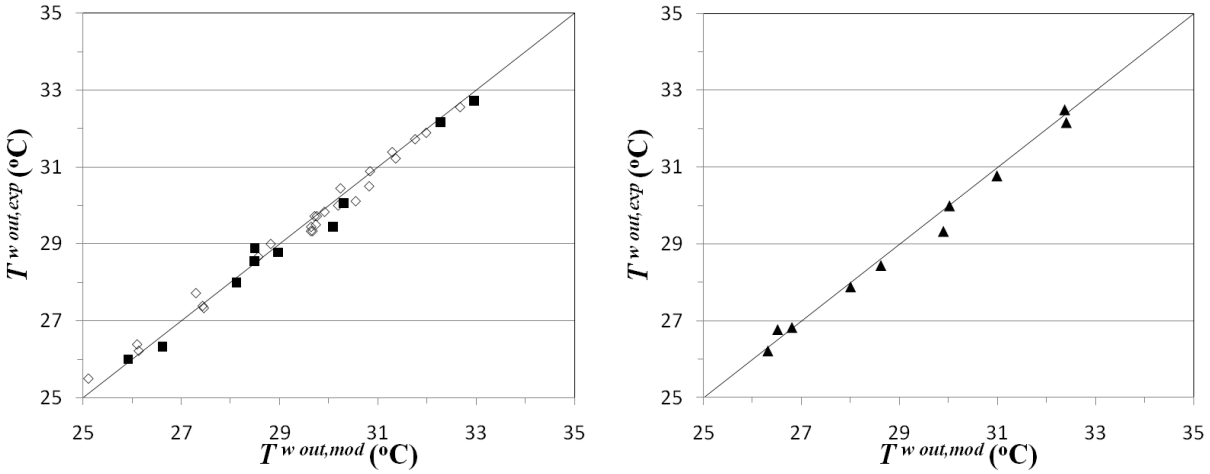

Figure 3.10 – Water outlet temperature model predictions vs. observed value for tower R-1: (a) Training [◊] + validation [■] and (b) test [▲]. Assuming a constant P^{atm} of 101.3 kPa.

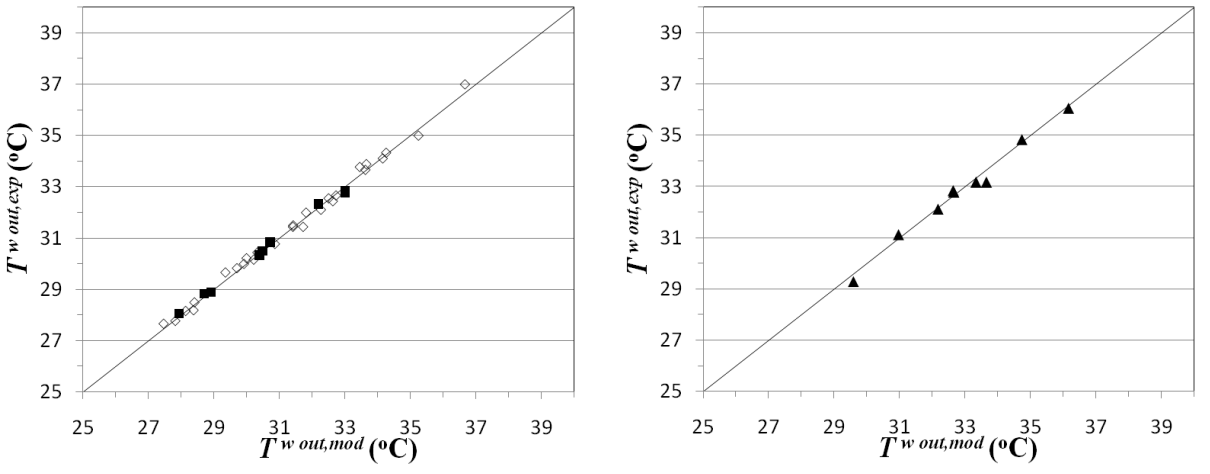

Figure 3.11 – Water outlet temperature model predictions vs. observed value for tower R-2: (a) Training [◊] + validation [■] and (b) test [▲]. Assuming a constant P^{atm} of 101.3 kPa.

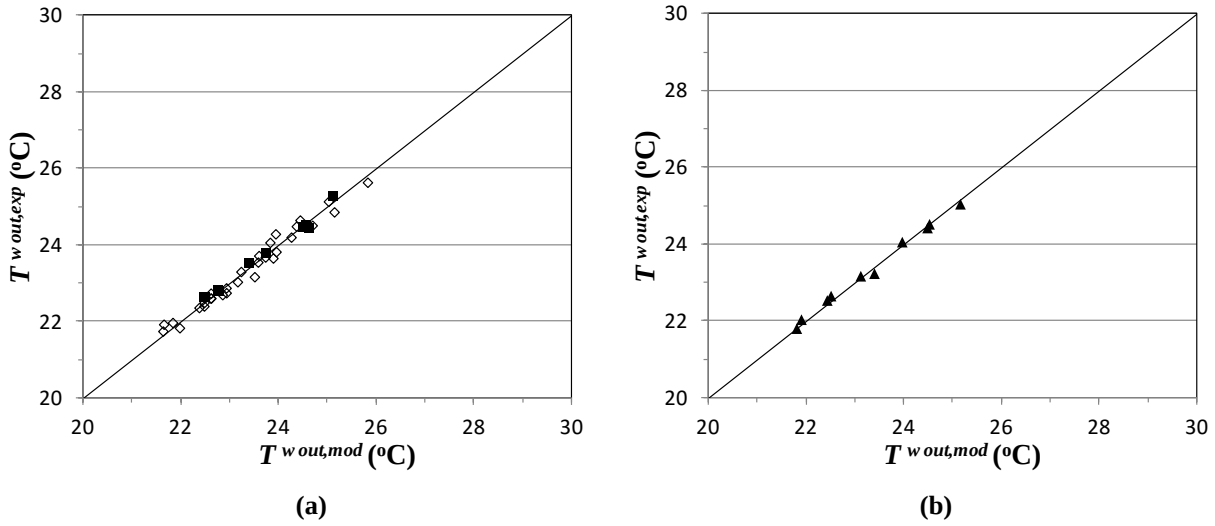

Figure 3.12 – Water outlet temperature model predictions vs. observed value for Dow's tower: (a) Training [◊] + validation [■] and (b) test [▲].

Due to the fact that air outlet temperature is often unmonitored (as in Estarreja Dow's cooling tower), the model was trained by minimizing the error between model prediction and experimental outlet water temperature. However, Figure 3.13 shows that the model output for air outlet temperatures is also in good agreement with the experimental values.

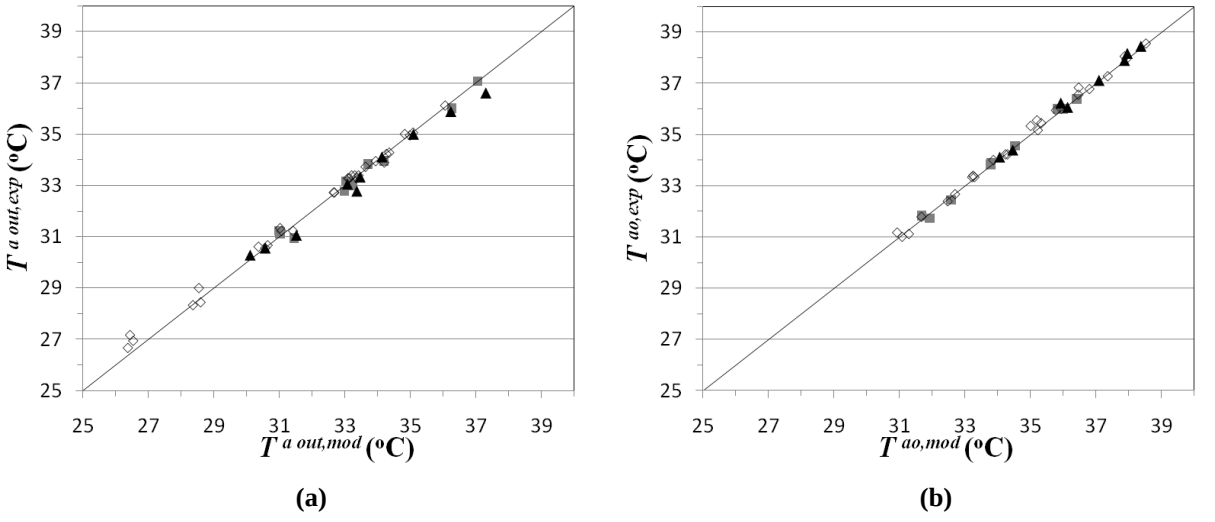

Figure 3.13 – Air outlet temperature model predictions vs. observed value for training [◊], validation [■] and test [▲] in: (a) Tower R-1 and (b) tower R-2. Assuming a constant P^{atm} of 101.3 kPa.

Step 5 - Model performance evaluation

To quantitatively evaluate the performance of the model, the following statistical parameters were calculated: correlation coefficient, (R) and root mean squared error ($RMSE$). The correlation coefficient provides a variability measure of the data reproduced in the model and the root mean squared error provides the measure of residual errors and gives a global idea of the difference between the observed and modeled values. These parameters are given by Eqs. (3.7) and (3.8) [85] where Y_l is the model output, $\bar{Y}$ is the average value of the model output and, $\hat{Y}_l$ is the experimental value.

$$R = \sqrt{\frac{\sum_{l=1}^{m}(Y_l - \bar{Y})^2 - \sum_{l=1}^{m}\left(Y_l - \hat{Y}_l\right)^2}{\sum_{l=1}^{m}(Y_l - \bar{Y})^2}} \quad \textbf{(3.7)}$$

$$RMSE = \sqrt{\frac{1}{m}\sum_{l=1}^{m}\left(Y_l - \hat{Y}_l\right)^2} \quad \textbf{(3.8)}$$

Model performance parameters regarding outlet water temperature ($T^{w\,out}$) are summarized in Table 3.6. For the test data sub-sets of tower R-1 and R-2, respectively, $RMSE_{test}$ is: 0.23; 0.218 and R_{test}: 0.994; 0.993, as for Dow's industrial cooling tower the test sub-set $RMSE_{test}$ is: 0.129 and R_{test}: 0.991. The values of the model evaluation parameters indicate a good fit between experimental and model values for both the laboratory setup (Tower R-1 and R-2) and the industrial application (Dow's cooling tower).

Table 3.6 – Model performance parameters for the different data sets. The variable that is being analyzed is the water outlet temperature, $T^{w\,out}$.

	Training			**Validation**			**Test**		
	R-1	R-2	Dow	R-1	R-2	Dow	R-1	R-2	Dow
RMSE	0.206	0.172	0.175	0.291	0.129	0.102	0.236	0.218	0.118
R	0.997	0.997	0.984	0.991	0.997	0.996	0.994	0.993	0.996

Although the model was trained using only water outlet temperatures the model performance parameters regarding air outlet temperatures ($T^{a\ out}$) in tower R-1 and R-2 also indicate an acceptable fit between model predictions and experimental values: $RMSE_{test}$ = 0.349; R_{test} = 0.988 for tower R1 and $RMSE_{test}$ = 0.130; R_{test} = 0.997 for tower R-2. In an industrial context air outlet temperature is not a critical variable to be controlled, therefore these values are not available for Dow's case study and the comparison between model and experimental air outlet temperatures was not possible to accomplish.

All predicted values are within a margin of ±2 % from the experimental values for water outlet temperatures and ±3 % for air outlet temperatures (tower R-1 and R-2).

3.1.3 Cooling system thermodynamic model

The hydraulic performance of the network is evaluated with the developed hydraulic model, *i.e.*, the cooling water flow rates flowing through the heat exchangers were determined. On the other hand, with the ASPEN PLUS thermodynamic model, the temperature on each point of the network was evaluated.

Figure 3.14 shows the cooling water system as a block diagram. The cooling water system is composed by a combination of the cooling water network, where heat is transferred from the process to the cooling water, and the cooling tower, where heat is transferred from the cooling water to ambient air. By combining each heat exchanger duty and cooling water flow with the cooling tower model, it is possible to establish an accurate model that describes the plant cooling water system. The thermodynamic model of the cooling water system was developed with the ASPEN PLUS simulator. The global property method used in the flowsheet was set to IDEAL and is applied throughout.

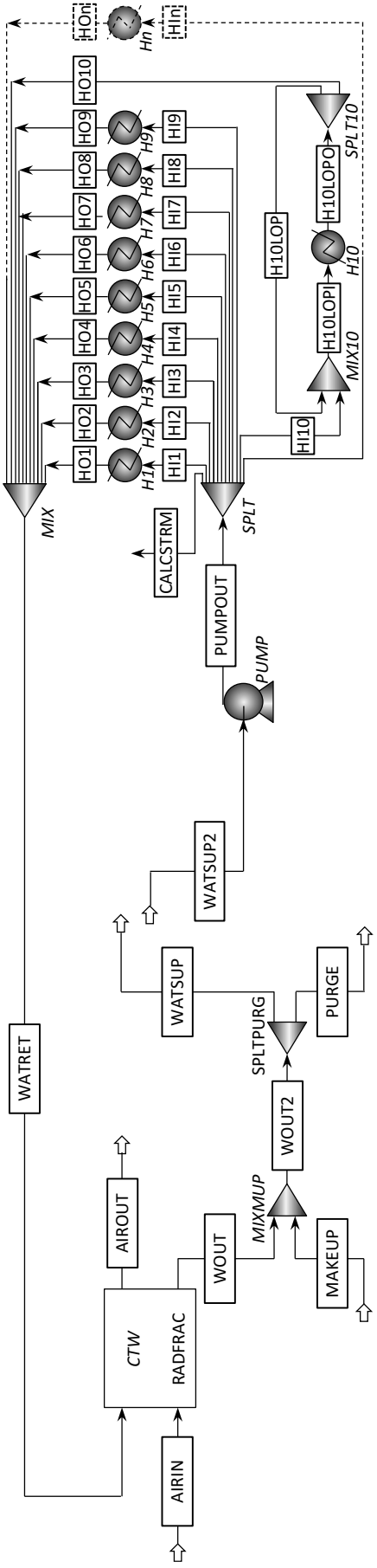

Figure 3.14 – Block diagram of the cooling water system model.

3.1.3.1 *Cooling tower model*

The graphical display of the cooling tower (*CTW*) model implemented in ASPEN PLUS is shown in Figure 3.15. A detailed description of the model was previously described in Section *3.1.2* The *Cooling Tower Model* and consists on a RADFRAC block without reboiler and condenser, two equilibrium stages with the calculation type set as 'Equilibrium'. At the bottom stage "dry" air (AIRIN) enters 'On-stage' and cooled water (WOUT) exits; at the top stage "humid" air (AIROUT) exits and hot water (WATRET) enters 'Above-Stage'. The Murphree efficiency of the top stage is $Eff_{w,1}^{M}$ = 0.96 and the Murphree efficiency of the bottom stage is $Eff_{w,2}^{M}$ = 0.70.

The intermediary stream (WOUT2) that resulted from mixing the cooled outlet water stream (WOUT) with the makeup stream (MAKEUP) enters in a SPLIT block where it is divided into the stream that feeds the cooling water network (WATSUP) and a purge stream (PURGE). The purge flow is set within the SPLIT block to 5 m^3/h.

The cooling water system is semi-closed system in terms of mass balance since the majority of the flow circulates cyclically. However, there are losses during the process: by evaporation in the cooling tower and because of the purge flow that is required to maintain an acceptable quality of the cooling water. To account these losses, a makeup of fresh water is required. So, the cooled outlet water stream (WOUT) is mixed with the makeup stream (MAKEUP) in a MIXER block (*MIXMUP*), resulting in an intermediary stream (WOUT2).

The "Design Spec" tool of the ASPEN PLUS was used for determining the flow of fresh makeup. The mass flow of the supply (WATSUP) and return (WATRET) streams were as defined as variables. Then, it was defined that the mass flow of WATSUP should be equal to the one of WATRET by varying the MAKEUP mass flow.

Although the purge flow rate of 5 m^3/h is relatively small when compared to the total flow rate, 5678 m^3/h, it would make sense that the purge was taken ahead of the makeup so that the purge would be more effective. However, the makeup takes place in the cooling tower basin whereas the purge is taken from the outlet stream.

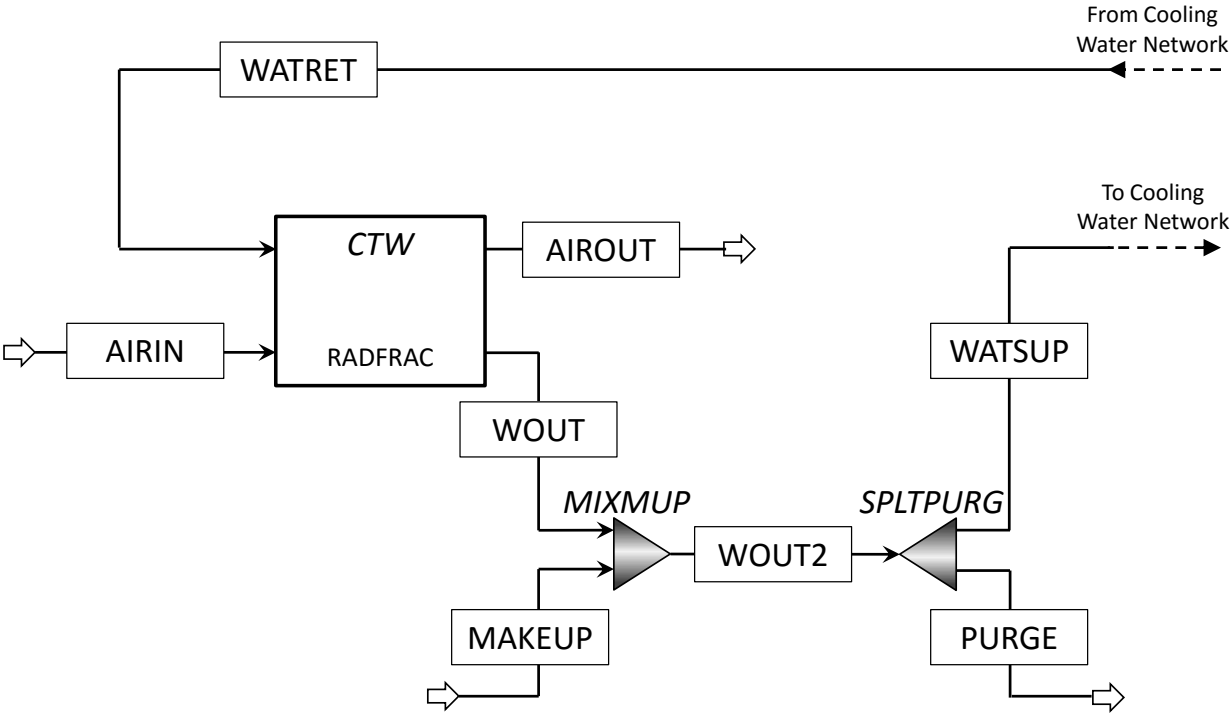

Figure 3.15 – Detail of the cooling tower thermodynamic model implemented in ASPEN PLUS.

3.1.3.2 *Cooling water network*

Each heat exchanger in the network was described by a HEATER block. The input variables of each block were pressure drop and heat duty. Heat duty of each heat exchanger was based on design values.

In Figure 3.16,the graphical display of the cooling water network model implemented in ASPEN PLUS is shown. The water living the cooling tower (WATSUP2) goes through a cooling water pump (*PUMP*) where it is pressurized from 0 barg to 5.3 barg, increasing 0.1 C in the compression process. The outlet stream of the PUMP block (*PUMPOUT*) then enters a SPLIT block (*SPLT*), which can be interpreted as the cooling water supply header, dividing the inlet stream into each individual heat exchanger flow (HI1, HI2,…, HIn). The specific flow of each heat exchanger was previously determined with the hydraulic model of the cooling water network, as described above. Cooling water then enters each heat exchanger (*H1*, *H2*,…,*Hn*), where it is heated by the process stream. The heat duty of each exchanger and pressure drop of each heat exchanger are inputs of the each HEATER block. Since cooling water is a liquid stream and no flash is involved, the pressure drop defined in the heat exchangers has little influence on the outlet stream conditions in regard to temperature and physical state so, an arbitrary value of 0.8 barg for the pressure drop was assumed. The outlet streams (HO1, HO2,…, HOn) are combined in a MIXER block (MIX), which can be interpreted as the cooling water return header. The combined outlet stream (WATRET) follows to the cooling water to complete the cooling water system cycle. The IDEAL property method was used to simulate every block.

Due to process requirements, there were some heat exchangers where the inlet temperature had to be higher than the one supplied by the cooling water distribution network. In these cases, a recycling loop was used such as shown in Figure 3.16. The inlet stream of the cooler (H10LOPI) was fed into the heat exchanger (H10) and heated by a given duty. The outlet stream (H10LOPO) then entered in a SPLIT block (SPLT10) where it was divided into two streams: one was recycled (H10LOP) and the other (H10O) followed to the return header. The recycled stream (H10LOP) was then mixed with "fresh" cooling water (H10) in a MIXER block (*MIX10*), generating a "warm" stream and thus completing the loop.

The known variables regarding the heat exchangers with recycling loops were the heat exchanger's flow rate and temperature of the inlet stream (H10LOP) and the exchanger's (H10) heat duty. The unknown variables were the recycled stream (H10LOP) flow rate and "fresh" water flow rate. To determine the flow rate of "fresh" cooling water a 'Design Spec' was used. The temperature of the "warm" inlet temperature of the cooler (H10LOPI) was as defined as variable. Then, it was defined that the temperature of the heat exchanger inlet stream (H10LOPI) should be equal to a given temperature by varying the "fresh" cooling water (H10) mass flow rate.

The recycled stream (H10LOP) flow rate was determined using a CALCULATOR block. This block allowed some Fortran code to be implemented defining the loop mass balance. By declaring the heat exchanger's inlet flow rate (H10LOPI), which is a known variable, and stating that the recycled mass flow rate is equaled to the inlet flow rate minus the "fresh" water flow rate (Eq. (3.9)), which was manipulated by the abovementioned 'Design Spec', it was possible to calculate in the recycle stream flow rate.

$$H10LOP\left[\frac{kg}{h}\right] = H10LOPI\left[\frac{kg}{h}\right] - HI10\left[\frac{kg}{h}\right] \quad \textbf{(3.9)}$$

The SPLIT block determines the flow of one of the block's outlet streams based on the difference between the inlet stream and the sum of the other stream flow rates. So, to simplify the cooling water network model by avoiding the necessity of varying the cooling water inlet flow (WATSUP2) to the SPLIT block, an auxiliary stream was applied (CALCSTRM). This stream's mass flow rate is the difference between the inlet cooling water flow rate to the SPLIT block (WATSUP2) and the total sum of the mass flow rates of the streams feeding the heat exchangers (HI1, HI2,…, HIn). Therefore, by assigning a sufficiently large mass flow rate to the WATSUP2 stream, the SPLIT block was always in mass balance despite variations in the network mass balance.

To work around the fact that cyclic systems are harder to converge in ASPEN PLUS and the cooling water system is a semi-closed structure the WATSUP and the WATSUP2 streams are not connected to each other (as seen in Figure 3.14). To ensure that both streams were at the same temperature a CALCULATOR block was implemented. The WATSUP and WATSUP2 temperatures were declared as 'Tear' variables with the Fortran statements declaring that the WATSUP2 temperature was equal to the WATSUP temperature. In the CALCULATOR block 'Sequence' options, it was defined that it should be executed after the *SPLTPURG* block.

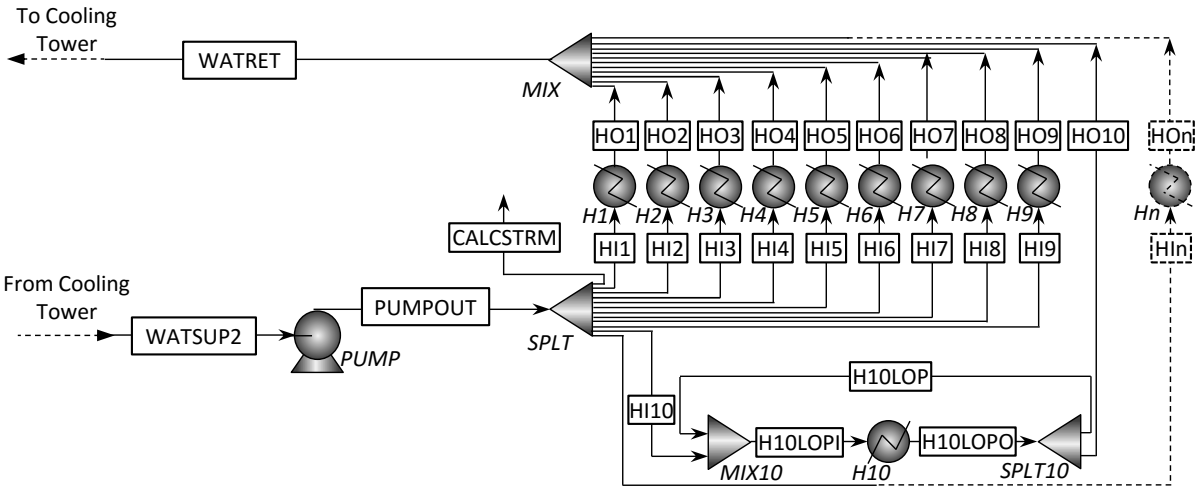

Figure 3.16 – Detail of the cooling water network thermodynamic model implemented in ASPEN PLUS.

In Figure 3.17, the cooling water system flowsheet implemented in ASPEN PLUS is presented. There are a total of 37 heat exchangers in the network of which 4 are integrated in loop and fed with “warm” water.

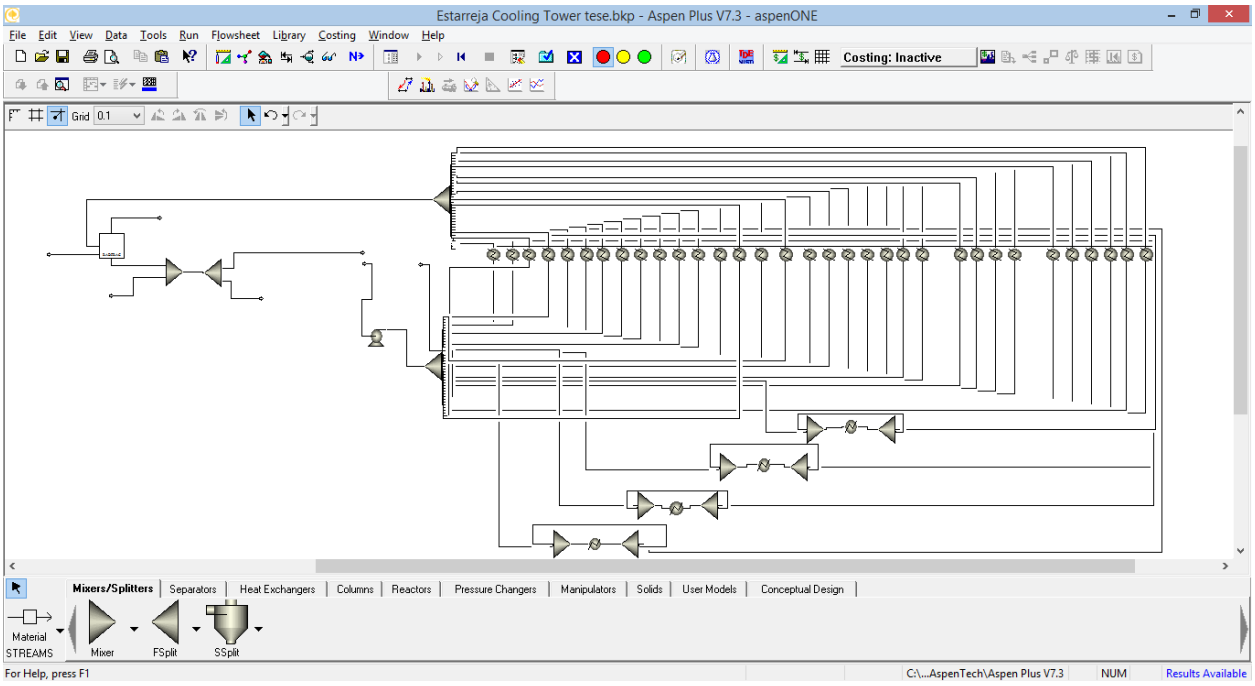

Figure 3.17 – ASPEN PLUS model of cooling water network integrated with cooling tower.

3.1.4 Evaluation of the performance of the cooling water system

Some cooling water parameters determined using the thermodynamic model for a 21 C air wet-bulb temperature are presented in Table 3.7.

The thermodynamic model showed that the temperature range between the supply and overall return streams is approximately 6 C for the Dow's cooling water network. The fact that the range value is not an exact figure results from the fact that it slightly varies with the air wet-bulb temperature. This is due to the presence of loops in the cooling water network that influences the cooling water circulating flow. For instance, since the cooling duty is constant, when the cooling water supply temperature decreases due to a lower air wet-bulb temperature, the required "fresh" water flow rate to each loop will also decrease, therefore reducing the cooling water overall circulating flow rate and therefore increasing the range. However, since the heat duty of the heat exchanger with loop corresponds to only 5% of the total heat duty, the range variation is not significant, varying 0.08 C with a 3 C variation in the air wet-bulb temperature.

Table 3.7 – Dow's cooling water network parameters for a 21 C air wet-bulb temperature.

Range ($T_{return} - T_{supply}$)	6 C
Cooling duty of the network	37.6 MW
Circulating cooling water flow rate	5678 t/h
Water lost due to evaporation	30.6 t/h

Figure 3.18 shows the results of performing a sensitivity analysis using the thermodynamic model of the cooling system, where the cooling water network supply temperature is calculated by varying air wet-bulb temperature for different cooling ranges are shown.

The maximum design cooling water supply temperature for the process is set to 26 C. Taking the results shown in Figure 3.18 into consideration, which corresponds to a 21 C air wet-bulb temperature *i.e.* if the air wet-bulb temperatures rises above 21 C the cooling water supply temperature will be above design. To work within design boundaries, it is necessary to reduce the cooling water range (decrease cooling duty) and therefore reduce production rate.

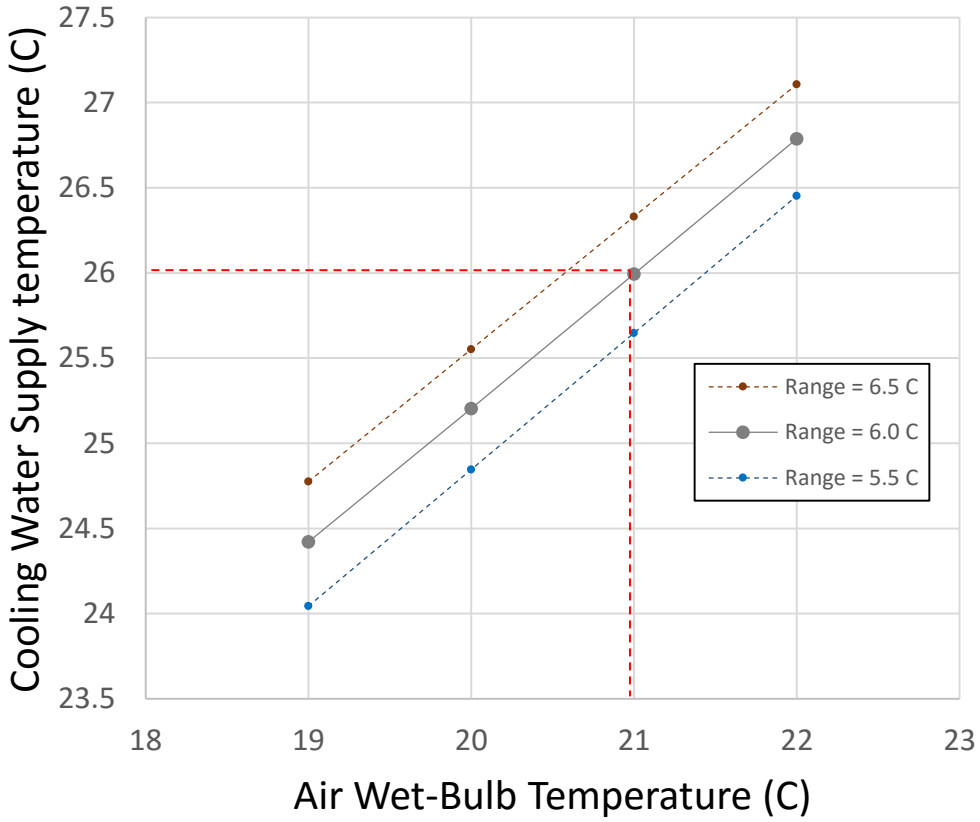

Figure 3.18 – Cooling water supply temperature *vs* Air wet bulb temperature for the Dow's cooling tower.

Given the limit air wet-bulb temperature of 21 C, it is now relevant to determine how the cooling water system design is adequate to the environmental conditions at the Estarreja site.

A cooling tower with lower capacity implies that the plant rate is limited by the cooling tower for longer periods whereas a cooling tower with high capacity might mean that the cooling tower is overdesigned and a higher capital investment is required.

Given a set of historic weather data, it is possible to determine how long throughout the year was the air wet-bulb temperature above a given temperature. Combining this information with the limit value of the wet-bulb temperature of cooling water system, the time during which the cooling tower would be limiting the production rate can be determined.

Records regarding weather data at the Dow's Estarreja MDI plant were not available. Therefore, to estimate the wet-bulb temperature's annual frequency, data was retrieved from the Ovar weather station, which is approximately 15 km away from the plant, corresponding to the whole of year 2010 [84].

Figure 3.19 displays the frequency of occurrence of different wet-bulb temperatures is presented. The figure can be used to answer the following question: During 2010, what was the percentage of the year during which the temperature was higher than a given wet-bulb temperature? For example, the wet-bulb temperature was higher than 13.8 C during approximately half of the year.

At maximum plant rate, the abovementioned cooling tower maximum outlet temperature was set to be 26 C and to achieve this temperature, the ambient air wet-bulb temperature must lower than 21 C. It is possible to observe in Figure 3.19 that during 2010 the wet-bulb temperature was above 21 C, which is the temperature above which the cooling tower limits the production rate, during approximately 4.5% of the year. This represents 394 hours of disrupted production rate due to cooling tower limitations.

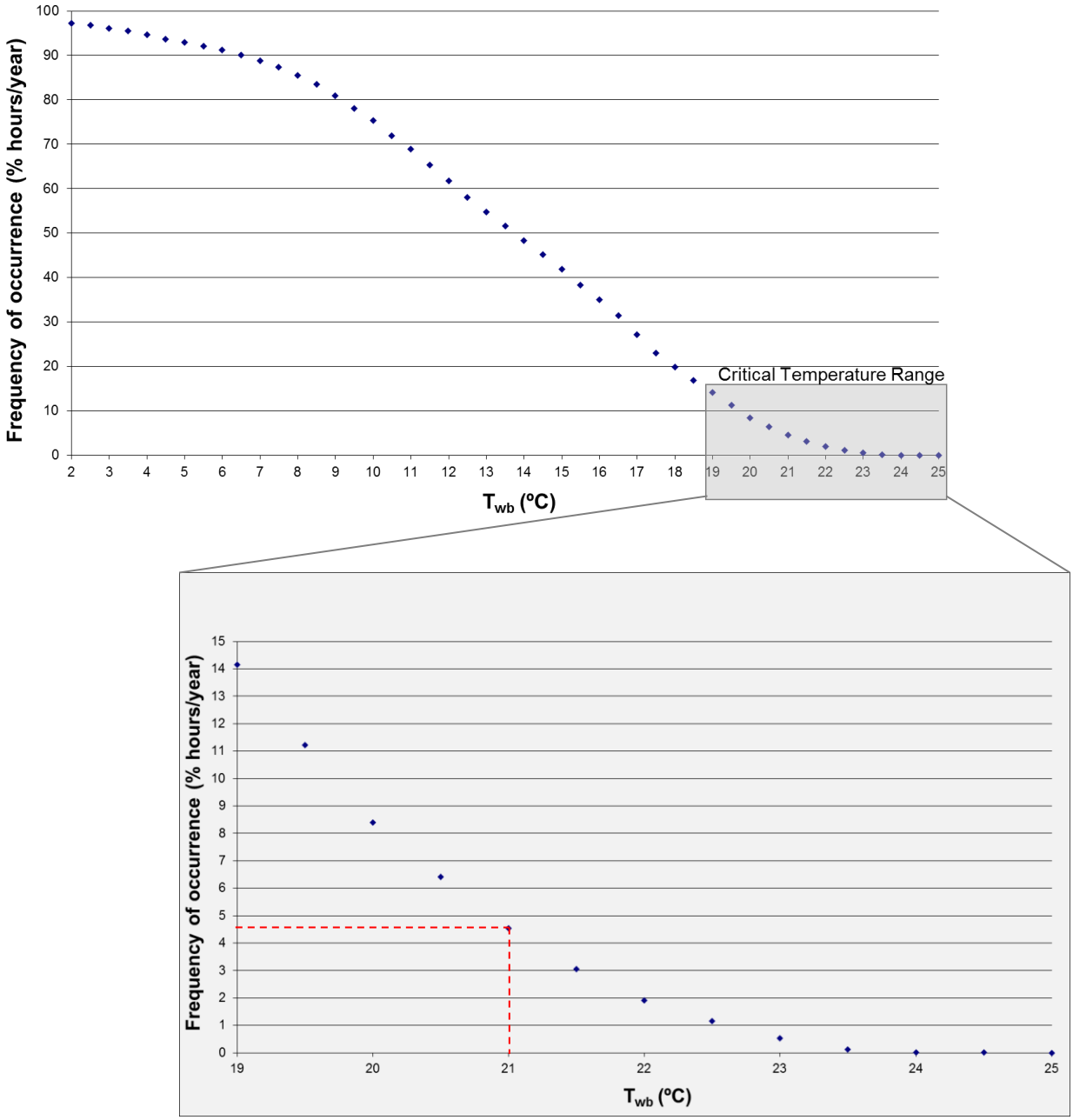

Figure 3.19 – Estimated wet-bulb temperature frequency of occurrence in 2010 at Dow's Estarreja MDI plant.

3.2 Steam system analysis

3.2.1 Steam generator

Steam is one of the most widely used media for conveying thermal energy within several industries. Some reasons that make steam so attractive for utilization in a process is the fact that water is readily available, relatively inexpensive, non-toxic and environmentally safe. In its vapor form, it is a safe and efficient energy carrier. Steam has a high energy density and can hold much more potential energy as an equivalent mass of liquid water and since the heat transfer coefficient of steam is so high, the required heat transfer area is relatively small. This enables the use of heat exchangers with smaller heat transfer areas, which are cheaper and with a lower footprint.

Steam is often generated in one or more boilers and then distributed to the various consumption points through a piping network. This centralized arrangement means that the boiler is an obvious target for optimization efforts that promote the improvement of its efficiency.

The performance test code for fired steam generators from the American Society of Mechanical Engineers [86] describes two different methods for determining the boiler efficiency: the direct and the indirect method.

The direct method, also known as the input-output method, is essentially the ratio between the energy that is transferred to the steam and the total energy supplied by the fuel. Eq. (3.10) describes the boiler efficiency calculated through the direct method, η_{dm}, where Q_{stm} is the energy transferred to the steam and Q_{fuel} is the total energy contained in the fuel fed to the boiler.

$$\eta_{dm} = \frac{Q_{stm}}{Q_{fuel}} \tag{3.10}$$

On the other hand, the indirect method, Eq. (3.11), computes boiler efficiency, η_{im}, based on the total energy contained in the fuel fed to the boiler subtracted by the boiler losses, where X_{losses} is the ratio between Q_{fuel} and the total boiler losses.

$$\eta_{im} = \frac{Q_{fuel} - Q_{fuel} \cdot X_{losses}}{Q_{fuel}} = 1 - X_{losses} \tag{3.11}$$

For determining boiler efficiency using the direct method it is only necessary to quantify the inlet fuel enthalpy and the enthalpy transferred to the steam. The uncertainty of the direct method is directly proportional to the uncertainty of measurement of the feed water/steam flow rate, feed water and steam specific enthalpy, fuel flow rate and fuel heating value. As for the indirect method, it does not rely on the flow rate measurement of fuel and feed water/steam but instead on the determination of boiler losses through a detailed energy balance.

So, while boiler efficiency is simpler to compute using the direct method, the indirect method is the preferred approach to determine boiler efficiency [86]. This is because the direct method requires very

sensitive flowmeters to accurately determine steam and fuel flow, which are not commonly found in industrial boilers, whereas in the indirect method measurement errors impact only on the losses rather than all the total energy.

As an example, if the real boiler efficiency calculated through the direct method is considered as being $\eta_{dm\ real}$ and $\eta_{dm\ dev}$ the boiler efficiency deviated by an error, if there is an error in steam flow measurement of 1%, Eq. (3.12) , assuming a 90% boiler efficiency this will impact on the calculated efficiency ± 0.9%.

$$\eta_{dm\ dev} = \frac{Q_{stm\ real} \cdot (1 \mp 1\%)}{Q_{fuel}} = \eta_{dm\ real} \cdot (1 \mp 1\%) \quad \textbf{(3.12)}$$

If $\eta_{dm\ real}$ = 90%

Then,

$$\eta_{dm\ dev} = \eta_{dm\ real} \mp 0.9\% \quad \textbf{(3.13)}$$

As for the indirect method,

$$\eta_{im\ dev} = \frac{Q_{fuel} - Q_{fuel} \cdot X_{losses} \cdot (1 \mp 1\%)}{Q_{fuel}} = 1 - X_{losses} \cdot (1 \mp 1\%)$$

$$\eta_{im\ dev} = 1 - X_{losses} \mp X_{losses} \cdot 1\% = \eta_{im\ real} \mp X_{losses} \cdot 1\% \quad \textbf{(3.14)}$$

If X_{losses} = 10%

$$\eta_{im\ dev} = \eta_{im\ real} \mp 0.1\% \quad \textbf{(3.15)}$$

Figure 3.20 shows a diagram of the energy balance of the steam generator where the input and output heat streams are shown as well as a list of the potential losses in the boiler. A detailed description of the methodology used to calculate each parameter of the energy balance is well described elsewhere in the American Society of Mechanical Engineers (ASME) performance test code for fired steam generators [86] and therefore will not be detailed here.

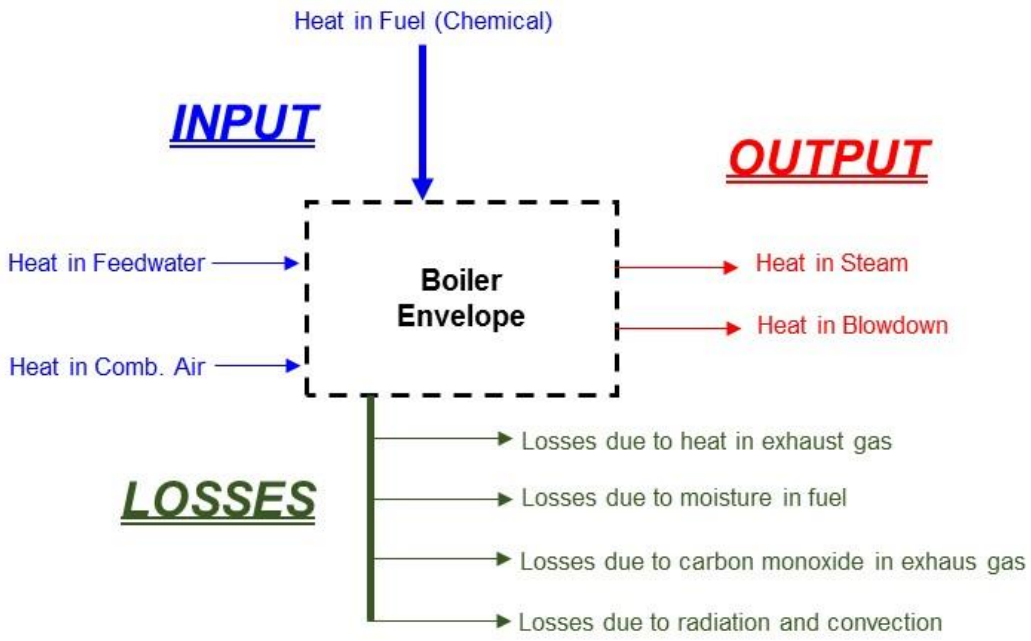

Figure 3.20 – Energy balance of steam generator envelope.

The boiler efficiency calculation method described on ASME manual is based on the fuel high heat value (HHV) and therefore takes into account air moisture and losses due to moisture from burning hydrogen. The reference state is liquid water so, unless the boiler system has a recovery unit that allows the condensation of water present in the flue gas, boiler efficiency based on HHV is significantly lower than the efficiency based on the lower heating value (LHV).

The process variables and assumed parameters considered for the boiler efficiency calculation are stated in Table 3.8. Although the indirect method does not calculate efficiency directly from fuel flow rates, it does require entry of flowrates to determine relative fractions of fuels and losses due to surface radiation.

Carbon monoxide is not measured online, so the value stated in Table 3.8 is assumed that carbon monoxide concentration in the flue gas is 80% of the upper limit imposed by the environmental permit [87] and is considered to be constant for all three boilers. Additionally, since the boilers use natural gas as fuel, unburned carbon is considered to be negligible.

Boiler efficiency was calculated assuming the fuel composition detailed in Table 3.9. The natural gas property data was provided by the natural gas supplier regarding the average composition during a one month period. The main constituent of the fuel stream is methane, with a molar fraction of 89.9%, followed by ethane, with a molar fraction of 6.79%. The rest of the fuel constituents are inert gases, totalling 0.92%, and other longer chain hydrocarbons corresponding to 2.38%.

Table 3.8 – Model parameters for calculating boiler efficiency using the indirect method.

Inlet combustion air temperature	Online measurement
Exhaust gas temperature	Online measurement
Fuel flow rate	Online measurement
Ambient temperature	23 ºC
Air relative humidity	80%
Boiler skin area	184 m^2
Boiler skin temperature	50 ºC
Carbon monoxide in stack	400 mg/Nm^3
Unburned fuel as total organic carbon	(Neglectable)

Table 3.9 – Average fuel composition during April 2011 (composition provided by fuel supplier) and high and low heating values [88].

Component	HHV ($kJ.kg^{-1}$)	LHV ($kJ.kg^{-1}$)	Formula	Mol. Fraction
Nitrogen	-	-	N_2	0.32%
Carbon Dioxide	-	-	CO_2	0.60%
Methane	37 620	33 866	CH_4	89.90%
Ethane	65 904	60 285	C_2H_6	6.79%
Propane	93 799	86 316	C_3H_8	1.90%
n-Butane	121 543	111 874	C_4H_{10}	0.21%
IsoButane	121 192	111 798	C_4H_{10}	0.27%
TOTAL	***48 240***	***43 560***		***100 %***

Figure 3.21 to Figure 3.23 show the variation of boiler efficiency based on LHV with stack temperature and excess oxygen in exhaust gas for different fuel flows. A higher stack temperature means that less energy is being recovered from the flue gas to generate steam and therefore is being lost to the environment. On the other hand, higher excess oxygen in stack implies that the flow of combustion air admitted to the boiler is too high, meaning that energy is being lost by heating up an unnecessary quantity of combustion air. As mentioned earlier, the indirect method does not calculate efficiency directly from fuel flow rates. However, since it is assumed that the radiation losses are constant and independent from the fuel flow rate, specific radiation losses will vary inversely to fuel flow rate, *i.e.*, radiation losses per "unit" of fuel will decrease for higher rates and decrease for lower rates, thus impacting on the overall boiler efficiency.

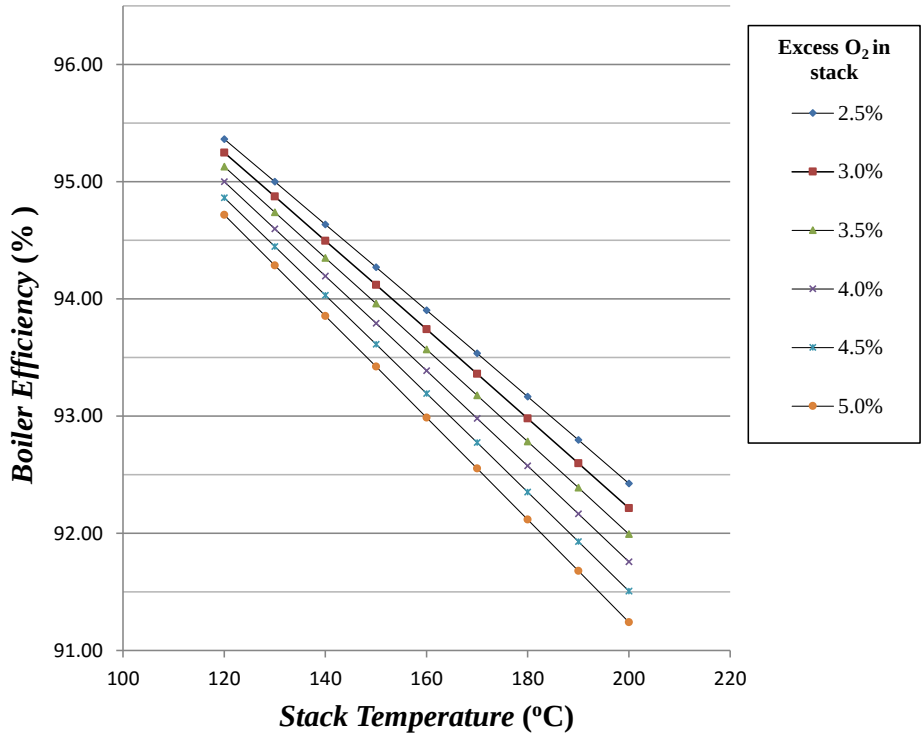

Figure 3.21 – Boiler efficiency based on LHV *vs.* stack temperature calculated using the indirect method for different values of oxygen content in stack. Fuel flow = 500 kg/h

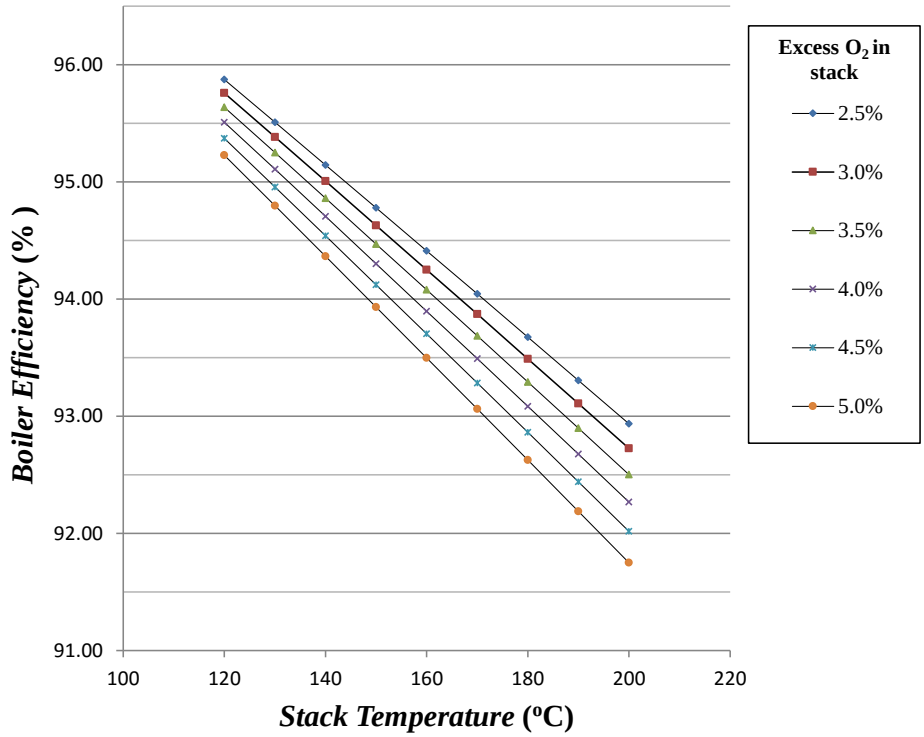

Figure 3.22 – Boiler efficiency based on LHV *vs.* stack temperature calculated using the indirect method for different values of oxygen content in stack. Fuel flow = 1000 kg/h

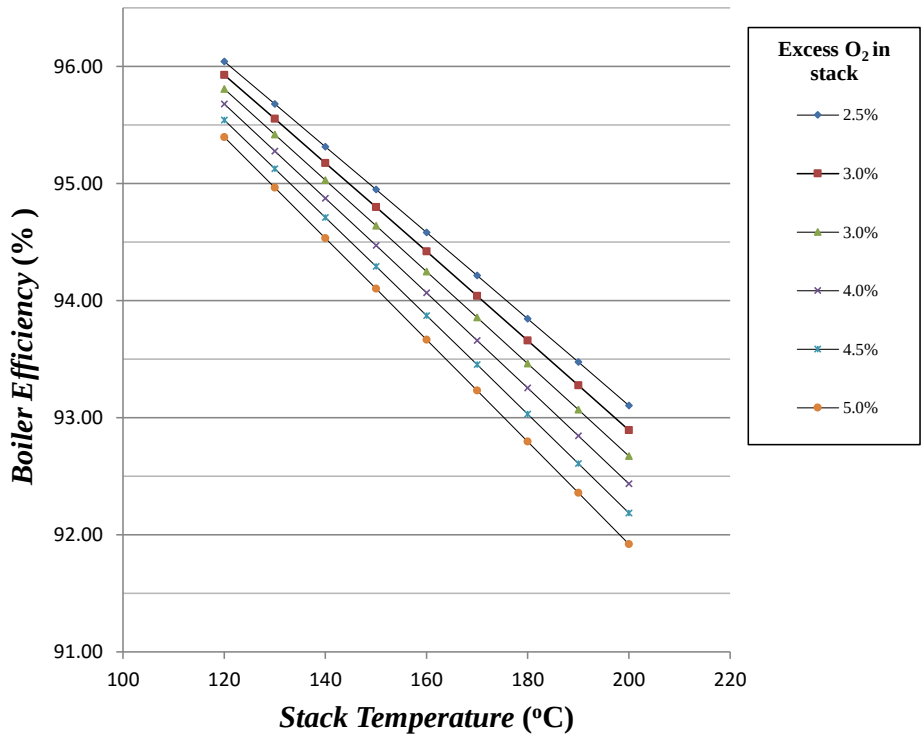

Figure 3.23 – Boiler efficiency based on LHV *vs.* stack temperature calculated using the indirect method for different values of oxygen content in stack. Fuel flow = 1500 kg/h

Plots in Figure 3.21 to Figure 3.23, showing the relation between stack temperature, excess oxygen in stack and boiler efficiency for different fuel loads are useful tools for assessing boiler efficiency at a given operating point.

By observing Figure 3.21 to Figure 3.23, some remarks can also be taken: While keeping the same stack temperature, lowering oxygen content in stack does not have an effect on boiler efficiency by the same magnitude, *i.e.* lowering oxygen content by 1% does necessarily means that boiler efficiency will increase by 1%.

Figure 3.24 to Figure 3.26 illustrate the comparison between the results obtained when using the direct and the indirect method. The comparison is done for the three boilers in the Estarreja plant.

It is possible to observe from Figure 3.24 to Figure 3.26 that boiler efficiency calculated with the direct method is much more disperse than when using the indirect method. The reason for the evident difference between both methods is explained by the different approaches in the abovementioned calculation methods. While the indirect method takes into account more reliable measurements, such as fuel flow rates, stack temperatures and flue gas oxygen contents, the direct method relies on the correct measurement of steam generated by the boiler, which is known to be a difficult medium to retrieve a precise flow rate quantification.

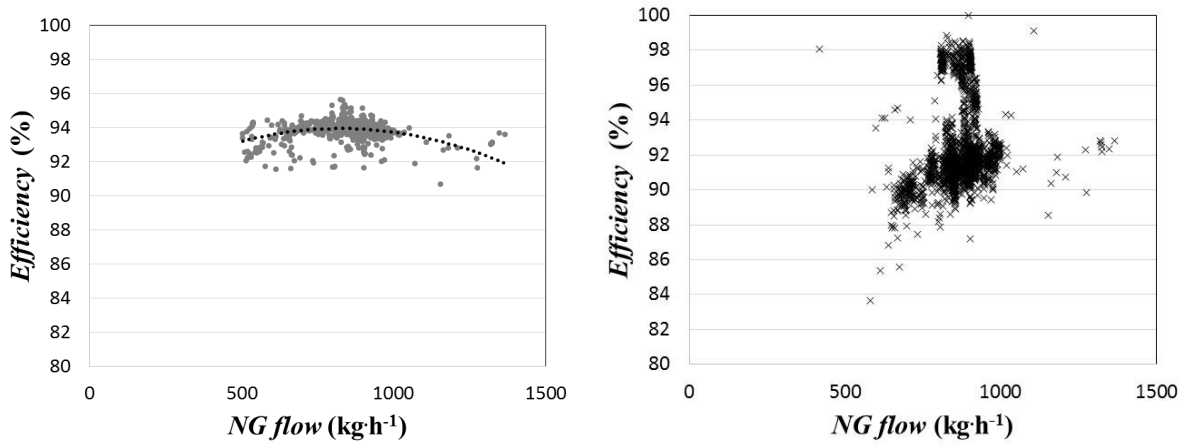

(a) **(b)**

Figure 3.24 – B4001 boiler efficiency using the input-output method (●) and the direct method (×).

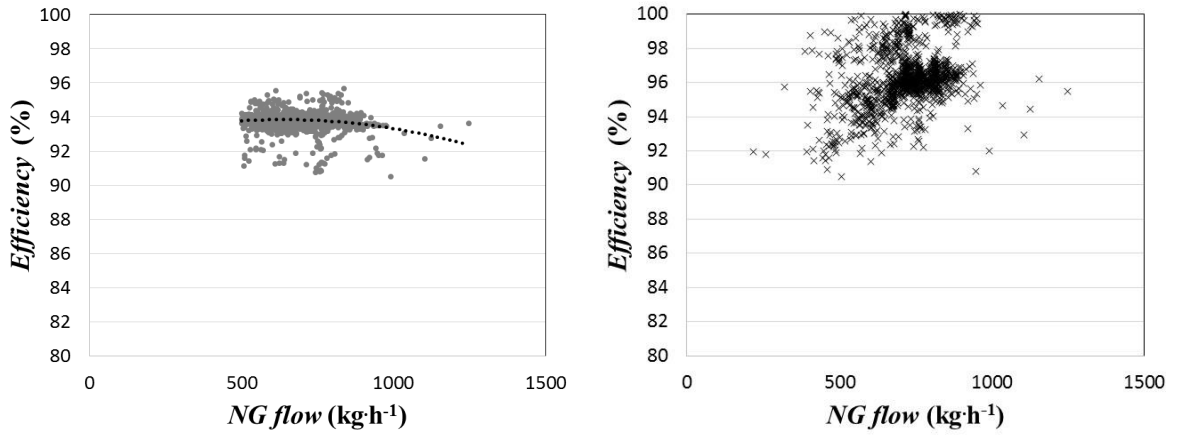

(a) **(b)**

Figure 3.25 – B4002 boiler efficiency using the input-output method (●) and the direct method (×).

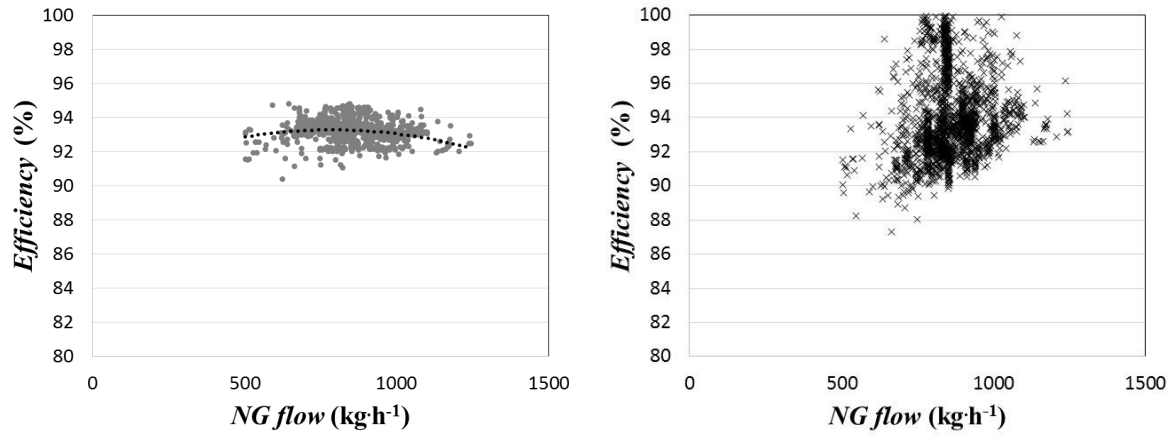

Figure 3.26 – B4003 boiler efficiency using the input-output method (●) and the direct method (×).

A polynomial trend line was fitted to the data regarding the boiler efficiency and natural gas flow for all three boilers. The quadratic equation that was adjusted to the data shown in Figure 3.24 to Figure 3.26 regarding the relation between fuel flow (Q_{fuel}) and boiler efficiency calculated with the indirect method (η_{im}) is given by Equation (3.16).

$$\eta_{im}\ (\%) = a \times {Q_{fuel}}^2 + b \times Q_{fuel} + c \qquad \textbf{(3.16)}$$

The adjusted parameters for each boiler used in Equation (3.16) are shown in Table 3.10. Although the squared correlation coefficient (R^2) is very low for all three boilers: 0.14, 0.03 and 0.06 for B4001, B4002 and B4003, respectively, the equations are still useful for estimating the average boiler efficiency given any given fuel flow.

Table 3.10 – Parameters for describing the relation between boiler efficiency and fuel flow, described by Equation (3.16), regarding the three boilers.

	a	***b***	***c***
B4001	-6.96×10^{-6}	1.15×10^{-2}	89.2
B4002	-4.03×10^{-6}	5.14×10^{-3}	92.2
B4003	-5.05×10^{-6}	7.95×10^{-3}	90.1

Figure 3.27 shows the relation between efficiency, based on LHV, and boiler load provided by the vendor [89]. The plot shows this relation for different boilers, characterized by their efficiencies when operating at 100% load. In the case of the Estarreja MDI plant, the vendor states that efficiency at 100% load is 91%, meaning that the maximum achievable efficiency is approximately 91.5% when operating at 80% of maximum capacity. However, the data provided by the vendor was based upon the assumption that the

boiler would operate with fuel oil. Additionally, excess oxygen content and stack temperature is not specified.

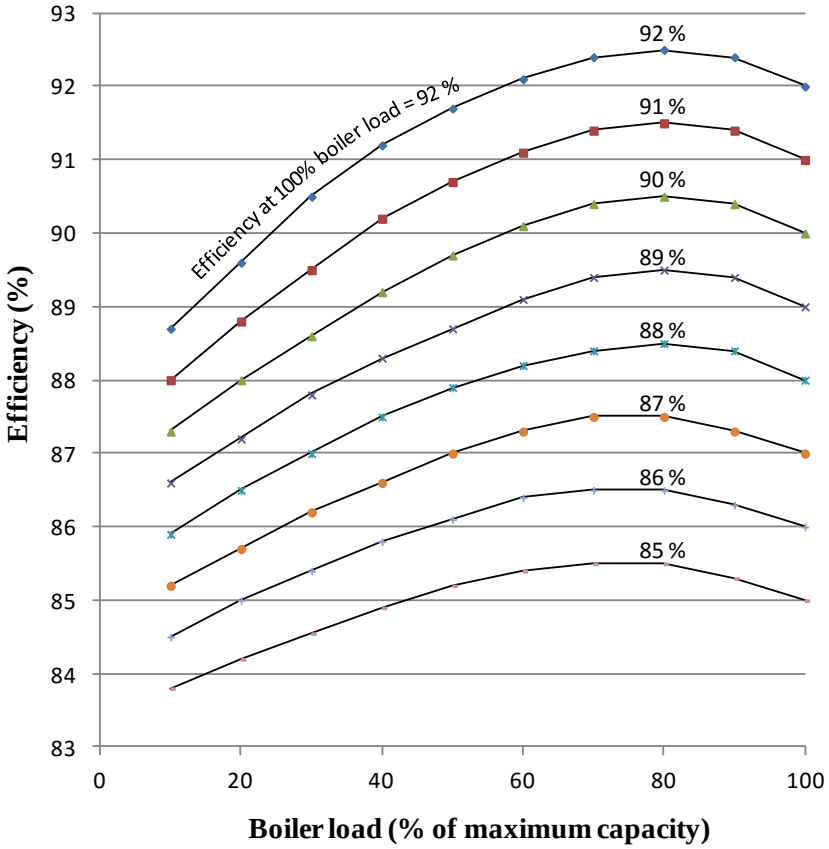

Figure 3.27 – Efficiency curves for different boilers provided by the vendor [89].

When comparing the calculated efficiency for each boiler with the data provided by the vendor, it is possible to verify that the calculated efficiency for each boiler is generally higher, usually above 93%. This can be due to the fact that natural gas is a "cleaner" fuel and does not produce as much soot as fuel oil, rendering a more efficient burn with less heat exchanger fouling. Also, vendor data does specify oxygen content in stack, meaning that the efficiency curves provided by the vendor might be assuming a higher oxygen content in stack than the one that the boilers are normally operated.

By determining each boiler efficiency, it is then possible to calculate the steam produced by each boiler based on the fuel flow.

Boiler efficiency, η, the ratio between the energy transferred to the steam and the energy input is calculated using Eq. (3.17). This efficiency is referred to the fuel low heat value (LHV).

$$\eta = \frac{Q \cdot (H_V - H_{BFW})}{B \cdot LHV} \times 100 \quad \textbf{(3.17)}$$

Where, Q is the steam load (kg/h), H_v and H_{BFW} are the steam and boiler feed water enthalpy (kJ/kg), B is the fuel load (kg/h) and LHV is the low heat value of the fuel.

Based on the boilers behavior described by the parameters stated in Table 3.10, different operating methods were analyzed: Either steam production was equally distributed across the three boilers or the load was distributed so that fuel consumption was minimized.

For finding the load distribution that rendered the minimum fuel consumption the Solver tool available in Microsoft Excel 2013 [90] was used.

The chosen method for solving the optimization problem was the GRG nonlinear method, but since the problem in highly non-linear, a global minimum cannot be guaranteed. However, to ensure that the solver provided the "best" solution, constraints regarding minimum (Q > 0 kg/h) and maximum (Q < 25000 kg/h) boiler steam production were considered. Additionally, several initialization points, within the stated boiler limits, were tested.

Considering an equal steam load distribution scheme, where each boiler has the same steam production, fuel consumption for various steam production levels is stated in Table 3.11. In Table 3.12, the same information is shown but instead regarding an optimal distribution scheme, where the fuel consumption is minimized. Table 3.13 presents the comparison between both schemes in regard to fuel consumption.

Table 3.11 –Estimated fuel consumption for different steam production levels assuming an equal steam load distribution.

Equal load distribution

Fuel Consumption (kg/h)			Steam Production (kg/h)			
B4001	B4002	B4003	B4001	B4002	B4003	Total
398	394	398	6667	6667	6667	*20000*
494	491	496	8333	8333	8333	*25000*
591	589	593	10000	10000	10000	*30000*
687	687	691	11667	11667	11667	*35000*
785	786	789	13333	13333	13333	*40000*
883	886	889	15000	15000	15000	*45000*

Table 3.12 – Estimated fuel consumption for different steam production levels assuming an optimal steam load distribution.

Optimal load distribution						
Fuel Consumption (kg/h)			Steam Production (kg/h)			
B4001	B4002	B4003	B4001	B4002	B4003	Total
779	400	0	13233	6767	0	*20000*
736	737	0	12493	12507	0	*25000*
935	833	0	15875	14125	0	*30000*
807	578	680	13707	9818	11475	*35000*
811	774	775	13780	13131	13090	*40000*
876	859	922	14891	14545	15565	*45000*

Table 3.13 – Comparison between total fuel consumption regarding equal and optimal load distribution schemes. Improvement in fuel consumption of the optimal load distribution relatively to the equal load distribution scheme.

	Equal load distribution	**Optimal load distribution**	
Total Steam Production (kg/h)	Total Fuel Consumption (kg/h)	Total Fuel Consumption (kg/h)	Fuel Consumption Reduction
20000	*1190*	*1178*	**-0.94%**
25000	*1482*	*1475*	**-0.60%**
30000	*1773*	*1768*	**-0.28%**
35000	*2066*	*2065*	**-0.05%**
40000	*2360*	*2360*	**-0.01%**
45000	*2657*	*2657*	**0.00%**

Taking into account the comparison between fuel consumption of both load distribution schemes stated in Table 3.13, it is possible to observe that the improvement in fuel consumption is higher for lower steam production rates and decreases as steam production rate increases, reaching a negligible improvement margin for higher rates.

The results lead to the conclusion that, in this specific case, distributing the load equally across the three boilers is in fact a good option in regard to fuel efficiency. Nonetheless, the described methodology is useful for accessing boiler performance and providing an optimization strategy for distributing boiler load, being especially useful in cases where boilers have higher efficiency discrepancies.

3.2.2 Steam network

Since the centralized steam production is often the preferred arrangement for industrial applications, it is then essential to have an efficient steam distribution network that delivers steam to the various consumption

points. Furthermore, it is essential to have a clear understating of the steam network when assessing process modifications that involve the usage of steam as they impact on the overall balance of the network.

The purpose of producing steam in Estarreja MDI plant is solely for heating process steams. The plant uses steam at two different grades: The abovementioned steam generation system produces high pressure (HP) steam, at 22 barg and 275 C. Additionally, low pressure (LP) steam, at 3.8 barg and 151 C is also used in the plant.

The steam system can be described as follows: HP steam is produced in three boilers that use natural gas as fuel, which is then distributed to the HP steam consumers. The generated HP condensates are fed into a flash drum, where LP steam is generated. When pressure in the LP steam header drops below a given set-point, a pressure control valve lets down HP steam to rise the pressure in the header, whereas when the header pressure increases, LP steam is vented to atmosphere. Some LP steam is directly injected into the process while the remaining is distributed to LP steam consumers. The resulting LP condensates, then go to a flash drum where they depressurize to atmospheric pressure. The condensates from the atmospheric flash drum together with the condensates from the LP flash drum, fresh demineralized water and a small stream of LP steam are fed into a deaerator which is at 2.1 barg to remove non-condensable gases and therefore prevent corrosion issues. Finally, the system is closed when the condensates are fed into the boiler through the boiler feed pumps.

A schematic view of the steam system showing the main branches of the network is presented in Figure 3.28. LP steam is vented to atmosphere when the high pressure control valve in the LP steam header is open. However, since it is normally closed, was not depicted in Figure 3.28.

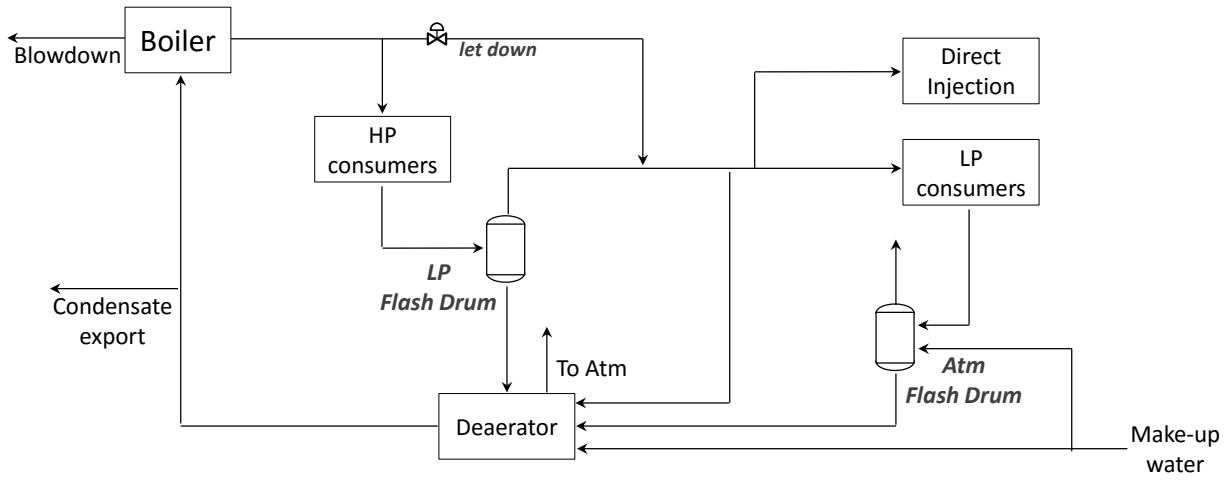

Figure 3.28 – Steam network block diagram.

3.2.3 Steam system thermodynamic model

The ASPEN PLUS thermodynamic model allows the determination of the steam and condensate flow rates and temperature on each point of the network. With this information, it is possible to build the process flow diagram (PFD). The global property method used in the flowsheet was set to STEAMNBS, which is the property method that is based on the steam tables developed by the National Bureau Standards in cooperation with the National Research Council of Canada [91] and is applied throughout the steam system model.

In Figure 3.29, the steam system is represented with a block diagram. In this diagram, the boiler, the high pressure steam network and the low pressure steam network envelopes are highlighted. Other relevant components include the low pressure (*LPDRUM*) and atmospheric (*ATMDRUM*) flash drums, the letdown valve (*LDVALVE*), low pressure (*LPPUMP*) and atmospheric (*ATMPUMP*) condensate pumps, and the deaerator (*DEAERATOR*).

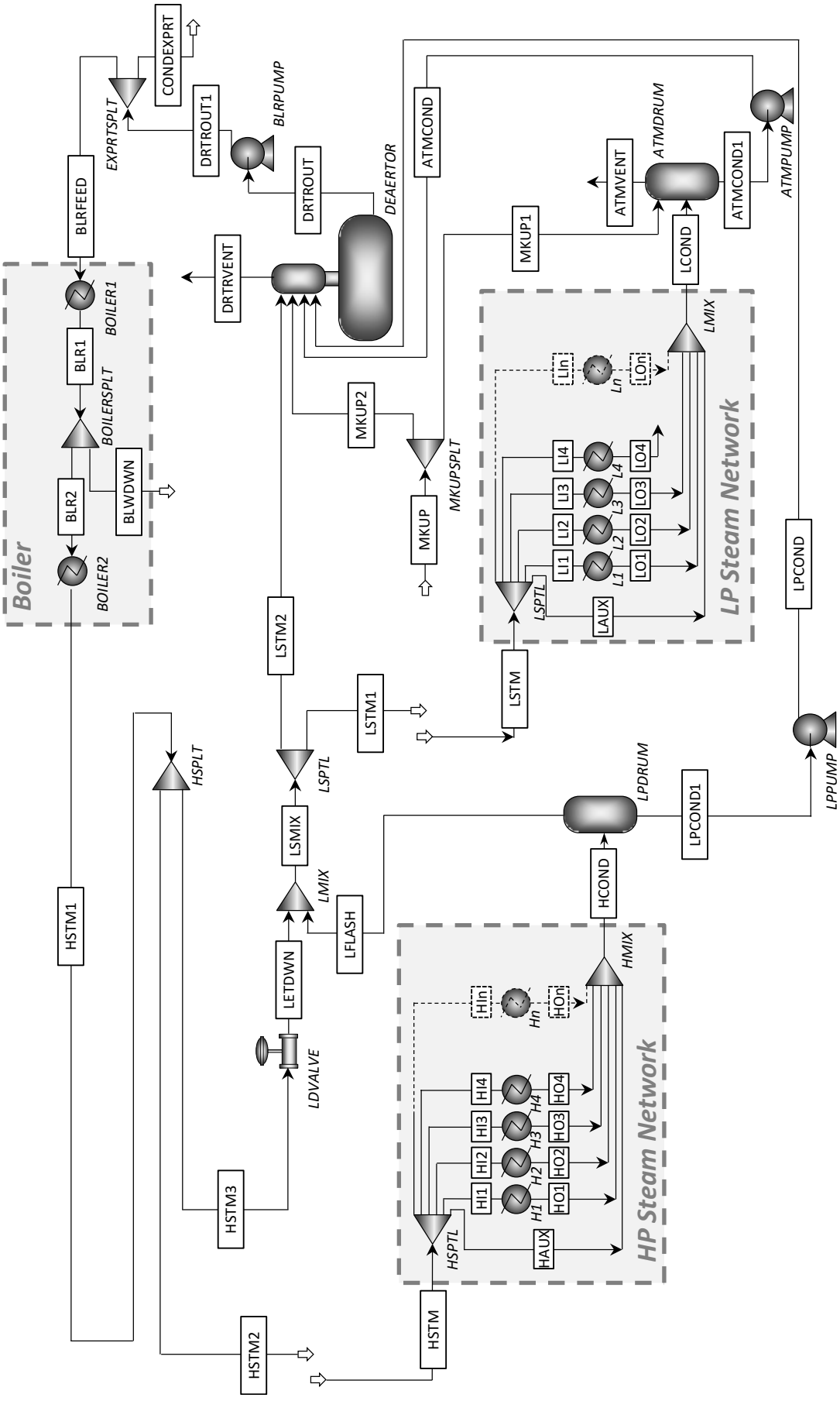

Figure 3.29 – Block diagram of the steam system model implemented in ASPEN PLUS.

3.2.3.1 *Boiler*

The boiler envelope shown in Figure 3.30 consists of three blocks. The first HEATER block (*BOILER1*) simulates the liquid phase in the boiler, where the condensates are heated up to the specified outlet conditions, 22 barg and vapor fraction = 0. With a SPLIT block (*BOILERSPLT*), to avoid over-concentrating scaling and corrosive components in the boiler, the stream leaving the heat exchanger is split to generate a blowdown stream of 500 kg/h (BLWDOWN) that is sent to waste water treatment. The BLR2 stream then follows to the second heat exchanger (*BOILER2*), where the outlet conditions are specified as being 22 barg and 285 C.

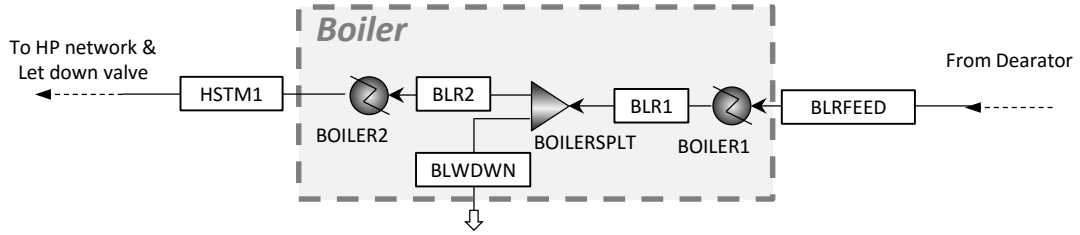

Figure 3.30 – Boiler envelope in ASPEN PLUS.

3.2.3.1 *HP steam letdown to LP steam*

LP steam is mainly generated by the flash of HP condensates in the LP flash drum. However, to meet the demand and keep the pressure in the LP steam header, a letdown valve is responsible for generating LP steam from HP steam.

In Figure 3.31, the HP steam produced in the boiler (HSTM1) is divided in a SPLIT block (*HSPLT*) to generate the stream that is fed to the HP steam network (HSTM2) and the stream that is used to produce LP steam (HSTM3) in the letdown valve (*LDVALVE*).

LP steam (LSMIX) is generated by mixing both the steam from the LP flash drum (LFLASH) and the HP steam letdown (LETDWN) in the MIXER block (*LMIX*). The letdown valve is set in ASPEN PLUS as a VALVE block where the outlet pressure was specified as being 3.8 barg.

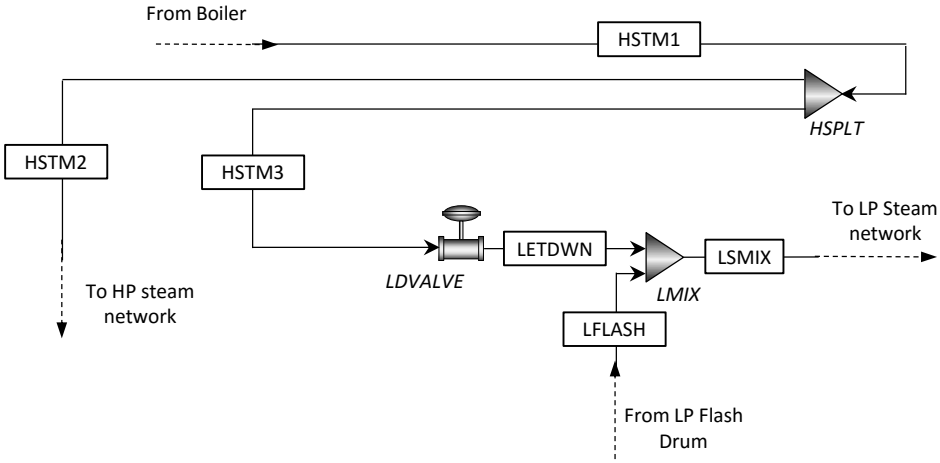

Figure 3.31 – HP and LP steam generation in ASPEN PLUS.

3.2.3.2 *HP steam network*

The HP steam network consists in a set of heat exchangers, fed from a distribution network arranged in parallel*, i.e.,* steam or condensate passes only once through each heat exchanger.

In Figure 3.32, the HP steam network diagram is shown. Steam generated in the boiler (previously split in *HSPLT* block, *vide* Figure 3.31) is fed to a SPLIT block (*HSPLT*) that simulates the supply header and where flow is distributed across all consumers (HI1, HI1, …, HIn). The heat exchangers (*H1, H1, …, Hn*) are set as HEATER blocks where outlet pressure is set to 21.8 barg and outlet temperature to 218.1 C, which are conditions where vapor fraction is 0. The condensate streams (HO1, HO1, …, HOn) are mixed in a MIXER block (*HMIX*), which simulates the return header.

The high pressure condensate stream (HCOND) then follows to a flash drum (*LPDRUM*) that is set in ASPEN PLUS as a FLASH2 block, where pressure is set to 3.8 barg and heat duty to 0 kW. The outlet streams are LP steam (LPFLASH) and LP condensate (LPCOND1). LP steam is fed to the LP steam network, whereas LP condensate is fed to a pump (*LPPUMP*), where pressure increase is set to 0.5 barg. The resulting stream (LPCOND) then follows to the deaerator.

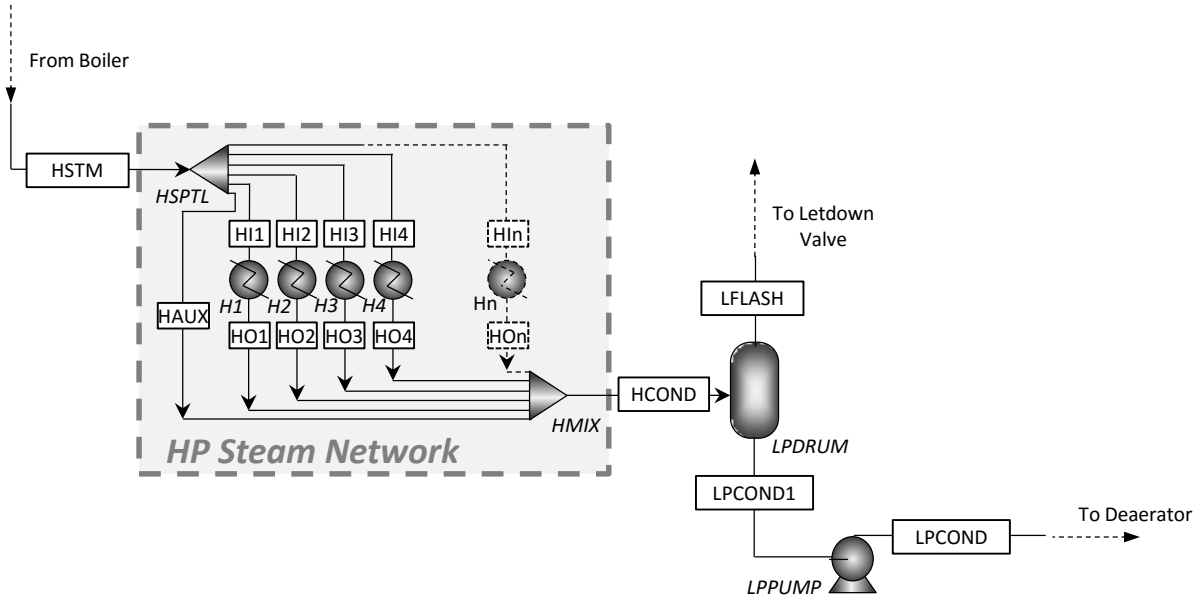

Figure 3.32 – HP network in ASPEN PLUS.

3.2.3.3 *LP steam network*

The LP steam network configuration is similar to the HP steam network. The LP steam network is shown in Figure 3.33.. The main differences from the HP steam network are: the network is fed with LP steam instead of HP steam, the outlet conditions of the heat exchanger blocks are set to 3.3 barg and 145.6 C and there are cases where steam is injected directly into de process, as in the case of stream LI4-*L4*-LO4.

As for the flash drum (*ATMDRUM*), pressure is set to 0 barg and heat duty to 0 kW with the resulting flashed steam being vented to atmosphere (ATMVENT). To drop down the temperature in the flash drum and therefore minimize losses, a cool makeup stream at 23 C (MKUP1) is fed to the drum. Condensates (ATMCOND1) are fed into a pump (*ATMPUMP*) that rises the pressure to 4 barg and sends the condensates (ATMCOND) to the deaerator.

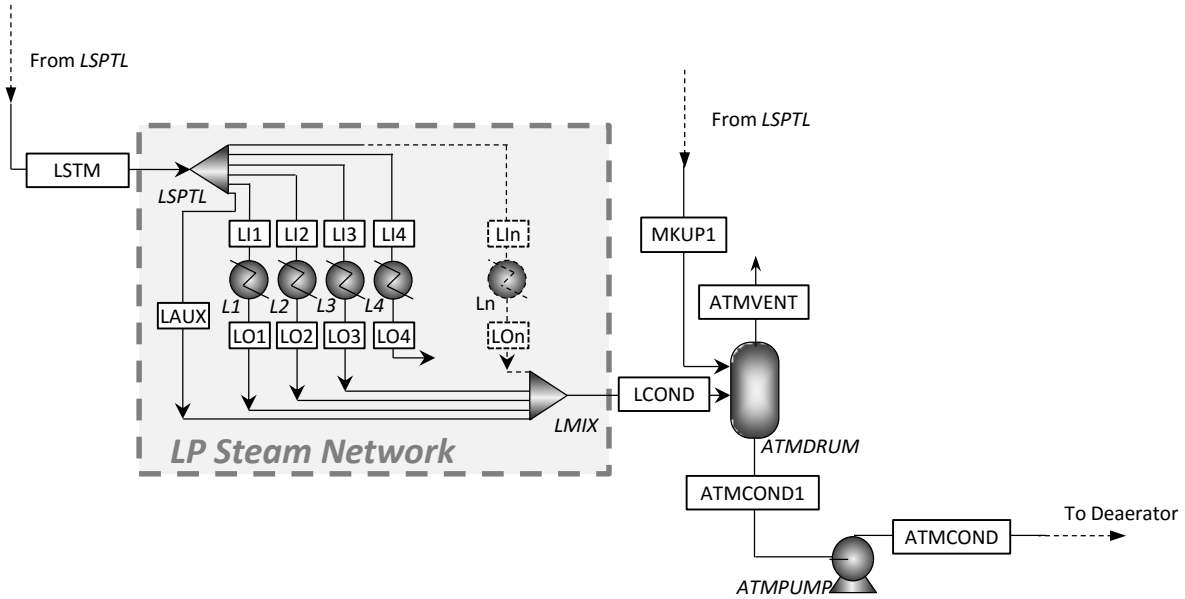

Figure 3.33 – LP network in ASPEN PLUS.

3.2.3.4 ***Deaerator***

Figure 3.34 shows the deaerator system as implemented in ASPEN PLUS. The exact image of the deaerator block in ASPEN PLUS is in fact similar to a flash drum as the ones shown before, however, to have a clearer picture of the equipment a different image was used herein.The deaerator (*DEAERTOR*) is responsible for collecting the condensates from the various sources, removing the non-condensables from the system by applying steam as a scrubbing agent (LSTM2) and then venting to atmosphere (DRTVENT). The *DEAERTOR* is simulated in ASPEN PLUS using a FLASH2 block, where pressure is set to 3 barg and heat duty to 0 kW.

Condensate streams entering in the deaerator are fresh water makeup (MKUP2), condensates generated in the LP steam flash drum (LPCOND) and condensates generated in the atmospheric flash drum (ATMCOND). The total makeup water (MKUP) enters a SPLIT block *MKUPSPLT* where the flow is divided (10% of the total makeup flow (MKUP1) goes to the atmospheric flash drum where the remaining (MKUP2) goes to the deaerator).

A stream (DRTOUT1) then leaves the deaerator and goes to a PUMP block (BLRPUMP), where it is pumped to 24 barg. From the outlet stream DRTOUT1, the flow is divided in a SPLIT block (*EXPRTSPLT*), 100 kg/h of condensates are exported to outside boundary limits (CONDEXPRT). The remaining flow (BLRFEED) follows to the boiler to generate HP steam and therefore complete the cycle.

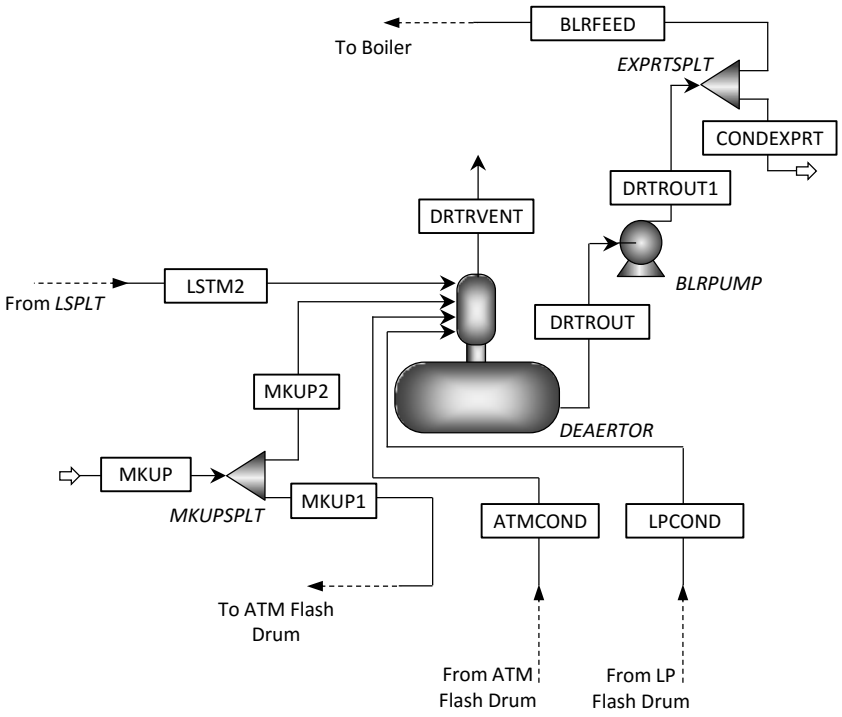

Figure 3.34 – Deaerator in ASPEN PLUS.

3.2.3.5 *Design Specs and Calculator blocks*

To calculate some of variables of the steam system, several Design Specs and Calculator blocks were used in the ASPEN PLUS simulation.

Design specs

For each heat exchanger, the calculated net-duty of the exchanger was specified as being a variable. The target specification for this variable was then set to the known heat duty of the exchanger by manipulating steam flow in the *HSPLT* or *LSPLT* block, depending if the exchanger was part of the HP or LP steam network. This Design Spec facility allowed the simulator to manipulate the inlet steam flow until the desired heat duty was achieved.

Like the cooling water system, the steam system is a semi-closed structure in terms of mass balance. To work around the fact that cyclic systems are harder to converge in ASPEN PLUS, the LSTM and the LSTM2 streams are not connected to each other (as seen in Figure 3.29). A Design Spec is then used to vary LSTM flow with the objective that the LAUX stream flow is negligible, here set to 0.1 kg/h. Another Design Spec is used to manipulate LSTM1 flow in block *LSPLT* so that it is equal LSTM flow.

The required steam flow to work with the deaerator is 1140 kg/h. To accomplish this, a Design Spec is used to vary the flow of the HP stream (HSTM3), being fed to the let-down valve (*LDVALVE*) in block *HSPLT*. The objective is to obtain a steam flow being fed to the deaerator (LSTM2) equal to 1140 kg/h.

As for the HP steam network, a Design Spec is used so that HSTM flow is varied and HAUX stream flow is negligible and equal 0.1 kg/h. Finally, a design spec is used to manipulate the makeup flow (MKUP) so that HSTM2 flow is equal to the one of stream HSTM.

Calculator block

Since the let-down valve generates superheated steam, the mixture of the saturated steam generated in the LP flash drum and the steam generated in the letdown valve generates steam that is slightly superheated. Thus, the temperature of steam in stream LSTM1 is set to be equal to the one in stream LSTM by means of a CALCULATOR block.

3.2.3.6 *Model outputs*

The thermodynamic model of the steam network is used to determine process conditions on each point of the network and evaluate the overall balance of the network. Figure 3.35 shows the process flow diagram with the mass flow on the main branches of the steam network.

This model is then used to evaluate the impact that the heat integration options have on the steam network.

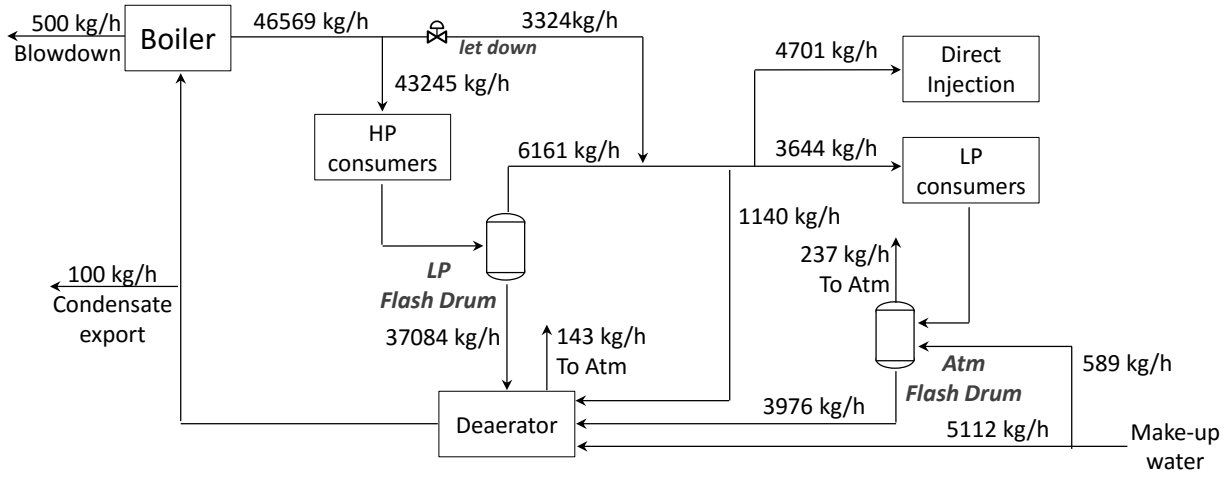

Figure 3.35 – Steam network block diagram.

Taking into account the steam balance shown in Figure 3.35, there is a drive for reducing 3324 kg/h of LP steam consumption without having to make any change in the network configuration of parameters. It is possible however that less than predicted LP steam is generated by the let-down valve. This might be due to steam trap malfunctions or bypasses, enabling HP steam to be let-down to the HP condensates and consequently generating a higher quantity of flashed LP steam. In this case, LP steam would be generated in the steam traps instead of the letdown valve. Therefore, any modification to the system aiming towards

decreasing LP consumption should be preceded by the implementation of programs that monitor the maintenance of the steam straps.

3.2.4 Steam cost estimation

For evaluating the economic viability of the various heat exchanger configurations, it is essential to properly determine steam cost.

Table 3.14 shows the base parameters used to determine steam cost: Demineralized water and natural gas price refer to 2012 price; boiler efficiency is an average value based on the analysis performed in Section 3.2.1; process heat consumption, steam generated in boiler and demineralized water consumption were determined by the mass and heat balances of the steam network; boiler feed water enthalpy refers to liquid water at 22 barg and 135.2 C and steam enthalpy to superheated steam at 23 barg and 285.0 C, with the reference state being 0 barg and 0 C [92].

For clearness sake, a variable number X_i is attributed to each parameter. In Table 3.15, this variable numbers are employed for showing the formulas used to calculate each parameter.

Table 3.14 – Parameters for steam cost estimation

X_1	Demin Water price	1.367 €/t
X_2	Boiler efficiency (LHV)	93.6 %
X_3	Natural Gas (LHV) price	29.4 €/MWh
X_4	Process heat consumption	30.1 MW
X_5	Steam generated in boiler	45.0 t/h
X_6	Demin Water consumption	5.6 t/h
X_7	Boiler feed water enthalpy	570.0 kJ/kg
X_8	HP Steam enthalpy	2977.7 kJ/kg

Table 3.15 shows the intermediate parameters, which lead to the determination of HP steam. HP steam cost was estimated as 0.021 €/kg or 39 €/MWh.

Table 3.15 – Steam cost estimation intermediate calculation parameters.

X_9	$= {X_5 \cdot (X_8 - X_7)}/{3600}$	Q_{in} to HP steam	30.1 MW
X_{10}	$= {X_9}/{X_2 - X_9}$	Q_{lost} boiler	2.1 MW
X_{11}	$= X_9 + X_{10}$	Total Q_{in} on NG	32.1 MW
X_{12}	$= {X_{11}}/{1}$	Hourly Natural gas duty =	32.1 $MW.h^{-1}$
X_{13}	$= X_{12} \cdot X_3$	Cost of Natural gas	944 €/h
X_{14}	$= X_1 \cdot X_6$	Cost of Demin H_2O	8 €/h
X_{15}	$= {(X_{13} - X_{14})}/{X_5}$	Cost of HP steam	21 €/te
X_{16}	$= {(X_{13} - X_{14})}/{X_9}$	Cost of HP steam	39 €/MWh

4 Stream match methodology

Pinch analysis is an useful methodology for identifying the minimum utility targets based on the heat and temperature availability in each range. However, in industrial contexts, there are several layout constraints that involve particular costs when modifications are to be implemented in a new or existent network.

The common framework for applying pinch methodology is focused mainly on the energy minimization of the heat exchanger network. Nevertheless, for industrial applications, it is often necessary to consider other costs such as piping, special materials, process incompatibilities, etc. When designing or retrofitting a heat exchanger network, these limitations are often bypassed by relying on heuristics and experience. Other limitation of the basic pinch methodology is that the approach temperature is fixed for all heat exchangers located at the pinch. However, an optimal global temperature approach does not mean that the local temperature approach of each heat exchanger is optimal. The new stream match methodology proposed in this chapter allows a relaxation of the approach temperature of the heat exchangers located at the pinch, therefore further optimizing the designs.

An important concept that pinch technology defines in the one that gives the name to the methodology itself: The ‘Process pinch’. This concept is important because it defines the temperature at which the process is most constrained in terms of temperature gradient [93]. The new stream match methodology uses this concept to apply different rules depending on whether the stream is above, bellow or crossing the pinch.

Although pinch methodology allows the consideration of forbidden matches to determine hot and cold energy targets, it is not straightforward how to build the network taking into account the forbidden matches as well as the piping costs associated with the heat exchanger physical location, which can represent a significant percentage of the capital costs.

The methodology presented herein is suitable for retrofitting existent heat exchanger networks or for design purposes. The methodology can take into account parameters introduced by the user such as costs associated with: piping, specific heat exchanger configurations or materials, etc.

This methodology is adequate for finding matches that have a positive return on investment in the design activity in such a way that information could avoid or benefit some particular configuration alternative.

4.1 Methodology framework

The methodology proposed in this work relies on the calculation of several matrixes with variables regarding each possible match and a procedure for calculating the heat exchanger duty, Q_{HX}, in- and outlet cold temperature, $T_{c\ in\ HX}$ and $T_{c\ out\ HX}$, in- and outlet hot temperature, $T_{h\ in\ HX}$ and $T_{h\ out\ HX}$, depending on whether the streams are above or below the pinch. The methodology evolves through the following 17 steps:

1. Identify the hot and cold streams, stating in- and outlet temperature, heat duty and heat transfer coefficient for each one. With an available pinch tool determine the pinch temperature of the network. Use an approach temperature that is typical for the industry;
2. Determine which streams are above, crossing or below the pinch;
3. Build a matrix stating the feasibility of each match;
4. Build a matrix stating the piping cost of each possible match. Takes into account all the parameters that influence cost such as distance, piping material, insulation requirements, accessibility, etc.;
5. Build a matrix stating the duty of each possible match (Q_{HX});
6. Build a matrix stating the cold inlet temperature of each possible match ($T_{c\ in\ HX}$);
7. Build a matrix stating the cold outlet temperature of each possible match ($T_{c\ out\ HX}$);
8. Build a matrix stating the hot inlet temperature of each possible match ($T_{h\ in\ HX}$);
9. Build a matrix stating the hot outlet temperature of each possible match ($T_{h\ out\ HX}$);
10. Build a matrix stating the logarithmic mean temperature difference of each possible match ($LMTD$);
11. Build a matrix stating the overall heat transfer coefficient of each possible match (U);
12. Build a matrix stating the heat exchange area for each possible match (A);
13. Build a matrix stating the annualized capital cost for each possible match ($Cost_{yr}$);
14. Build a matrix stating the yearly return for each possible match (YR);
15. Match the streams that give the highest return. If above the pinch start with the hot stream with the lowest outlet temperature and gradually move out of the pinch, if below the pinch start with the cold streams with the highest outlet temperature and gradually move out of the pinch;
16. For each match, go back to step 3 and recalculate the variables until no more matches with positive return are possible (see A3 (Stream match tools) for further information on the developed tool)

This method is based on the formulation of matrixes containing specific information of each match that in combined into a single matrix that gives the annualized return of each match. An iterative process is then applied to find the matches that provide maximum return.

The several steps of this methodology are illustrated in next subsections and some information about the implementation on Excel worksheet is also given in A3 (Stream match tools).

Step 1 and 2 - Traditional pinch technology tools are applied to determine the pinch temperature and evaluate which streams are above, crossing or below the pinch.

Step 3 - Since there are constraints that prevent some streams to be matched, such as safety issues or process incompatibilities, a matrix with the possible (✓) and forbidden (✘) matches is built. The construction of this matrix is based on the process constraints as well as physical limitations. Therefore, a deep understating of the process and the physical constraints is required to build the feasibility matrix.

Table 4.1 shows an example of a matrix with the feasible and forbidden matches in the process with cold streams as lines and hot streams as columns. If a match is possible but for example involves a costly design or unsafety exchange it should still be considered as unfeasible.

Table 4.1 – Example of the feasibility matrix. In this example match C1-H1 would not be feasible.

	H1	⋯	Hn
C1	✘		✓
⋮	⋮	⋱	⋮
Cn	✓	⋯	✓

In the Excel worksheet where the methodology is implemented the possible matches assume a value of 1 and forbidden matches a 0 in the feasibility matrix.

Step 4 - There might be some additional costs associated with the piping of each possible match. Therefore, a matrix stating these costs is stated.

Table 4.2 – Example of the piping cost, $Cost_{piping}$, relative to each match.

	H1	⋯	Hn
C1	$Cost_{piping\ C1H1}$		$Cost_{piping\ C1Hn}$
⋮	⋮	⋱	⋮
Cn	$Cost_{piping\ CnH1}$	⋯	$Cost_{piping\ CnHn}$

Steps 5 to 9 - Next, matrixes with the heat duty Q_{HX}, in- and outlet cold temperature, $T_{c\ in\ HX}$ and $T_{c\ out\ HX}$, in- and outlet hot temperature, $T_{h\ in\ HX}$ and $T_{h\ out\ HX}$, are determined according the steps presented in Section **4.2**, for the possible matches . As described in the aforementioned section, the calculation procedure will depend on whether the streams are above, crossing or below the pinch. For each variable, a set of matrixes like the ones shown in Table 4.3 to 4.8 are determined.

Table 4.3 – Example of the heat duty matrix, Q_{HX}, relative to each match.

	H1	⋯	Hn
C1	Q_{C1H1}		Q_{C1Hn}
⋮	⋮	⋱	⋮
Cn	Q_{CnH1}	⋯	Q_{CnHn}

Table 4.4 – Example of the cold inlet temperature matrix, $T_{c\ in\ HX}$, relative to each match.

	H1	⋯	Hn
C1	$T_{c\ in\ C1H1}$		$T_{c\ in\ C1Hn}$
⋮	⋮	⋱	⋮
Cn	$T_{c\ in\ CnH1}$	⋯	$T_{c\ in\ CnHn}$

Table 4.5 – Example of the cold outlet temperature matrix, $T_{c\ out\ HX}$, relative to each match.

	H1	⋯	Hn
C1	$T_{c\ out\ C1H1}$		$T_{c\ out\ C1Hn}$
⋮	⋮	⋱	⋮
Cn	$T_{c\ out\ CnH1}$	⋯	$T_{c\ out\ CnHn}$

Table 4.6 – Example of the hot inlet temperature matrix, $T_{h\ in\ HX}$, relative to each match.

	H1	⋯	Hn
C1	$T_{h\ in\ C1H1}$		$T_{h\ in\ C1Hn}$
⋮	⋮	⋱	⋮
Cn	$T_{h\ in\ CnH1}$	⋯	$T_{h\ in\ CnHn}$

Table 4.7 – Example of the hot outlet temperature matrix, $T_{h\ out\ HX}$, relative to each match.

	H1	⋯	Hn
C1	$T_{h\ out\ C1H1}$		$T_{h\ out\ C1Hn}$
⋮	⋮	⋱	⋮
Cn	$T_{h\ out\ CnH1}$	⋯	$T_{h\ out\ CnHn}$

Step 10 - Based on the Q_{HX}. $T_{c\ in\ HX}$, $T_{c\ out\ HX}$, $T_{h\ in\ HX}$ and $T_{h\ out\ HX}$ a matrix with the logarithmic mean temperature difference (LMTD) for each match is calculated.

Table 4.8 – Example of the Logarithmic Mean Temperature Difference matrix, *LMTD*, relative to each match.

	H1	⋯	Hn
C1	$LMTD_{C1H1}$		$LMTD_{C1Hn}$
⋮	⋮	⋱	⋮
Cn	$LMTD_{CnH1}$	⋯	$LMTD_{CnHn}$

Step 11 - Next, a matrix with the overall heat transfer coefficient, *U,* for each match is calculated according to Eq. (4.1). Where HTC_c and HTC_h are the heat transfer coefficients for the cold and hot side, respectively. Wall resistance was ignored in this approach.

$$\mathrm{U} = \frac{1}{{}^{1}/_{\mathrm{HTC_C}} + {}^{1}/_{\mathrm{HTC_H}}} \tag{4.1}$$

Table 4.9 – Example of the Overall Heat Transfer Coefficient, *U,* relative to each match.

	H1	⋯	Hn
C1	U_{C1H1}		U_{C1Hn}
⋮	⋮	⋱	⋮
Cn	U_{CnH1}	⋯	U_{CnHn}

Step 12 - For determining the matrix with the required heat transfer area of each match Eq. (4.2) was used. The parameters in the equation are retrieved from the previously calculated matrixes.

$$\mathrm{Area} = \frac{\mathrm{Q_{HX}}}{\mathrm{LMTD} \cdot \mathrm{U}} \tag{4.2}$$

Table 4.10 – Example of the Area, *A,* relative to each match.

	H1	⋯	Hn
C1	A_{C1H1}		A_{C1Hn}
⋮	⋮	⋱	⋮
Cn	A_{CnH1}	⋯	A_{CnHn}

Step 14 - Capital cost ($Cost_{Cap}$) is the investment needed to fulfill any given match. It is based on the heat exchange area, piping and pumping costs and requirements for special materials.

In this work, only the area cost is considered and the $Cost_{Cap}$ is calculated according to Eq.(4.3), where parameters *a*, *b*, and *c* are specified. However, it would be possible to include other costs by changing the cost function in the $Cost_{Cap}$ matrix. Additionally, it is possible to have different equations in the same matrix, for example for streams with special material requirements.

$$\mathrm{Cost_{cap}}[€] = \mathrm{a} + \mathrm{b} \cdot (\mathrm{Area}[\mathrm{m^2}])^{\mathrm{c}} + Cost_{piping} \tag{4.3}$$

For a leveled comparison between different configurations, the capital cost was converted to an annualized cost, $Cost_{yr}$, by multiplying the capital cost by an annualization factor ($A_{n,i}$), as shown in Eq. (4.4).

$$\mathrm{Cost_{yr}[€/yr]} = \mathrm{Cost_{cap}} \cdot \mathrm{A_{n,i}} \quad \textbf{(4.4)}$$

The annualized factor, $A_{n,i}$, is given by Eq. (4.5), where *i* is the interest rate and *n* the equipment life span in years.

$$\mathrm{A_{n,i}} = \left(\frac{\mathrm{i}(1+\mathrm{i})^{\mathrm{n}}}{(1+\mathrm{i})^{\mathrm{n}}-1}\right) \quad \textbf{(4.5)}$$

Table 4.11 – Example of the yearly cost, *Cost$_{yr}$*, relative to each match.

	H1	⋯	Hn
C1	*Cost $_{yr\ C1H1}$*		*Cost $_{yr\ C1Hn}$*
⋮	⋮	⋱	⋮
Cn	*Cost $_{yr\ CnH1}$*	⋯	*Cost $_{yr\ CnHn}$*

Step 15 - The yearly return (*YR*) is calculated taking into consideration the cost of hot utility and cold utility used to heat up or cool down each stream, where *OH* is the operating hours per year.

$$\mathrm{YR} = \mathrm{Q_{HX}} \cdot \mathrm{OH[h \cdot yr^{-1}]} \cdot (\mathrm{Cost_{Cold\ util}[€ \cdot kWh^{-1}]} + \mathrm{Cost_{hot\ util}[€ \cdot kWh^{-1}]}) - \mathrm{Cost_{yr}[€/yr]} \quad \textbf{(4.6)}$$

Table 4.12 – Example of the yearly return, YR$_{yr}$, relative to each match.

	H1	⋯	Hn
C1	*YR $_{C1H1}$*		*YR $_{C1Hn}$*
⋮	⋮	⋱	⋮
Cn	*YR $_{CnH1}$*	⋯	*YR $_{CnHn}$*

Step 15 and 16 - Finally, streams above and below the pinch are matched according to the highest return.

4.2 Stream matching illustrated with Case Study 1

For a clearer perception of the stream match methodology, a case study will be used throughout the description of the proposed approach as an example for the various steps of the methodology. The example is taken from FI^{2}EPI [94] and shows a system with 2 hot streams and 2 cold streams. In Table 4.13, the inlet (T_{in}) and outlet (T_{out}) temperatures, heat capacity flow rate (CP), heat transfer coefficient (HTC) and heat load (Q) of each stream data regarding the example is shown.

Table 4.13 – Stream data for CS 1.

	T_{in} [C]	T_{out} [C]	CP [kW·C^{-1}]	Q [kW]	HTC [kW·m^{-2}·C^{-1}]	Cost [€·kWh^{-1}]
H1	200	90	40	4400	0.5	
H2	180	60	20	2400	0.5	
C1	30	165	30	4050	0.5	
C2	110	170	50	3000	0.5	
CU	25	40	-	-	3.5	4 x 10^{-3}
HU	190	190	-	-	3.5	25 x 10^{-3}

The values shown in Table 4.14 are the economic and cost law parameters used by the authors in their work FI^{2}EPI [94]. Parameters *i* and *n* are used in by Eq. (4.5) to determine the annualized factor whereas parameters *a*, *b* and *c* shall be used in Eq. (2.1) to determine the capital cost of each heat exchanger.

Table 4.14 – Economic data regarding CS 1.

Rate of return (*i*)	4%
Plant life (*n*)	5 years
Hours of operation per year	8500
a	7786.7
b	1778.8
c	0.83

<u>Step 1</u> - Determine process pinch temperature

The determination of the process pinch is done by using the traditional pinch technology methods, as described in Section 4.

Knowing the pinch temperatures allow the evaluation of which streams are above, below or crossing the pinch. For the stream matching methodology described ahead there will be a clear distinction between above and below pinch areas. In the case of a stream that is crossing the pinch then this stream will be divided into two, above and below the pinch, requiring the calculation of the heat load in each zone.

Case study 1 (Step 1)

Assuming a 12 C global minimum approach (ΔT_{min}), which is a typical temperature approach for the chemical industry and is the value used in by the authors FI^{2}EPI [94]. The approach of each match will be individually adjusted in a later step of the methodology so this parameter is important at this stage for determining the position of each stream in regard to the pinch point.

The cold pinch temperature is 110 C and the hot pinch temperature is 122 C. Figure 4.1 shows the network from CS1 with the pinch line also represented. It is possible to observe that stream H1, H2 and C1 are crossing the pinch while the others are either above or below the pinch. Stream C2 is above the pinch with the inlet temperature of this stream located exactly at the pinch.

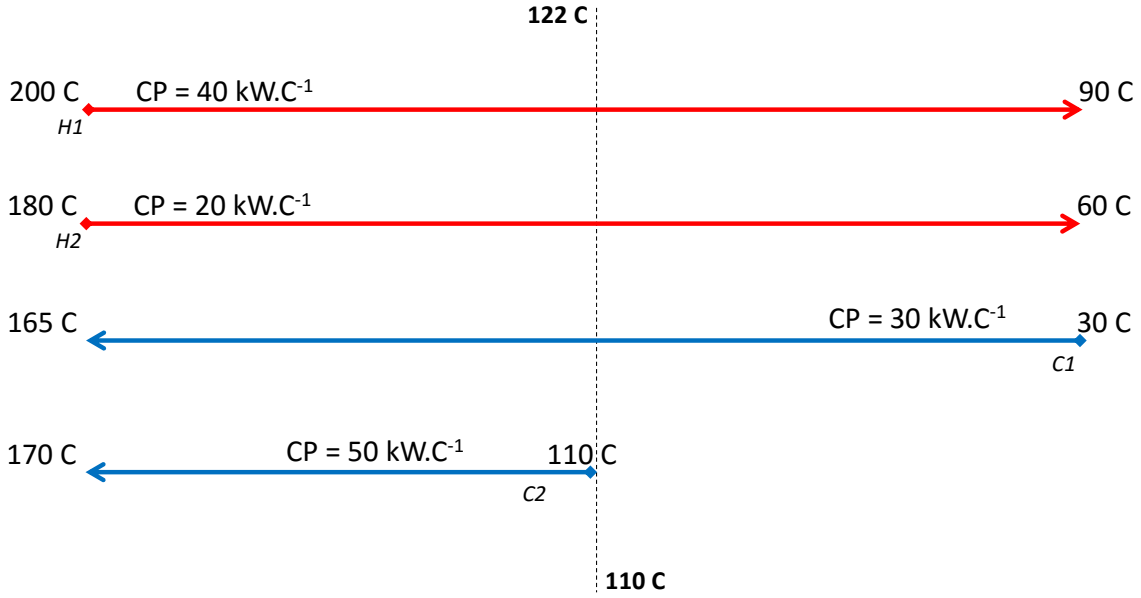

Figure 4.1 – Representation of hot and cold streams of case study 1 with the pinch line.

Figure 4.2 and Figure 4.3 show the streams that are located above and below the pinch, respectively. Streams H1, H2 and C1 are cut at the pinch, *i.e.*, they are crossing the pinch. Stream C2 is exactly at the pinch but is not crossing it.

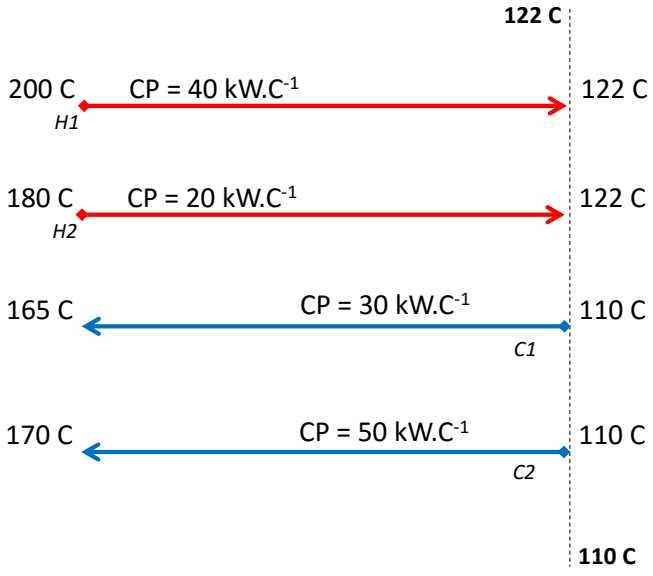

Figure 4.2 – Representation of hot and cold streams of CS 1 above the pinch. Streams H1, H2 and C1 are cut at the pinch.

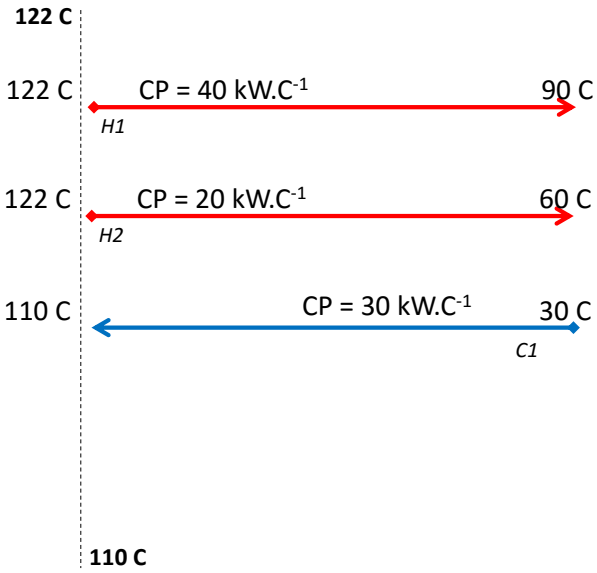

Figure 4.3 – Representation of hot and cold streams of CS 1 below the pinch. Streams H1, H2 and C1 are cut at the pinch.

In Table 4.15, the temperatures and heat load of the streams above and below the pinch are presented. In the cases where streams don't show any value means that they are not present in that zone.

Table 4.15 – Heat load and temperatures of streams of CS 1 above and below the pinch.

	Above pinch			*Below pinch*		
	T_{in} [C]	T_{out} [C]	Q [kW]	T_{in} [C]	T_{out} [C]	Q [kW]
H1	200	122	3120	122	90	1280
H2	180	122	1160	122	60	1240
C1	110	165	1650	30	110	2400
C2	110	170	3000	-	-	-

Step 2 - Split streams at the pinch according to pinch rules

Pinch methodology states that, when exactly at the pinch temperature, the number of hot streams (N_{hot}) and CP_{hot} should be lower than the number of cold streams (N_{cold}) and CP_{cold} if above the pinch and vice-versa if bellow the pinch. If any of these rules is not satisfied then a steam should be split so that the rules are fulfilled. Table 4.16 summarizes the abovementioned pinch rules.

Table 4.16 – Rules for splitting streams at the pinch.

Above pinch	Below pinch
$N_{hot} \leq N_{cold}$	$N_{cold} \leq N_{hot}$
$CP_{hot} \leq CP_{cold}$	$CP_{cold} \leq CP_{hot}$

Case study 1 (Step 2)

Taking into account the pinch rules for splitting streams and the network depicted in Figure 4.1, the need for splitting streams will be evaluated.

Above the pinch, the number of hot steams is lower than the number of cold streams. Additionally, for each hot stream at the pinch there is at least one cold stream with a higher CP.

Bellow the pinch, the number of cold steams is lower than the number of hot streams and there is a cold stream with a higher CP than the hot stream.

These conditions mean that it is not necessary to split streams above or below the pinch. Table 4.17 and 4.18 show the results of applying the stream splitting rules to the CS1 network.

Table 4.17 – Stream splitting rules for CS1 regarding the number of streams immediately above/bellow the pinch.

Above pinch	Below pinch
$N_{hot} \leq N_{cold}$	$N_{cold} \leq N_{hot}$
$N_{hot} = 2 = N_{cold}$ ✓	$N_{cold} = 1 < 2 = N_{hot}$ ✓

Table 4.18 – Stream splitting rules for CS1 regarding the CP of streams immediately above/bellow the pinch.

Above pinch	Below pinch
$CP_{hot} \leq CP_{cold}$	$CP_{cold} \leq CP_{hot}$
$CP_{H1} \leq CP_{C2}$ ✓	$CP_{C1} \leq CP_{H1}$ ✓
$CP_{H2} \leq CP_{C1,C2}$ ✓	

<u>Step 3</u> - Match streams above the pinch

Above the pinch, every hot stream should cross exchange with a cold stream and therefore only hot utility should be used. To maximize the heat recovery above the pinch, the strategy used for matching the streams above the pinch was to assume that the heat exchanger hot outlet temperature is equal to the hot stream outlet temperature, *i.e.*, $T_{H\,out\,HX} = T_{H\,out}$.

In Figure 4.4 (a - d) the matching options of the streams that satisfy the condition $T_{C\,out} > T_{H\,out} - \Delta T_{min}$ and are above the pinch with a $CP_{hot} > CP_{cold}$ are shown.

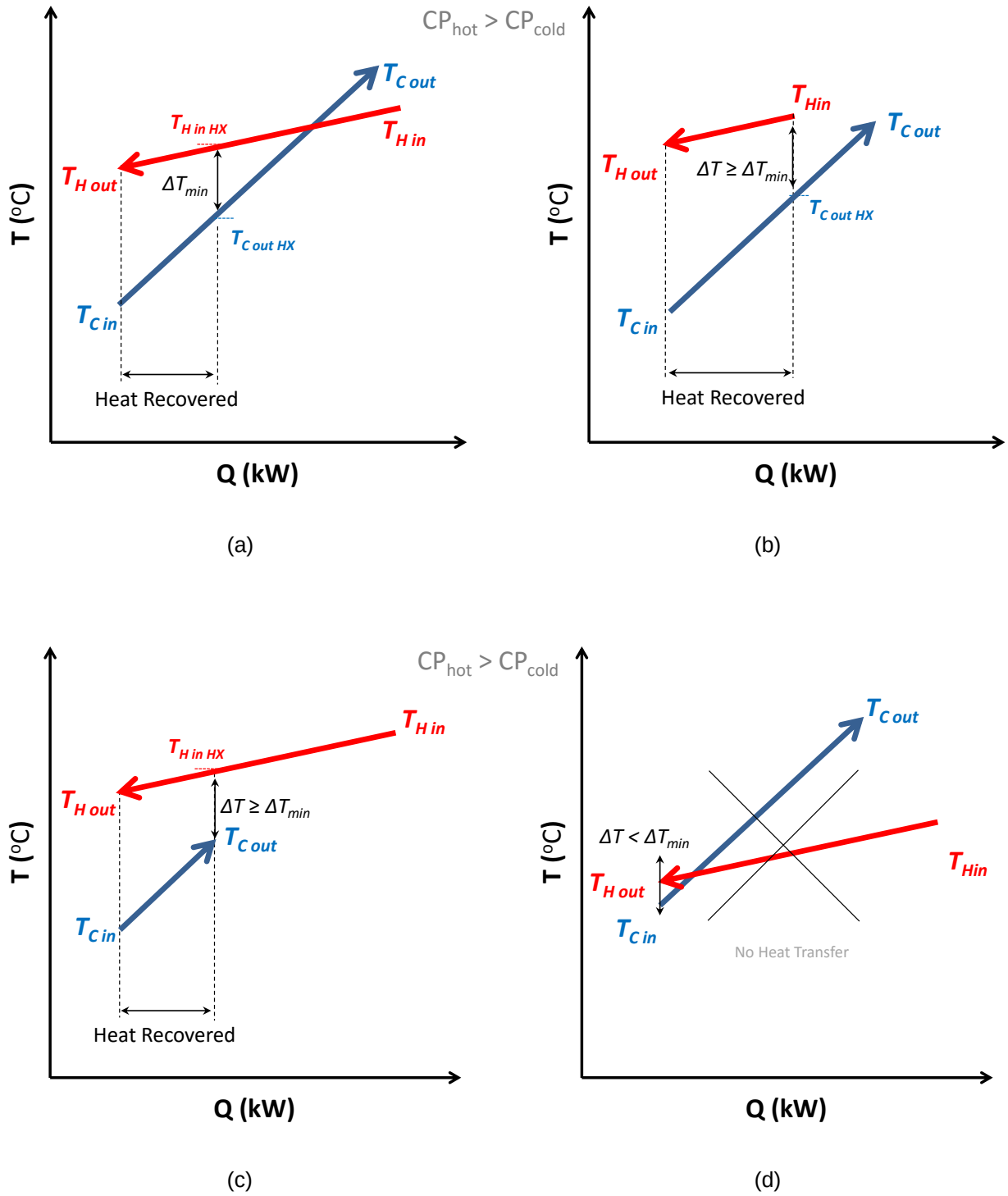

Figure 4.4 – Possible cross-exchange scenarios when $CP_{hot} > CP_{cold}$ with a pinch point for streams that are above the pinch point.

Similarly, for $CP_{hot} < CP_{cold}$ of pinched streams above the pinch, the possible scenarios are shown in Figure 4.5 (a - c)

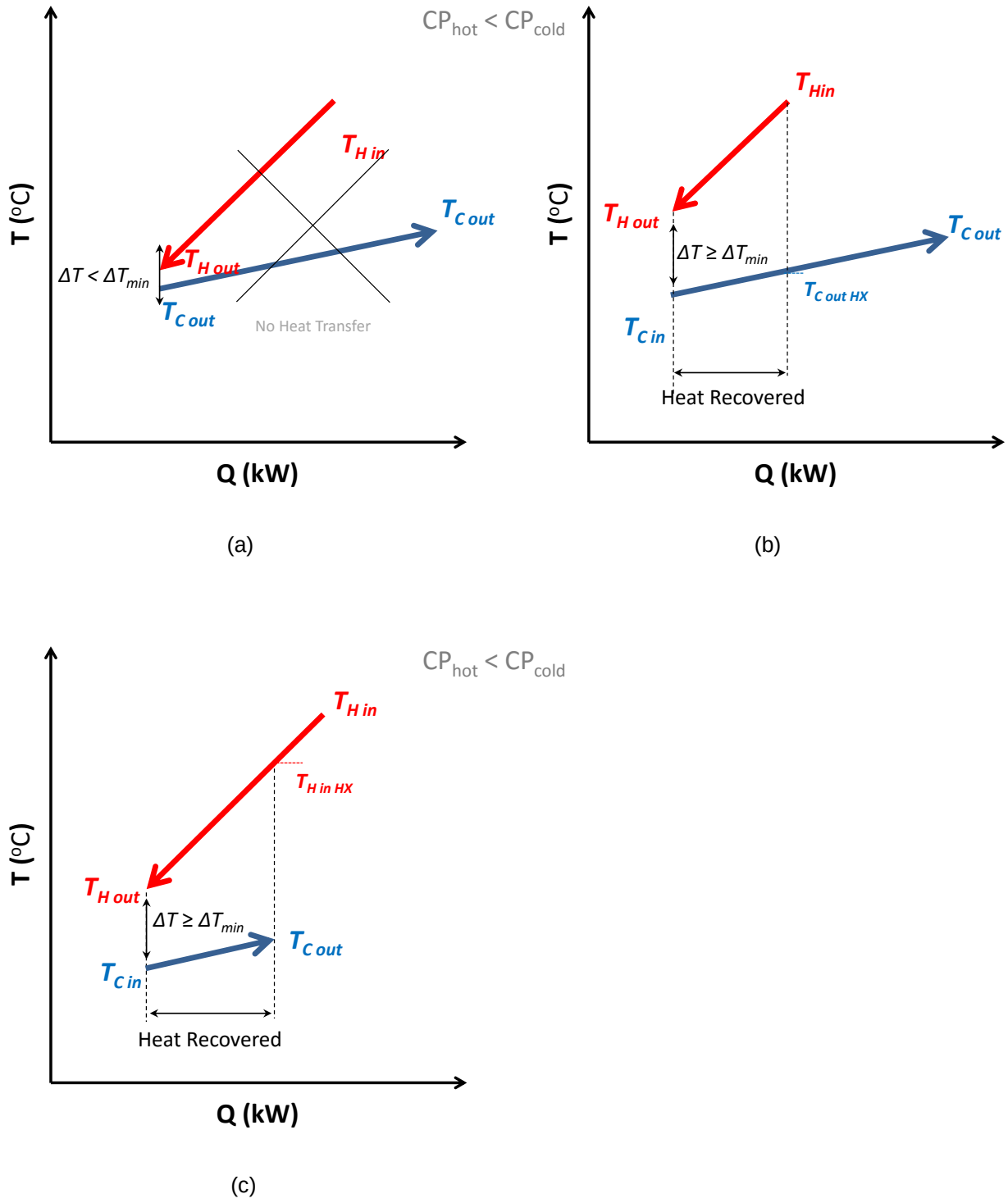

Figure 4.5 – Possible cross-exchange scenarios when $CP_{hot} < CP_{cold}$ with a pinch point for streams that are above the pinch point.

If streams are not pinched amongst them ($T_{C\,out} < T_{H\,out} - \Delta T_{min}$) and are above the pinch then the possible scenarios are shown in Figure 4.6 (a - b).

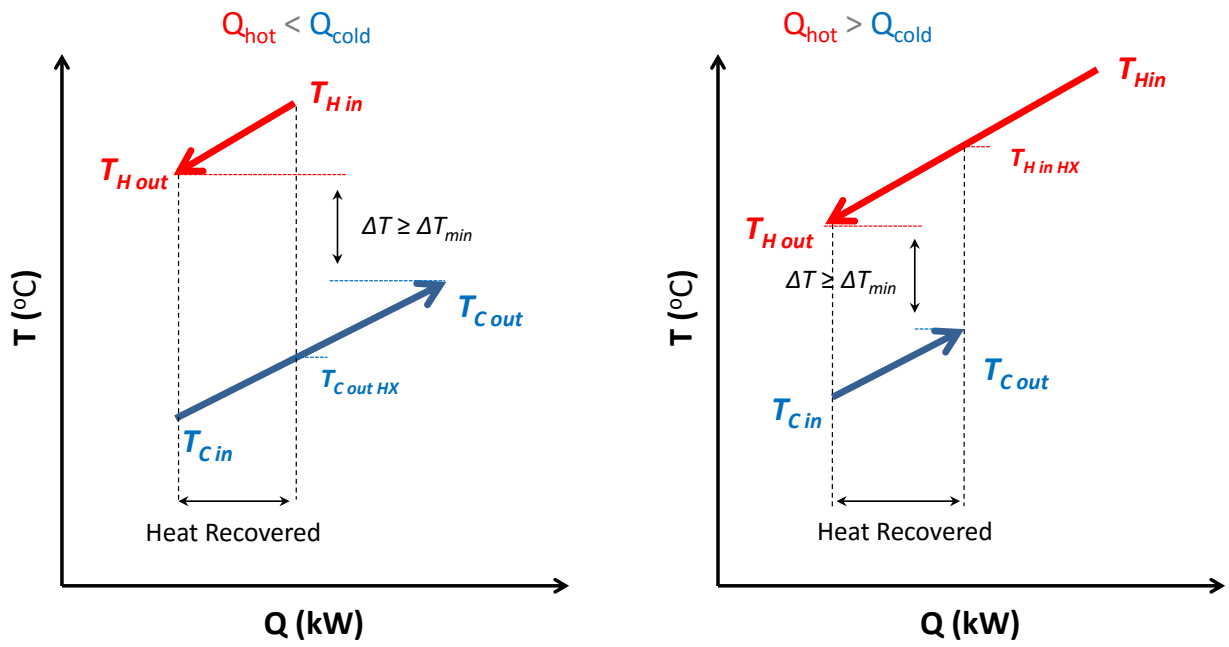

Figure 4.6 – Possible cross-exchange scenarios when streams are not pinched and are above the pinch point.

Taking into consideration the possible scenarios shown in Figure 4.4, Figure 4.5 and Figure 4.6, the algorithm for determining Q_{HX}. $T_{c\,in\,HX}$, $T_{c\,out\,HX}$, $T_{h\,in\,HX}$ and $T_{h\,out\,HX}$ is detailed in Figure 4.7.

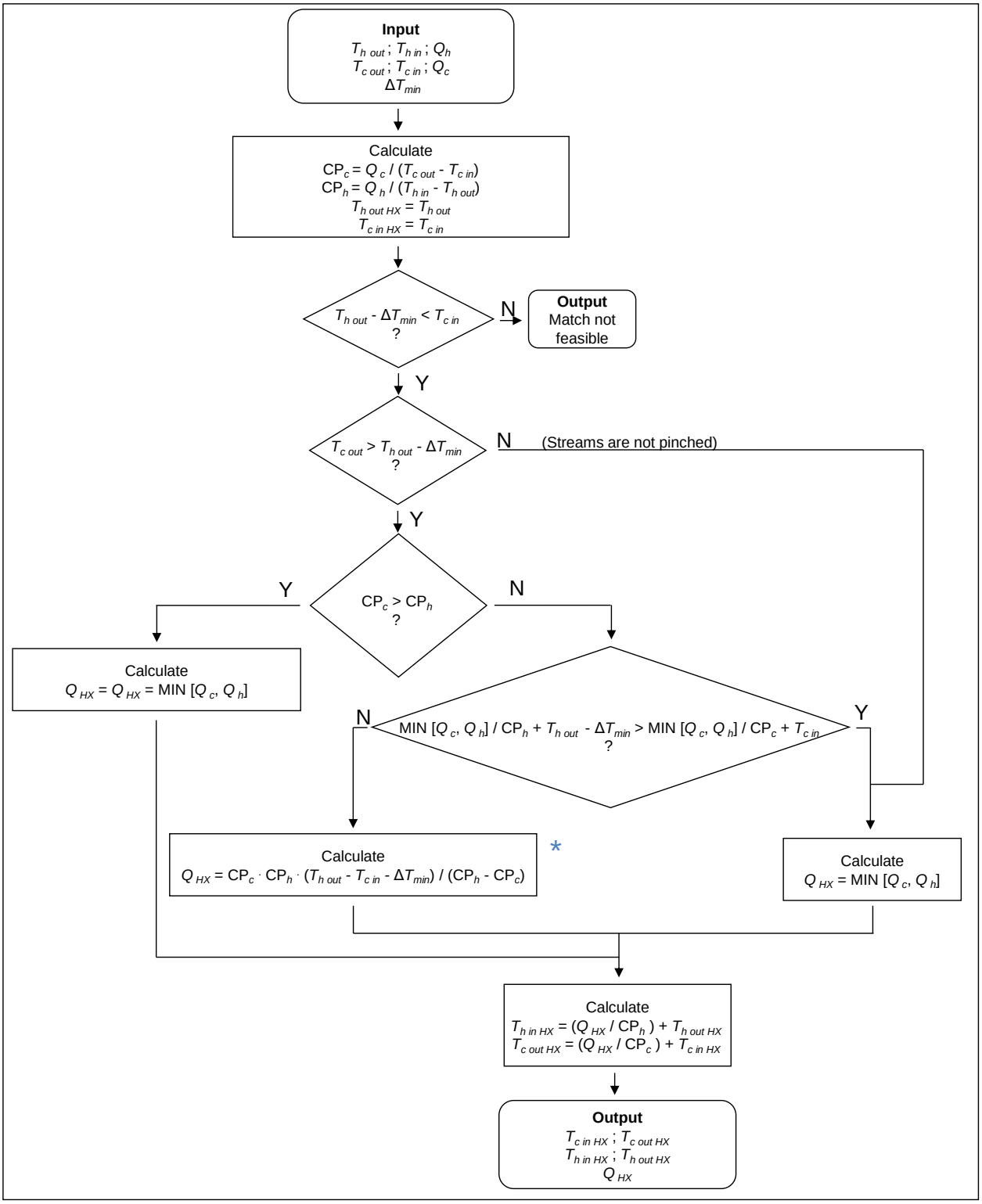

Figure 4.7 – Algorithm used to determine the in- and outlet temperature and duty of each match for the streams located above the pinch. The expression marked with an "*" is detailed in Appendix A2.

The described algorithm returns Q_{HX}. $T_{c\,in\,HX}$, $T_{c\,out\,HX}$, $T_{h\,in\,HX}$, $T_{h\,out\,HX}$. This information is used to determine the *LMTD*, *A*, $Cost_{yr}$ and *YR* matrixes.

After the Yearly Return matrix is determined, select the hot stream with the lowest outlet temperature, *i.e.*, closest to the pinch. For this stream, choose the match with the highest return and match the streams. If there is no match with a positive return proceed to the next hot stream. Gradually move out of the pinch, recalculating the matrixes whenever a match is made, until the hot stream with the highest inlet temperature is matched.

Case study 1 (Step 3)

For matching the streams above the pinch start with the hot streams with the lowest outlet temperature. In the case of streams H1 and H2 share the same inlet temperature, therefore the selected match will be the one with the highest return between both streams.

In Table 4.19, the yearly return relative to each match after the first pass above the pinch shows that the match with the highest return is H1-C2. The duty of C2 is fulfilled with this match.

Table 4.19 –Yearly return relative to each match in CS 1 (1st pass above the pinch).

	H1	H2
C1	181 969	248 800
C2	**654 415**	255 357

Accordingly, Figure 4.8 shows the CS 1 network showing the H1-C2 match.

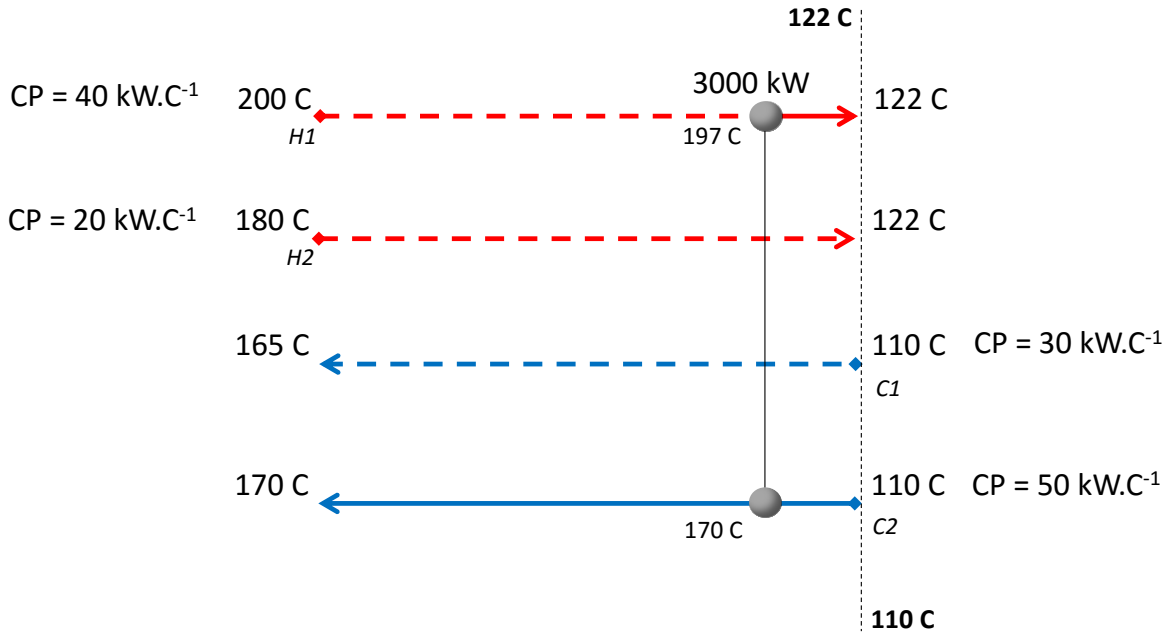

Figure 4.8 – CS 1 network configuration, above the pinch, with match between H1 and C2.

The matching procedure continues with stream H2, which is now the hot stream with the lowest inlet temperature. In Table 4.20, the yearly return relative to each match in CS 1 after the second pass above

the pinch shows that the only possible match is H2-C1 and has a positive return. The duty of H2 is fulfilled with this match.

Table 4.20 –Yearly return relative to each match in CS 1 (2nd pass above the pinch).

	H1	H2
C1	26 289	**248 800**
C2	-	-

Accordingly, Figure 4.9 shows the CS 1 network showing the H1-C2 match.

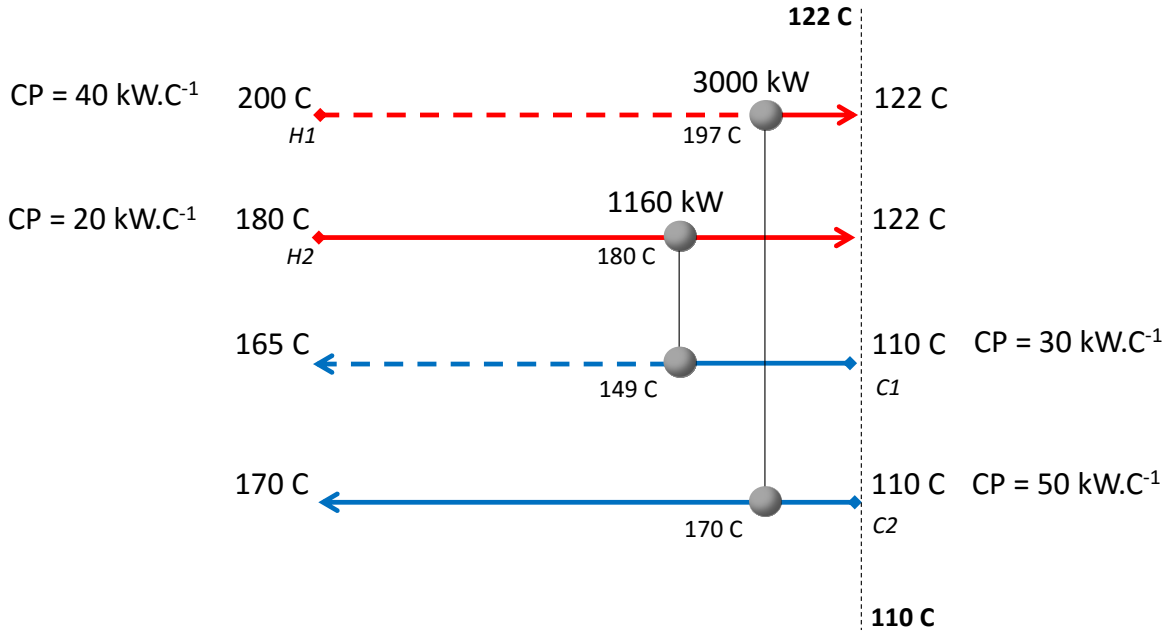

Figure 4.9 – CS 1 network configuration, above the pinch, with match between H2 and C1.

The third pass in the matching procedure will match stream H1, which the remaining hot stream that is still not complete. In Table 4.21, the yearly return relative to the matching of stream H1 with C1 has a positive return.

Table 4.21 –Yearly return relative to each match in CS 1 (3rd pass above the pinch).

	H1	H2
C1	**25 237**	-
C2	-	-

Accordingly, Figure 4.10 shows the CS 1 network showing the H1-C1 match.

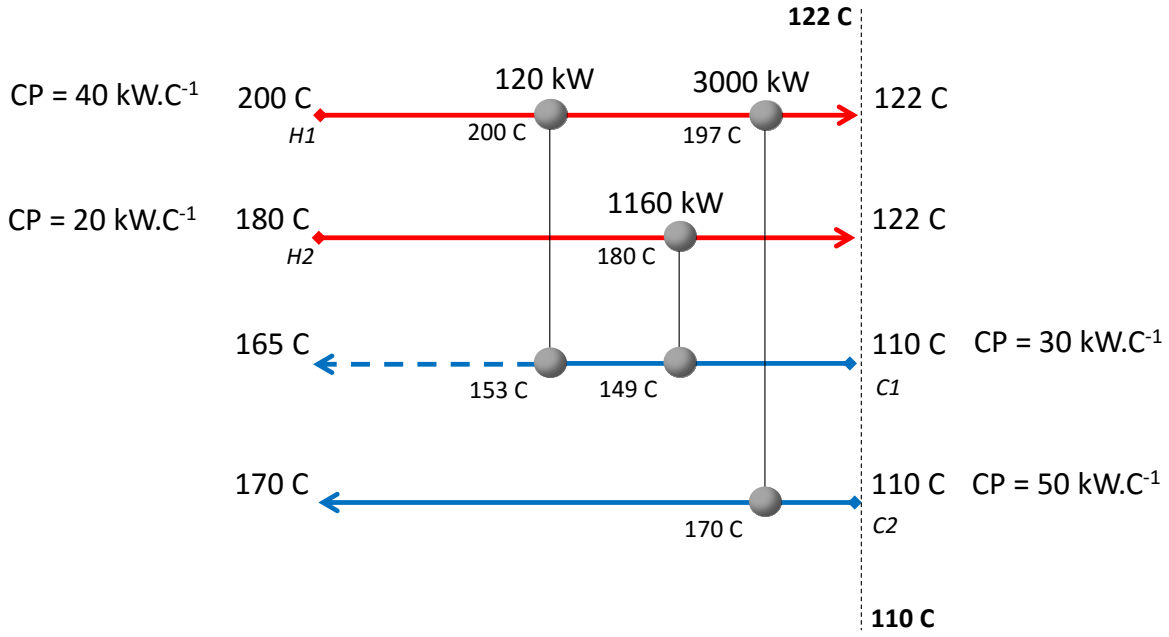

Figure 4.10 – CS 1 network configuration, above the pinch, with match between H1 and C1.

Finally, the remaining duty in the C1, 370 kW, is fulfilled with hot utility.

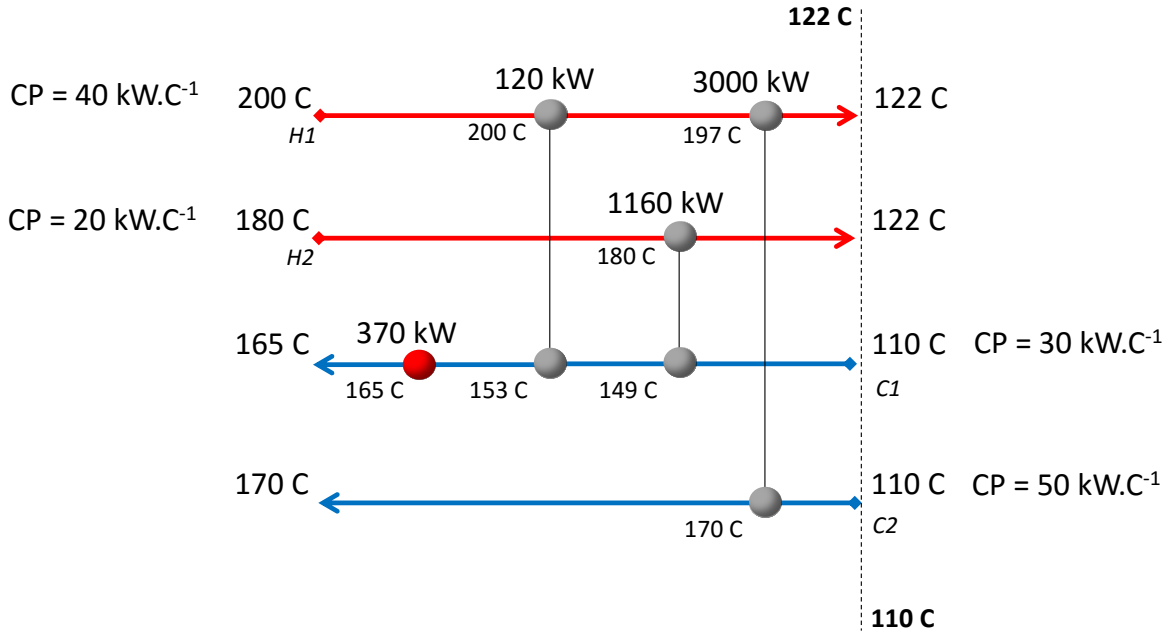

Figure 4.11 – CS 1 network configuration, above the pinch, with all the streams duty fulfilled. Hot utility consumption is 370 kW.

The capital cost, savings and yearly return of each match above the pinch are listed in Table 4.22.

Table 4.22 – Area, capital cost, savings and yearly return relative to each match in CS 1 above the pinch.

	Area [m²]	*Capital Cost [€]*	*Savings [€/yr]*	*YR [€/yr]*
C1-H1	*10*	*19 848*	*29 695*	*25 237*
C1-H2	*230*	*170 305*	*287 055*	*248 800*
C2-H1	*649*	*391 625*	*742 384*	*654 415*

Step 4 - Match streams below the pinch

Below the pinch, every cold stream should cross exchange with a hot stream and therefore only cold utility should be used. To maximize the heat recovery below the pinch, the strategy used for matching the streams below the pinch was to assume that the heat exchanger cold outlet temperature is equal to the cold stream outlet temperature, *i.e.*, $T_{C\,out\,HX} = T_{C\,out}$.

In Figure 4.12 (a - c), the matching options of the streams that satisfy the condition $T_{C\,out} > T_{H\,out} - \Delta T_{min}$ and are above the pinch with a $CP_{hot} > CP_{cold}$ are shown.

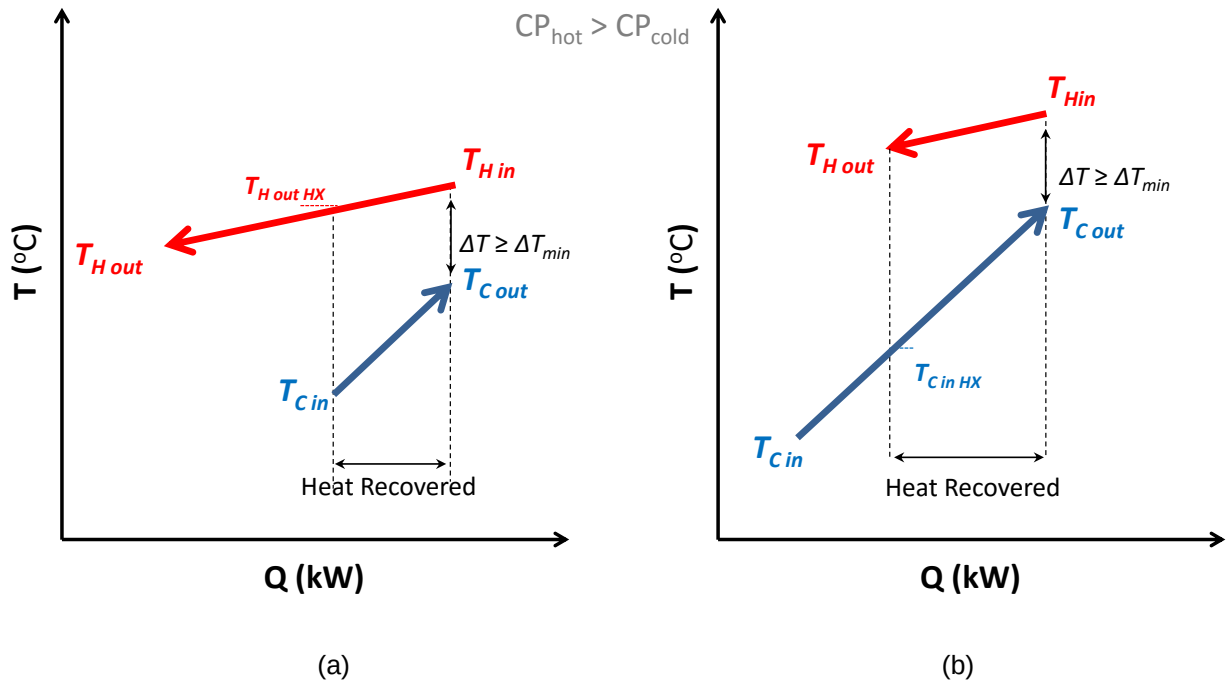

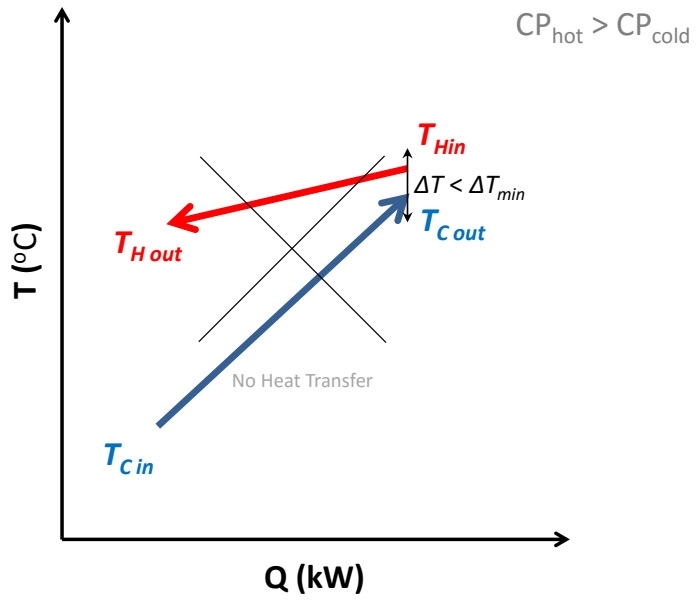

(c)

Figure 4.12 – Possible cross-exchange scenarios when $CP_{hot} > CP_{cold}$ with a pinch point for streams that are below the pinch point.

Similarly, for $CP_{hot} < CP_{cold}$ of pinched streams below the pinch, the possible scenarios are shown in Figure 4.13 (a - d).

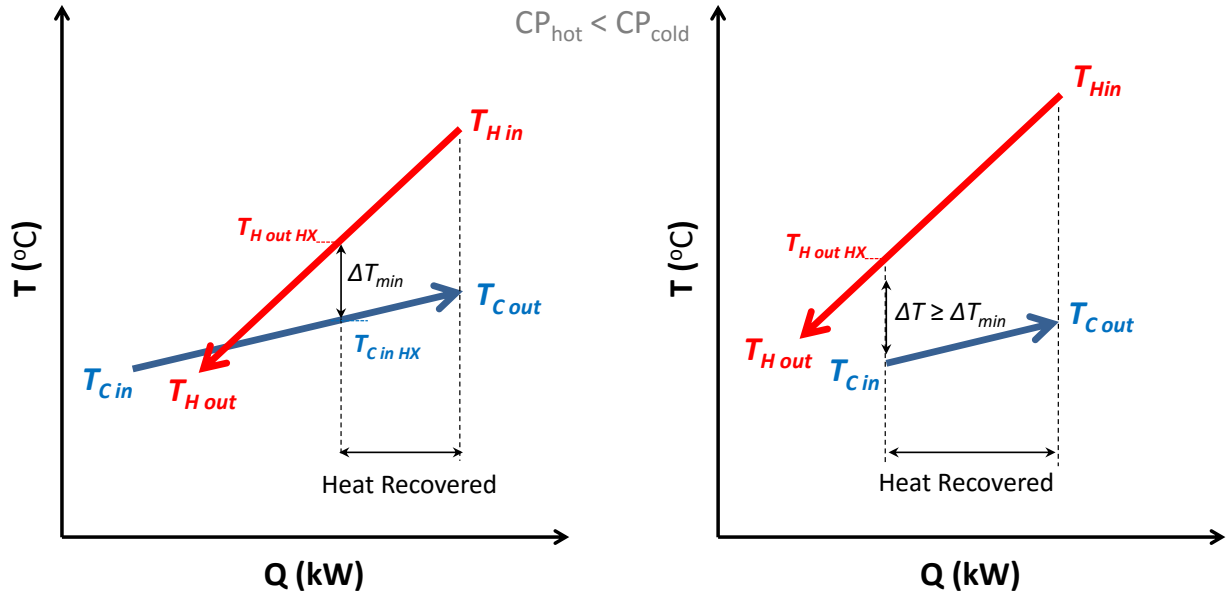

(a) (b)

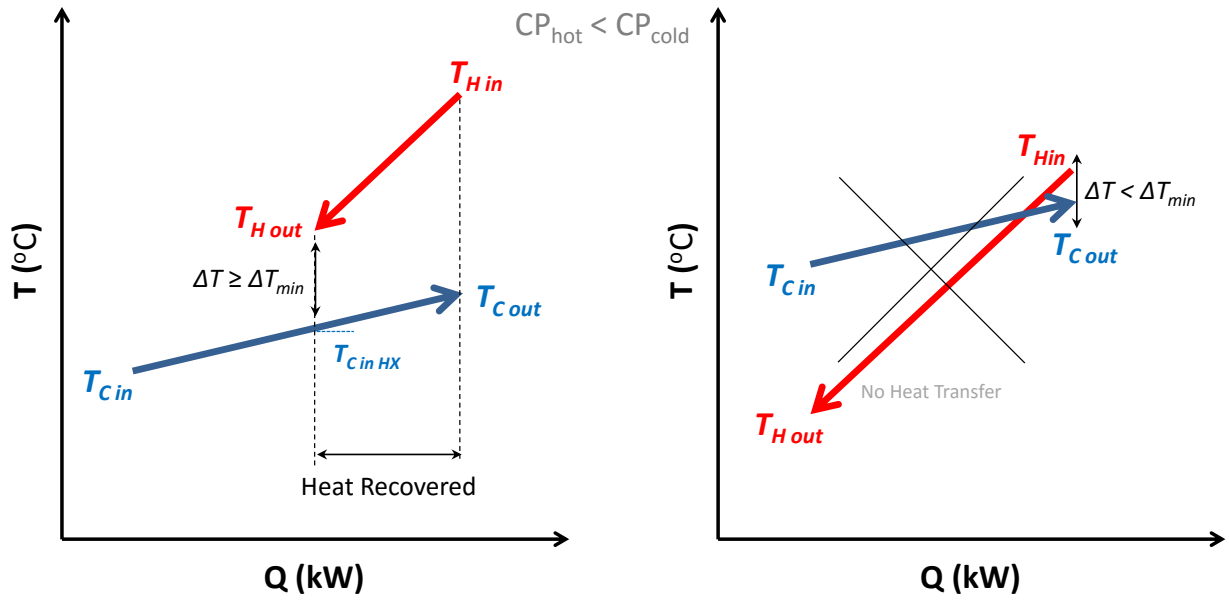

(c) (d)

Figure 4.13 – Possible cross-exchange scenarios when $CP_{hot} < CP_{cold}$ with a pinch point for streams that are below the pinch point.

If streams are not pinched amongst them ($T_{C\,out} < T_{H\,out} - \Delta T_{min}$) and are below the pinch then the possible scenarios are shown in Figure 4.14(a - b).

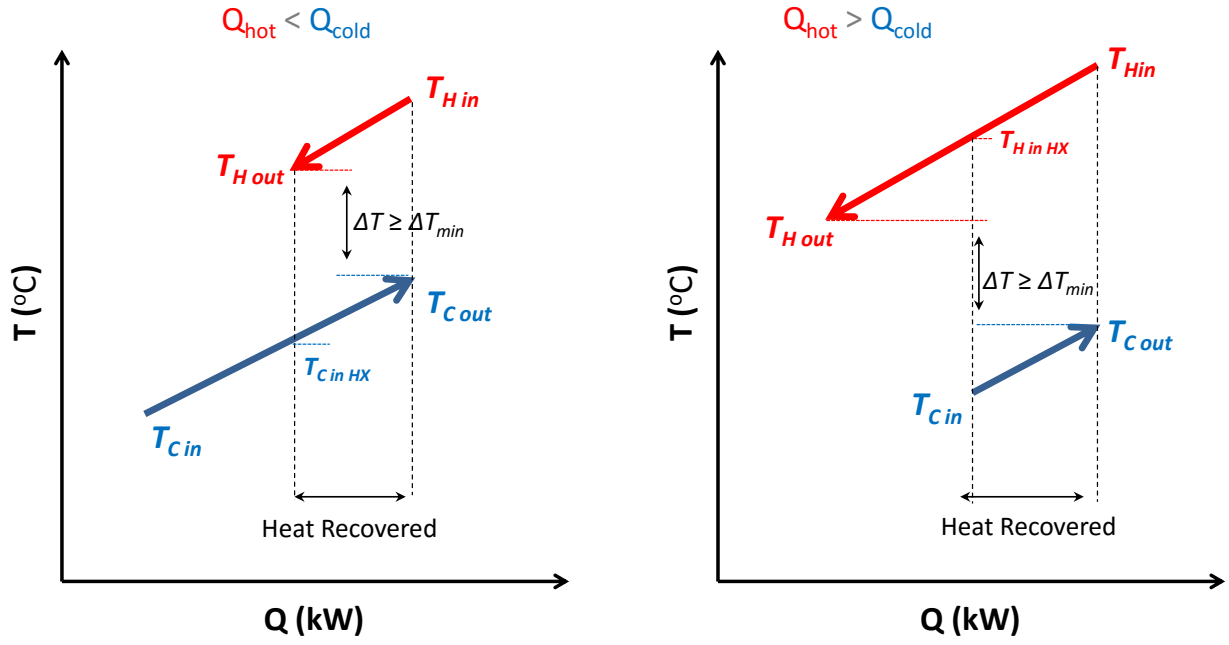

(a) (b)

Figure 4.14 – Possible cross-exchange scenarios when streams are not pinched and are above the pinch point.

Taking into consideration the possible scenarios shown in Figure 4.12, Figure 4.4, Figure 4.13 and Figure 4.14, the algorithm for determining Q_{HX}. $T_{c\ in\ HX}$, $T_{c\ out\ HX}$, $T_{h\ in\ HX}$ and $T_{h\ out\ HX}$ is detailed in Figure 4.15.

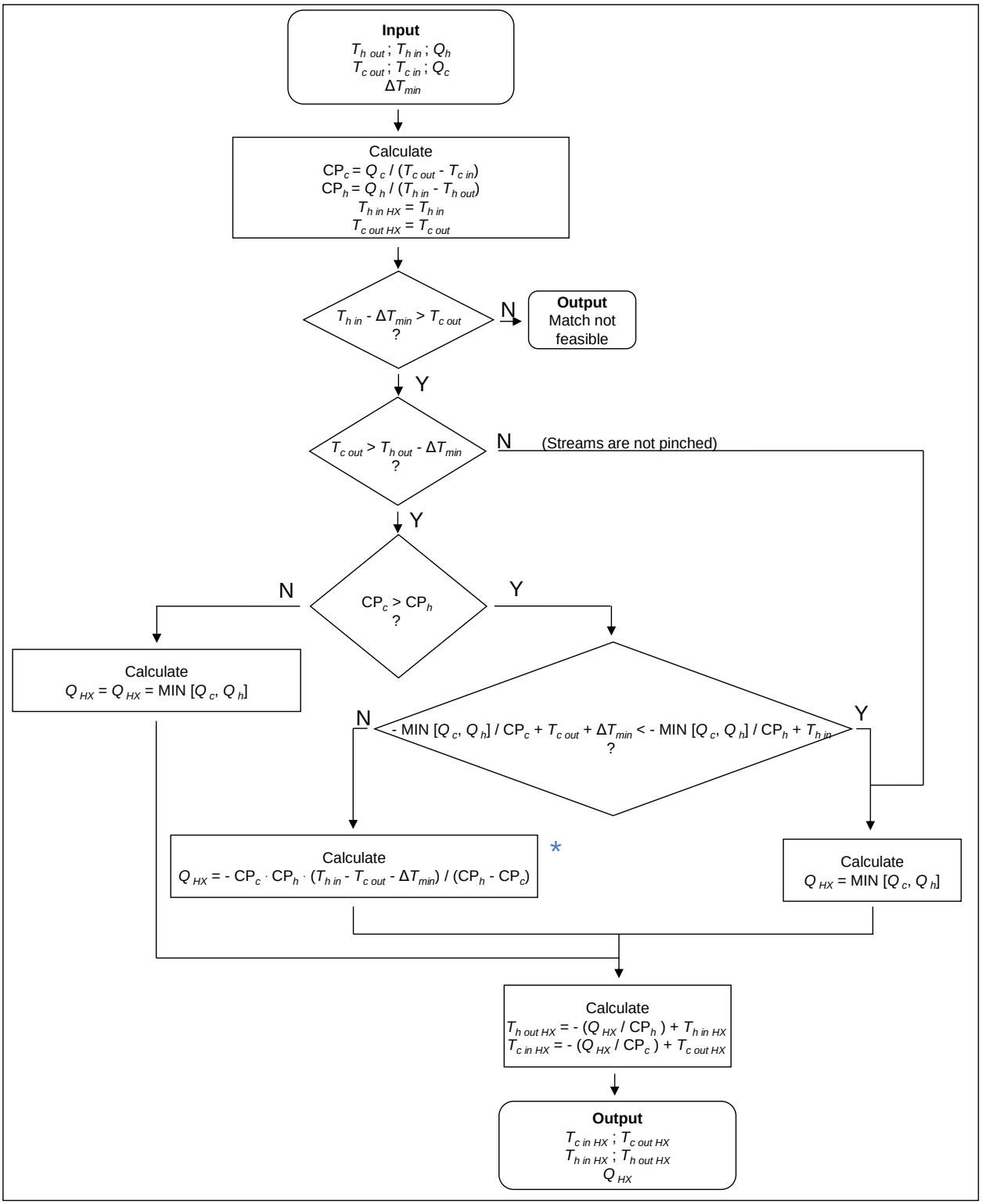

Figure 4.15 – Algorithm used to determine the in- and outlet temperature and duty of each match for the streams located below the pinch. The expression marked with an "*" is detailed in Appendix A2.

As detailed before for the above pinch scenario, the described algorithm returns Q_{HX}. $T_{c\ in\ HX}$, $T_{c\ out\ HX}$, $T_{h\ in\ HX}$, $T_{h\ out\ HX}$. This information is used to determine the *LMTD*, *A*, $Cost_{yr}$ and *YR* matrixes.

After the Yearly Return matrix is determined, select the cold stream with the highest outlet temperature, *i.e.*, closest to the pinch. For this stream, choose the match with the highest return and match the streams. If there is no match with a positive return proceed to the next cold stream. Gradually move out of the pinch until the cold stream with the lowest outlet temperature is matched.

Case study 1 (Step 4)

For matching the streams bellow the pinch start with the cold streams with the highest outlet temperature. In the case of CS 1, there is only one cold stream bellow the pinch so the matching sequence is straightforward and all the matches have positive returns. Figure 4.16 shows the CS 1 network with all the matches bellow the pinch.

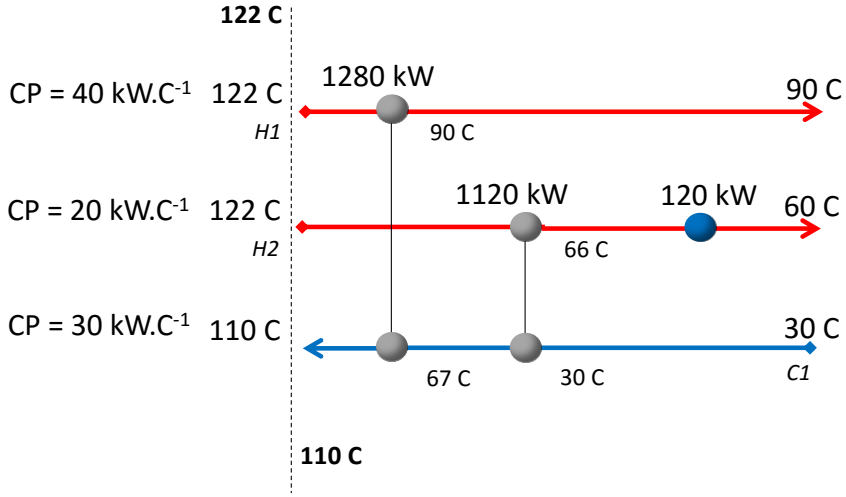

Figure 4.16 – CS 1 network configuration, bellow the pinch, with all the streams duty fulfilled. Cold utility consumption is 120 kW.

The capital cost, savings and yearly return of each match below the pinch are listed in Table 4.23Table 4.22.

Table 4.23 – Area, capital cost, savings and yearly return relative to each match in CS 1 below the pinch.

	Area [m²]	*Capital Cost [€]*	*Savings [€/yr]*	*YR [€/yr]*
C1-H1	***305***	***213 102***	***316 751***	***268 882***
C1-H2	***100***	***89 267***	***277 157***	***257 105***

Step 5 - Optimize temperature approach of heat exchangers at the pinch

After the streams are matched, the next step is to optimize the temperature approach of the streams that are crossing the pinch to minimize the total annual cost, which is the sum of the annual capital cost and the annual operating cost, as shown in Eq. (4.7). The annual capital cost corresponds to the annualized investment and the operating cost corresponds to the annual cost spent on utilities.

$$Tot\ annual\ cost[€] = Annual\ cost_{cap}[€] + Annual\ cost_{op}[€] \quad \textbf{(4.7)}$$

Case study 1 (Step 5)

The minimization is performed with Microsoft Excel Solver by manipulating the independent variables, which are the stream temperatures at the pinch and the split stream ratios. In CS 1 there are no split streams but in CS 2 it is possible to see an example where split streams are present.

Thus, the number of independent variables is equal to the number of streams that are crossing the pinch plus the number of split stream minus 1.

In Figure 4.17, the network showing the independent variables to be optimized is shown. In the case of CS1 there are 3 streams crossing the pinch and 0 splits, therefore there are 3 independent variables.

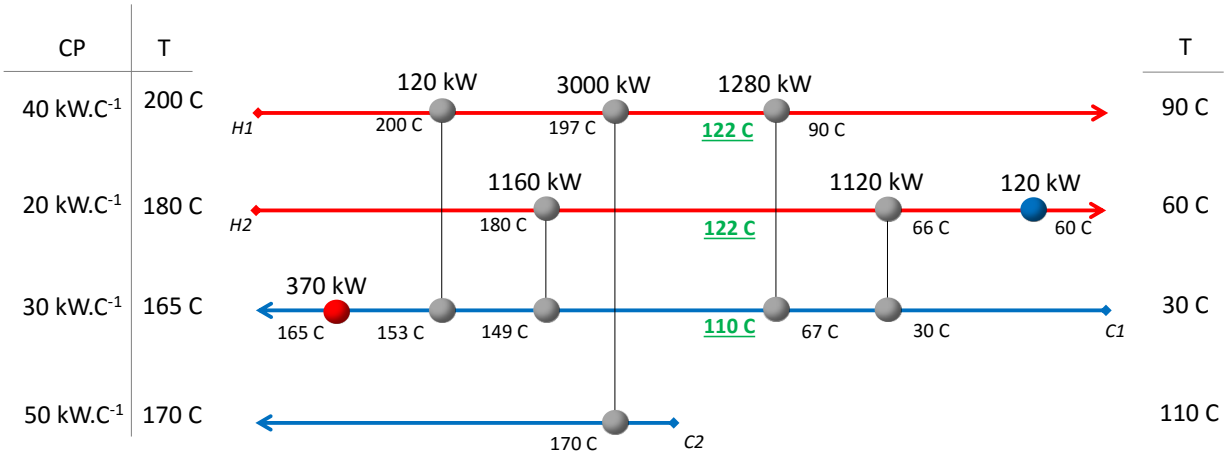

Figure 4.17 – CS 1 heat exchanger network, without heat being transferred across the pinch.

Table 4.24 presents a summary of the temperatures, duty, area, annual capital cost and operating cost associated with each heat exchangers placed above and below the pinch without the optimization of the independent variables.

Table 4.24 – Summary of CS 1 base case network, without heat being transferred across the pinch.

		Hot		Cold		Q [kW]	Area [m²]	Annual Capital Cost [€·yr⁻¹]	Operating Cost [€·yr⁻¹]
		T_{in} [C]	T_{out} [C]	T_{in} [C]	T_{out} [C]				
Above Pinch	H1-C2	197	122	110	170	3000	649	87 970	-
	H2-C1	180	122	110	149	1160	230	38 255	-
	H1-C1	200	197	149	153	120	10	4 458	-
	HU-C1	190	190	153	165	370	48	11 713	78 980
Below Pinch	H1-C1	122	90	67	110	1280	305	47 868	-
	H2-C1	122	66	30	67	1120	100	20 052	-
	CU-H2	66	60	25	40	120	15	5 483	4 080
							Total:	215 800	83 061
							Total annual cost: 298 860 €·yr⁻¹		

In Figure 4.18, the CS1 network with the independent variables already optimized is shown. It is possible to observe that the cold utility heat exchanger previously located in steam H2 disappeared after the optimization step therefore eliminating the need for cold utility altogether.

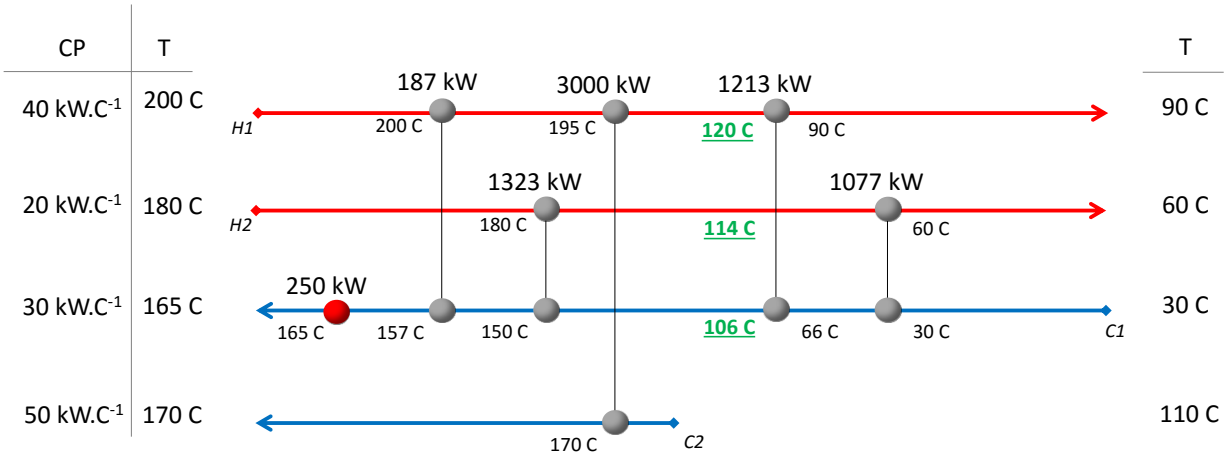

Figure 4.18 – CS 1 heat exchanger network, with optimized temperatures.

Table 4.25 summarizes the temperatures, duty, area, annual capital cost and operating cost associated with each heat exchangers of the CS1 network, after the optimization step.

Table 4.25 – Summary of CS 1 base case network, relaxing the pinch temperatures and allowing heat to be transferred across the pinch.

		Hot		Cold		Q [kW]	Area [m²]	Annual Capital Cost [€·yr⁻¹]	Operating Cost [€·yr⁻¹]
		T_{in} [C]	T_{out} [C]	T_{in} [C]	T_{out} [C]				
Above Pinch	H1-C2	195	120	110	170	3000	718	95 548	-
	H2-C1	180	114	106	150	1323	329	50 780	-
	H1-C1	200	195	150	153	187	17	5 941	-
	HU-C1	190	190	153	165	**250**	35	9 314	53 365
Below Pinch	H1-C1	120	90	66	106	1213	261	42 219	-
	H2-C1	114	60	30	66	1077	113	21 893	-
							Total:	225 694	53 365
							Total annual cost: 279 059 €·yr⁻¹		

The methodology allowed the design of a heat exchanger network, which provided lower operating costs that the more traditional pinch methodology used by the Pereira *et al.* [94] , as shown in Table 4.26.

Before the optimization step, the total operating cost provided by the methodology was 0.4% higher than the result presented by the authors, while the result after the optimization step allowed the removal of the cold utility and resulted in a 6.2% reduction in the annual cost when comparing with the annual cost presented by the authors.

Table 4.26 – Comparison between the results achieved by the authors [94] and the proposed methodology for CS 1.

	ΔT_{min} [C]	Number of heat exchangers	Annual Capital Cost [€·yr⁻¹]	Operating Cost [€·yr⁻¹]	Total annual cost [€·yr⁻¹]	Annual cost reduction
Authors [94]	8	6	214 510	83 084	297 595	0
With retrofit (not optimized)	12	7	215 800	83 061	298 860	+0.4%
With retrofit (optimized)	8	6	225 694	53 365	279 059	-6.2%

4.3 Case study 2 - Retrofit heat exchanger network (Industrial application)

The industrial case study is a system with 25 cold streams and 37 hot streams. Table 4.27 and Table 4.28 present the data regarding cold and hot streams, namely: the inlet (T_{in}) and outlet (T_{out}) temperatures, heat capacity flow rate (CP), heat transfer coefficient (HTC) and heat load (Q).

Table 4.27 – Cold Stream data for CS 2.

	T_{in} [C]	T_{out} [C]	CP [kW·C^{-1}]	Q [kW]	HTC [kW·m^{-2}·C^{-1}]
C0	42.5	85.0	22.0	934.4	1.50
C1	30.7	58.9	46.8	1320.3	1.46
C2	-34.4	25.0	3.1	186.6	0.02
C3	187.2	188.1	6623.3	5961.0	0.20
C4	197.8	198.3	15572.8	7786.4	0.20
C5	196.0	202.0	50.3	301.9	0.20
C6	199.2	203.7	814.8	3666.7	1.39
C7	35.9	158.0	3.7	455.6	0.20
C8	163.0	187.0	9.4	226.1	0.20
C9	196.0	200.5	72.2	325.0	0.20
C10	149.6	150.2	3777.8	2266.7	0.20
C11	144.8	145.3	180.0	90.0	0.20
C12	32.0	88.0	0.8	46.9	0.20
C13	205.0	211.7	31.1	208.3	0.93
C14	25.0	198.0	0.1	15.2	0.03
C15	35.5	45.7	31.3	317.1	3.25
C16	33.2	101.5	9.1	620.8	4.15
C17	35.2	74.5	0.1	5.4	2.17
C18	39.8	63.3	30.2	708.8	1.58
C19	178.0	201.0	191.7	4409.0	0.20
C20	82.6	120.0	14.9	556.8	0.20
C21	82.6	120.0	14.9	556.8	0.20
C22	-37.9	-35.0	9.2	26.6	0.20
C23	-37.9	-31.0	10.7	74.1	0.20
C24	-37.9	-37.7	6.8	1.4	0.20

Table 4.28 – Hot Stream data for CS 2.

	T_{in} [C]	T_{out} [C]	CP [kW·C^{-1}]	Q [kW]	HTC [kW·m^{-2}·C^{-1}]
H0	-11.7	-37.0	10.7	270.0	0.20
H1	193.9	39.1	19.0	2941.1	1.26
H2	39.9	26.4	13.9	186.6	1.18
H3	68.0	54.9	100.9	1320.4	0.33
H4	70.0	50.0	57.4	1148.2	0.53
H5	-11.7	-34.4	3.3	74.1	0.03
H6	39.5	32.0	8.8	66.0	0.20
H7	51.4	39.0	287.7	3562.0	2.21
H8	109.1	32.0	52.8	4067.9	0.64
H9	138.0	39.5	19.0	1872.0	0.68
H10	99.8	99.7	46280.0	4628.0	0.20
H11	31.0	-31.0	0.4	26.6	0.20
H12	135.0	60.0	5.9	444.4	0.20
H13	144.2	100.0	149.2	6594.4	0.20
H14	185.2	34.0	3.0	457.8	0.20
H15	175.8	48.6	1.6	200.8	0.20
H16	35.1	28.0	92.1	650.0	0.20
H17	200.0	52.0	9.7	1430.6	0.20
H18	67.0	-13.0	0.0	1.4	0.20
H19	146.0	33.0	0.4	46.9	0.20
H20	33.0	32.0	0.7	0.7	0.20
H21	95.5	28.9	2.6	171.7	4.09
H22	100.3	74.9	0.2	5.4	0.20
H23	87.3	34.9	0.1	7.1	4.31
H24	82.5	37.6	33.5	1500.7	3.39
H25	118.2	48.0	36.8	2585.7	4.90
H26	118.5	85.0	52.4	1755.9	2.59
H27	99.7	35.0	5.1	327.6	0.20
H28	81.0	35.0	22.5	1037.0	1.85
H29	75.9	35.0	1.3	54.9	0.20
H30	110.0	46.0	29.3	1876.8	0.20
H31	95.5	54.0	15.2	633.2	0.20
H32	39.9	38.0	194.5	359.7	0.20
H33	42.8	38.0	185.8	888.3	0.20
H34	42.1	38.0	188.8	777.7	0.20
H35	121.0	113.0	31.0	248.0	0.20
H36	-17.0	-37.9	41.4	865.0	0.20

In Table 4.29, the cost of each utility for CS2 is discriminated.

Table 4.29 – Utility cost for CS 2.

Utility	Cost (€·MWh^{-1})
CW	2.7
Air	0.01
HP Steam	39
K-1001	11.4
K-1002	12.1

The total cooling duty of the cooling tower is 37.6 MW, as shown in Chapter 3, but the duty presented in Table 4.30 only accounts for 26.9 MW of cooling water duty. This is because 10.7 MW of cooling duty is not available for retrofitting purposes and therefore is not accounted for in this section.

Taking into consideration the utility cost and the consumed duty of each utility, the operating cost associated with each utility as well as the total annual cost for the CS2 base case is given in Table 4.30.

It was assumed that the hot utility was provided solely by HP steam. Cold utility was provided by CW, Air, K-1001 and K-1002.

Table 4.30 – Consumption of each utility and associated operating cost for CS 2 base case network.

		Q [kW]	Operating Cost [k€·yr^{-1}]
Utilities	CW	26 946	582.0
	Air	11 470	0.9
	HP steam	27 534	8 591.6
	K-1001	865	79.0
	K-1002	270	26.2

Total operating cost:	9 278.7 k€·yr^{-1}
Annual Capital Cost :	0
Total annual cost:	**9 278.7 k€·yr^{-1}**

Since the industrial network already has some level of heat integration, the existent heat exchangers are shown in Table 4.31.

Table 4.31 – Existent heat exchanger data for cross exchange streams in the Estarreja MDI plant.

	Cold Stream	T_{in} (C)	T_{out} (C)	Hot Stream	T_{in} (C)	T_{out} (C)	Q (kW
C17-H22	PROCESS	35	74	PROCESS	100	75	5
C15-H27	PROCESS	36	46	PROCESS	100	37	317
C16-H25	PROCESS	33	102	PROCESS	118	101	621
C12-H19	PROCESS	32	88	PROCESS	146	33	47
C1-H3	PROCESS	31	59	PROCESS	68	55	1320
C2-H2	PROCESS	-34	25	PROCESS	40	26	187
C0-H1	PROCESS	43	85	PROCESS	194	145	934
C22-H11	PROCESS	-38	-31	PROCESS	-12	-34	74
C23-H5	PROCESS	-38	-35	PROCESS	31	-31	27
C24-H18	PROCESS	-38	-38	PROCESS	67	-13	136

Taking into consideration the list given in Table 4.31 and the hot and cold stream data given in Table 4.27 and Table 4.28 and using the traditional pinch tools to identify the heat exchangers that crossing the pinch, heat exchanger C0-H1 was identified as cross-pinching 710.2 KW. Therefore, this heat exchanger was discarded and the streams that were used in this HX were used for crossing with other stream within the network.

The values shown in Table 4.32 refer to the economic parameters. Parameters *i* and *n* are used in by Eq. (4.5) to determine annualized factor whereas parameters *a*, *b* and *c* shall be used in Eq. (2.1) to determine the capital cost of each heat exchanger.

Table 4.32 – Economic data regarding CS 2.

Rate of return (*i*)	13%
Plant Life (*n*)	10 yrs
Hours of operation per year	8000
a	40972
b	1947
c	0.7

Possible matches

As stated before, one the advantages of the proposed methodology is that it allows the user to define the process incompatibilities and therefore eliminate the possibility of matching the defined streams. In Table 4.33, the feasibly matrix concerning CS2 network is given.

Table 4.33 – Feasibility matrix for the CS 2 network.

	C0	C1	C2	C3	C4	C5	C6	C7	C8	C9	C10	C11	C12	C13	C14	C15	C16	C17	C18	C19	C20	C21	C22	C23	C24
H0	✓	✓	✓	✓	✓	✓	✓	✓	✓	✓	✓	✓	✓	✓	✓	✓	✓	✓	*	✓	*	*	✓	✓	✓
H1	✓	✓	✓	✓	✓	✓	✓	✓	✓	✓	✓	✓	✓	✓	✓	✓	✓	✓	*	✓	*	*	✓	✓	✓
H2	✓	✓	✓	✓	✓	✓	✓	✓	✓	✓	✓	✓	✓	✓	✓	✓	✓	✓	*	✓	*	*	✓	✓	✓
H3	*	✓	✓	✓	✓	✓	✓	✓	✓	✓	✓	✓	✓	✓	✓	✓	✓	✓	*	✓	*	*	✓	✓	✓
H4	*	✓	✓	✓	✓	✓	✓	✓	✓	✓	✓	✓	✓	✓	✓	✓	✓	✓	*	✓	*	*	✓	✓	✓
H5	✓	✓	✓	✓	✓	✓	✓	✓	✓	✓	✓	✓	✓	✓	✓	✓	✓	✓	*	✓	*	*	✓	✓	✓
H6	✓	✓	✓	✓	✓	✓	✓	✓	✓	✓	✓	✓	✓	✓	✓	✓	✓	✓	*	✓	*	*	✓	✓	✓
H7	✓	✓	✓	✓	✓	✓	✓	✓	✓	✓	✓	✓	✓	✓	✓	✓	✓	✓	*	✓	*	*	✓	✓	✓
H8	✓	✓	✓	✓	✓	✓	✓	✓	✓	✓	✓	✓	✓	✓	✓	✓	✓	✓	*	✓	*	*	✓	✓	✓
H9	✓	✓	✓	✓	✓	✓	✓	✓	✓	✓	✓	✓	✓	✓	✓	✓	✓	✓	*	✓	*	*	✓	✓	✓
H10	✓	✓	✓	✓	✓	✓	✓	✓	✓	✓	✓	✓	✓	✓	✓	✓	✓	✓	*	✓	*	*	✓	✓	✓
H11	✓	✓	✓	✓	✓	✓	✓	✓	✓	✓	✓	✓	✓	✓	✓	✓	✓	✓	*	✓	*	*	✓	✓	✓
H12	*	✓	✓	✓	✓	✓	✓	✓	✓	✓	✓	✓	✓	✓	✓	✓	✓	✓	✓	✓	✓	✓	✓	✓	✓
H13	*	✓	✓	✓	✓	✓	✓	✓	✓	✓	✓	✓	✓	✓	✓	✓	✓	✓	✓	✓	✓	✓	✓	✓	✓
H14	*	✓	✓	✓	✓	✓	✓	✓	✓	✓	✓	✓	✓	✓	✓	✓	✓	✓	✓	✓	✓	✓	✓	✓	✓
H15	*	✓	✓	✓	✓	✓	✓	✓	✓	✓	✓	✓	✓	✓	✓	✓	✓	✓	✓	✓	✓	✓	✓	✓	✓
H16	*	✓	✓	✓	✓	✓	✓	✓	✓	✓	✓	✓	✓	✓	✓	✓	✓	✓	✓	✓	✓	✓	✓	✓	✓
H17	*	*	*	*	*	*	*	*	*	*	✓	*	*	*	✓	*	*	*	*	*	*	*	*	*	*
H18	*	✓	✓	✓	✓	✓	✓	✓	✓	✓	✓	✓	✓	✓	✓	✓	✓	✓	✓	✓	✓	✓	✓	✓	✓
H19	*	✓	✓	✓	✓	✓	✓	✓	✓	✓	✓	✓	✓	✓	✓	✓	✓	✓	✓	✓	✓	✓	✓	✓	✓
H20	*	✓	✓	✓	✓	✓	✓	✓	✓	✓	✓	✓	✓	✓	✓	✓	✓	✓	✓	✓	✓	✓	✓	✓	✓
H21	*	✓	✓	✓	✓	✓	✓	✓	✓	✓	✓	✓	✓	✓	✓	✓	✓	✓	✓	✓	✓	✓	✓	✓	✓
H22	*	✓	✓	✓	✓	✓	✓	✓	✓	✓	✓	✓	✓	✓	✓	✓	✓	✓	✓	✓	✓	✓	✓	✓	✓
H23	*	✓	✓	✓	✓	✓	✓	✓	✓	✓	✓	✓	✓	✓	✓	✓	✓	✓	✓	✓	✓	✓	✓	✓	✓
H24	*	✓	✓	✓	✓	✓	✓	✓	✓	✓	✓	✓	✓	✓	✓	✓	✓	✓	✓	✓	✓	✓	✓	✓	✓
H25	*	✓	✓	✓	✓	✓	✓	✓	✓	✓	✓	✓	✓	✓	✓	✓	✓	✓	✓	✓	✓	✓	✓	✓	✓
H26	*	✓	✓	✓	✓	✓	✓	✓	✓	✓	✓	✓	✓	✓	✓	✓	✓	✓	✓	✓	✓	✓	✓	✓	✓
H27	*	✓	✓	✓	✓	✓	✓	✓	✓	✓	✓	✓	✓	✓	✓	✓	✓	✓	✓	✓	✓	✓	✓	✓	✓
H28	*	✓	✓	✓	✓	✓	✓	✓	✓	✓	✓	✓	✓	✓	✓	✓	✓	✓	✓	✓	✓	✓	✓	✓	✓
H29	*	✓	✓	✓	✓	✓	✓	✓	✓	✓	✓	✓	✓	✓	✓	✓	✓	✓	✓	✓	✓	✓	✓	✓	✓
H30	*	✓	✓	✓	✓	✓	✓	✓	✓	✓	✓	✓	✓	✓	✓	✓	✓	✓	✓	✓	✓	✓	✓	✓	✓
H31	*	✓	✓	✓	✓	✓	✓	✓	✓	✓	✓	✓	✓	✓	✓	✓	✓	✓	✓	✓	✓	✓	✓	✓	✓
H32	*	✓	✓	✓	✓	✓	✓	✓	✓	✓	✓	✓	✓	✓	✓	✓	✓	✓	✓	✓	✓	✓	✓	✓	✓
H33	*	✓	✓	✓	✓	✓	✓	✓	✓	✓	✓	✓	✓	✓	✓	✓	✓	✓	✓	✓	✓	✓	✓	✓	✓
H34	*	✓	✓	✓	✓	✓	✓	✓	✓	✓	✓	✓	✓	✓	✓	✓	✓	✓	✓	✓	✓	✓	✓	✓	✓
H35	*	✓	✓	✓	✓	✓	✓	✓	✓	✓	✓	✓	✓	✓	✓	✓	✓	✓	✓	✓	✓	✓	✓	✓	✓
H36	✓	✓	✓	✓	✓	✓	✓	✓	✓	✓	✓	✓	✓	✓	✓	✓	✓	✓	✓	✓	*	*	✓	✓	✓

CS2 Step 1 - Determine process pinch temperature

To determine the process pinch, a 10 C global minimum approach (ΔT_{min}) was assumed, which is a typical temperature approach for the chemical industry. The approach of each match will be individually adjusted in a later step of the methodology, so this parameter is only important at this stage for determining the position of each stream in regard to the pinch point.

The cold pinch temperature is 149.6 C and the hot pinch temperature is 159.6 C. In Table 4.34, the temperatures and heat load of the streams above and below the pinch are presented. In the cases where streams don't show any value means that they are not crossing the pinch and therefore were not divided.

Cold streams C7 and C14 are crossing the pinch while the others are either above or below the pinch. Stream C10 inlet temperature is exactly at the pinch.

Table 4.34 – Heat load and temperatures of cold streams of CS 2 above and below the pinch. A "-" indicates that there is no duty above or below the pinch. Streams with "*" are already cross-exchanging, so only the duty that is being supplied by HU is considered.

	Above pinch			*Below pinch*		
	T_{in} [C]	T_{out} [C]	Q [kW]	T_{in} [C]	T_{out} [C]	Q [kW]
C0	-	-	-	42.5	85.0	934.4
*C1	-	-	-	58.9	58.9	0
*C2	-	-	-	25.0	25.0	0
C3	187.2	188.1	5961.0	-	-	-
C4	197.8	198.3	7786.4	-	-	-
C5	196.0	202.0	301.9	-	-	-
C6	199.2	203.7	3666.7	-	-	-
C7	149.6	158.0	31.3	35.9	149.6	424.2
C8	163.0	187.0	226.1	-	-	-
C9	196.0	200.5	325.0	-	-	-
C10	149.6	150.2	2266.7	-	-	-
C11	-	-	-	144.8	145.3	90.0
*C12	-	-	-	88.0	88.0	0
C13	205.0	211.7	208.3	-	-	-
C14	149.6	198.0	4.3	25.0	149.6	11.0
C15	-	-	-	35.5	45.7	0.1
*C16	-	-	-	101.5	101.5	0
*C17	-	-	-	74.5	74.5	0
C18	-	-	-	39.8	63.3	708.8
C19	178.0	201.0	4409.0	-	-	-
C20	-	-	-	82.6	120.0	556.8
C21	-	-	-	82.6	120.0	556.8
*C22	-	-	-	-35.0	-35.0	0
*C23	-	-	-	-31.0	-31.0	0
*C24	-	-	-	-37.7	-37.7	0

Hot streams H1, H14, H15 and H17 are crossing the pinch while the others are below the pinch.

Table 4.35 – Heat load and temperatures of hot streams of CS 2 above and below the pinch. A "-" indicates that there is no duty above or below the pinch. Streams with "*" are already cross-exchanging, so only the duty that is being removed by cold utility is considered.

	Above pinch			*Below pinch*		
	T_{in} [C]	T_{out} [C]	Q [kW]	T_{in} [C]	T_{out} [C]	Q [kW]
H0	-	-	-	-11.7	-37.0	270.0
H1	193.9	159.6	651.2	159.6	39.1	2290.0
*H2	-	-	-	26.4	26.4	0
*H3	-	-	-	54.9	54.9	0
H4	-	-	-	70.0	50.0	1148.2
*H5	-	-	-	-34.4	-34.4	0
H6	-	-	-	39.5	32.0	66.0
H7	-	-	-	51.4	39.0	3562.0
H8	-	-	-	109.1	32.0	4067.9
H9	-	-	-	138.0	39.5	1872.0
H10	-	-	-	99.8	99.7	4628.0
*H11	-	-	-	-31.0	-31.0	0
H12	-	-	-	135.0	60.0	444.4
H13	-	-	-	144.2	100.0	6594.4
H14	185.2	159.6	77.5	159.6	34.0	380.3
H15	175.8	159.6	25.6	159.6	48.6	175.3
H16	-	-	-	35.1	28.0	650.0
H17	200.0	159.6	390.5	159.6	52.0	1040.1
*H18	-	-	-	-13.0	-13.0	0
*H19	-	-	-	33.0	33.0	0
H20	-	-	-	33.0	32.0	0.7
H21	-	-	-	95.5	28.9	171.7
*H22	-	-	-	74.9	74.9	0
H23	-	-	-	87.3	34.9	7.1
H24	-	-	-	82.5	37.6	1500.7
*H25	-	-	-	101.3	48.0	1963.1
H26	-	-	-	118.5	85.0	1755.9
*H27	-	-	-	43.7	35.0	44.1
H28	-	-	-	81.0	35.0	1037.0
H29	-	-	-	75.9	35.0	54.9
H30	-	-	-	110.0	46.0	1876.8
H31	-	-	-	95.5	54.0	633.2
H32	-	-	-	39.9	38.0	359.7
H33	-	-	-	42.8	38.0	888.3
H34	-	-	-	42.1	38.0	777.7
H35	-	-	-	121.0	113.0	248.0
H36	-	-	-	-17.0	-37.9	865.0

CS2 Step 2 - Split streams at the pinch according to pinch rules

Immediately above the pinch, the number of hot steams is lower than the number of cold streams. Additionally, the CP of stream C2 is higher than the CP of stream H1. These conditions mean that there is no necessity for splitting stream above the pinch.

Bellow the pinch, the number of hot steams is also lower than the number of cold streams, meaning that one of the rules is not fulfilled and a hot stream should be split. If stream H3 is split in half, then the number of hot stream will equal the number of cold streams and the CP of stream H3/1 and H3/2 is higher than the CP of both stream C2 and C4. Table 4.36 and 4.37 show the results of applying the pinch stream splitting rules to the CS 2 network.

Table 4.36 – Stream splitting rules for CS 2 regarding the number of streams immediately above/bellow the pinch.

Above pinch	Below pinch
$N_{hot} \leq N_{cold}$ ✗	$N_{hot} \geq N_{cold}$ ✓
$N_{hot} = 4 > 3 = N_{cold}$	$N_{hot} = 4 > 2 = N_{cold}$

Table 4.37 – Stream splitting rules for CS 2 regarding the CP of streams immediately above/bellow the pinch.

Above pinch	Below pinch
$CP_{hot} \leq CP_{cold}$ ✓	$CP_{hot} \geq CP_{cold}$ ✓
$CP_{H1} < CP_{C10}$	$CP_{H1,H17} > CP_{C7}$
$CP_{H14} < CP_{C7,C10}$	$CP_{H1,H14,H15,H17} > CP_{C14}$
$CP_{H15} < CP_{C7,C10}$	
$CP_{H17} < CP_{C10}$	

From Table 4.37, it is possible to observe that in the region above the pinch only tot cold streams, C7 and C10, have a CP higher than the CP of the 4 hot streams. This means that two additional cold streams with a CP higher than the CP of the hot streams are required. This is achieved by splitting stream C10 in three, as shown in Figure 4.19. With the splits in place the $N_{hot} \leq N_{cold}$ condition is also fulfilled.

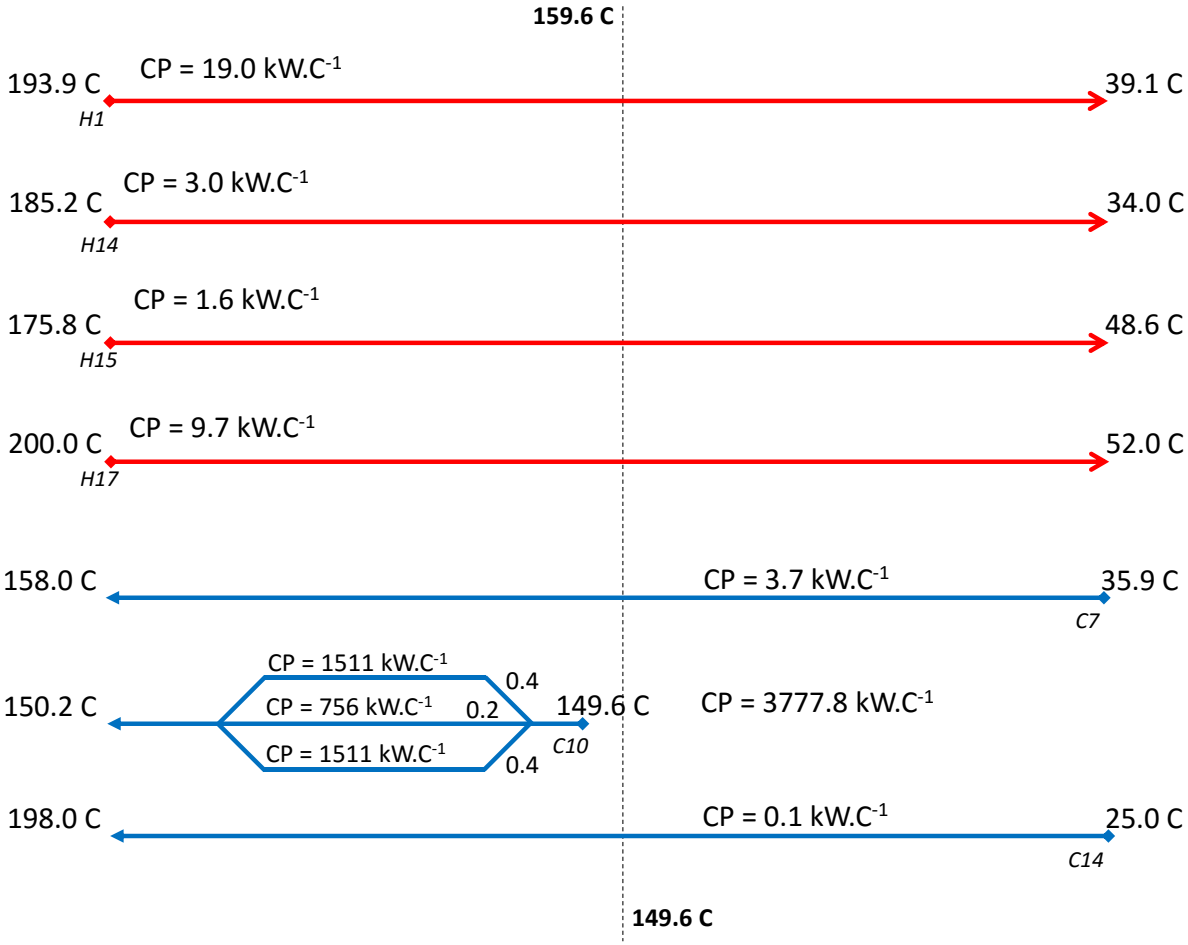

Figure 4.19 – CS2 streams crossing the pinch. Cold stream C10 with two splits.

CS2 Step 3 - Match streams above the pinch

After the Yearly Return matrix is determined, select the hot stream with the lowest outlet temperature, *i.e.*, closest to the pinch. For this stream, choose the match with the highest return and match the streams. If there is no match with a positive return proceed to the next hot stream. Gradually move out of the pinch until the hot stream with the highest inlet temperature is matched.

In this step the streams above the pinch are matched according to the methodology. In Figure 4.20, the matches above the pinch are shown.

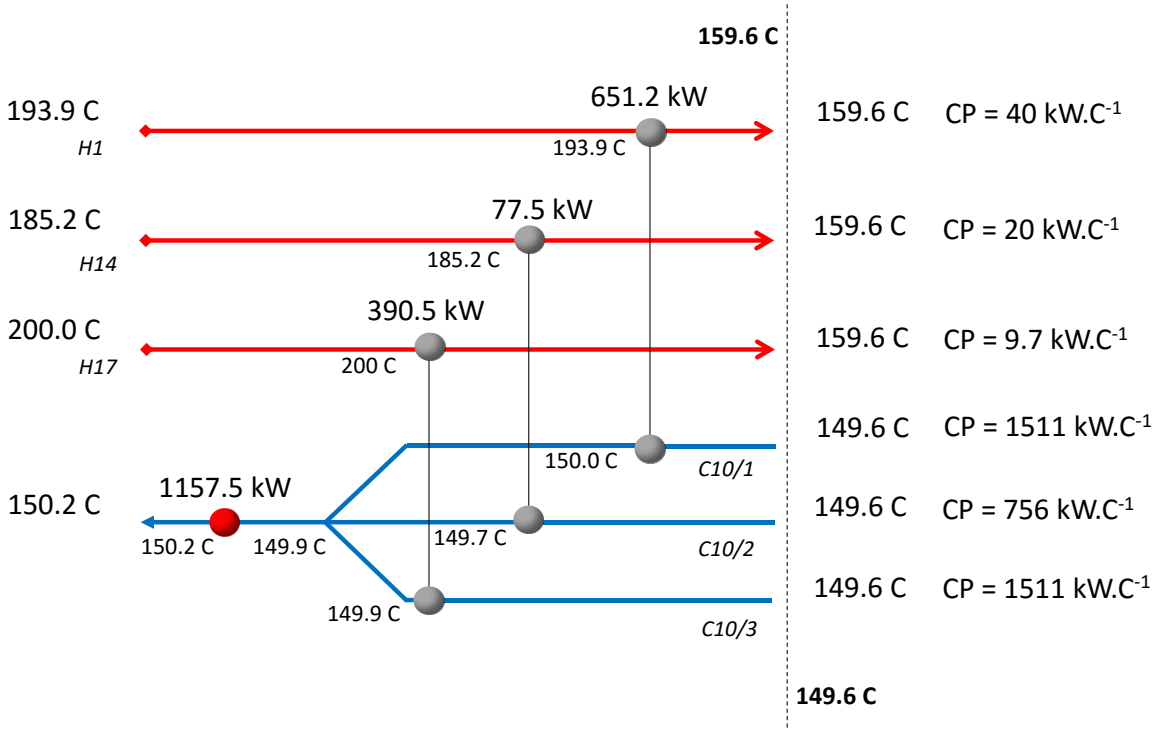

Figure 4.20 – CS 2 matches above the pinch.

Stream H1, H14 and H17 were matched with cold streams and all the duty above the pinch was fulfilled. Stream H15 and C14 were not matched since there were not available matches that gave a positive yearly return. This was mainly because the available duty above the pinch was only 25.6 kW for stream H15 and 4.3 kW for stream C14, as seen in Table 4.35.

Three new heat exchangers were added to network above the pinch. It is assumed that hot utility heat exchanger does not need to be replaced. In a further stage of analysis, it would be necessary to verify if the overdimensioning of the heat exchanger would be problematic and, if yes, the cost of replacement must also be accounted for in the economic analysis.

In Table 4.38, the capital cost, yearly savings and yearly return of the three matches above the pinch are presented.

Table 4.38 – Yearly return relative to each match in CS 2 (above pinch)

	Area [m²]	*Capital Cost [€]*	*Savings [€/yr]*	*YR [€/yr]*
C10/1-H1	158	104 500	203 217	183 959
C10/2-H14	39	64 520	24 188	12 298
C10/3-H17	165	102 400	121 868	102 997

CS2 Step 4 - Match streams below the pinch

After the Yearly Return matrix is determined, select the cold stream with the highest outlet temperature, *i.e.*, closest to the pinch. For this stream, choose the match with the highest return and match the streams. If there is no match with a positive return proceed to the next cold stream. Gradually move out of the pinch until the cold stream with the lowest outlet temperature is matched.

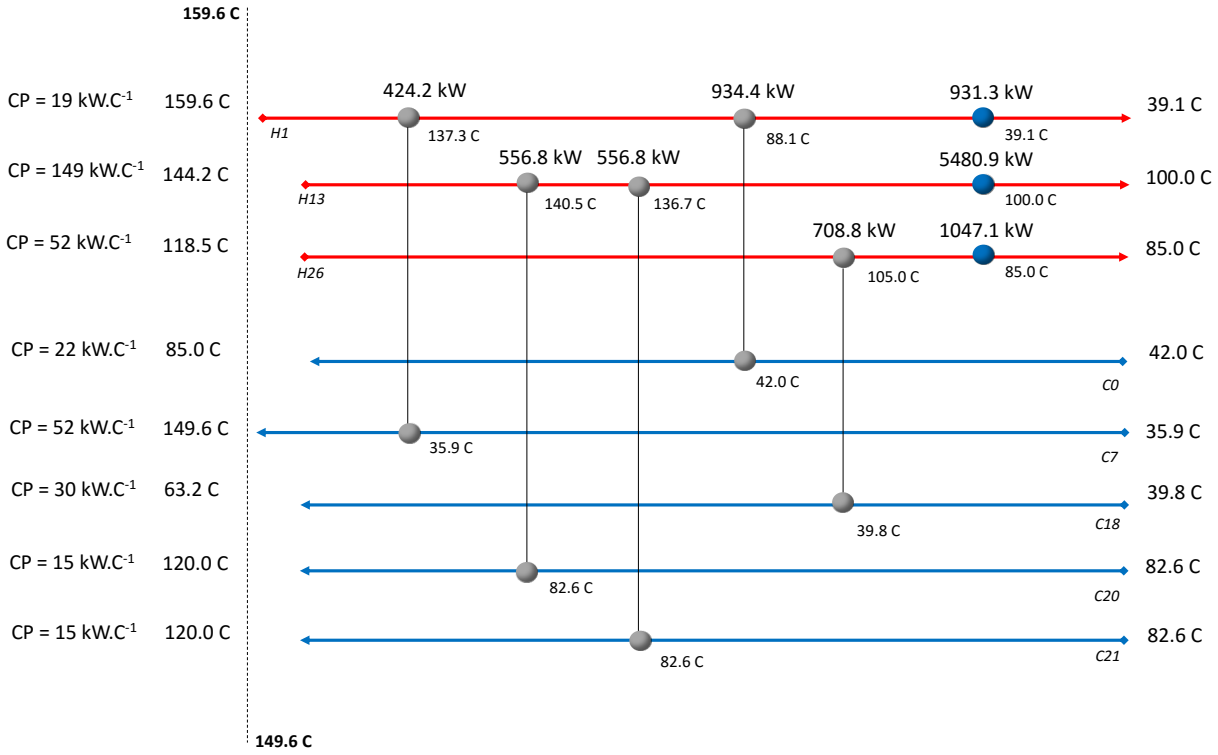

Figure 4.21 – CS 2 matches bellow the pinch.

Four new heat exchangers were added to the network below the pinch. Again, like in the above pinch case, it is considered that, although overdimensioned, the existent cooling utility heat exchangers can still be used and don't need to be replaced.

In Table 4.39, the capital cost, yearly savings and yearly return of the three matches below the pinch are presented.

Table 4.39 – Yearly return relative to each match in CS 2 (below pinch)

	Area [m²]	*Capital Cost [€]*	*Savings [€/yr]*	*YR [€/yr]*
C7-H1	62	73 666	132 393	118 817
C20-H13	144	98 969	173 755	155 516
C21-H13	161	103 469	173 755	154 686
C0-H1	28	59 854	291 606	280 576
C18-H26	12	51 601	221 191	211 682

CS2 Step 5 - Optimize temperature approach of heat exchangers at the pinch

In this step, the independent variables are optimized so that the total annual cost of the network is minimal. Since the number of independent variables is equal to the number of streams that are crossing the pinch plus the number of split stream minus 1, in the case of CS2 the number of streams crossing the pinch is 4 (H1, H14, H17 and C7) and the number of splits is 3, which result in the total of 4 + 3 - 1 = 6 independent variables.

In Figure 4.22, the retrofitted network, without temperature approach optimization yet performed, is shown. The independent variables are the variables in green.

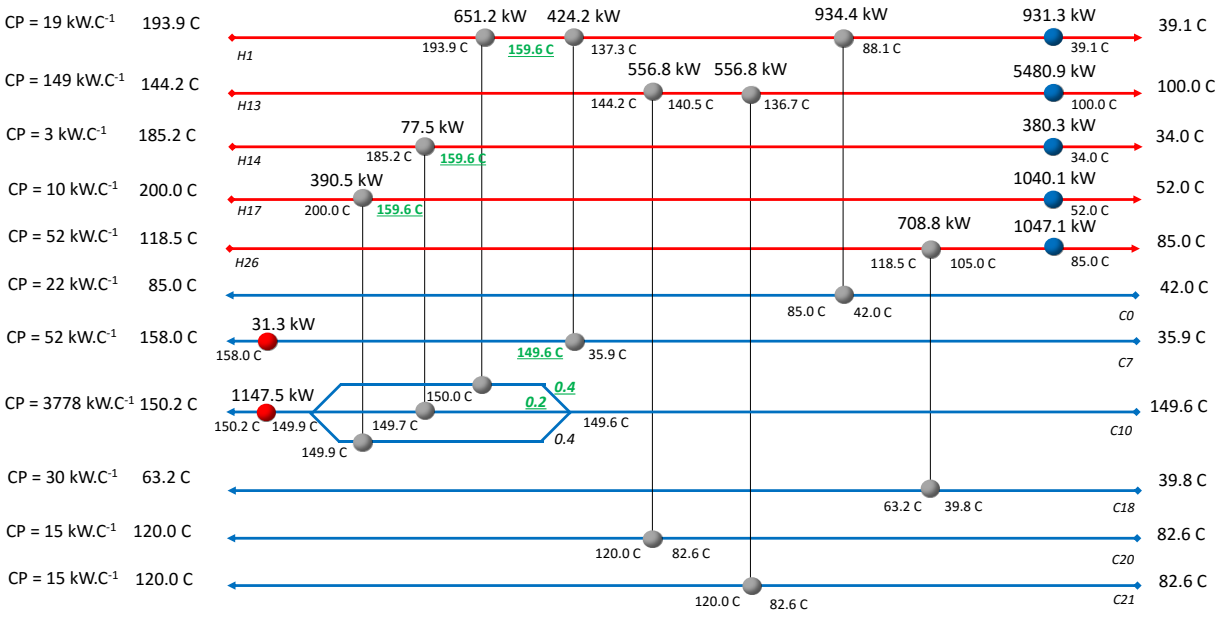

Figure 4.22 – CS 2 base case heat exchanger network, without heat being transferred across the pinch.

A summary of each utility heat duty and associated operating costs for the retrofitted network, without independent variables optimization, is shown in Table 4.40.

Table 4.40 – Summary of CS 2 base case network. Retrofit without optimization.

	Retrofit without optimization	
	Q [kW]	Operating Cost [k€·yr^{-1}]
CW	8 880	191.8
HP steam	1 179	367.8
Total operating cost		559.6 k€·yr^{-1}
Total capital cost		659.4 k€
Annual capital cost		121.5 k€·yr^{-1}
Total annual cost		**681.1 k€·yr^{-1}**

Next, the independent variables are changed so that the total annual cost is minimized. This minimization was performed using Microsoft Excel Solver [90], changing the independent variables and setting the objective as minimization of the total annual cost (a more comprehensive explanation of the tool is detailed in Appendix A3).

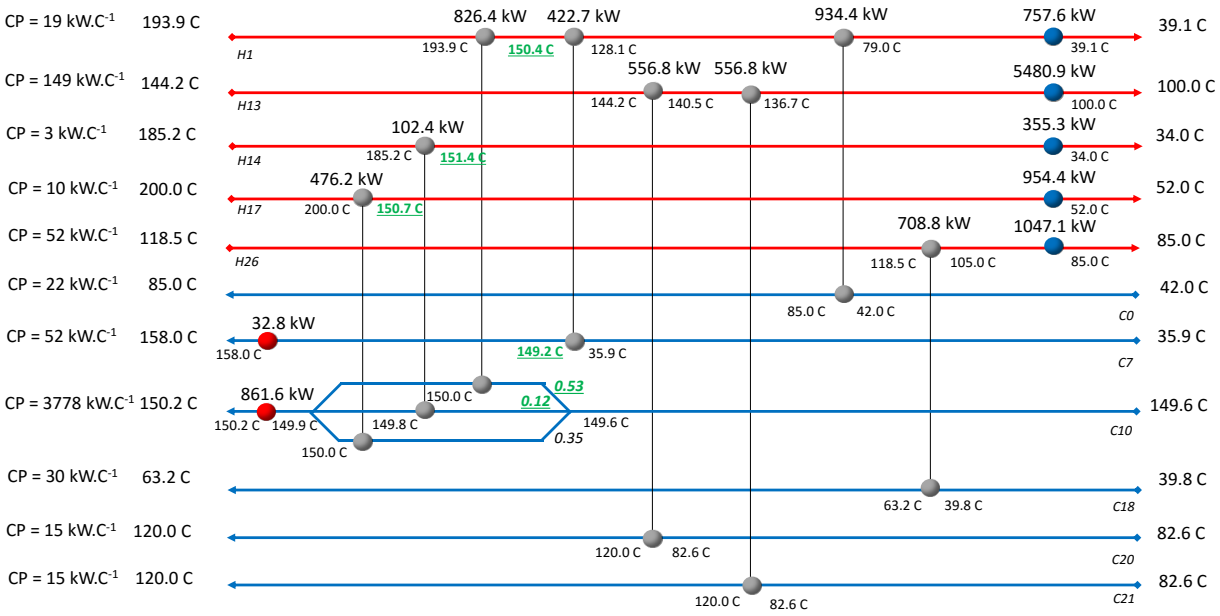

Figure 4.23 – CS 2 heat exchanger network, with optimized temperatures.

The optimization step does not take into account the previously imposed ΔT_{min} and the independent variables are manipulated so that the total annual cost of the network is minimized. The resulting network has a ΔT_{min} of 0.8 C in heat exchanger C10/1-H1. Although this temperature approach is not very typical the fact that the heat transfer coefficient of stream H1, 1.26 kW·m^{-2}·C^{-1}, is relatively high results in this network configuration.

The capital cost, savings and yearly return of each match after temperature optimization are listed in Table 4.41.

Table 4.41 – Area, capital cost, savings and yearly return relative to each match in CS 2. After temperature optimization

	Area [m^2]	*Capital Cost [€]*	*Savings [€/yr]*	*YR [€/yr]*
C10/1-H1	***370***	***151 295***	***148 601***	***120 719***
C10/2-H14	***92***	***83 606***	***31 958***	***16 551***
C10/3-H17	***449***	***167 025***	***257 902***	***227 121***
C7-H1	***177***	***91 329***	***131 929***	***115 098***
C20-H13	***144***	***98 969***	***173 755***	***155 516***
C21-H13	***160***	***103 469***	***173 755***	***154 686***
C0-H1	***34***	***62 728***	***291 606***	***280 046***
C18-H26	***12***	***51 601***	***221 191***	***211 682***

A summary of each utility heat duty and associated operating costs for the retrofitted network, after optimization, is shown in Table 4.42.

Table 4.42 – Summary of CS 2 base case network. Retrofit with optimization

	Retrofit with optimization	
	Q [kW]	**Operating Cost [k€·yr^{-1}]**
CW	8 595	185.7
HP steam	894	279.1
Total operating cost		464.8 k€·yr^{-1}
Total capital cost		810.0 k€
Annual capital cost		149.3 k€·yr^{-1}
Total annual cost		**614.0 k€·yr^{-1}**

For the abovementioned scenario stream C10 was split and the outlet temperature of each split stream was not fixed. This situation is normal when there is no phase change. However, when working with reboilers or condensers, the outlet temperature should be the same for all split streams since there is a phase change. In these cases, the hot/cold utility is in parallel with the other split streams.

If this consideration is taken into account in the case of stream C10 and the outlet temperature of each split stream is fixed than the split fractions are no longer be an independent variables and the CS 2 network would be as shown in Figure 4.24. In this case, the heat exchanger with the hot utility in stream C10 is placed in parallel with the other heat exchangers.

The number of independent variables also changes from 6 to 4 as the split ratio is calculated instead of being an independent variable. This is because the in- and outlet temperatures are fixed and, for fulfilling a given heat duty, the split ratio is calculated and is no longer a variable that can be varied.

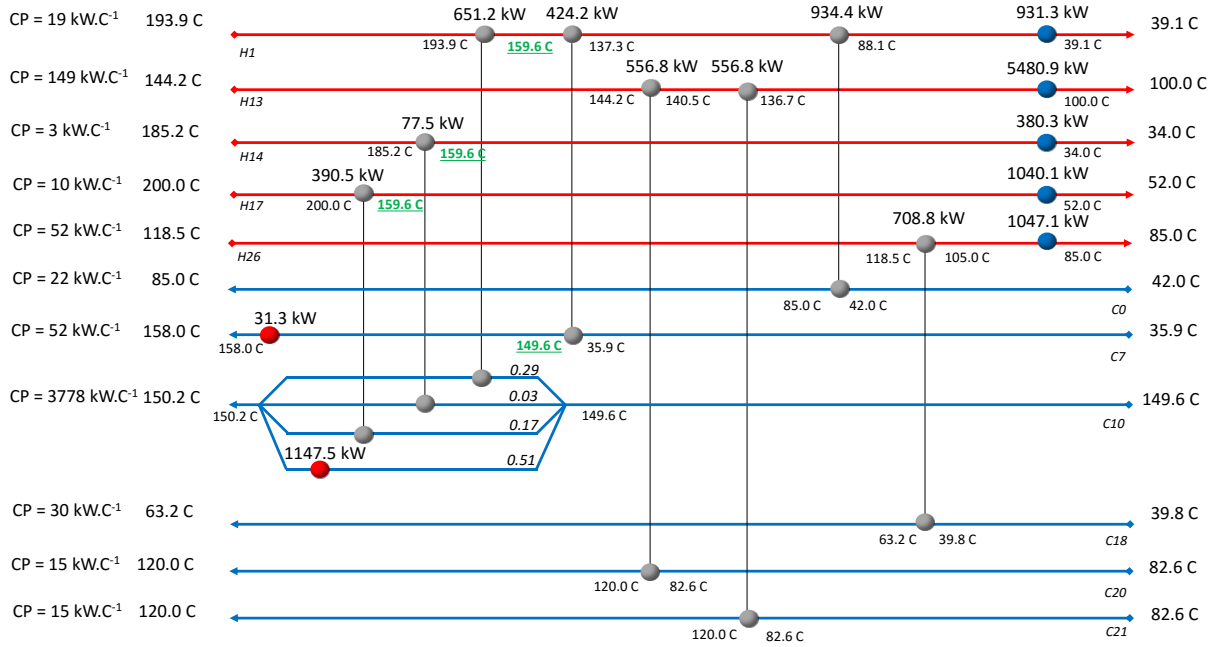

Figure 4.24 – CS 2 base case heat exchanger network, without heat being transferred across the pinch. Stream C10 split streams with fixed outlet temperatures.

The optimized network is shown in Figure 4.25.

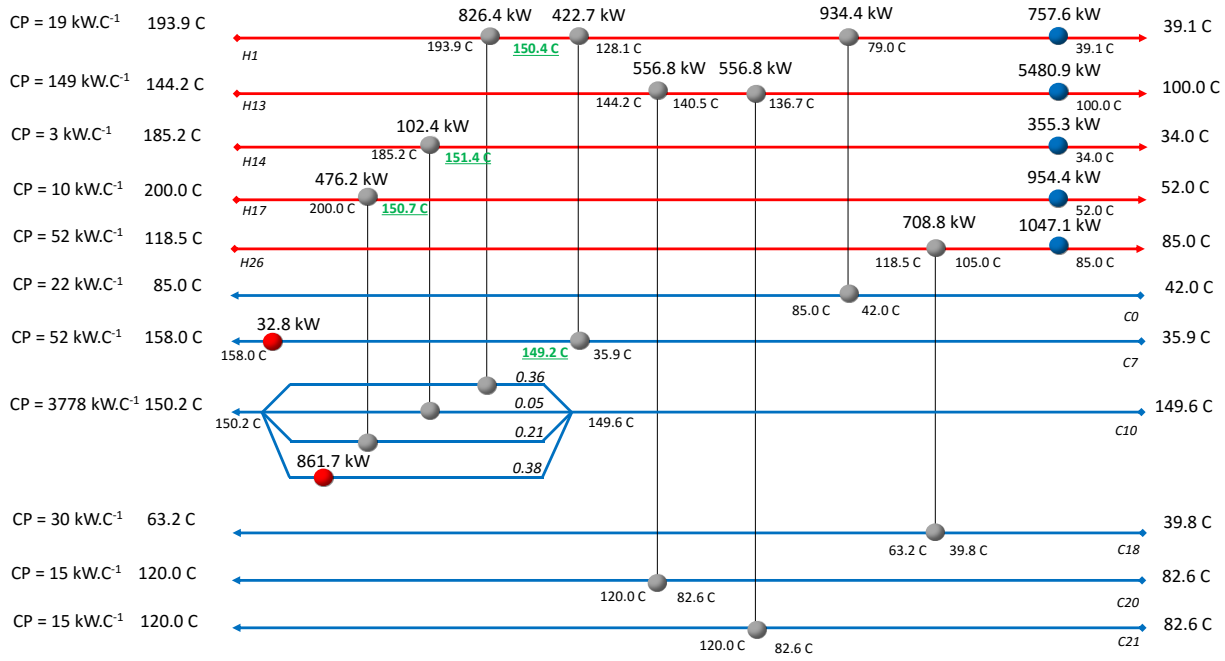

Figure 4.25 – CS 2 heat exchanger network, with optimized temperatures. Stream C10 split streams with fixed outlet temperatures.

For this specific heat exchanger network, the total annual cost is similar independently of fixing the split streams outlet temperatures or not. Nonetheless, it is important to present both approaches as it might be relevant when applying the methodology to other networks.

Table 4.43 compares the utility duty, total operating cost, annual capital cost and total annual cost for the different scenarios. The base case scenario, which has several exchangers that are violating pinch rules, has the highest total annual cost of 1540.3 k€·yr^{-1}. After retrofitting the network with the stream matching methodology the total annual cost of the network was reduced to 681.1 k€·yr^{-1}. After optimizing the network a 614.0 k€·yr^{-1} total annual cost was achieved. The total operating cost is reduced by 1075 k€·yr^{-1} when comparing the base case with the optimized network.

Table 4.43 – Summary of CS 2 base case network. Retrofit with optimization.

	Base case		Retrofit without optimization		Retrofit with optimization	
	Q [kW]	**Operating Cost [k€·yr^{-1}]**	**Q [kW]**	**Operating Cost [k€·yr^{-1}]**	**Q [kW]**	**Operating Cost [k€·yr^{-1}]**
CW	12 245	264.5	8 878	191.8	8 595	185.7
HP steam	4 089	1 275.8	1 148	358.0	862	268.9
Total operating cost	1 540.3 k€·yr^{-1}		559.6 k€·yr^{-1}		464.8 k€·yr^{-1}	
	-		659.4 k€		810.0 k€	
Annual capital cost	-		121.5 k€·yr^{-1}		149.3 k€·yr^{-1}	
Total annual cost	**1 540.3 k€·yr^{-1}**		**681.1 k€·yr^{-1}**		**614.0 k€·yr^{-1}**	

It is possible to apply the methodology for retrofitting industrial networks. The results summarized in Table 4.44 show that applying the methodology without the optimization step allows a 56.4% annual cost reduction and, with the optimization step, allows a further 7.7% reduction when comparing with the base case scenario.

Table 4.44 – Annual cost of the base case, with retrofit and with retrofit (optimized) networks of CS 2. Considers only the streams that were subject to retrofit.

	Annual cost [k€·yr^{-1}]	Annual cost reduction
Base case	1 540.3	0
With retrofit	671.3	-55.8%
With retrofit (optimized)	603.8	-63.5%

Table 4.45 summarizes the annual cost of the base case, with retrofit and with retrofit (optimized) networks but, differently from Table 4.44 that considers only the streams that were subject to retrofit efforts, considers the whole network. The overall reduction on the annual cost after optimization is 11.3% when compared to the base case scenario.

Table 4.45 – Annual cost of the base case, with retrofit and with retrofit (optimized) networks of CS 2. Considers the whole network.

	Annual cost [k€·yr^{-1}]	Annual cost reduction
Base case	9 278.7	0
With retrofit	8 301.3	-10.5%
With retrofit (optimized)	8 234.2	-11.3%

4.4 Impact on cooling tower operation

Adding to the fact that the total annual cost will be reduced, the cooling tower will also operate under the design limit during a higher percentage of the year. In Chapter 3, a plot showing the variation of the cooling water supply temperature with the air wet-bulb temperature was presented. If the retrofit measures were to be implemented the cooling water range would decrease from 6 C to 5.5 C, meaning that the network would still operate within the design limit of 26 C for the cooling water supply temperature with an air wet-bulb temperature of 21.5 C (Figure 4.26).

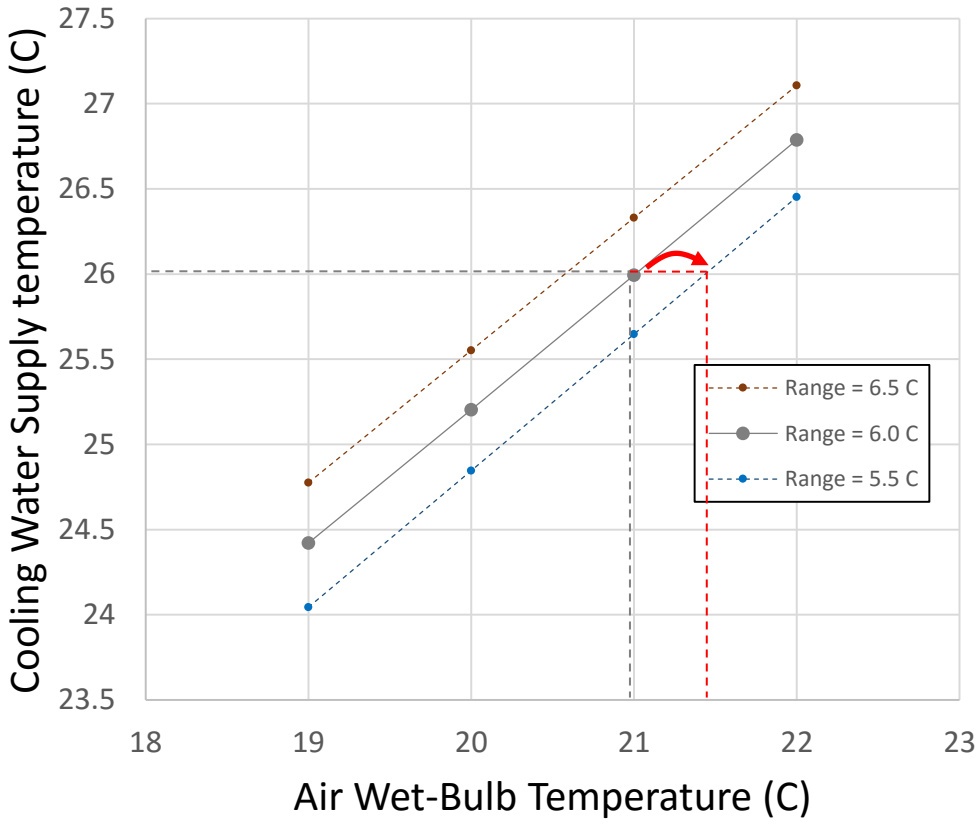

Figure 4.26 – Cooling water supply temperature *vs* Air wet bulb temperature for the Dow's cooling tower with the retrofit measures implemented.

Looking at Figure 4.27, it is possible to observe that if the retrofit measures were implemented the cooling tower would only be above its design limit during 3% of the year instead of 4.5% for the base case scenario.

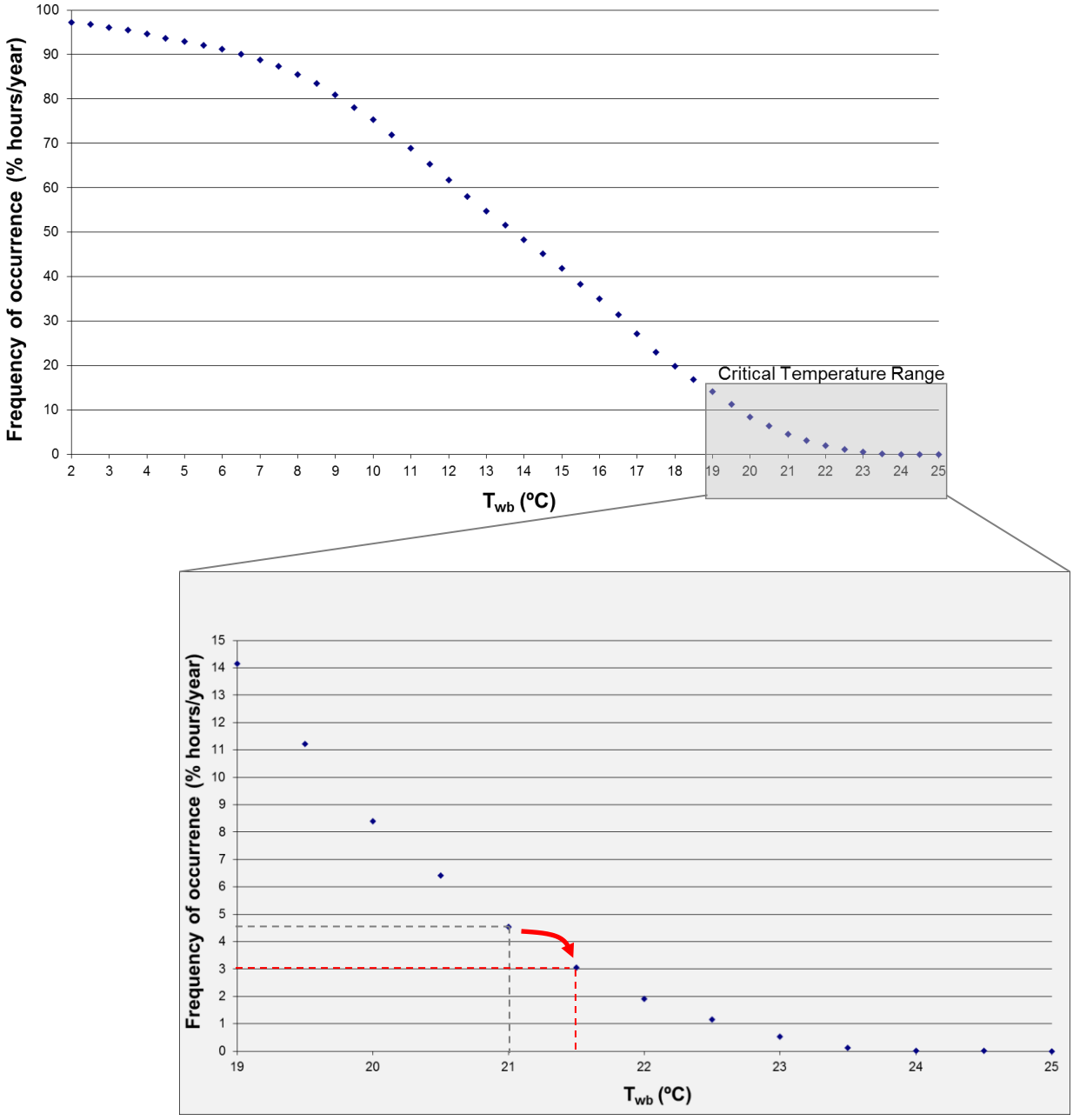

Figure 4.27 – Estimated wet-bulb temperature frequency of occurrence in 2010 at Dow's Estarreja MDI plant with the retrofit measures implemented.

4.5 Impact on the steam network

LP steam can be produced by either flashing HP condensates or by letting down HP steam. This has clear impacts on the plant overall energy analysis as reducing LP steam is only advantageous to the point where LP steam is only related to the steam that is being generated by the let-down valve. Considering the case

where a process optimization would lead to a situation where no letdown would be necessary, if LP steam consumption was further reduced without carrying out any other modification in the system, LP steam header pressure would increase and vent to atmosphere, consequently rendering this reduction useless.

When evaluating any process modification, it is necessary to analyze how it will impact on the steam network balance. It is therefore necessary to assess the overall heat and mass balance of the steam network and check if no LP steam will be vented to the atmosphere.

Updating the thermodynamic model presented in Chapter 3 with the optimized network scenario a new process flowsheet was calculated as shown in Figure 4.28. Some important differences between the steam network process flowsheet before (Figure 3.35) and after (Figure 4.28) the implementation of the stream match methodology arise. It is possible to observe that HP to LP steam letdown dropped from 3324 kg/h to 12 kg/h, meaning that all the LP steam requirements are being met by flashing the HP condensates in the LP flash drum. Total make-up water decreased from 5691 kg/h to 5466 kg/h and it was possible to eliminate the vented steam from the atmospheric flash drum.

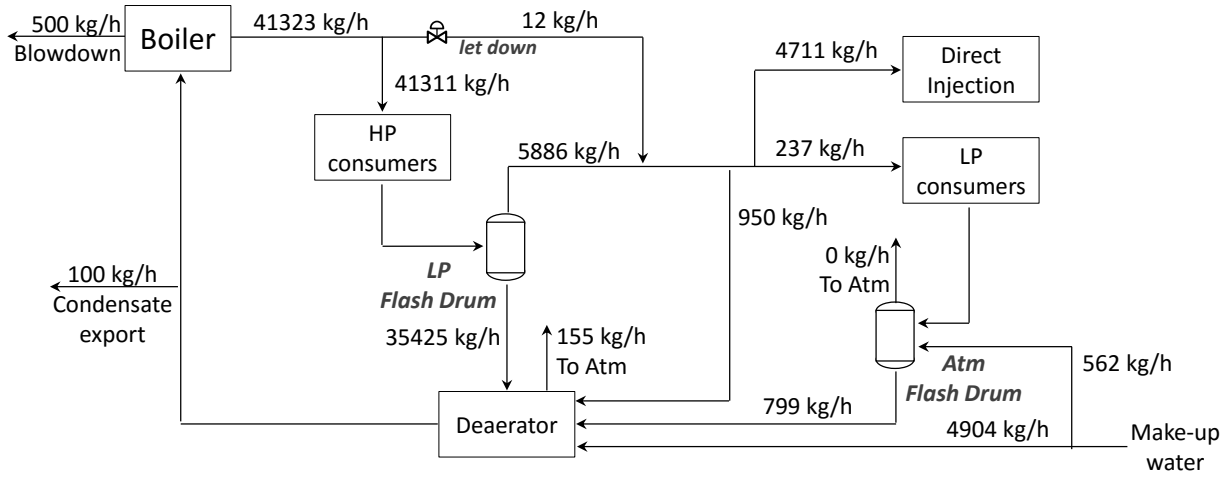

Figure 4.28 – Steam network block diagram after implementing optimized network scenario.

The resulting steam network is balanced in terms of HP and LP steam consumption. However, if further actions were taken to reduce LP steam consumption an unbalanced situation would arise due to the overproduction of LP steam by flashing the HP condensates. To avoid this situation, a possible solution would be to install a new HP knock out drum that would separate the HP condensate phases and pump the condensate directly to the boiler and the vapor phase to the LP steam header. Depending on the LP steam consumption, the HP condensate would either go directly to the boiler, for lower LP steam requirements, or to the LP flash drum, for higher LP steam requirements. The proposed scheme is presented in Figure 4.29.

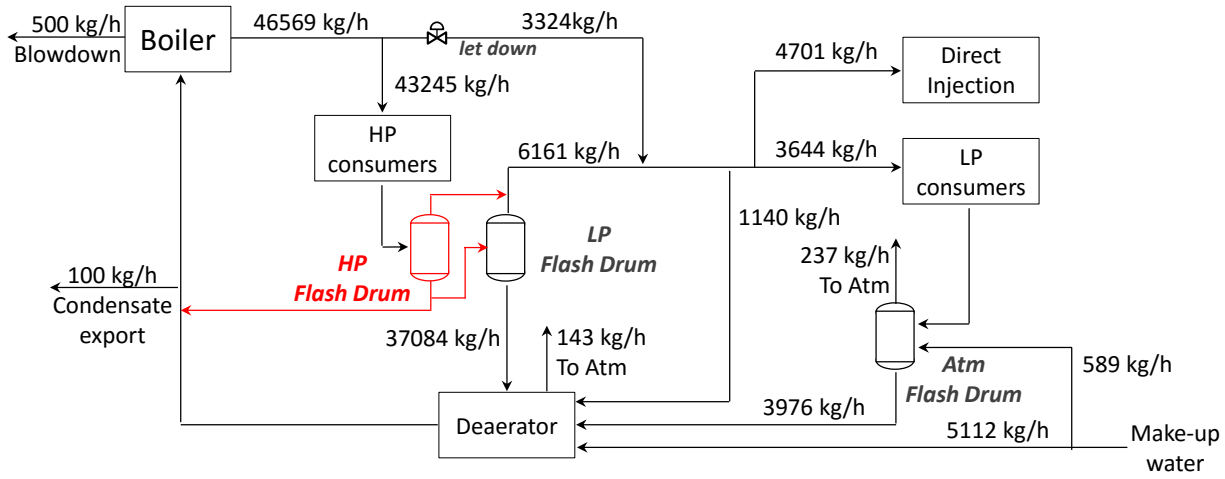

Figure 4.29 – Steam network configuration that allows the control of LP steam generated in the LP flash drum.

5 Conclusions and Recommendations

5.1 General conclusions

The approach suggest a methodology for the implementation of the cooling water and steam systems models. These models allow the performance evaluation of existent networks and serve as a basis for optimization studies. Furthermore, a heat integration methodology was developed that aimed for the reduction of utilities consumption.

A new approach based on an equilibrium stage method for modeling an existent cooling towers was developed and validated with experimental data, both from previous works and data collected from an industrial facility [76]. The presented methodology can be implemented in ASPEN PLUS models and integrated with the cooling water network model.

To develop an accurate model of the cooling system the flow on each point of the network was required and for that a hydraulic model of the cooling water network was implemented. The hydraulic model not only permitted the calculation of the accurate flow on each point of the network but also allowed the identification and improvement of heat exchangers where the cooling water flow differed from design.

The models of the case study plant suggested that the maximum wet-bulb temperature after which the cooling tower is not able to supply cooling water at a temperature lower then design was 20.5 C which, for the year of 2010, corresponded to 4.5% of the time.

A framework for analyzing the steam generators' performance was also presented. This methodology allows the performance evaluation of the steam generators as well as the multiple steam generators system optimization by managing the load of each steam generator. It was shown that using the direct method for determining boiler performance rendered better results that using the direct method due to the high variation in steam flow measurement.

For the boilers operation it was found that distributing the load across the three boilers was the better option and stopping a boiler while increasing the load of the other two did not add significant savings. Additionally, operating with only two boilers would also decrease reliability of the plant.

A detailed description of the steps taken for the implementation of the steam system thermodynamic model in ASPEN PLUS was also presented in this chapter. This model is used to build the steam network process flowsheet. The case study network has 3314 kg/h of LP steam that can be reduced before any change has to be implemented on the steam network configuration to avoid venting LP steam to atmosphere.

A new methodology for heat integration based on pinch analysis concepts was described in Chapter 4. The procedure can be used for the grassroots design or for retrofitting a heat exchanger network.

The stream match methodology takes into account forbidden matches and describes how the network is built in a sequential manner considering the yearly return of each match. The last step of the methodology is to "relax" the ΔT_{min} that was imposed at the beginning of the design phase and optimize the independent

variables, which are the pinch temperatures and split ratios, to minimize the overall yearly cost of the network.

The methodology was applied to a grassroots design of a network with 2 hot and 2 cold streams and the resulting network had an annualized cost 6.2% lower than the configuration achieved by Pereira *et al.* [94] who used traditional design pinch methodology.

For retrofitting an industrial network the approach was to determine which heat exchangers were violating any of the pinch rules and apply the stream matching methodology to the streams that were being serviced by these heat exchangers. In terms of annual cost the retrofitted network was 11.3% more efficient than the base case scenario. An investment of 810.0 k€ would represent savings of 1075 k€/yr, meaning a payback of less than 1 year.

The models of the steam and cooling water systems were used to evaluate the performance of the retrofitted industrial network. It was found that the cooling tower would be underdimensioned during 3% of the year instead of the 4.5% of the base case scenario. As for the steam network the HP steam let-down to generate LP steam would be reduced from 3324 kg/h to 12 kg/h and demineralized water consumption from 5691 kg/h to 5466 kg/h.

5.2 Recommendations for future work

Some of the themes addressed in this work can be subject of further study and development. Energy integration in industrial facilities is a relevant field of study that will most certainly remain actual in the foreseeable future.

A model of the cooling tower using equilibrium stage was developed in ASPEN PLUS. Such model could also be formulated using thermodynamic equilibrium equations and then be used in other platforms other than ASPEN PLUS. The cooling tower model could then be integrated into mathematical formulations regarding cooling water systems.

The methodology for evaluating the performance of the steam generators using the indirect method and for optimizing load distribution was presented. This methodology should be applied to other case studies where the performance of each steam generator differ from one another.

As for the stream match methodology it would be interesting to apply the methodology to other case studies to further validate it. Also, the developed tools can be automated to turn them into an integrated user-friendly tool that uses the concepts of the stream matching methodology. This tool could be of great value for designing and retrofitting industrial facilities.

6 References

[1] Key World Energy Statistics Report. International Energy Agency 2015

[2] Polyurethane MDI Handbook. BASF Corporation 2000.

[3] R. Sood, J.-L. Roser, R. De Genova. Advances in pure and polymeric MDI chemistry to meet changing product, process and performance needs. Utech Asia '97, Singapore, 1997.

[4] F.J.M. Neves. Modelling and Optimization of Large-Scale Processes—Application to the liquid-phase aniline production. Departamento de Engenharia Química. Faculdade de Ciências e Tecnologia da Universidade de Coimbra 2007.

[5] S.R. Wan Alwi, N.E. Mohammad Rozali, Z. Abdul-Manan, J.J. Klemeš. A process integration targeting method for hybrid power systems. Energy. 44 (2012) 6-10.

[6] S.-G. Yoon, J. Lee, S. Park. Heat integration analysis for an industrial ethylbenzene plant using pinch analysis. Applied Thermal Engineering. 27 (2007) 886-93.

[7] M. Ebrahim, A. Kawari. Pinch technology: an efficient tool for chemical-plant energy and capital-cost saving. Applied Energy. 65 (2000) 45-9.

[8] T. Gundersen. International Energy Agency. Implementating agreement on process integration. Annex I - A Process Integration Primer. SINTEF Energy Research 2000.

[9] B. Linnhoff, D.R. Mason, I. Wardle. Understanding heat exchanger networks. Computers & Chemical Engineering. 3 (1979) 295-302.

[10] B. Linnhoff, J.R. Flower. Synthesis of heat exchanger networks: I. Systematic generation of energy optimal networks. AIChE Journal. 24 (1978) 633-42.

[11] B. Linnhoff, J.R. Flower. Synthesis of heat exchanger networks: II. Evolutionary generation of networks with various criteria of optimality. AIChE Journal. 24 (1978) 642-54.

[12] J.J. Klemeš. Handbook of Process Integration (PI): Minimisation of Energy and Water Use, Waste and Emissions - Process Integration (PI): An Introduction. Woodhead Publishing Limited 2013.

[13] Aspen Plus V7.3 [25.0.1.5015]. Aspen Technology Inc. 2011.

[14] F. Benyahia. Flowsheeting packages: reliable or fictitious process models? Trans IChemE. 78 (2000).

[15] F.G. Martins. "Process simulators". Engenharia de processos e sistemas; Programa doutoral em Engenharia da Refinação, Petroquímica e Química 2010.

[16] A.C. Dimian. Integrated design and simulation of chemical processes 2003.

[17] Structural representations of systems. Norwegian University of Science and Technology. Notes of TKP9 & KP8100 2007 course, 2007.

[18] S.H. Kim, S.G. Yoon, S.H. Chae, S. Park. Economic and environmental optimization of a multi-site utility network for an industrial complex. Journal of environmental management. 91 (2010) 690-705.

[19] J.-K. Kim, R. Smith. Cooling water system design. Chemical Engineering Science. 56 (2001) 3641-58.

[20] M.H. Agha, R. Thery, G. Hetreux, A. Hait, J.M. Le Lann. Integrated production and utility system approach for optimizing industrial unit operations. Energy. 35 (2010) 611-27.

[21] W.S. Goh, Y.K. Wan, C.K. Tay, R.T.L. Ng, D.K.S. Ng. Automated targeting model for synthesis of heat exchanger network with utility systems. Applied Energy. 162 (2016) 1272-81.

[22] G.-Y. Jin, W.-J. Cai, L. Lu, E.L. Lee, A. Chiang. A simplified modeling of mechanical cooling tower for control and optimization of HVAC systems. Energy Conversion and Management. 48 (2007) 355-65.

[23] D.J. Benton, C.F. Bowman , M. Hydeman, P. Miller. An improved cooling tower algorithm for the CoolTools simulation model. ASHRAE Transactions. 108 (2002) AC-02-9-4.

[24] J.C. Kloppers, D.G. Kröger. A critical investigation into the heat and mass transfer analysis of counterflow wet-cooling towers. International Journal of Heat and Mass Transfer. 48 (2005) 765-77.

[25] J.R. Picardo, J.E. Variyar. The Merkel equation revisited: A novel method to compute the packed height of a cooling tower. Energy Conversion and Management. 57 (2012) 167-72.

[26] M.M. Castro, T.W. Song, J.M. Pinto. Minimization of Operational Costs in Cooling Water Systems. Chemical Engineering Research and Design. 78 (2000) 192-201.

[27] J.-U.-R. Khan, B.A. Qureshi, S.M. Zubair. A comprehensive design and performance evaluation study of counter flow wet cooling towers. International Journal of Refrigeration. 27 (2004) 914-23.

[28] R. Al-Waked, M. Behnia. CFD simulation of wet cooling towers. Applied Thermal Engineering. 26 (2006) 382-95.

[29] E. Rubio-Castro, M. Serna-González, J.M. Ponce-Ortega, M.A. Morales-Cabrera. Optimization of mechanical draft counter flow wet-cooling towers using a rigorous model. Applied Thermal Engineering. 31 (2011) 3615-28.

[30] M. Hosoz, H.M. Ertunc, H. Bulgurcu. Performance prediction of a cooling tower using artificial neural network. Energy Conversion and Management. 48 (2007) 1349-59.

[31] T.-H. Pan, S.-S. Shieh, S.-S. Jang, W.-H. Tseng, C.-W. Wu, J.-J. Ou. Statistical multi-model approach for performance assessment of cooling tower. Energy Conversion and Management. 52 (2011) 1377-85.

[32] M. Serna-González, J.M. Ponce-Ortega, A. Jiménez-Gutiérrez. MINLP optimization of mechanical draft counter flow wet-cooling towers. Chemical Engineering Research and Design. 88 (2010) 614-25.

[33] R.V. Rao, V.K. Patel. Optimization of mechanical draft counter flow wet-cooling tower using artificial bee colony algorithm. Energy Conversion and Management. 52 (2011) 2611-22.

[34] X. Qi, Y. Liu, Q. Guo, J. Yu, S. Yu. Performance prediction of seawater shower cooling towers. Energy. 97 (2016) 435-43.

[35] M.H. Sadafi, S. González Ruiz, M.R. Vetrano, I. Jahn, J. van Beeck, J.M. Buchlin, et al. An investigation on spray cooling using saline water with experimental verification. Energy Conversion and Management. 108 (2016) 336-47.

[36] J.M. Ponce-Ortega, M. Serna-González, A. Jiménez-Gutiérrez. MINLP synthesis of optimal cooling networks. Chemical Engineering Science. 62 (2007) 5728-35.

[37] K.V. Gololo, T. Majozi. On Synthesis and Optimization of Cooling Water Systems with Multiple Cooling Towers. Industrial & Engineering Chemistry Research. 50 (2011) 3775-87.

[38] J. Sun, X. Feng, Y. Wang. Cooling-water system optimisation with a novel two-step sequential method. Applied Thermal Engineering. 89 (2015) 1006-13.

[39] S.-C. Georgescu, A.-M. Georgescu, A. Jumara, V.-F. Piraianu, G. Dunca. Numerical Simulation of the Cooling Water System of a 115 MW Hydro-Power Plant. Energy Procedia. 85 (2016) 228-34.

[40] M. Kljajić, D. Gvozdenac, S. Vukmirović. Use of Neural Networks for modeling and predicting boiler's operating performance. Energy. (2012).

[41] S.K. Behera, E.R. Rene, M.C. Kim, H.-S. Park. Performance prediction of a RPF-fired boiler using artificial neural networks. International Journal of Energy Research. 38 (2014) 995-1007.

[42] D. Strušnik, M. Golob, J. Avsec. Artificial neural networking model for the prediction of high efficiency boiler steam generation and distribution. Simulation Modelling Practice and Theory. 57 (2015) 58-70.

[43] Ø. Andreassen, T.O. Olsen. Optimal Load Allocation. Modeling, Identification and Control: A Norwegian Research Bulletin. 4 (1983) 107-16.

[44] A.C. Dunn, Y.Y. Du. Optimal load allocation of multiple fuel boilers. ISA transactions. 48 (2009) 190-5.

[45] C.D. Rocco, R. Morabito. Um modelo de otimização para as operações de produção de vapor em caldeiras industriais. Gestao e Producao. 19 (2012) 273-86.

[46] C.-L. Chen, H.-C. Chen. A mathematical approach for retrofit and optimization of total site steam distribution networks. Process Safety and Environmental Protection. 92 (2014) 532-44.

[47] Y. Majanne. Model predictive pressure control of steam networks. Control Engineering Practice. 13 (2005) 1499-505.

[48] S.W.A. Coetzee, T. Majozi. Steam System Network Synthesis Using Process Integration. Industrial & Engineering Chemistry Research. 47 (2008) 4405-13.

[49] W. Zhong, H. Feng, X. Wang, D. Wu, M. Xue, J. Wang. Online hydraulic calculation and operation optimization of industrial steam heating networks considering heat dissipation in pipes. Energy. 87 (2015) 566-77.

[50] T. Umeda, T. Harada, K. Shiroko. A thermodynamic approach to the synthesis of heat integration systems in chemical processes. Computers & Chemical Engineering. 3 (1979) 273-82.

[51] T.F. Yee, I.E. Grossmann. Simultaneous optimization models for heat integration—II. Heat exchanger network synthesis. Computers & Chemical Engineering. 14 (1990) 1165-84.

[52] R. Nordman. New process integration methods for heat-saving retofit projects in industrial systems. Department of Energy and Environment. Chalmers University of Technology, Göteborg, Sweden, 2005.

[53] N. Jiang, J.D. Shelley, S. Doyle, R. Smith. Heat exchanger network retrofit with a fixed network structure. Applied Energy. 127 (2014) 25-33.

[54] B.K. Sreepathi, G.P. Rangaiah. Review of Heat Exchanger Network Retrofitting Methodologies and Their Applications. Industrial & Engineering Chemistry Research. 53 (2014) 11205-20.

[55] I.C. Kemp. Pinch Analysis and Process Integration, 2nd Edition: A User Guide on Process Integration for the Efficient Use of Energy 2007.

[56] Pinch analysis for the efficient use of energy, water and hydrogen. in: N.R. Canada, (Ed.).2003.

[57] P. Castro, H. Matos, M.C. Fernandes, C. Pedro Nunes. Improvements for mass-exchange networks design. Chemical Engineering Science. 54 (1999) 1649-65.

[58] J.J. Alves, G.P. Towler. Analysis of Refinery Hydrogen Distribution Systems. Industrial & Engineering Chemistry Research. 41 (2002) 5759-69.

[59] T.N. Tjoe, B. Linnhoff. Using Pinch Technology for Process Retrofit. Chemical Engineering. 93 (1986) 47-60.

[60] M. Bagajewicz, G. Valtinson, D. Nguyen Thanh. Retrofit of Crude Units Preheating Trains: Mathematical Programming versus Pinch Technology. Industrial & Engineering Chemistry Research. 52 (2013) 14913-26.

[61] A. Carlsson, P.-A.k. Franck, T. Berntsson. Design better heat exchanger network retrofits. Chemical Engineering Progress March 1993. pp. 87–96.

[62] N.D.K. Asante, X.X. Zhu. An Automated and Interactive Approach for Heat Exchanger Network Retrofit. Chemical Engineering Research and Design. 75 (1997) 349-60.

[63] J. Cerda, A.W. Westerberg, D. Mason, B. Linnhoff. Minimum utility usage in heat exchanger network synthesis A transportation problem. Chemical Engineering Science. 38 (1983) 373-87.

[64] J. Cerda, A.W. Westerburg. Synthesizing heat exchanger networks having restricted stream/stream matches using transportation problem formulations. Chemical Engineering Science. 38 (1983) 1723-40.

[65] S.A. Papoulias, I.E. Grossmann. A structural optimization approach in process synthesis—II. Computers & Chemical Engineering. 7 (1983) 707-21.

[66] A. Barbaro, M.J. Bagajewicz. New rigorous one-step MILP formulation for heat exchanger network synthesis. Computers & Chemical Engineering. 29 (2005) 1945-76.

[67] D.Q. Nguyen, A. Barbaro, N. Vipanurat, M.J. Bagajewicz. All-At-Once and Step-Wise Detailed Retrofit of Heat Exchanger Networks Using an MILP Model. Industrial & Engineering Chemistry Research. 49 (2010) 6080-103.

[68] Y. Wang, R. Smith, J.-K. Kim. Heat exchanger network retrofit optimization involving heat transfer enhancement. Applied Thermal Engineering. 43 (2012) 7-13.

[69] Calgavin hiTRAN Thermal systems (Company website consulted on October 2015). Tube side heat transfer enhancement device

[70] Y. Wang, M. Pan, I. Bulatov, R. Smith, J.-K. Kim. Application of intensified heat transfer for the retrofit of heat exchanger network. Applied Energy. 89 (2012) 45-59.

[71] M. Pan, I. Bulatov, R. Smith, J.-K. Kim. Optimisation for the retrofit of large scale heat exchanger networks with different intensified heat transfer techniques. Applied Thermal Engineering. 53 (2013) 373-86.

[72] H. Becker, F. Maréchal. Energy integration of industrial sites with heat exchange restrictions. Computers & Chemical Engineering. 37 (2012) 104-18.

[73] Engineers Aide SiNET XLC 8.3. Epcon International.

[74] W. Simpson, T.K. Sherwood. Performance of small mechanical draft cooling towers. ASRAE Journal of Refrigerating Engineering. 52 (1946) 543-76.

[75] Aspen Plus V7.1. Aspen Technology Inc. 2008.

[76] J.A. Queiroz, V.M.S. Rodrigues, H.A. Matos, F.G. Martins. Modeling of existing cooling towers in ASPEN PLUS using an equilibrium stage method. Energy Conversion and Management. 64 (2012) 473-81.

[77] A. Aktepe, Ç. Öncel, S. Ersöz. An artificial neural network model on welding process control of 155 mm. artillery ammunition. 6th International Advanced Technologies Symposium (IATS'11), Elazığ, Turkey, 2011.

[78] Microsoft Office Excel 2007. Microsoft Corporation 2007.

[79] Aspen Simulation Workbook V7.1. Aspen Technology Inc. 2009.

[80] Q. Fang. Distinctions between Levenberg-Marquardt method and Tikhonov regularization. Thayer School of Engineering, Dartmouth College, Hanover, USA, 2004.

[81] Aspen Simulation Workbook User Guide V7.1. Aspen Technology Inc. 2009.

[82] B.A. Qureshi, S.M. Zubair. A complete model of wet cooling towers with fouling in fills. Applied Thermal Engineering. 26 (2006) 1982-9.

[83] G. Heidarinejad, M. Karami, S. Delfani. Numerical simulation of counter-flow wet-cooling towers. International Journal of Refrigeration. 32 (2009) 996-1002.

[84] Weather Underground. Atmospheric pressure data corresponding to the period between January and December 2010 Retrived on February 2011.

[85] S.I.V. Sousa, F.G. Martins, M.C.M. Alvim-Ferraz, M.C. Pereira. Multiple linear regression and artificial neural networks based on principal components to predict ozone concentrations. Environmental Modelling & Software. 22 (2007) 97-103.

[86] American Society of Mechanical Engineers ASME PTC 4-1998 - Fired Steam Generators. 1998.

[87] Licença Ambiental LA nº 467/1.0/2013 Dow Portugal – Produtos Químicos, Sociedade Unipessoal Limitada. in: A.P.d. Ambiente, (Ed.).2013.

[88] R.E. Bolz. CRC Handbook of Tables for Applied Engineering Science. 2nd ed1976.

[89] Boiler efficiency as a function of the load. Standardkessel Duisburg 1979.

[90] Microsoft Office Excel 2013. Microsoft Corporation 2007.

[91] V.L. Haar, J.S. Gallagher, G.S. Kell. NBS/NRC steam tables: Thermodynamic and Transport Properties and Computer Programs for Vapor and Liquid States of Water in S.I. Units. Hemisphere Publishing Corp, Washington–New York–London Chemie Ingenieur Technik. 57 (1984) 812-1985.

[92] International site for Spirax Sarco - Steam Tables. International site for Spirax Sarco 2013.

[93] KBC. Pinch technology introduction. KBC Energy Services.

[94] P. Pereira, H. Matos, M.C. Fernandes, C. Pedro Nunes. FI2EPI: A heat management tool for Process Integration. Applied Thermal Engineering (preliminary accepted under revision, 2016).

[95] American Society of Agricultural and Biological Engineers /(ASAE) D271.2 Psychrometric Data. 1984.

[96] ASHRAE fundamentals Handbook. Chapter 6 Psychrometrics 1997.

[97] Aspen Energy Analyzer V7.1. Aspen Technology Inc. 2008.

Appendix

A1 *(Air properties)*

Air Properties

Some properties of the system air-water are calculated using equations, which were retrieved from the American Society of Agricultural and Biological Engineers document *ASAE Standard Psychrometric Data ASAE D2* [95] and ASHRAE Fundamental Handbook [96].

To determine the wet-bulb temperature based on dry-bulb temperature and relative humidity, it is necessary to evaluate several intermediate variables, namely: humidity ratio, latent heat of vaporization of water at saturation, dew point temperature, vapor pressure, vapor pressure at saturation and enthalpy.

Nomenclature:

- h = enthalpy of air-vapor mixture, J/kg
- h_{fg} = latent heat of vaporization of water at T_{dp}, J/kg
- h_{ig} = heat of sublimation of ice at T_{dp}, J/kg
- H = humidity ratio, kg of water/kg of dry air
- P_{atm} = atmospheric pressure, Pa
- P_s = saturation vapor pressure at temperature T, Pa
- P_v = vapor pressure, Pa
- rh = relative humidity, decimal
- T = dry bulb temperature, K
- T_{dp} = dewpoint temperature, K
- T_{wb} = wet-bulb temperature, K

Saturation line, P_s as a function of T:

$$\ln(P_S) = 31.9602 - \frac{6270.3605}{T} - 0.46057 \cdot \ln(T) \qquad 255.38 \le T \le 273.16 \qquad \textbf{(A1.1)}$$

$$\ln\left(P_S / R\right) = \frac{A + BT + CT^2 + DT^3 + ET^4}{FT - GT^2} \qquad 273.16 \le T \le 533.16 \qquad \textbf{(A1.2)}$$

where:

- R = 22 105 649.25
- A = -27 405.526
- B = 97.5413
- C = -0.146244
- D = 0.12558 x 10^{-3}

- E = -0.48502 x 10^{-7}
- F = 4.34903
- G = 0.39381 x 10^{-2}

Saturation line, T_{dp} as a function of P_{vs}:

$$T_{dp} - 255.38 = \sum_{i=0}^{i=8} A_i \left[\ln(0.00145 \cdot P_S)\right]^i \qquad 620.52 \le P_S \le 4\,688\,396.00 \qquad \textbf{(A1.3)}$$

where:

- A_0 = 19.5322
- A_1 = 13.6626
- A_2 = 1.17678
- A_3 = -0.189693
- A_4 = 0.087453
- A_5 = -0.0174053
- A_6 = 0.00214768
- A_7 = -0.138343 x 10^{-3}
- A_8 = 0.38 x 10^{-5}

Latent heat of sublimation at saturation:

$$h_{ig} = 2\,839\,683.144 - 212.56384 \cdot (T - 255.38) \qquad 255.38 \le T \le 273.16 \qquad \textbf{(A1.4)}$$

Latent heat of vaporization at saturation:

$$h_{fg} = 2\,502\,535.259 - 2\,385.76424 \cdot (T - 273.16) \qquad 273.16 \le T \le 338.72 \qquad \textbf{(A1.5)}$$

$$h_{fg} = \left(7\,329\,155\,978.000 - 15\,995\,964.08 \cdot T^2\right)^{1/2} \qquad 338.72 \le T \le 533.16 \qquad \textbf{(A1.6)}$$

Humidity ratio:

$$H = \frac{0.6219 \cdot P_v}{P_{atm} - P_v} \qquad \begin{matrix} 255.38 \le T \le 533.16 \\ P_v < P_{atm} \end{matrix} \qquad \textbf{(A1.7)}$$

Enthalpy:

$$\begin{aligned} h &= 1006.92540 \cdot (T - 273.16) \\ &\quad - H \cdot \left[333\,432.1 + 2030.598 \cdot (273.16 - T_{dp})\right] + h_{ig} \cdot H \\ &\quad + 1875.6864 \cdot H \cdot (T - T_{dp}) \end{aligned} \qquad 255.38 \le T_{dp} \le 273.16 \qquad \textbf{(A1.8)}$$

and,

$$h = 1006.92540 \cdot (T - 273.16) + 4186.8 \cdot H \cdot (T - 273.16) + h_{fg} \cdot H + 1875.6864 \cdot H \cdot (T - T_{dp}) \qquad 273.16 \le T_{dp} \le 373.16 \qquad \textbf{(A1.9)}$$

Relative humidity:

$$rh = P_v / P_S \qquad \textbf{(A1.10)}$$

After estimating the enthalpy of moist air, the wet-bulb temperature is calculated through an iterative procedure. Assuming that the enthalpy at a given dry-bulb temperature and relative humidity are equal to the enthalpy at the wet-bulb temperature and saturation (Enthalpy (T_{db}, H [%]) = Enthalpy (T_{wb}, 100 %)), the wet-bulb temperature is iterated until this equality is verified.

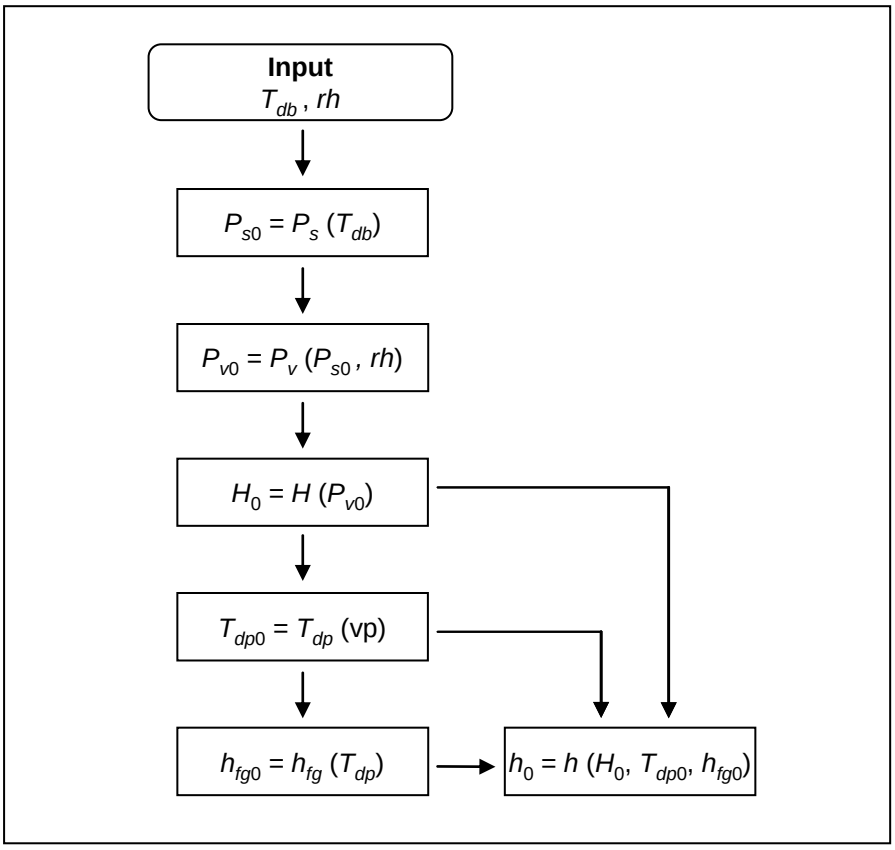

Figure A1.1 – Flow diagram describing the algorithm to calculate properties of humid air.

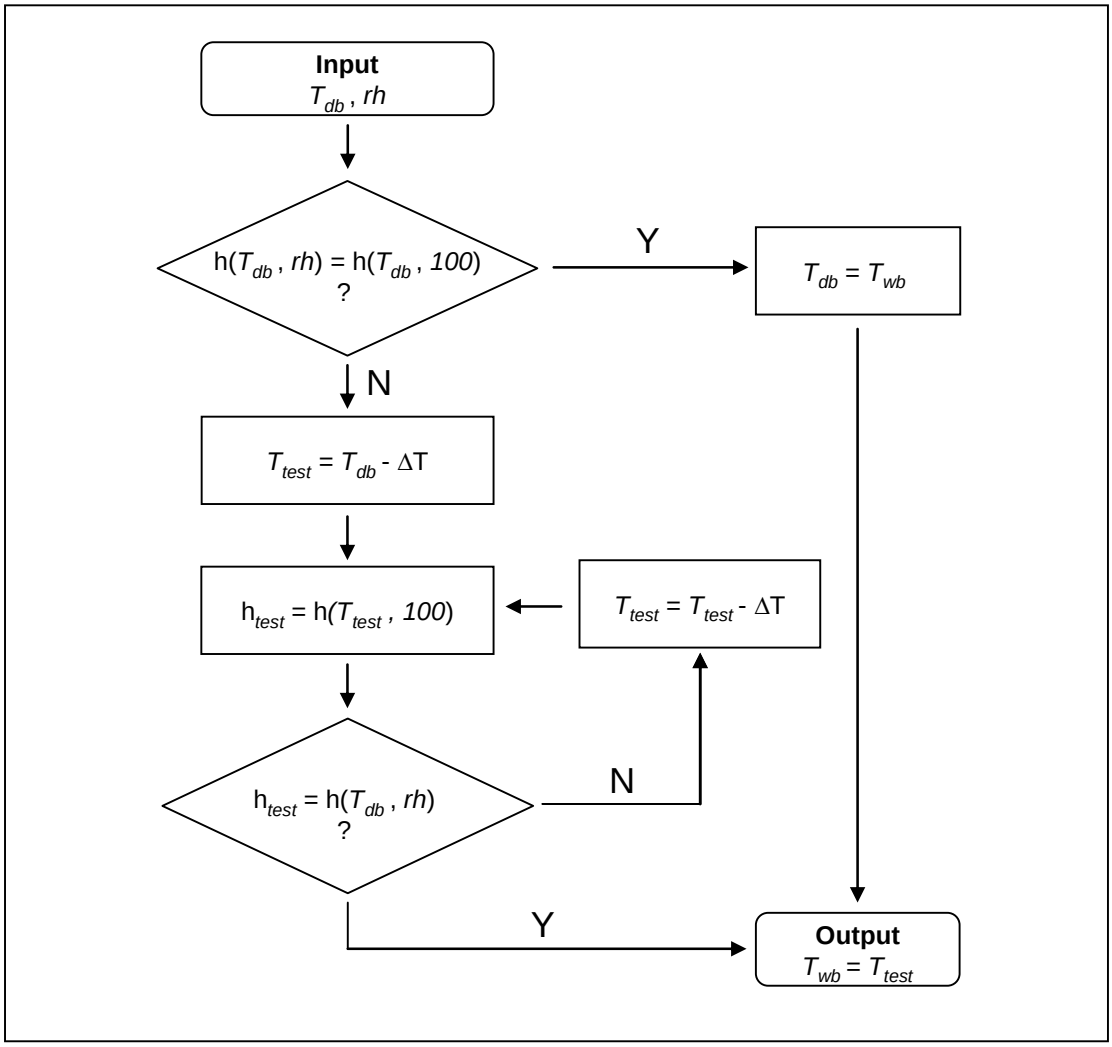

Figure A1.2 –Flow diagram describing the algorithm to calculate the wet-bulb temperature of humid air.

$$A(kg\ Dry\ Air / kg\ MoistAir) = \frac{1}{1 + H(kg\ H_2O / kg\ Dry\ Air)} \quad \textbf{(A1.11)}$$

$$W(kg\ H_2O / kg\ Moist\ Air) = 1 - A(kg\ H_2O / kg\ Dry\ Air) \quad \textbf{(A1.12)}$$

A2 *(Stream matching)*

Above the pinch

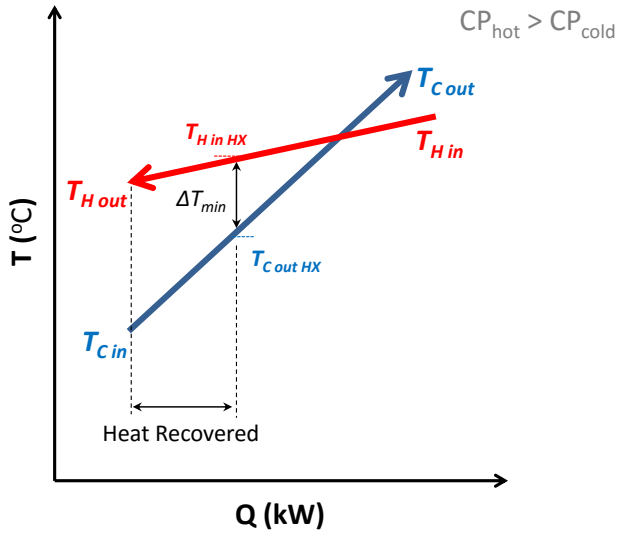

$$Q_{c\,HX} = CP_c \cdot (T_{c\,out\,HX} - T_{c\,in}) \Leftrightarrow T_{c\,out\,HX} = \frac{Q_{c\,HX} + CP_c \cdot T_{c\,in}}{CP_c} \quad \textbf{(A1.1)}$$

$$Q_{h\,HX} = CP_h \cdot (T_{h\,in\,HX} - T_{h\,out}) \Leftrightarrow T_{h\,in\,HX} = \frac{Q_{h\,HX} + CP_h \cdot T_{h\,out}}{CP_h} \quad \textbf{(A1.2)}$$

Heat transfer between both streams is the same:

$$Q_{c\,HX} = Q_{h\,HX} = Q_{HX} \quad \textbf{(A1.3)}$$

Cold steam outlet temperature and hot inlet temperature are related:

$$T_{c\,out\,HX} = T_{h\,in\,HX} - \Delta T_{min} \quad \textbf{(A1.4)}$$

Combining the equations:

$$\frac{Q_{HX} + CP_c \cdot T_{c\,in}}{CP_c} = \frac{Q_{HX} + CP_h \cdot T_{h\,out}}{CP_h} - \Delta T_{min} \quad \textbf{(A1.5)}$$

$$\Leftrightarrow \frac{Q_{HX} \cdot CP_h + CP_c \cdot CP_h \cdot T_{c\,in} - Q_{HX} \cdot CP_c - CP_h \cdot CP_c \cdot T_{h\,out}}{CP_c \cdot CP_h} = -\Delta T_{min} \quad \textbf{(A1.6)}$$

$$\Leftrightarrow \frac{Q_{HX} \cdot (CP_h - CP_c) + CP_c \cdot CP_h \cdot (T_{c\,in} - T_{h\,out})}{CP_c \cdot CP_h} = -\Delta T_{min} \quad \textbf{(A1.7)}$$

$$\Leftrightarrow \frac{Q_{HX} \cdot (CP_h - CP_c)}{CP_c \cdot CP_h} = T_{h\,out} - T_{c\,in} - \Delta T_{min} \quad \textbf{(A1.8)}$$

$$\Leftrightarrow Q_{HX} = \frac{CP_c \cdot CP_h \cdot (T_{h\,out} - T_{c\,in} - \Delta T_{min})}{(CP_h - CP_c)} \quad \textbf{(A1.9)}$$

Below the pinch

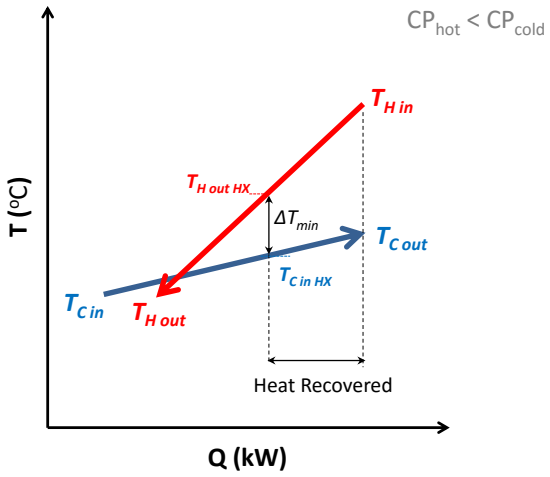

$$Q_{c\,HX} = CP_c \cdot (T_{c\,out} - T_{c\,in\,HX}) \Leftrightarrow T_{c\,in\,HX} = \frac{-Q_{c\,HX} + CP_c \cdot T_{c\,out}}{CP_c} \quad \textbf{(A1.10)}$$

$$Q_{h\,HX} = CP_h \cdot (T_{h\,in} - T_{h\,out\,HX}) \Leftrightarrow T_{h\,out\,HX} = \frac{-Q_{h\,HX} + CP_h \cdot T_{h\,in}}{CP_h} \quad \textbf{(A1.11)}$$

Heat transfer between both streams is the same:

$$Q_{c\,HX} = Q_{h\,HX} = Q_{HX} \quad \textbf{(A1.12)}$$

Cold steam inlet temperature and hot outlet temperature are related:

$$T_{c\,in\,HX} = T_{h\,out\,HX} - \Delta T_{min} \quad \textbf{(A1.13)}$$

Combining the equations:

$$\frac{-Q_{HX} + CP_c \cdot T_{c\,out}}{CP_c} = \frac{-Q_{HX} + CP_h \cdot T_{h\,in}}{CP_h} - \Delta T_{min} \quad \textbf{(A1.14)}$$

$$\Leftrightarrow \frac{-Q_{HX} \cdot CP_h + CP_c \cdot CP_h \cdot T_{c\,out} + Q_{HX} \cdot CP_c - CP_h \cdot CP_c \cdot T_{h\,in}}{CP_c \cdot CP_h} = -\Delta T_{min} \quad \textbf{(A1.15)}$$

$$\Leftrightarrow \frac{Q_{HX} \cdot (-CP_h + CP_c) + CP_c \cdot CP_h \cdot (T_{c\,out} - T_{h\,in})}{CP_c \cdot CP_h} = -\Delta T_{min} \quad \textbf{(A1.16)}$$

$$\Leftrightarrow \frac{Q_{HX} \cdot (-CP_h + CP_c)}{CP_c \cdot CP_h} = T_{h\,in} - T_{c\,out} - \Delta T_{min} \quad \textbf{(A1.17)}$$

$$\Leftrightarrow Q_{HX} = -\frac{CP_c \cdot CP_h \cdot (T_{h\,in} - T_{c\,out} - \Delta T_{min})}{(CP_h - CP_c)} \quad \textbf{(A1.18)}$$

A3 *(Stream match tools)*

A description of the tool developed for applying the stream match methodology is described herein. The tools were developed using Microsoft Excel. For applying the methodology three files are used:

Above pinch.xls Used to match the streams above the pinch.

Below pinch.xls Used to match the streams below the pinch.

HX network.xls Used to visualize the heat exchanger network and optimize the temperature approach.

A3.3.1 Above pinch.xls

1. In the "***INPUT***" sheet input the data related to each stream namely: T_{in} [C], T_{out} [C], FC_p [kW·C^{-1}], Q [kW], HTC [kW.m^2·C^{-1}]. In this sheet the hot and cold pinch temperature must also be stated. To determine the pinch temperature other tool should be used [97].

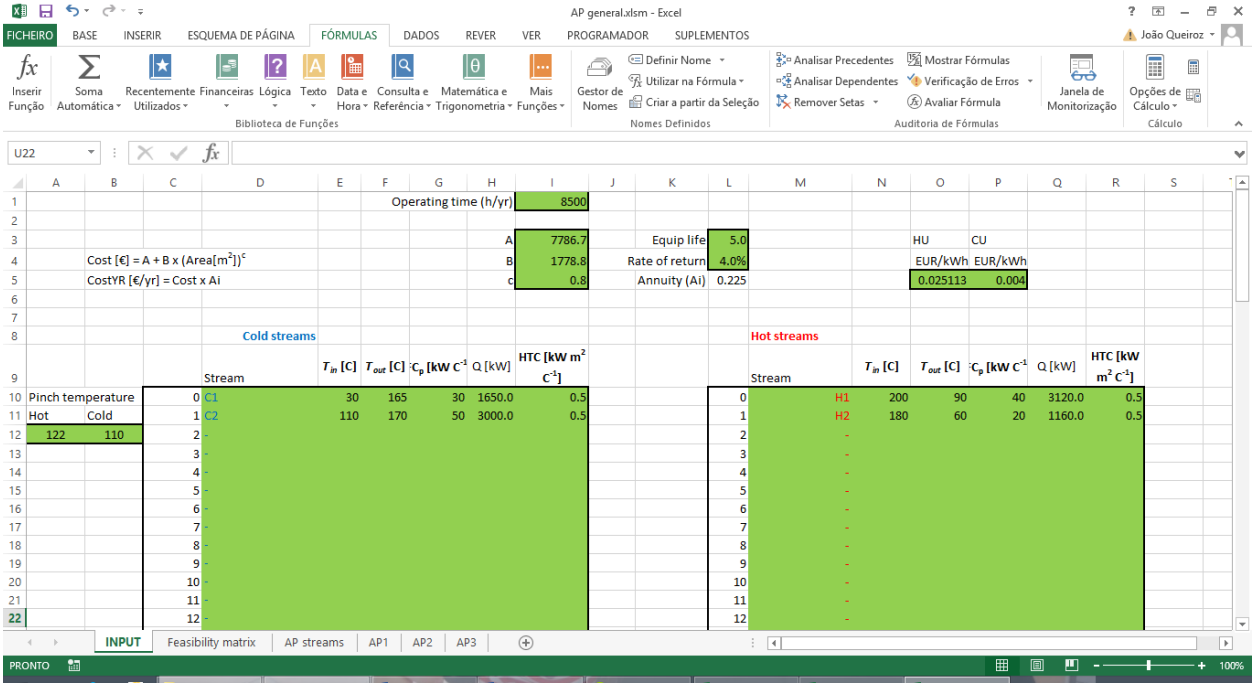

2. Then "***Feasibility matrix***", where 1 represents a feasible match and 0 a non-feasible match.

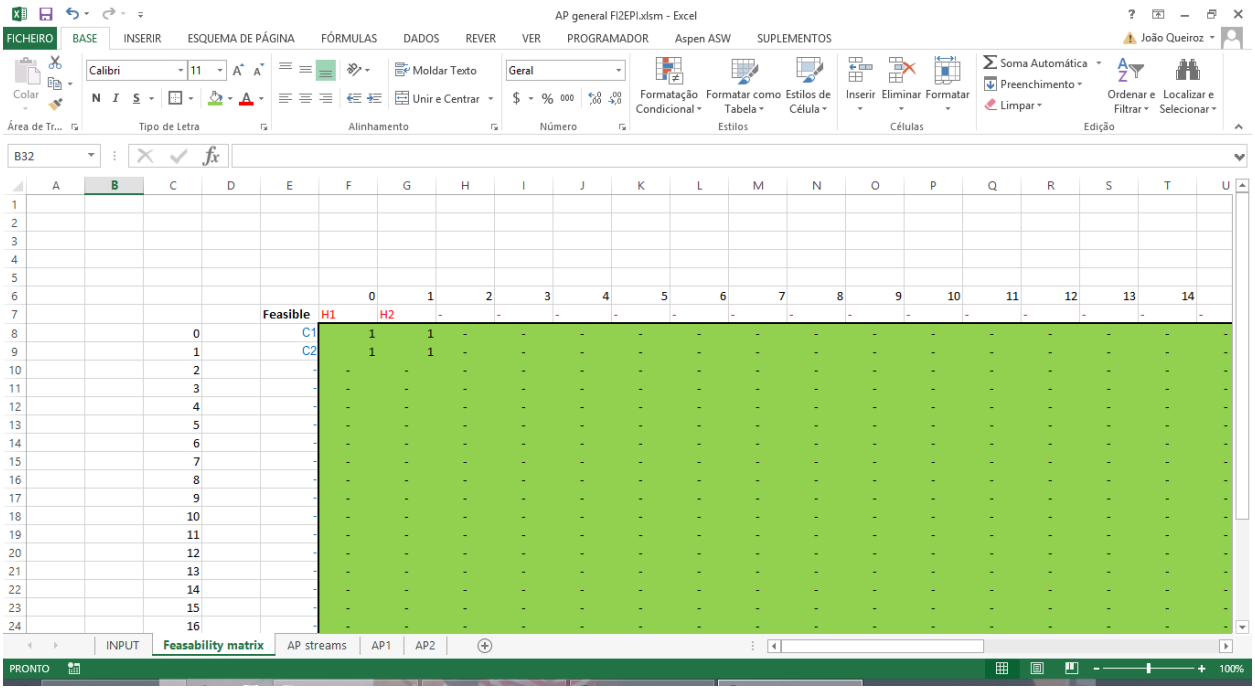

3. Based on the data states on the “INPUT” sheet the tool determines the duty and temperature of each stream that is located above the pinch. The summary is then presented in the “***AP streams***” sheet.

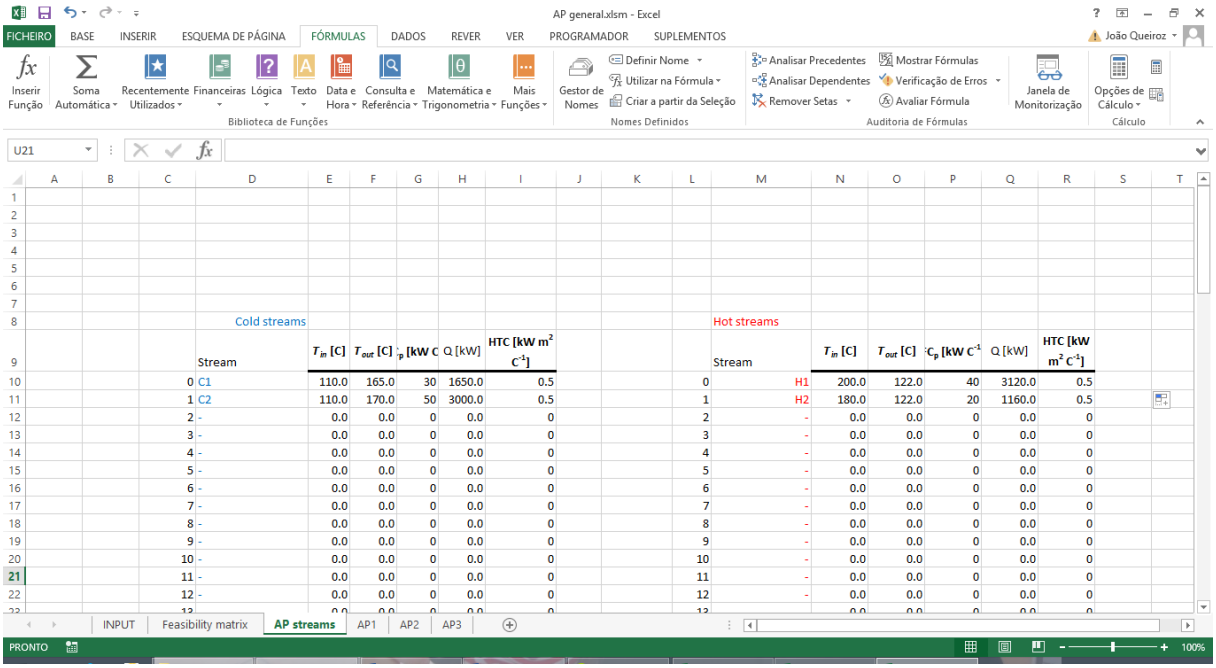

4. On sheet “AP1”, check which are the hot streams with the lowest outlet temperature. For these streams, choose the match with the highest return in the Cost-Saving matrix.
   Is this case streams H1 and H2 have the same inlet temperature, which is the pinch temperature, 122 C and the match with the highest return is C2-H1.

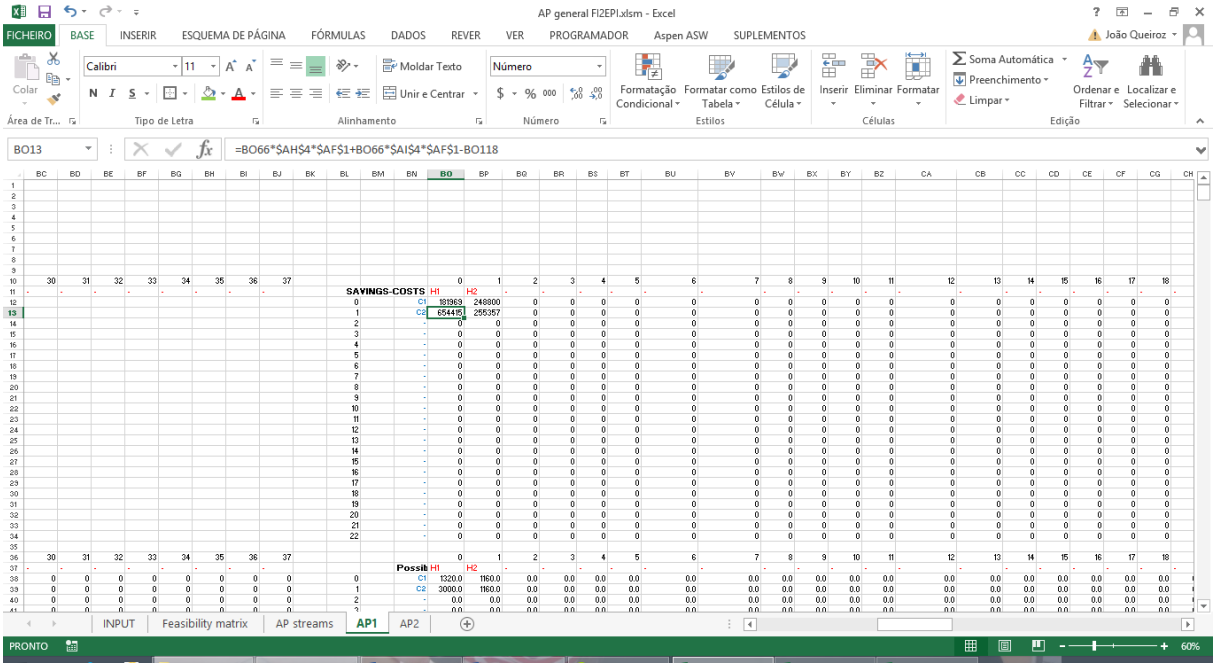

5. On sheet AP2 select the streams (green box) which were selected in the previous step.

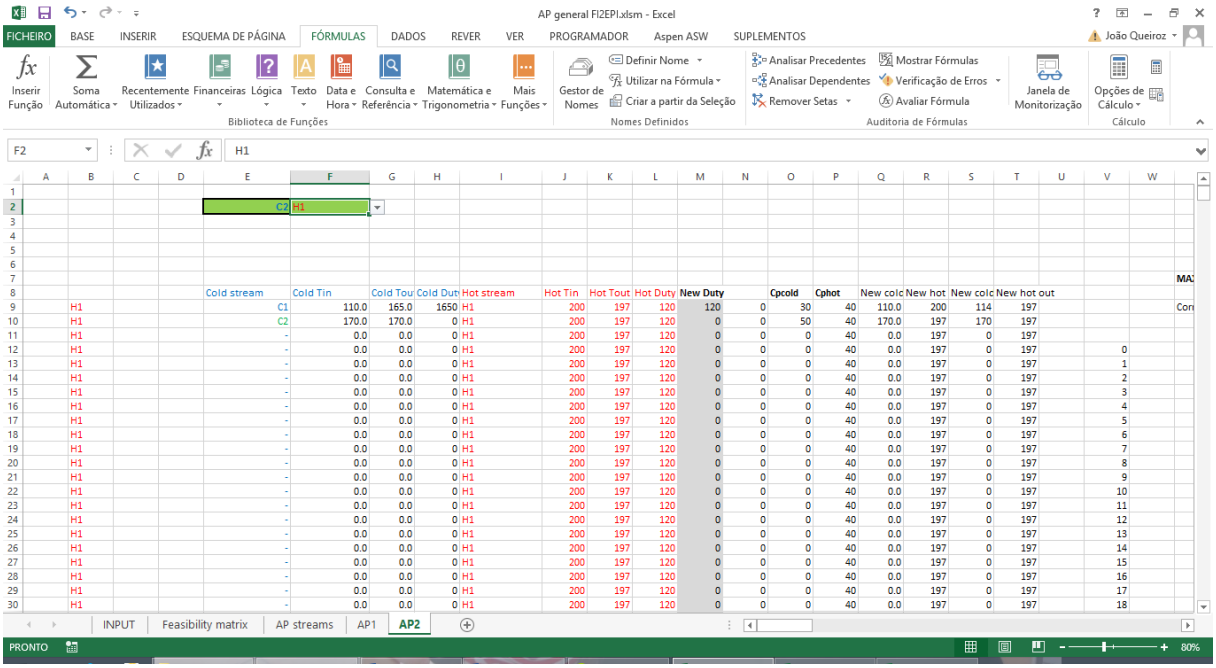

6. On sheet “AP2”, check which are the hot streams with the lowest inlet temperature. For these streams, choose the match with the highest return in the Cost-Saving matrix.

   In this case stream H1 has an inlet temperature of 197 C and stream H2 an outlet temperature of 122 C. Since stream H2 has an outlet temperature lower than stream H1, only this stream will be considered and the selected match will be C1-H2.

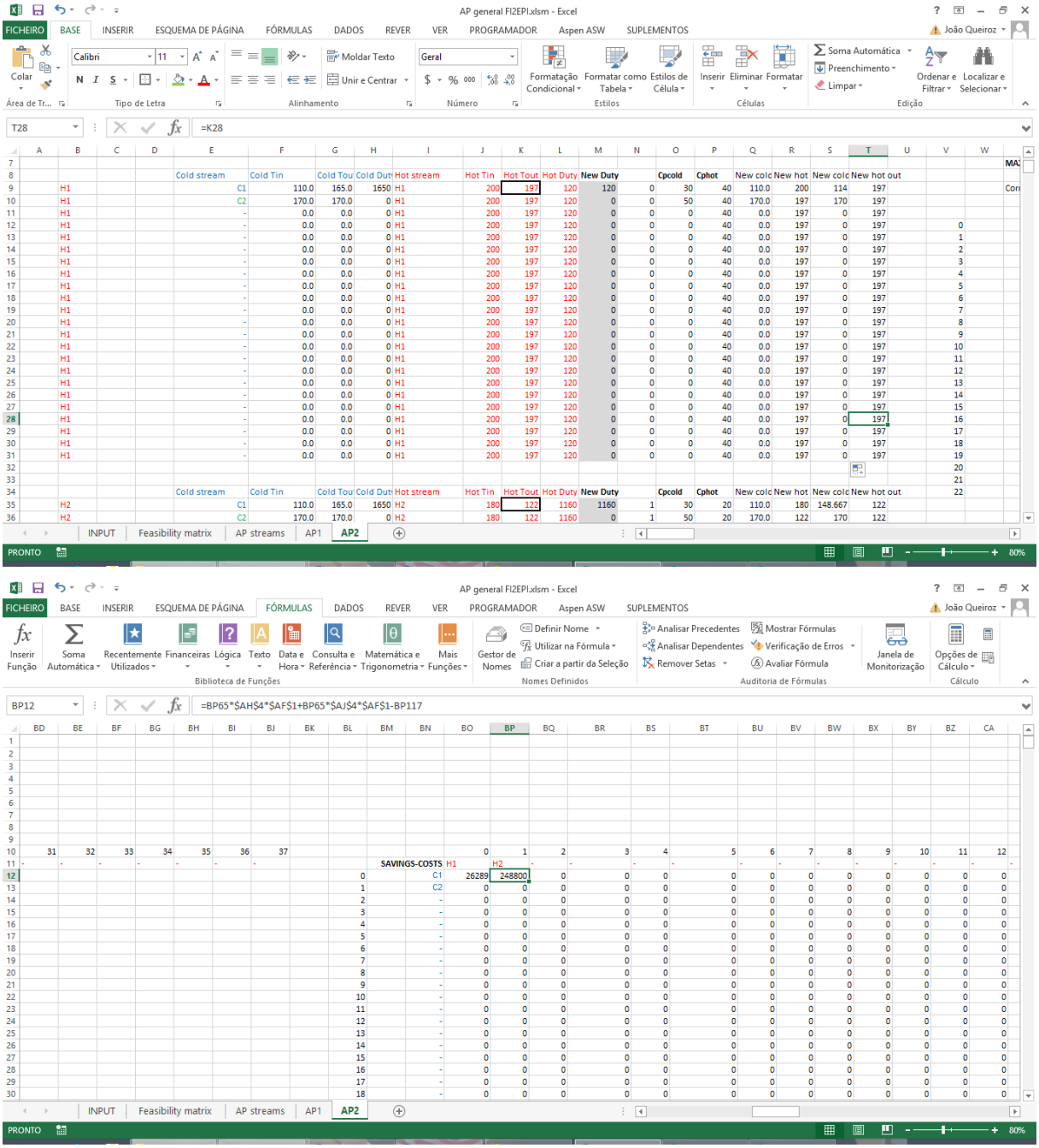

7. Copy the last sheet, in this case sheet AP2, and paste it at the end. Change the name of the sheet so that the sheets have a sequential numeration.

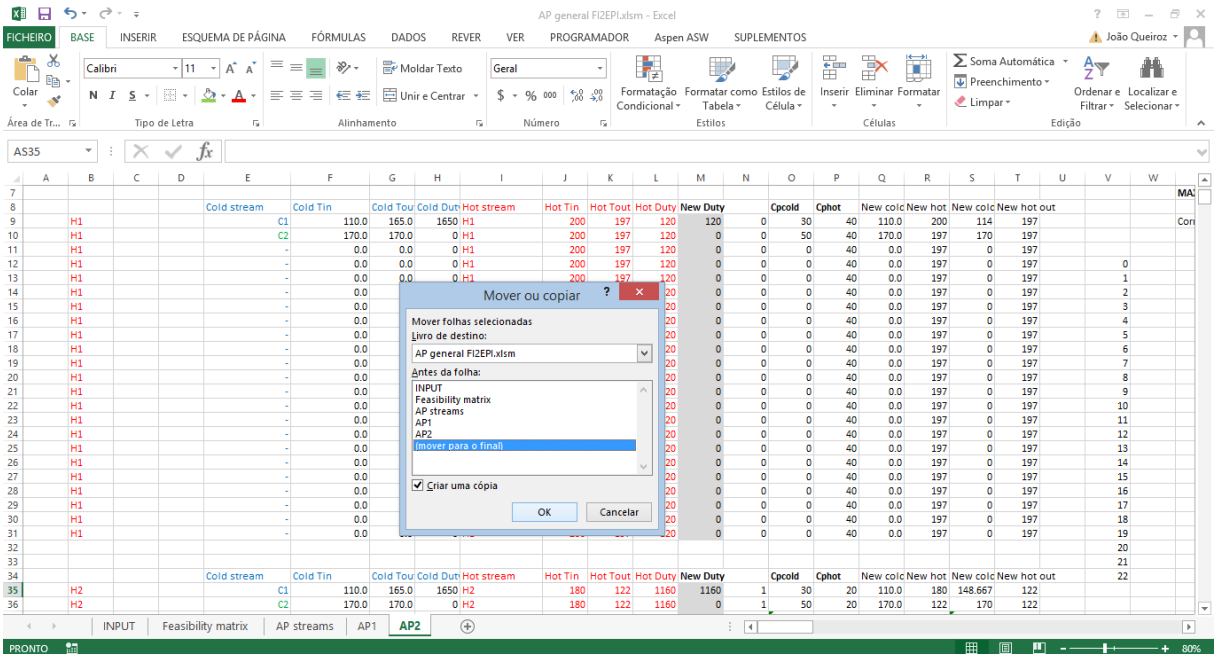

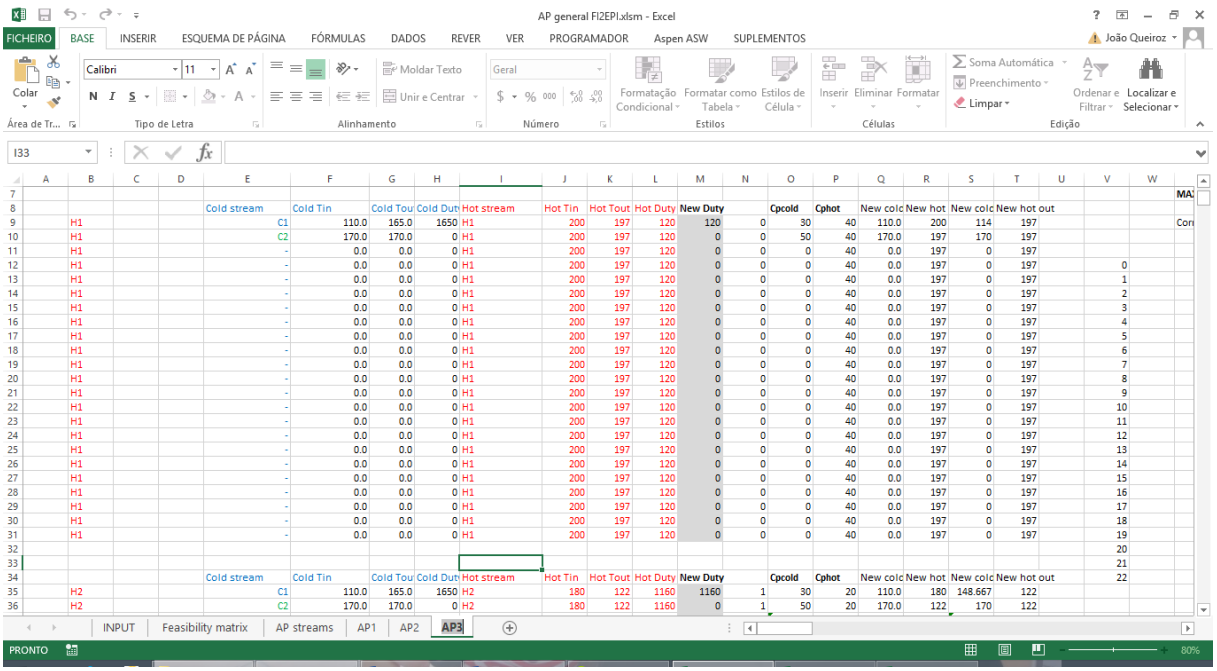

8. On sheet AP3 select the streams (green box) which were selected in the previous step.

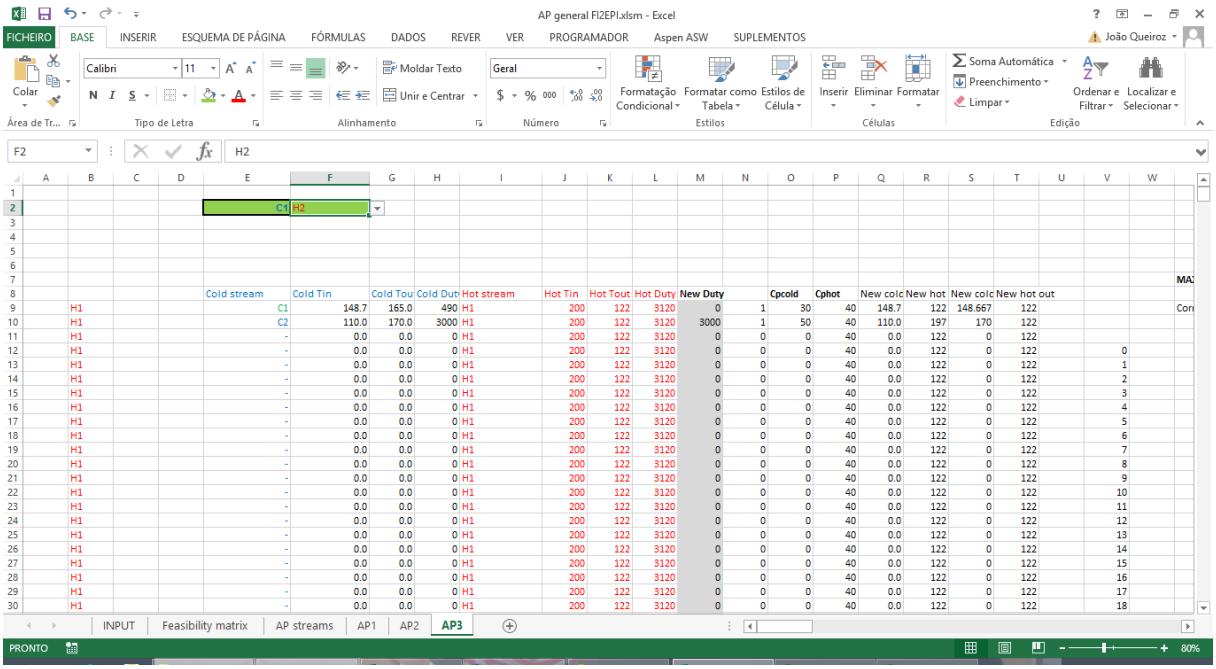

9. On Sheet AP3 “replace all” ’AP1’ with ‘AP2’.

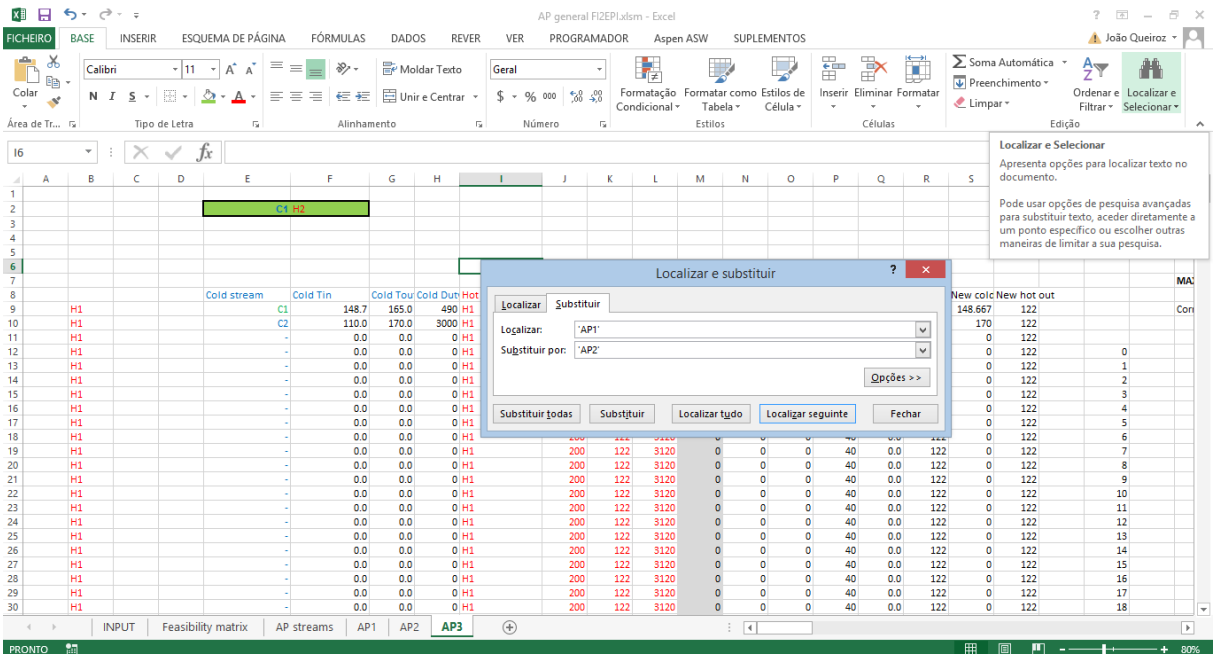

10. On sheet AP2 select the streams (green box) which were previously selected, C1-H2.

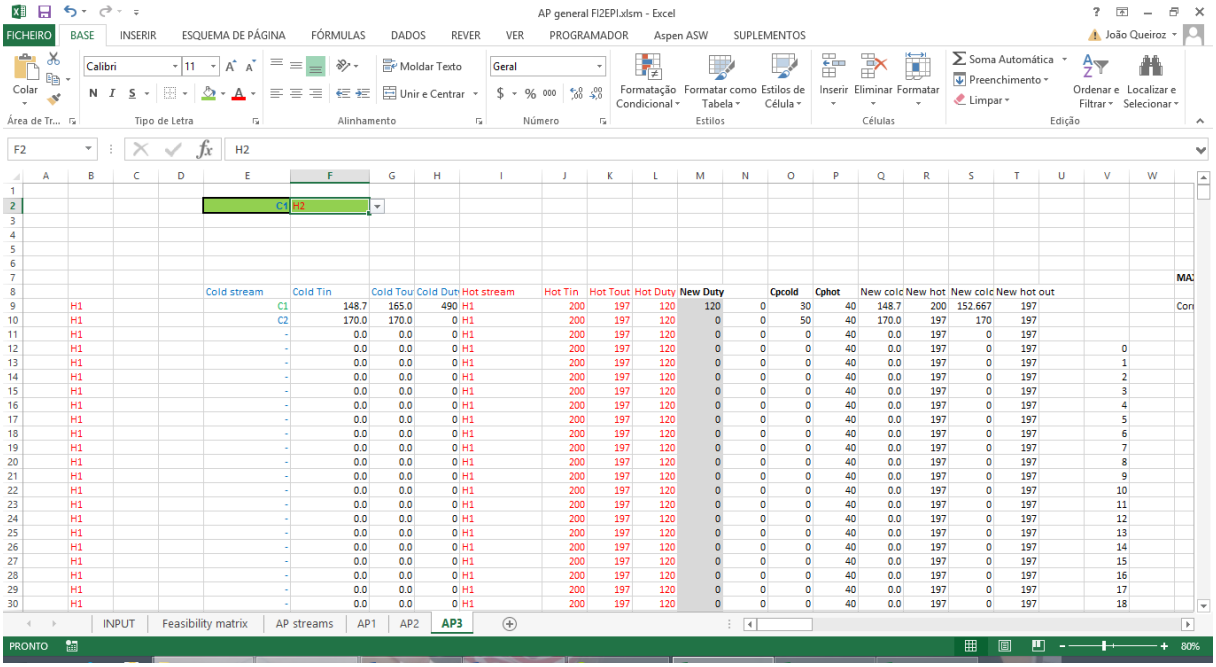

11. Choose the match with the highest return.

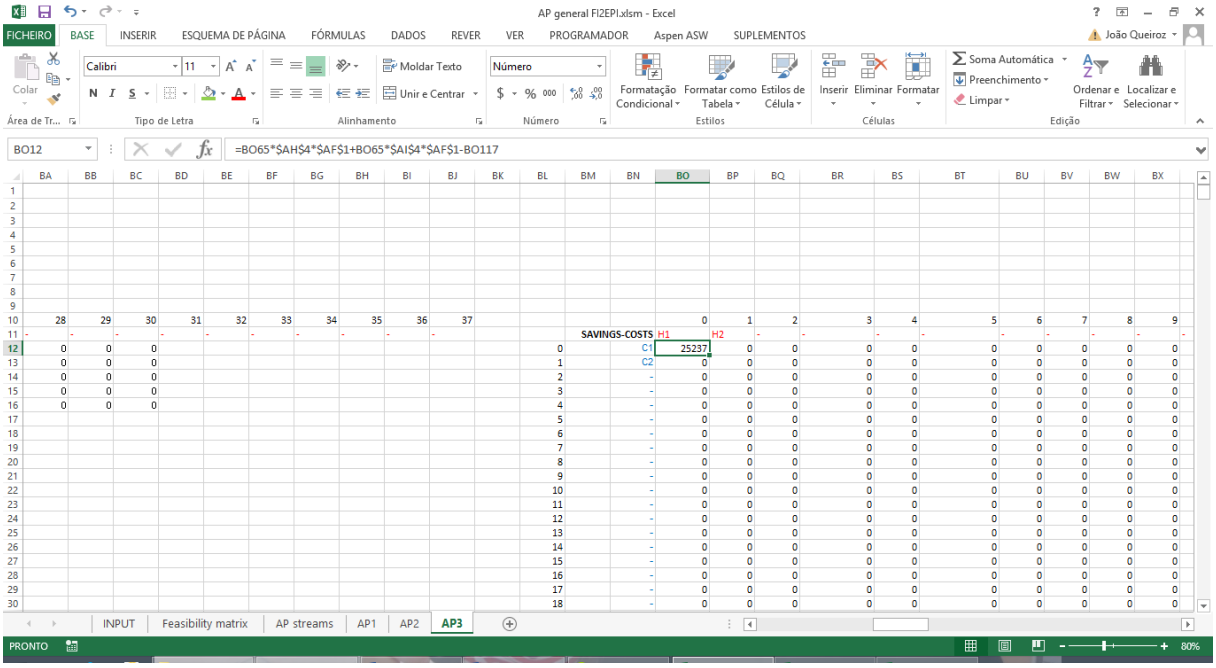

12. When no more streams are available to match stop the process.

A3.3.2 Bellow pinch.xls

Follow the same procedure as for the Above Pinch worksheet but in this case the order for choosing the matches start with the cold streams with the highest outlet temperature and gradually move out of the pinch.

A3.3.3 Pinch Tool.xls

1. Specify the input data in the green boxes

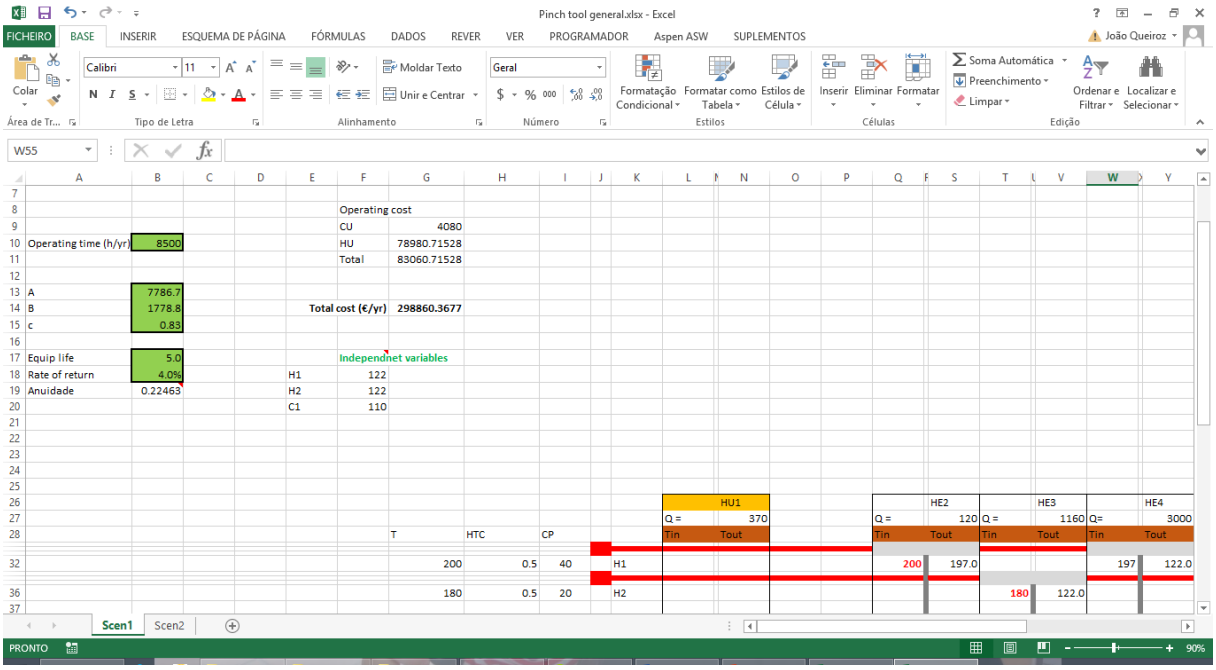

2. Build the network that was determined using the Above Pinch.xls and the Bellow Pinch.xls tools

To insert a new Heat exchanger copy an existent one.

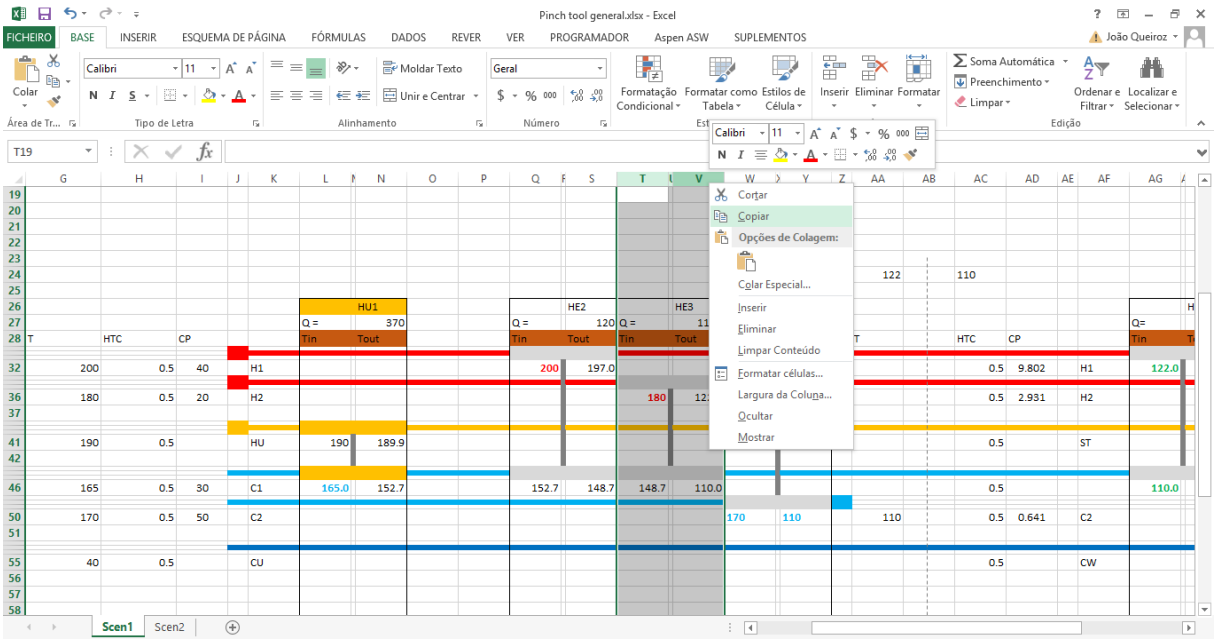

,and then insert the copied cells.

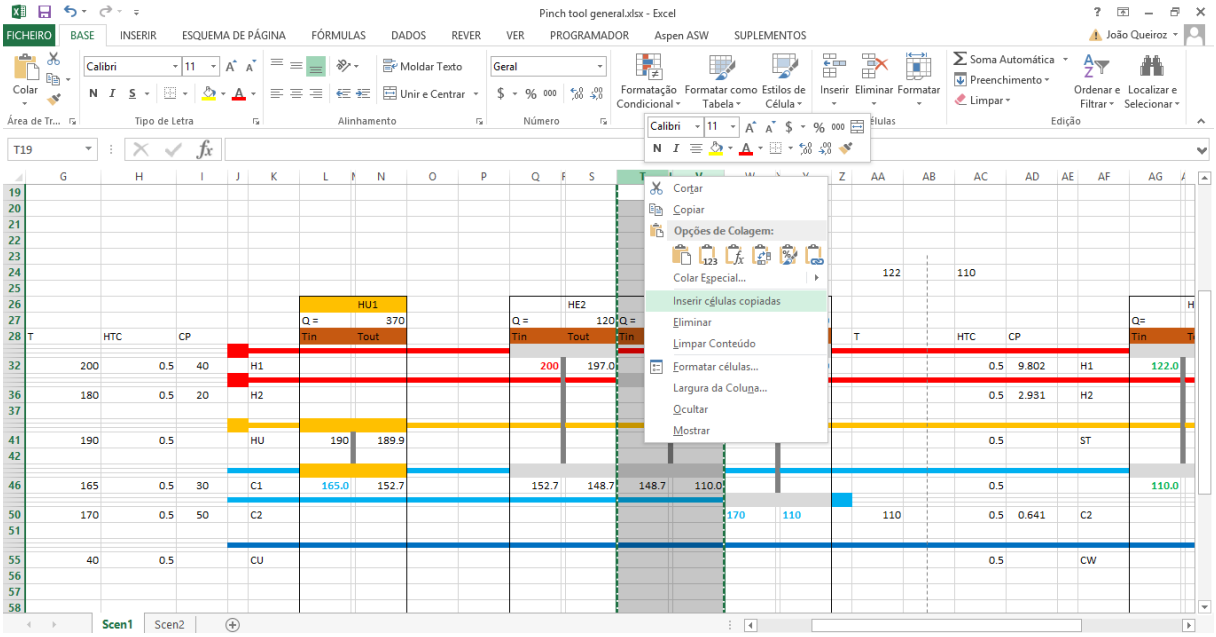

3. To insert a new stream follow the same procedure as with the heat exchanger but insert the copies cells in a row.

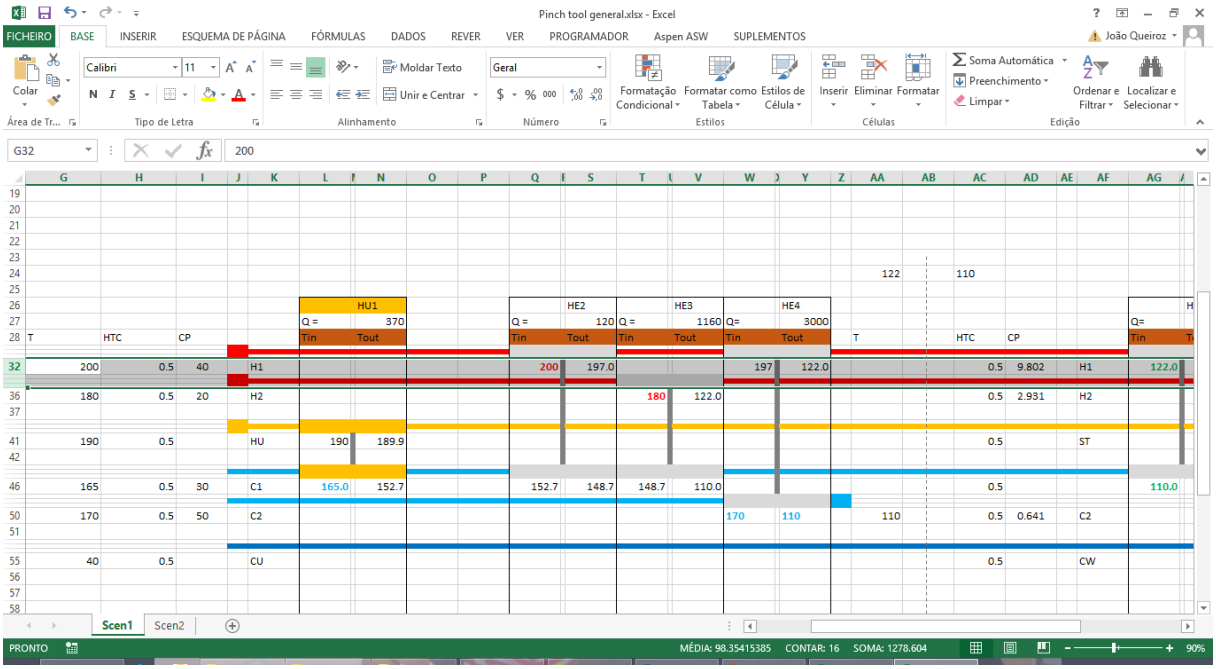

4. Link the cells that are dependent of each other. For example, the cold outlet of heat exchanger 2 equals the cold inlet of heat exchanger 3

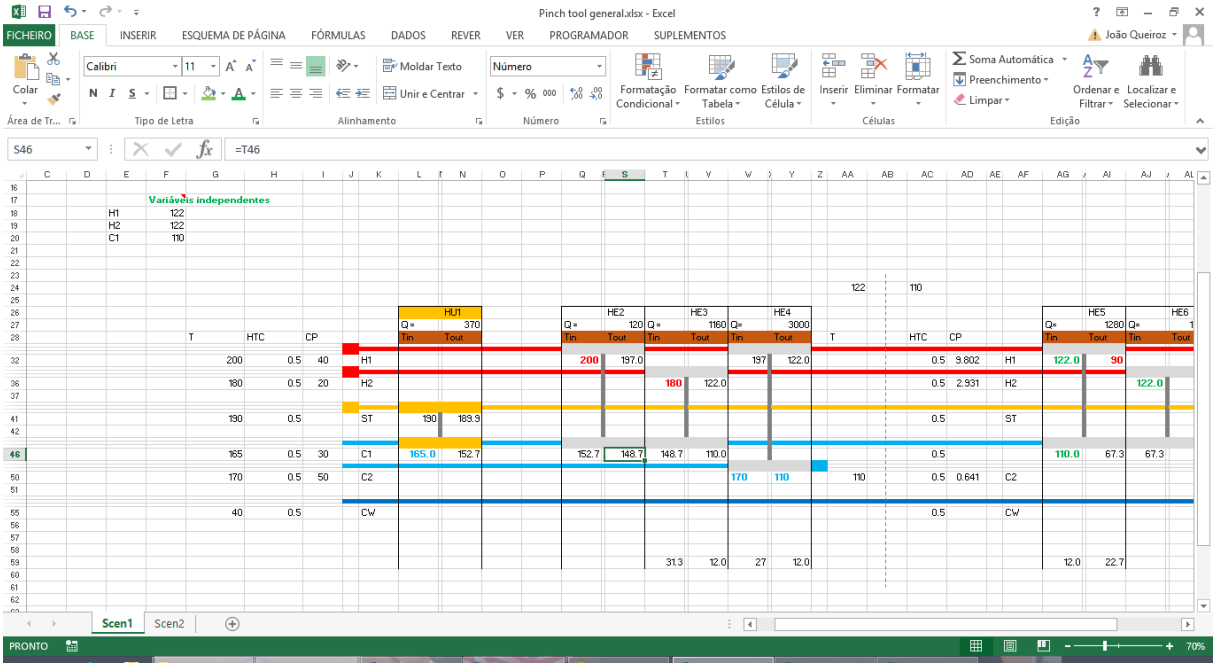

5. The temperatures at the pinch are considered independent variables, so they are explicated in a group of cells (on the HX network the independent variables are in green).

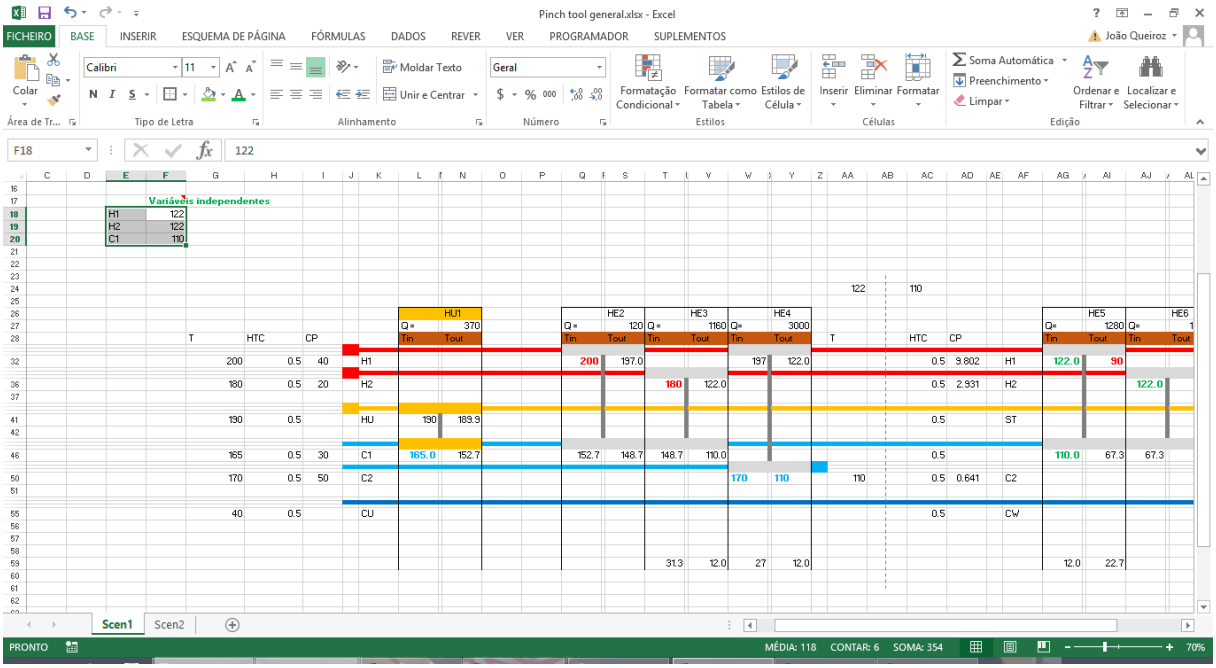

6. Use solver to find the minimum annual cost of the network.

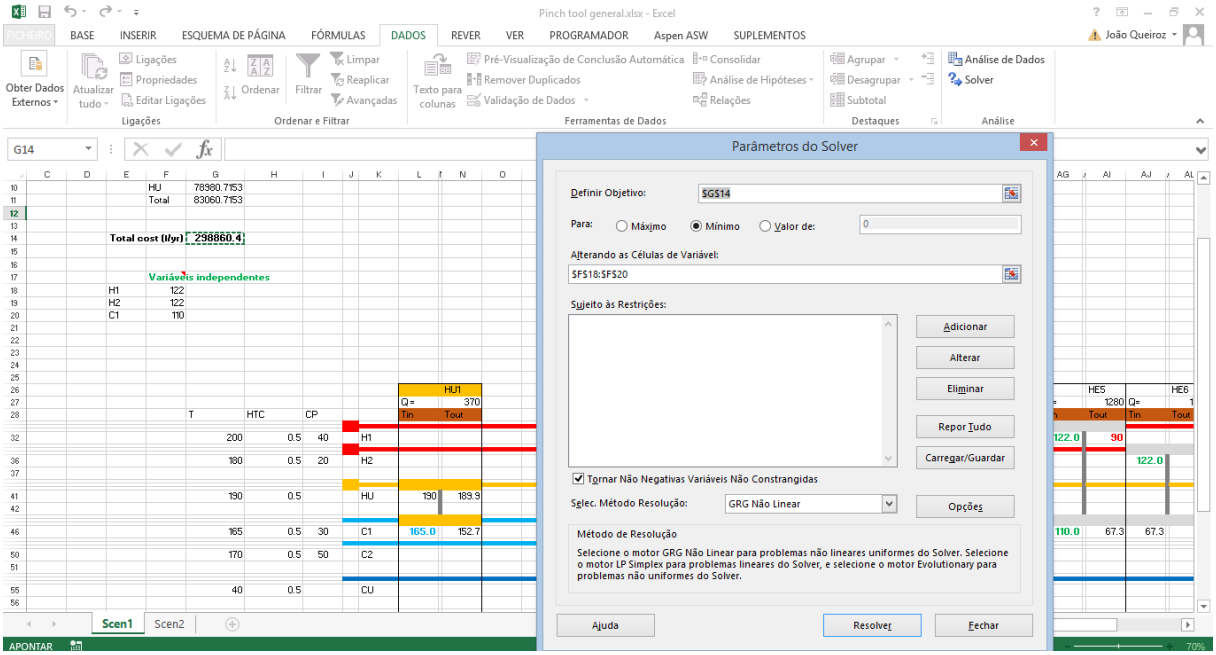

7. Check the network and evaluate the results.

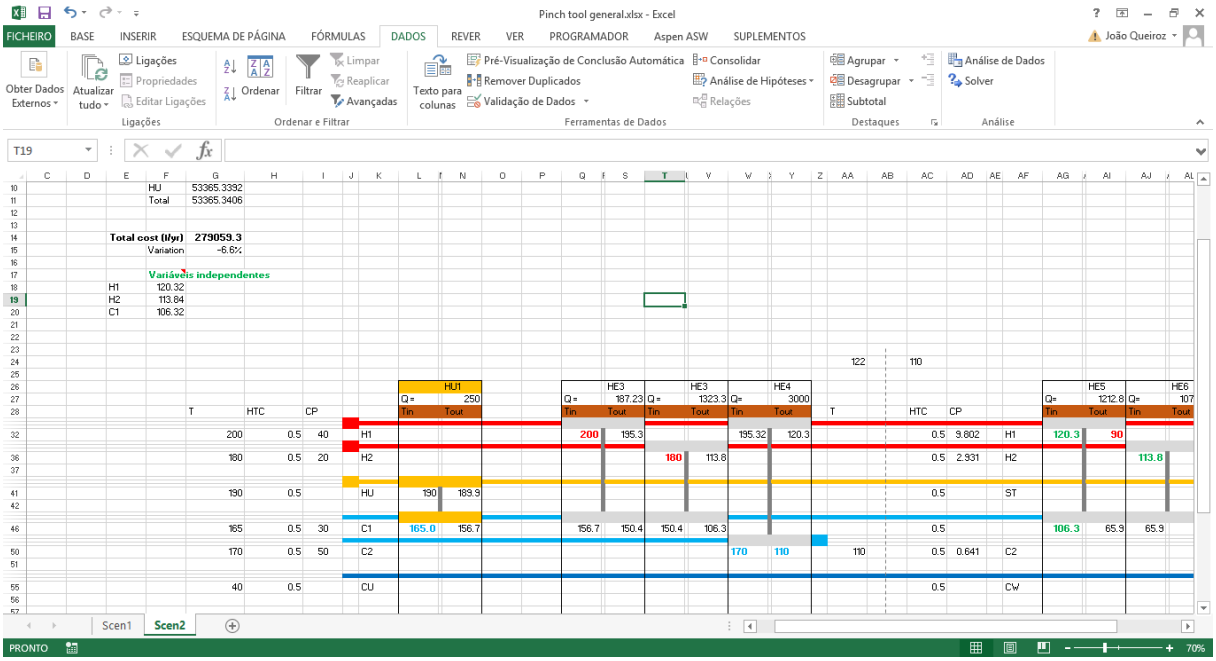

In this case cold utility could be removed.

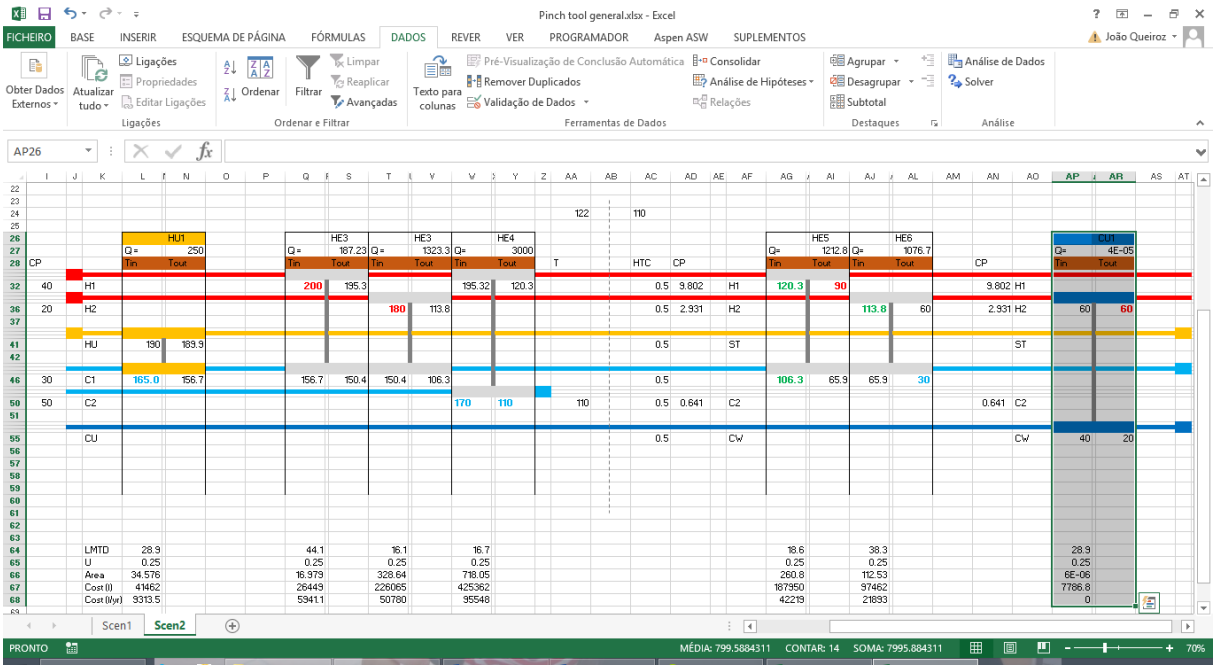
Pinch tool general.xlsx - Excel
FICHEIRO
BASE
INSERIR
ESQUEMA DE PÁGINA
FÓRMULAS
DADOS
REVER
VER
PROGRAMADOR
Aspen ASW
SUPLEMENTOS
João Queiroz
Obter Dados Externos
Atualizar tudo
Ligações
Propriedades
Editar Ligações
Ordenar
Filtrar
Limpar
Reaplicar
Avançadas
Texto para colunas
Pré-Visualização de Conclusão Automática
Remover Duplicados
Validação de Dados
Consolidar
Análise de Hipóteses
Relações
Agrupar
Desagrupar
Subtotal
Análise de Dados
Solver
Ligações
Ordenar e Filtrar
Ferramentas de Dados
Destaques
Análise
AP26
HU1
HE3
HE3
HE4
HE5
HE6
CU1
Scen1
Scen2
PRONTO
MÉDIA: 799.5884311
CONTAR: 14
SOMA: 7995.884311
70%